Technische Universität Berlin

Theoretical analysis of image separation and image inpainting: A compressed sensing approach

vorgelegt von

M.Sc.

Van Tiep Do

an der Fakultät II – Mathematik und Naturwissenschaften
der Technischen Universität Berlin
zur Erlangung des akademischen Grades

Doktor der Naturwissenschaften
– Dr. rer. nat. –

genehmigte Dissertation

Promotionsausschuss:

Vorsitzender:	Prof. Dr. Wilhelm Stannat
Gutachterin:	Prof. Dr. Gabriele Steidl
Gutachterin:	Prof. Dr. Gerlind Plonka-Hoch
Gutachter:	Prof. Dr. Nasser Aghazadeh

Tag der wissenschaftlichen Aussprache: 11. Januar 2023

Berlin 2023

Abstract

In image processing, problems of separation and reconstruction of missing pixels from incomplete digital images have been far more advanced in past decades. Many empirical results have produced very good results, however, providing a theoretical analysis for the success of algorithms is not an easy task, especially, for inpainting and separating multi-component signals. In this thesis, our primary goal is to develop a framework for these two problems.

In the first part of this thesis, we present a theoretical analysis of separating images consisting of pointlike and curvelike structures. Our approach is based on l_1-minimization, in which the sparsity of the desired solution is exploited by two sparse representation systems. It is well known that for such components wavelets provide an optimally sparse representation for point singularities, whereas α-shearlet type with flexible scaling might be best adapted to the curvilinear singularities. In our analysis, we first propose a reconstruction framework with theoretical guarantee on convergence, which is extended to use general frames instead of Parseval frames. We construct a dual pair of bandlimited α-shearlets which possesses a good time and frequency localization. We then apply the result to derive an asymptotic accuracy of the reconstructions. In addition, we show that it is possible to separate these two components as long as $\alpha < 2$, i.e., bandlimited α-shearlets which range from wavelet to shearlet type do not coincide with wavelets in the sense of isotropic fashion. Next, we present a theoretical analysis of recovering missing content in texture images. Our reconstruction algorithm is based on a modified basic pursuit denoising model. The success of this method relies on a compressed sensing technique that texture can be sparsely represented by Gabor frames. Different from papers in the literature which used a multi-scale approach to obtain asymptotic results, we propose a framework with recovery performance guarantees for the whole signal. Our analysis shows that if the region to be inpainted is sufficiently small we can then prove the success of the method by deriving a normalized L^2 error estimate of the reconstruction.

In the second part of this thesis, we introduce a comprehensive analysis showing that we can use two different representation systems to separate geometric components and fill-in the missing part of the original image simultaneously by utilizing the concept of clustered sparsity. Consequently, our theory shows that it is possible to inpaint or remove texture from an image that is the superposition of two distinct geometric components. We then extend our theory for separating N distinct geometric components and simultaneously filling-in the missing part of the observed image by two main algorithms, one is based on l_1 constrained and the other is based on unconstrained minimization. We present a theoretical guarantee for these algorithms using compressed sensing technique, which is based on a principle that each component can be sparsely represented by a suitably chosen dictionary. Those sparsifying systems are also extended to the case of general frames instead of Parseval frames which have been typically used in the past. We finally prove that the method does indeed succeed in separating point singularities from curvilinear singularities and texture as well as inpainting the missing band contained in curvilinear singularities and texture. Finally, some numerical experiments are performed to illustrate our theoretical results.

Zusammenfassung in deutscher Sprache

In der Bildverarbeitung sind die Ansätze zur Trennung und Rekonstruktion von fehlenden Pixeln aus unvollständigen digitalen Bildern in den letzten Jahrzehnten weit fortgeschritten. Viele empirische Ergebnisse haben sehr gute Resultate erbracht, aber eine theoretische Analyse für den Erfolg der Algorithmen ist keine leichte Aufgabe, insbesondere bei dem Inpainting und der Separation von Mehrkomponentensignale. In dieser Arbeit ist unser primäres Ziel die Entwicklung eines Rahmens für diese beiden Probleme.

Im ersten Teil dieser Arbeit präsentieren wir eine theoretische Analyse der Trennung von Bildern, die aus punktförmigen und kurvenförmigen Strukturen bestehen. Unser Ansatz basiert auf der l_1-Minimierung, bei der die Spärlichkeit der gewünschten Lösung durch zwei spärliche Darstellungssysteme ausgenutzt wird. Es ist bekannt, dass Wavelets für solche Komponenten eine optimal spärliche Darstellung für Punktsingularitäten bieten, während ein Shearlet-Typ mit flexibler Skalierung möglicherweise am besten für die krummlinigen Singularitäten geeignet ist. In unserer Analyse schlagen wir zunächst einen Rekonstruktionsrahmen mit theoretischer Konvergenzgarantie vor, der erweitert wird auf allgemeine Rahmen anstelle von Parseval-Rahmen. Wir konstruieren ein duales Paar von bandbegrenzten α-Shearlets, das eine gute Zeit- und Frequenzlokalisierung besitzt. Anschließend wenden wir das Ergebnis an, um eine asymptotische Genauigkeit der Rekonstruktionen abzuleiten. Darüber hinaus zeigen wir die Möglichkeit der Trennung beider Komponenten, solange $\alpha < 2$ ist, d. h., bandbegrenzte α-Shearlets, die vom Wavelet- zum Shearlet-Typ reichen, stimmen nicht mit Wavelets im Sinne einer isotropen Mode überein. Als nächstes stellen wir eine theoretische Analyse der Wiederherstellung fehlender Inhalte in Texturbildern vor. Unser Rekonstruktionsalgorithmus basiert auf einem modifizierten Basic pursuit-Entrauschungsmodell. Der Erfolg dieser Methode beruht auf einer Compressed-Sensing-Technik, bei der die Textur durch Gabor-Frames spärlich dargestellt werden kann. Im Gegensatz zu Arbeiten in der Literatur, die einen mehrskaligen Ansatz zur Erzielung asymptotischer Ergebnisse verwenden, schlagen wir einen Rahmen vor, der die Wiederherstellungsleistung für das gesamte Signal garantiert. Unsere Analyse zeigt, dass wir den Erfolg der Methode nachweisen können, wenn die zu übermalende Region ausreichend klein ist.

Im zweiten Teil dieser Arbeit stellen wir eine umfassende Analyse vor, die zeigt, dass wir zwei verschiedene Darstellungssysteme verwenden können, um geometrische Komponenten zu trennen und den fehlenden Teil des Originalbildes gleichzeitig aufzufüllen, indem wir das Konzept der geclusterten Sparsamkeit anwenden. Folglich zeigt unsere Theorie, dass es möglich ist, ein Bild, das aus der Überlagerung zweier unterschiedlicher geometrischer Komponenten besteht, zu übermalen oder Textur zu entfernen. Anschließend erweitern wir unsere Theorie für die Trennung von N verschiedenen geometrischen Komponenten und gleichzeitiges Auffüllen des fehlenden Teils des beobachteten Bildes durch zwei Hauptalgorithmen, einer basiert auf l1-gebundener und der andere auf ungebundener Minimierung. Wir stellen eine theoretische Garantie für diese Algorithmen vor, indem wir die Technik der komprimierten Abtastung verwenden, die auf dem Prinzip basiert, dass jede Komponente spärlich durch ein geeignetes Wörterbuch dargestellt werden kann. Diese Sparsifizierungssysteme werden auch auf den Fall allgemeiner Rahmen anstelle von Parseval-Rahmen, die in der Vergangenheit üblicherweise verwendet wurden, erweitert. Wir zeigen schließlich, dass die Methode tatsächlich erfolgreich Punktsingularitäten von krummlinigen Singularitäten und Textur trennt und das fehlende Band

in kurvilinearen Singularitäten und Textur. Schließlich werden einige numerische Experimente durchgeführt, um unsere theoretischen Ergebnisse zu illustrieren.

Acknowledgments

There are many people without whom this work would not have been possible. My first gratitude goes to Prof. Dr. Gitta Kutyniok for all her valuable advice and support over the past few years. Thank you for introducing me to the research directions and providing a pleasant environment for my research. I would also like to express my sincerest thanks to Prof. Dr. Gabriele Steidl, Prof. Dr. Gerlind Plonka-Hoch and Prof. Dr. Nasser Aghazadeh for agreeing to review this thesis.

I would like to thank Vietnam International Education Development (VIED) of the Ministry of Education and Training (MOET), Vietnam, for supporting me during my study in Germany through its “Project 911" fellowship.

I wish to sincerely thank all members of the working group, the former Applied Functional Analysis Group at the Institute of Mathematics of the Technische Universität Berlin. You were great colleagues and friends, and I enjoyed the time with you very much. It was a pleasure and an honor for me to be a member of the AFG. Specifically, my sincere appreciation goes to Dr. Ron Levie not only for all the discussions and scientific exchanges we have had, but also his support of my first project which is a part of this thesis. It has greatly improved the quality of my research. Apart from that, I would like to thank my office roommates, Alex and Ali, who have transformed the office into a second home for long periods of time.

My sincere thanks go to my co-authors, without whom this thesis would not have been possible. It was a pleasure working with my co-authors. Thanks for your productive collaboration and contribution to the theory. These acknowledgements are the reason I will use the pronoun ”we“ throughout this thesis. I am also thankful to the thousands of individuals that have dedicated their time and efforts to open-source projects for free. They have given the scientific community the ability to work with powerful tools due to their work.

The last thing I wish to do is to thank my parents, my entire family, who were constant sources of support during my academic career and motivated me to be where I am today. My special thanks go to my wife, Thi Thu Thuy Le, for the unending support on this journey, and my son, Viet Quan Do, for being my inspiration. I would not have been able to get this far without you all.

Contents

Preface **iii**
Abstract . . . iii
Zusammenfassung in deutscher Sprache . . . v
Acknowledgments . . . vii

List of Tables **xiii**

List of Figures **xiii**

Introduction **1**
Geometric Separation . . . 1
Image Inpainting . . . 2
Separation and Inpainting through Cluster Coherence . . . 3
Multiple Component Separation and Inpainting . . . 4
Structure of the Thesis . . . 5

1 Frames and Compressed Sensing **9**
1.1 Frames . . . 9
1.1.1 Gabor Frames . . . 12
1.1.2 Wavelet Frames . . . 13
1.1.3 Shearlet Frames . . . 14
1.2 Compressed Sensing . . . 17
1.2.1 l_0- Minimization . . . 17
1.2.2 Basic Pursuit . . . 18
1.2.3 Null Space Property . . . 18
1.2.4 Restricted Isometry Property . . . 19

2 Problem of Geometric Separation **21**
2.1 Problem Formulation . . . 21
2.1.1 General Component Separation . . . 21
2.1.2 Recovery via l_1-Minimization . . . 22
2.2 Theoretical Guarantee for Component Separation . . . 22
2.2.1 Joint Concentration Analysis . . . 22
2.2.2 Theoretical Guarantee via Cluster Coherence . . . 24
2.3 Component Separation . . . 26
2.3.1 Mathematical Model of Components . . . 26
2.3.2 Wavelet Frames . . . 27
2.3.3 A Pair of Bandlimited α-Shearlet Dual Frames . . . 27
2.4 Multi-scale Component Separation . . . 34
2.4.1 Estimate of Cluster Coherence . . . 36
2.4.2 Sparse Representation Error . . . 40

2.4.3 Proof of Main Theorem . . . 44
2.5 Conclusions and Further Discussion . . . 45

3 Problem of Image Inpainting **47**
3.1 Results on Images Governed by Edges . . . 47
3.2 Texture Inpainting- a Global Approach . . . 48
3.2.1 Formulation of Image Inpainting . . . 48
3.2.2 Recovery Algorithm . . . 49
3.2.3 Theoretical Analysis Tools . . . 50
3.3 Image Model Settings . . . 52
3.3.1 Model of Texture . . . 52
3.3.2 Missing Part Model . . . 53
3.4 Main Result . . . 53
3.4.1 Set of Significant Gabor Coefficients . . . 53
3.4.2 A Convergence for Image Inpainting . . . 54
3.4.3 Proof of Theorem 3.7 . . . 54

4 Simultaneous Separation and Inpainting **59**
4.1 Motivation . . . 59
4.2 Simultaneous Inpainting and Separation Approach . . . 60
4.2.1 The Separation Problem . . . 60
4.2.2 The Inpainting Problem . . . 61
4.2.3 The Simultaneous Separation and Inpainting problem . . . 61
4.3 General Separation and Inpainting Theory . . . 61
4.3.1 Joint Concentration . . . 62
4.3.2 Recovery Guarantee Through Joint Concentration . . . 62
4.3.3 Recovery Guarantee Through Cluster Coherence . . . 64
4.4 Mathematical Models of Texture and Cartoon . . . 67
4.4.1 Model of Texture . . . 67
4.4.2 The Local Cartoon Patch . . . 68
4.4.3 The Missing Part . . . 70
4.5 Sparsifying Systems for Texture and Cartoon . . . 70
4.5.1 Gabor Frame . . . 71
4.5.2 The Universal-scaling Shearlet Frame . . . 71
4.6 Inpainting and Separation of Cartoon and Texture . . . 74
4.6.1 Multi-scale Separation and Inpainting . . . 74
4.6.2 Balancing the Texture and Cartoon Parts . . . 76
4.6.3 Sparsity Assumptions on Texture . . . 80
4.6.4 Cluster Sets for Texture and Cartoon . . . 81
4.6.5 The Separation and Inpainting Theorem for Cartoon and Texture . . . 82
4.7 Extensions and Future Directions . . . 83
4.8 Relative Sparsity of Texture and Cartoon . . . 83
4.8.1 Decay Estimates of Shearlet and Gabor Elements . . . 84
4.8.2 Cartoon Patch . . . 86
4.8.3 Texture . . . 95
4.9 Cluster Coherence for Cartoon and Texture . . . 97
4.9.1 Cluster Coherence of the Un-projected Frames . . . 97

4.9.2 Cluster Coherence of the Projected Frames . . . 99
4.10 Proof of Theorem 4.16 . . . 104

5 Multiple Component Separation and Inpainting **105**
5.1 Mathematical Formulation . . . 105
5.1.1 Notations and Definitions . . . 105
5.1.2 Problem of Multiple Component Image Separation . . . 106
5.1.3 Problem of Image Inpainting . . . 107
5.1.4 Recovery via l_1-Minimization . . . 107
5.2 Theoretical Guarantee for Multiple Component Separation Problems . . . 107
5.2.1 Joint Concentration Analysis . . . 107
5.2.2 Cluster Coherence Analysis . . . 111
5.3 l_1 Optimization of Image Denoising . . . 114
5.4 Inpainting and Denoising of Multiple Component Images in Applications 118
5.4.1 Model of Components . . . 118
5.4.2 Sparse Representations . . . 119
5.4.3 Multi-scale Approach . . . 121
5.4.4 Main Results . . . 122
5.4.5 Estimate of Approximation Errors . . . 124
5.4.6 Estimate of Cluster Coherence for Separation Task . . . 126
5.4.7 Estimate of Cluster Coherence for Inpainting Task . . . 131
5.4.8 Proof of Theorem 5.16 and Theorem 5.17 . . . 132
5.5 Summary and Conclusion . . . 133

6 Numerical Implementation **135**
6.1 Algorithms . . . 135
6.2 Experiments . . . 136
6.3 Discussion . . . 138

Bibliography **139**

List of Tables

List of Figures

1.1 Mercedes-Benz frame 10

2.1 Frequency tiling of shearlets. 29
2.2 Cones $\mathcal{C}_{\mathrm{v}}$ (black) and $\mathcal{C}_{\mathrm{v}}^{d}$ (gray) with $\mathcal{C}_{\mathrm{v}}^{d} \subset \mathcal{C}_{\mathrm{v}}$ in frequency domain. 30
2.3 The frequency tilling of the vertical cone $\mathcal{C}_{\mathrm{v}}$, with the support of one shearlet highlighted. 34
2.4 Frequency support of shearlets with $\iota = \mathrm{v}, |l| > 1$ (gray) and shearlets with $\iota = \mathrm{h}$ (black). 42

3.1 Left: Barbara image. Right: Some popular texture samples. 47
3.2 Difference between l_1 and l_2 minimization for finding sparse solutions. 49
3.3 Model of the missing trip at scale j. 53

4.1 A corrupted photo, where the noise is a texture part together with missing stripes, and the clean image is the cartoon part. 60
4.2 Real valued texture sample produced by randomly choosing a sparse set of Fourier coefficients with random values and an appropriate symmetry in the frequency domain, with the rest of the Fourier coefficients set to zero. 67
4.3 A local cartoon patch. 70
4.4 Frequency tiling of a cone-adapted shearlet. 72
4.5 Left: Interaction between a cluster of Gabor elements (black small squares) and a shearlet (gray) in the frequency domain; Right: Some shearlet elements (gray) associated with $\Lambda_{1,j}$ in the spatial domain for $l = 0$. 81
4.6 Interactions between horizontal shearlets, vertical shearlets and the sub-image of cartoon part $w\mathcal{S}_j$. Left: Frequency support of horizontal shearlets at scale j (gray), $w\mathcal{S}_j$ (bold). Right: Frequency support of vertical shearlets with $|l| > 1$ (gray), $w\mathcal{S}_j$ (bold). 93
4.7 Left: Frequency support of a shearlet (trapezoidal) and Gabor elements (small squares). Right: Missing part (vertical band), essential spatial support of a shearlet (ellipse) and a cluster of Gabor elements (rectangle). The gap width does not exceed the essential length of the shearlet. 99

5.1 Interaction between Gabor elements (black) with wavelet and shearlet elements (gray) 119
5.2 Frequency tiling of a cone-adapted shearlet. 121

5.3 Model of the missing trip at scale j. 122

6.1 Right: Corrupted image Left: The recovered image by l_1 minimization. 136
6.2 Right: Corrupted image Left: The recovered image by l_1 minimization. 136
6.3 Zoom in 136
6.4 Reconstructions errors of four missing columns 137
6.5 left: original image of neuron, middle: extracted spines, right: extracted dendrites. Source: [KL12b] 138

Introduction

In the era of data analytics, the task of *geometric separation* is of interest for various applications. For instance, astronomers might want to extract stars from filaments, or neurologists might want to separate spines from dendrites. This task arises due to the fact that image data are often the superposition of different geometric components. In fact, numerous publications have been contributed to this area both in the mathematical and engineering communities.

Another interesting problem in applications is to fill-in holes in images due to damage or missing data. This process was known as "*image inpainting*" which originally referred to the task of recovering missing parts in corrupted paintings [BSCB00], but now also means automatic filling of specific regions in images or videos. The common ingredient of image inpainting methods is to exploit the surrounding information of regions to be inpainted to interpolate the hidden areas. Although there are many algorithms have been proposed for image inpainting, this task is still challenging to solve as there is no unique solution to the problem.

In this thesis, we study a theoretical analysis for these two problems.

Geometric Separation

Given an image f, we assume that f is a superposition of two geometric components, i.e.,

$$f = \mathcal{P} + \mathcal{C},$$

where $\mathcal{P}, \mathcal{C}$ are two unknown components which we want to reconstruct.

To turn this problem into a uniquely solvable problem, the first steps are assumptions onto the shape of the components to be recovered. Recently, the methodology of compressed sensing allows the efficient reconstruction of sparse or approximately sparse data from highly incomplete linear measurements by l^1-minimization or thresholding [CRT06a; CRT06b; Don06]. The key ingredient is to choose two appropriate dictionaries, each one sparsely representing the corresponding component but failing to sparsely represent the other. In recent decades, there have been various applications of compressed sensing techniques, including deblurring and deconvolution [PEH09; RMW12], image inpainting [GK14; KKZ14; KDJ20], data compression [DVDD98; BSO08], as well as geometric separation [DK09; KL12b; DK13; Kut14; DLK22]. Along the way, the task of separating pointlike and curvelike structures was first introduced in [DK13] with a theoretical recovery guarantee by using wavelet and curvelet Parseval frames. Indeed, wavelets are well adapted for pointlike phenomena, whereas curvelets provide optimal representation for images with edges. However, the limitation is that curvelets use rotation which ignores the discrete lattice structures. Later, shearlet systems, originally introduced in [GKL06] and then followed by other types [KL09; KKL12; GL13; GK14], make use of shearing instead of rotation. They have been shown to share similar optimal approximation behavior with curvelets, but they allow the unified treatment of the continuum and

digital realm leading to faithful implementations compared with other known sparse representation systems like wavelets [Mal98], ridgelets [Can98], curvelets [CD99], bandlets [LM05], and contourlets [DV05].

In addition, a class of shearlets appeared using flexible scaling to adapt the system according to the smoothness of the data. Among them, universal shearlets [GK14] form Parseval frames by changing scaling parameters at each scale which are best adapted to only high frequency part, whereas compactly supported α-shearlets [Kei12; KLL12a] with fixed scaling parameter provide superior localization but fail to form Parseval frames. Thus, although Parseval frames play a crucial role both in applications and theoretical studies, this property is not always achieved. Overall, each of them has its own advantages and disadvantages depending on the approach chosen in applications.

In chapter 2, we consider the problem of separating pointlike singularities and curvilinear singularities. For our analysis, we construct a dual pair of bandlimited α-shearlets with flexible scaling which adaptively match their decompositions to the smoothness of observed data, i.e., they provide an optimal sparse representation of C^β-curvilinear singularities, $\beta = 2/\alpha$. They range from wavelets ($\alpha = 1$) to shearlets ($\alpha = 2$). This problem is more involved than when restricting to Parseval frame pairs of wavelets-curvelets [DK13], or wavelets-shearlets [DK09; KL12b]. In our analysis, we provide a theoretical guarantee for geometric separation using general frames not restricted to Parseval frames.

Image Inpainting

Another problem of our interest is image inpainting. To model this problem , we suppose that the original image f which we want to recover is corrupted. Given the Hilbert space $\mathcal{H}$, we assume that $\mathcal{H}$ can be decomposed into the known space $\mathcal{H}_K$ and the missing space $\mathcal{H}_M$ by

$$\mathcal{H} = \mathcal{H}_K \oplus \mathcal{H}_M,$$

where the subspaces $\mathcal{H}_K, \mathcal{H}_M$ denote the *known part* and *missing part* respectively. Let P_M and P_K denote the orthogonal projection of $\mathcal{H}$ upon these two subspaces, respectively. In the inpainting problem, we assume that we are only given the image in the known part $P_K f$, and the goal is to reconstruct f.

In chapter 3, we focus on inpainting texture images due to the fact that *texture* is a common phenomenon present in a large number of natural images. It is often important information which plays a central role in identifying regions of interest in images. Due to the rapid growth of the digital world, the study on texture becomes an essential part in image processing. Indeed, texture analysis methods have proven successful in a wide range of applications including industrial, medical imaging [GKHDV02; TAGFG08; Jia11], remote sensing [PMSMA15] and face recognition [AHP06]. In many situations, we might have texture in hand for processing, for instance, they could be either pure texture or after extracting from compound images [Kut13; FHMZ17; Do22]. However, digital images might be corrupted due to several factors such as chemical processing or poor storage, this therefore requires a pressing need for studying image inpainting as well as texture inpainting. There are some approaches to address these problems in the literature. The first one is related to texture synthesis techniques [EL99; HJM10], or combined PDE and texture synthesis approach [Gro04; YSZTW10; BCL14]. Total variation methods have

also been effectively applied to image inpainting [CS01; CSZ06; CDOS12; LW12]. The more recent approaches are convolutional neural networks which have shown promising results in recent years [Yeh+17; CH18]. Another related work is the transform-based method using *compressed sensing* techniques [Don06] with theoretical analysis in the context of multi-scale approach [KKZ14; KDJ20]. There, the below inpainting algorithm was applied at each scale before recovering the original image by a combination of its sub-images,

$$f^\star = \underset{u}{\operatorname{argmin}} \|\Phi^* u\|_1, \quad \text{subject to } P_K u = P_K f. \tag{0.1}$$

However, there was no information on the error of the reconstruction for the whole signal by using this approach, only asymptotic results were shown.

In this chapter, we provide a theoretical study of the global inpainting strategy. The core idea of this method is based on the assumption that f is sparse under a certain frame. In our analysis, we first propose a novel algorithm based on a modified basic pursuit denoising model for inpainting missing parts of the desired object. We then provide a theoretical guarantee for the success of the proposed algorithm. Finally, we transfer the abstract theory to inpaint texture images by using Gabor frames for sparsely representing texture. We prove the success of the proposed algorithm by deriving a universal L^2-error estimate of the reconstruction compared with the multi-scale analysis framework which shown good results only at fine scales. More precisely, we show that the reconstruction method succeeds in filling missing trips in texture images if the size of the missing part is sufficiently small.

Separation and Inpainting through Cluster Coherence

In chapter 4, we focus on the problem of inpainting and separation of cartoon from texture which was proposed in various papers, for instance [ESQD05; CCS10; BVSO03]. The general approach is to find two dictionaries, each sparsely representing one image part, and not sparsely representing the other. For example, texture is sparsely represented by a Gabor system, and cartoon by curvelets/shearlets. Then, in the separation and inpainting algorithm, the image is decomposed to a sparse representation based on the combined Gabor-curvelet system, using some compressed sensing approach. However, in the above-mentioned papers, there is no theoretical analysis of the success of the proposed methods. In [CCS10] and [ESQD05], the separation and inpainting problem is formulated as the minimization of the sum of the two l_1 norms of the two dictionary coefficients of the image. Each of these papers proposed an algorithm for the minimization, but neither proved that the l_1 minimization problem actually separates the two components. In our paper, we consider a similar setting to the above papers, and give a full approximation analysis of the method, with convergence guarantees. Our paper is the first that proves that the l_1 minimization problem indeed inpaints and separates the two components of the image.

Our analysis is based on the theoretical machinery of joint concentration and cluster coherence. These notions were used in the past for analyzing separation problems and inpainting problems, but never (to the best of our knowledge) for the simultaneous problem. Given two dictionaries, both joint concentration and cluster coherence are definitions that quantify the ability of each dictionary to sparsely represent signals of one type, but not signals of another type. Some papers use joint concentration to do inpainting

[GK14; KKZ14], some to do separation [DK13; Kut13]. Proving theoretical results is typically easier when using joint concentration. However, checking joint concentration on dictionaries in practice is difficult. Thus the notion of cluster coherence was introduced in [DK13], which is strictly stronger than joint concentration, and makes checking the assumptions of the theory easier in practical examples. Papers like [DK13; Kut13; GK14; KKZ14] use the notions of cluster coherence either for separation or for inpainting, but not simultaneously.

In this chapter, we modify and extend the definitions of joint concentration to accommodate a simultaneous analysis of separation and inpainting. We then further extend the notion of cluster coherence to fit the modified definitions of joint concentration. With the new general definitions, we consider the problem of inpainting and separating texture from cartoon. We show that the universal shearlet systems [GK14] and Gabor systems [Chr03] satisfy the cluster coherence requirement, thus proving the success of our inpainting–separation method.

We summarize our main contributions in this chapter as follows.

- We modify the joint concentration and cluster coherence definitions to accommodate the simultaneous separation-inpainting problem (Section 4.3).
- Using the modified notions of joint concentration and cluster coherence we prove that the l_1 sparse decomposition method successfully inpaints and separates the two parts of an image in a generic setting (Theorem 4.8).
- We use the general theory to inpaint and separate cartoon from texture in images. Here, the sparse decomposition method is based on a Gabor basis, sparsifying texture, and a universal shearlet dictionary, sparsifying cartoons (Section 4.5). The two systems are shown to satisfy the cluster coherence property, thus proving the success of the inpainting-separation cartoon from texture method (Theorem 4.16).

Our theoretical results on the problem of simultaneous separation and inpainting, which will be presented in Chapter 4, have been published in [DLK22]:

VT. Do, R. Levie, G. Kutyniok, *"Analysis of simultaneous inpainting and geometric separation based on sparse decomposition"* , Analysis and Applications, Vol. 20, No. 02, pp. 303-352, 2022.

Multiple Component Separation and Inpainting

Also, the task of inpainting an image which is often composed of two or more components is of interest in many research fields. However, at the first sight the above problems seem unable to solve from a theoretical point of view because of the ill-poseness of the system that leads to infinitely many solutions. Recently, compressed sensing technique provides a firm foundation to recover a signal from incomplete measurements by exploiting the sparsity of the signal [Don06]. It is well known that l_1 minimization performs exceptionally well in locating sparse solutions of underdetermined linear systems. Based on this observation, a great number of sparsity-based algorithms have been introduced in this area. Various empirical works in the past have shown good results for either inpainting [CKS02] or geometric separation [KL12b]. The theoretical study [DK13] first introduced an asymptotic result for separating points from curves using Parseval

frames of wavelets and curvelets. It was then followed by some other works to either inpaint a single component image [GK14; KKZ14; KDJ20] or separate two components [DK13; DG21]. Later, our previous work [DLK22] proposed a framework to deal with simultaneous separation and inpainting for two-component signals. A critical premise of these methods is that each of the components has a sparse representation in a certain dictionary.

However, all aforementioned papers used Parseval frames and none of them deal with the case of multi-component separation and inpainting. The problem studied here is completely different since we have more intersections among components which makes the problem more challenging. Each underlying layer has distinctive features, for instance, pointlike structure (smooth apart from point singularities), cartoon (the piecewise smooth part of the image), and texture (consisting of repeated texels). There is still a lack of theoretical analysis to explain why simultaneous separation and inpainting are possible for multi-component signals. In an attempt to generalize the theory to multi-component case, the proceeding paper [DK13] introduced a theory which also exploited notions of joint concentration and cluster coherence that first appeared in [KKZ11]. However, the theory in [KKZ11] can be problematic to apply for problems of separating more than two components, which will be discussed in Section 5.2.

In chapter 5, motivated by our previous works [DG21; DLK22] we present a more general framework for simultaneous separation, inpainting, and denoising on degraded multi-component signals. We introduce two algorithms based on l_1 minimization for analyzing these tasks, one deals with noiseless images and the other with additional noise. We then provide a theoretical guarantee for these algorithms by establishing L_2 error of the reconstructions. In addition, our methodology works for non-Parseval frames if each of them possesses a well localized dual frame, see [DG21] for the case of separating two components. We further apply the results to the separation of points from curves and texture while inpainting the missing content of the image. The key idea to the success of our method lies in the morphological difference among these ground truth components. They are then encoded in three different sparse representation systems, wavelets for representing point singularities, shearlets for representing curvilinear singularities, and Gabor frames for representing texture. Based on that, we prove the success of the proposed algorithms using a multi-scale approach. These results have been published in [Do22]:

VT. Do, *Multi-component separation, inpainting and denoising with recovery guarantees*, preprint, arXiv:2202.02806 [math.FA], 2022.

Structure of the Thesis

We organize the thesis in four parts with two main topics "Image separation" and "Image inpainting". In the first part, chapter 1 provides the reader with background knowledge of frames theory including Gabor frames, wavelet frames and shearlet frames. Most of this part can be skipped by readers familiar with the topic. In the second part, we provides a framework for those who primarily concerned with the applications and results of geometric separation, which are described in chapter 2. Next, we present problem of images inpainting in chapter 3 with focusing on inpainting texture images. Chapter 4 and 5 are dedicated to extend results from previous sections to problem of simultaneous separation and inpainting. More generalized models on original images to be separated

and inpainted are also introduced in this part. There we consider multiple component images in our analysis. Finally, we end the thesis with some experiments for our theoretical results in chapter 6. Discussion and our further direction are also included in this part.

Nomenclature

α_j	$\operatorname{argmin}_{\tilde{\alpha}_j \in Z_j} \lvert\tilde{\alpha}_j - \alpha\rvert = \frac{\lfloor j\alpha + 0.5 \rfloor}{j}$
$M_{j,l,(\iota)}$	$\left[s_j^{-1} \cdot S_{(\iota)}^{-l} \cdot (\operatorname{supp} \hat{\psi}_{j,0,0}^{\alpha_j,(\iota)} + B_1(0,1)) \right] \cap \mathbb{Z}^2$
Z_j	$\left\{ \frac{m}{j} \mid m \in \mathbb{Z}, m \leq 2j-1 \right\}$
Δ	$\left\{ (j,l,k;\alpha_j,(\iota) \mid j \geq 0, \lvert l\rvert < 2^{(2-\alpha_j)j}, k \in \mathbb{Z}^2, (\iota) \in \{(\mathrm{h}),(\mathrm{v})\} \right\}$ $\bigcup \left\{ (j,l,k;\alpha_j,\varnothing) \mid j \geq 0, \lvert l\rvert = 2^{(2-\alpha_j)j}, k \in \mathbb{Z}^2 \right\}$
Δ_j	$\{(j',k,l;\alpha_j,(\iota)) \in \Delta \mid j' = j\}, \quad j \geq 0$
$\Delta_j^{\pm}$	$\Delta_{j-1} \cup \Delta_j \cup \Delta_{j+1}$
$\hat{F}_j(\xi)$	$W_j(\xi) = W(2^{-2j}\xi)$
$\Lambda_{1,j}$	$\{(j,l,k;\alpha_j,v) \mid \lvert l\rvert \leq 1, k = (k_1,k_2) \in \mathbb{Z}^2, \lvert k_2 - lk_1\rvert \leq 2^{\epsilon j}\}$
$\Lambda_{2,j}$	$\left(\mathbb{Z}^2 \cap B(0,M_j) \right) \times \left(I_T^{\pm} \cap A_{s,j} \right)$
$\langle \lvert x\rvert \rangle$	$(1+\lvert x\rvert^2)^{1/2}$
$\mathbb{S}(\mathbb{R}^d)$	$\left\{ f \in C^\infty(\mathbb{R}^d) \mid \forall K,N \in \mathbb{N}_0 : \sup_{x \in \mathbb{R}^d} (1+\lvert x\rvert^2)^{-N/2} \sum_{\lvert\alpha\rvert \leq K} \lvert D^\alpha f(x)\rvert < \infty \right\}$
$\mathcal{C}_{(\mathrm{h})}$	$\left\{ (\xi_1,\xi_2) \in \mathbb{R}^2 \mid \left\lvert \frac{\xi_2}{\xi_1} \right\rvert \leq 1 \right\}$
$\mathcal{C}_{(\mathrm{v})}$	$\left\{ (\xi_2,\xi_1) \in \mathbb{R}^2 \mid \left\lvert \frac{\xi_1}{\xi_2} \right\rvert \leq 1 \right\}$
(h)	Horizontal
(v)	Vertical
A_j	$[-2^{2j-1}, 2^{2j-1}]^2 \setminus [-2^{2j-4}, 2^{2j-4}]^2$
$A_{\alpha,(\mathrm{h})}$	$\begin{bmatrix} 2^2 & 0 \\ 0 & 2^\alpha \end{bmatrix}$
$A_{\alpha,(\mathrm{v})}$	$\begin{bmatrix} 2^\alpha & 0 \\ 0 & 2^2 \end{bmatrix}$
$A_{s,j}$	$\{\xi \in \mathbb{R}^2 : s_j \xi \in A_j\}$
$I_T^{\pm}$	$\{n' \in \mathbb{Z}^2 \mid \exists n \in I_T : \lvert n' - n\rvert \leq 1\}$

M_j $2^{\epsilon j/6}$

$S_{(\mathrm{h})}$ $\begin{bmatrix} 1 & 1 \\ 0 & 1 \end{bmatrix}$

$S_{(\mathrm{v})}$ $\begin{bmatrix} 1 & 0 \\ 1 & 1 \end{bmatrix}$

$t^{(\mathrm{h})}$ $(t_1^{(\mathrm{h})}, t_2^{(\mathrm{h})}) := A_{\alpha_j,(\mathrm{h})}^{-j} S_{(\mathrm{h})}^{-l} k = (2^{-2j}(k_1 - lk_2), 2^{-\alpha_j j} k_2)$

$t^{(\mathrm{v})}$ $(t_1^{(\mathrm{v})}, t_2^{(\mathrm{v})}) := A_{\alpha_j,(\mathrm{v})}^{-j} S_{(\mathrm{v})}^{-l} k = (2^{-\alpha_j j} k_1, 2^{-2j}(k_2 - lk_1)$

$V_{(\mathrm{h})}(\xi)$ $v\left(\frac{\xi_2}{\xi_1}\right)$

$V_{(\mathrm{v})}(\xi)$ $v\left(\frac{\xi_1}{\xi_2}\right)$

$W_j(\xi)$ $W(\xi/2^{2j})$

1

Frames and Compressed Sensing

The purpose of this chapter is to provide a variety of notations, definitions, and preliminary results about representation systems that will be needed later in this thesis. Section 1.1 gives a brief review of frame theory including three common frames, Gabor frames, wavelet frames and shearlet frames. Next, Section 1.2 is devoted to the theory of Compressed sensing, a framework for acquiring sparse signals with few measurements. A fundamental idea here is that many types of signals are sparse in the sense that they can be well-represented by a small number of non-zero coefficients in a suitable basis or frames. This viewpoint is also a key to the efficiency of many lossy compression techniques such as JPEG, MP3 etc, in which a suitable wavelet system can be used.

1.1 Frames

We first start with some basic notions and definitions.

For $f, F \in L^1(\mathbb{R}^2)$ we define the *Fourier transform* and *inverse Fourier transform* by

$$\hat{f}(\xi) = \int_{\mathbb{R}^2} f(x) e^{-2\pi i x^T \xi} dx,$$

$$\check{F}(x) = \int_{\mathbb{R}^2} F(\xi) e^{2\pi i \xi^T x} d\xi,$$

with the usual extension to $L^2(\mathbb{R}^2)$.

Definition 1.1 A *frame* for a separable Hilbert space $\mathcal{H}$ is a countable family $\Phi = \{\phi_i\}_{i \in I}$ in $\mathcal{H}$ for which there exist constants $0 < A \leq B < +\infty$ such that

$$A\|f\|_2^2 \leq \sum_{i \in I} |\langle f, \phi_i \rangle|^2 \leq B\|f\|_2^2, \quad \forall f \in \mathcal{H}. \tag{1.1}$$

The constants A and B are called the *lower* and *upper frame bounds*, respectively. If A = B, this system is called an A-tight frame. In addition, if $A = B = 1$, then it is called a *Parseval frame*.

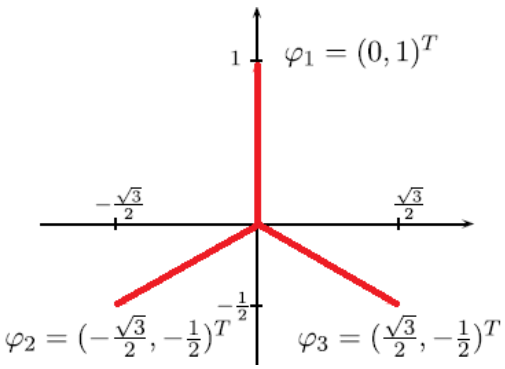

Figure 1.1: Mercedes-Benz frame

Example 1.2 1. Let $(e_i)_{i=1}^{\infty}$ be an orthonormal basis for $\mathcal{H}$, then $(e_1, e_1, e_2, e_3, e_4 \dots)$ form a frame for $\mathcal{H}$ with frame bounds 1 and 2.

2. *Mercedes-Benz frame*: we consider $\phi_1 = (0,1)^T, \phi_2 = (\frac{-\sqrt{3}}{2}, -\frac{1}{2})^T, \phi_3 = (\frac{\sqrt{3}}{2}, -\frac{1}{2})^T \in \mathbb{R}^2$. These vectors form a tight frame for $\mathbb{R}^2$ with frame bound $\frac{3}{2}$.

3. Let $(e_i)_{i=1}^{\infty}$ be an orthonormal basis for $\mathcal{H}$, then $(e_1, \frac{1}{\sqrt{2}}e_2, \frac{1}{\sqrt{2}}e_2, \frac{1}{\sqrt{3}}e_3, \frac{1}{\sqrt{3}}e_3, \frac{1}{\sqrt{3}}e_3, \frac{1}{2}e_4 \dots)$ form a Parseval frame for $\mathcal{H}$.

$\Diamond$

Definition 1.3 Let $\Phi = \{\phi_i\}_{i\in I}$ be a frame for $\mathcal{H}$. We have slightly abused notation by writing Φ again to denote the *synthesis operator*

$$\Phi : l_2(I) \to \mathcal{H}, \quad \Phi(\{c_i\}_{i\in I}) = \sum_{i\in I} c_i \phi_i.$$

We denote by Φ^* the *analysis operator*

$$\Phi^* : \mathcal{H} \to l_2(I), \quad \Phi^*(f) = (\langle f, \phi_i \rangle)_{i\in I}.$$

And the *frame operator* $\mathbb{S}$ is the operator

$$\mathbb{S} = \Phi\Phi^* : \mathcal{H} \to \mathcal{H}, \quad \mathbb{S}f = \sum_{i\in I} \langle f, \phi_i \rangle \phi_i.$$

Given a frame $\Phi = \{\phi_i\}_{i\in I}$ for $\mathcal{H}$, there exists a sequence $\Phi^d = \{\phi_i^d\}_{i\in I}$ in $\mathcal{H}$ such that

$$f = \Phi(\Phi^d)^* f = \sum_{i\in I} \langle f, \phi_i^d \rangle \phi_i, \ \forall f \in \mathcal{H}, \tag{1.2}$$

and

$$f = (\Phi^d)\Phi^* f = \sum_{i\in I} \langle f, \phi_i \rangle \phi_i^d, \ \forall f \in \mathcal{H}. \tag{1.3}$$

If both equations hold, Φ^d is called an *alternative dual frame* (or simply a *dual frame*) of Φ. Respectively, we call Φ^d an *analysis pseudo-dual* of the frame Φ, if only (1.2) holds and a *synthesis pseudo-dual* in case only (1.3) holds. In addition, the inequality (1.1) implies that

$\mathbb{S}$ is a self-adjoint, invertible operator on $\mathcal{H}$ [Chr03]. This leads to a special dual frame $\{\mathbb{S}^{-1}\phi_i\}_{i\in I}$ called the *canonical dual frame* of $\Phi = \{\phi_i\}_{i\in I}$ with frame bounds (B^{-1}, A^{-1}). In our analysis, we denote by $\mathbb{D}_\Phi$ the set of all synthesis pseudo-dual of the frame Φ, i.e.,

$$\mathbb{D}_\Phi = \Big\{\Phi^d = \{\phi_i^d\}_{i\in I} \in \mathcal{H} \mid f = \Phi^d\Phi^* f = \sum_{i\in I}\langle f, \phi_i\rangle\phi_i^d,\ \forall f \in \mathcal{H}\Big\}.$$

Obviously, $\mathbb{D}_\Phi \neq \emptyset$ since for each frame Φ the frame

$$\mathbb{S}^{-1}\Phi = \{\mathbb{S}^{-1}\phi_i\}_{i\in I}$$

is dual to Φ and therefore in $\mathbb{D}_\Phi$. Consequently, if Φ is a Parseval frame we have $\Phi \in \mathbb{D}_\Phi$. For more details on frame theory we refer to [DS52; Cas00; Chr03].

In sense of approximation theory, we would like to introduce another concept named *dictionary* which includes all frames or countable unions of frames. Let $\mathcal{H}$ be a Hilbert space, a dictionary is a sequence of vectors $\{\psi_i\}_{i\in I} \subset \mathcal{H}$ with I being finite or countable or countably infinite. In term of efficient representations, we need the notion of *best N-term approximation*. Let $\{\psi_i\}_{i\in I} \subset \mathcal{H}$ be a dictionary. For $f \in \mathcal{H}, N \in \mathbb{N}$, the best N-term approximation of f with respect to $\{\psi_i\}_{i\in I}$ is defined by the solution of the following minimization problem

$$\min_{I_N, (c_i)_{i\in I_N}} \|f - \sum_{i\in I_N} c_i\psi_i\|_{\mathcal{H}} \quad \text{s.t. } I_N \subseteq I, \#I_N \leq N.$$

In this context if $\{\psi_i\}_{i\in I}$ forms an orthonormal basis for $\mathcal{H}$, then the best N-term approximation is given by the N largest coefficients $|\langle f, \psi\rangle|$ in magnitude.

We intend to present some applications that mainly involve natural images the class of images of our interest in this thesis. To model natural images, *Cartoon-like functions* are often used as a standard model in image processing. Here, the class of Cartoon-like functions $\mathcal{E}^2(\mathbb{R}^2)$ is defined as the set of functions $f : \mathbb{R}^2 \to \mathbb{C}$ of the form

$$f = f_0 + f_1 \cdot \mathbb{1}_{B_\tau},$$

where $f_i \in C^2(\mathbb{R}^2)$, $\operatorname{supp} f_i \subseteq [0,1]^2$ and $\|f_i\|_{C^2} \leq 1,\ i = 0, 1$ and B_τ denotes the interior of a closed, non-intersecting curve τ in $C^2(\mathbb{R}^2)$. These functions are roughly speaking compactly supported functions that are C^2 apart from a C^2-discontinuity curve, see [Don01; KLL12b] for the details. Considering a cartoon like function $f \in \mathcal{E}^2(\mathbb{R}^2)$, the following shows a benchmark result, i.e., the optimal rate for representing f using a frame for $L^2(\mathbb{R}^2)$.

Theorem 1.4 ([Don01])
Let $\phi_{i\in I} \subseteq L^2(\mathbb{R}^2)$ be a frame for $L^2(\mathbb{R}^2)$. Then the optimal best N-term approximation rate for any $f \in \mathcal{E}^2(\mathbb{R}^2)$ is

$$\sigma(f, \{\phi_i\}_{i\in I}) := \inf_{I_N \subseteq I, \#I_N = N} \|f - c_i\phi_i\| = O(N^{-2}).$$

In what follows, we present a short overview of the most common frames, i.e., Gabor frames, wavelet frames and shearlet frames.

1.1.1 Gabor Frames

The first class of frames for $L^2(\mathbb{R}^2)$ we will discuss in this section is Gabor frames. This system appears naturally as a discretization of the short-time Fourier transform, which will be introduced next.

Definition 1.5 Let $g \in L^2(\mathbb{R}^2)$. Then the *short-time Fourier transform* of a function $f \in L^2(\mathbb{R}^2)$ with respect to g is defined by

$$\mathcal{S}_g f(t,\xi) = \int_{\mathbb{R}^2} f(x)\overline{g(x-t)}e^{-2\pi i x\xi}dx, \quad t,\xi \in \mathbb{R}^2.$$

Observing that

$$\mathcal{S}_g f(t,\xi) = \langle f, M_\xi T_t g\rangle = (\widehat{f \cdot T_t \overline{g}})(\xi), \quad t,\xi \in \mathbb{R}^2,$$

where the *translation operator* $T_t : L^2(\mathbb{R}^2) \to L^2(\mathbb{R}^2)$ is given by

$$T_t f(x) = f(x-t),$$

and *the modulation operator* $M_\xi : L^2(\mathbb{R}^2) \to L^2(\mathbb{R}^2)$ is given by

$$M_\xi f(x) = e^{2\pi i \xi x} f(x).$$

By this way, a Fourier transform is localized to a window of f and then moved over the entire domain by moving the window. In sense of representation, since the system $(M_\xi T_t g)_{(t,\xi)\in\mathbb{R}^2\times\mathbb{R}^2}$ is highly incomplete we might want to discretize the index set $\Lambda = (t,\xi) \subset \mathbb{R}^2 \times \mathbb{R}^2$ such that the resulted system still forms a frame for $L^2(\mathbb{R}^2)$, hence allows for a stable reconstruction of the function $f \in \mathbb{R}^2$ from the set of coefficients $(M_\xi T_t g)_{(t,\xi)\in\mathbb{R}^2\times\mathbb{R}^2}$.

Considering that translation in time and frequency are equally important, it seems natural to discretize each variable in a similar manner. In fact, the set of indexes Λ is typically chosen to be the lattice

$$\Lambda := m\mathbb{Z}^2 \times n\mathbb{Z}^2, \quad 0 < m,n \in \mathbb{Z}^2.$$

As a result, this leads to the definition of a Gabor frame.

Definition 1.6 Let $g \in L^2(\mathbb{R}^2)$ be a window function, we denote

$$g(x,y)(t) = g(t-x)e^{2\pi i t^T y}.$$

For $a,b > 0$, a *Gabor system* generated by g is given by $G(g,a,b) := \{g(ma,nb) \mid m,n \in \mathbb{Z}^2\}$. If this system forms a frame we call it a *Gabor frame*.

We now consider a necessary and sufficient condition for Gabor system to form a frame. In the following theorem we will see how the bounds of the frames are related to the parameters of the lattice and the window function.

Theorem 1.7 (Painless Nonorthogonal Expansions)

Let $a, b > 0$ and let $g \in L^2(\mathbb{R}^2)$ be a window function such that $G(g, a, b)$ forms a frame with frame bounds A and B. Then, we have

$$A \leq \frac{1}{b} \sum_{m \in \mathbb{Z}^2} |g(t - am)|^2 \leq B, \quad \text{for } a.e.\ t \in \mathbb{R}^2.$$

For an A-tight frame, we obtain

$$\frac{1}{b} \sum_{m \in \mathbb{Z}^2} \sum_{m \in \mathbb{Z}^2} |g(t - am)|^2 = A, \quad \text{for } a.e.\ t \in \mathbb{R}^2.$$

We now present a Gabor frame which we will later use in our analysis. Let $g \in L^2(\mathbb{R}^2)$ be a window function such that $\hat{g} \in C^\infty(\mathbb{R}^2)$, $\operatorname{supp} \hat{g} = [-1, 1]^2$ and

$$\sum_{n \in \mathbb{Z}^2} |\hat{g}(\xi + n)|^2 = 1, \quad \xi \in \mathbb{R}^2.$$

We define the Gabor system $\mathcal{G} = \{g_{m,n}(x)\}_{(m,n) \in \mathbb{Z}^2 \times \mathbb{Z}^2}$ by its Fourier transform as follows

$$\hat{g}_{m,n}(\xi) = \hat{g}(\xi - n) e^{2\pi i \xi^T \frac{m}{2}}.$$

As a result of Theorem 1.7, this system constitutes a Parseval frame for $L^2(\mathbb{R}^2)$.

1.1.2 Wavelet Frames

The theory of wavelets is mathematically rich and has many practical applications. We will not cover the entire wavelet theory in this section , but will concentrate on portions that will be useful in our need. Particularly, our discussion will be restricted to discrete wavelets, e.g., wavelet bases or redundant wavelet frames, the theory of continuous wavelets will not be discussed here. Also, wavelet theory exhibits a number of beautiful mathematical properties, but this is beyond the scope of this thesis.

The term wavelet, which means a 'small wave', usually refers to a function that is well-localized in the space and in the frequency domains. We first start with the definition of a *discrete wavelet system* in $L^2(\mathbb{R})$.

Definition 1.8 Let $\psi \in L^2(\mathbb{R})$, we define a *wavelet system* as the set of all translated and dyadically rescaled versions of ψ, i.e.,

$$\left\{ \psi_{j,m} = 2^{j/2} \psi\Big(2^j (\cdot - m)\Big), \quad j, m \in \mathbb{Z} \right\},$$

If this system forms an orthonormal basis of $L^2(\mathbb{R}^2)$, it is called an *orthonormal wavelet system* , and ψ is called a *wavelet.*

If the function ψ is compactly supported, the system enables a zooming into finer resolution and the relocation of the analysed region. In this way, signals and their behavior can be analyzed at a very local level.

An orthonormal wavelet base can be constructed with a general machinery called *multiresolution analysis* (MRA). A sequence of closed subspaces $(V_j)_{j\in\mathbb{Z}}$ of $L^2(\mathbb{R})$ is called a multiresolution analysis if the following properties are fulfilled:

(i) $\{0\} \subset \cdots \subset V_j \subset V_{j+1} \subset \cdots \subset L^2(\mathbb{R}), \quad j \in \mathbb{Z},$

(ii) $\bigcap_{j\in\mathbb{Z}} V_j = \{0\},$

(iii) $\overline{\bigcup_{j\in\mathbb{Z}} V_j} = L^2(\mathbb{R}),$

(iv) $f \in V_j \Leftrightarrow f(2\cdot) \in V_{j+1},$

(v) there exist a *scaling function* $\phi \in L^2(\mathbb{R})$ such that

$$\{\phi_{0,m} := \phi(\cdot - m) : m \in \mathbb{Z}\}$$

constitutes an orthonormal basis for V_0.

The associated *wavelet spaces* $(W_j)_{j\in\mathbb{Z}}$ are then defined by

$$V_{j+1} = V_j \oplus W_j.$$

As a result, $L^2(\mathbb{R})$ can be broken up as the direct sum of wavelet spaces. Given an MRA, it's well-known to construct an orthonormal basis of the form $\{\psi_{j,m} : \ j,m \in \mathbb{Z}\}$, for $L^2(\mathbb{R})$. Another construction of an orthonormal basis using MRA is of the following form:

$$\{\phi(\cdot - m) : \ m \in \mathbb{Z}\} \cup \{\psi_{j,m} : \ j \geq 0, m \in \mathbb{Z}\},$$

where the translates of the scaling function ϕ are used for the low frequency region, and the wavelet terms take care of of the high frequency region.

Additionally, there have been extensions of wavelet theory to higher dimensions using tensor product based constructions, which we will not state here. We merely rewrite the definition of a discrete wavelet system in $L^2(\mathbb{R}^2)$ which will be our main focus in this thesis. For a function $\psi \in L^2(\mathbb{R}^2)$, we call the following set a wavelet system in $L^2(\mathbb{R}^2)$

$$\psi_{j,m} := 2^j \psi\Big(A \cdot - m\Big), \quad m \in \mathbb{Z}^2,$$

where A is the scaling matrix

$$A = \begin{pmatrix} 2^j & 0 \\ 0 & 2^j \end{pmatrix}.$$

We would like to remark that an explicit construction of wavelet systems will be given in applications in later chapters.

1.1.3 Shearlet Frames

Shearlets were first introduce in [GKL06] by K. Guo, G. Kutyniok, D. Labate, W.-Q Lim as a powerful representation system that yields optimal rate for a the class of *cartoon like images*. Although constructions for higher dimensions of shearlets for both consinuous

and discrete versions are known in the literature [KLL12a; KLR15], we will restrict our presentation to the case of 2D-discrete shearlets which is our main interest in this thesis.

We first start by rewriting the definition of a shearlet system. Let

$$A_j := \begin{pmatrix} 2^j & 0 \\ 0 & 2^{j/2} \end{pmatrix}, \quad j \in \mathbb{Z},$$

be the *parabolic scaling matrix*, and

$$S_k =: \begin{pmatrix} 1 & k \\ 0 & 1 \end{pmatrix}, \quad k \in \mathbb{Z},$$

be the *shearing matrix*. Given $\psi \in L^2(\mathbb{R}^2$, then the *shearlet system* with respect to ψ is defined as

$$\mathcal{SH}(\psi) := \{2^{3j/4}\psi(S_k A_j x - k) : j,k \in \mathbb{Z}, m \in \mathbb{Z}^2\}.$$

One of the first type of shearlet system is so-called *classical shearlets*.

Definition 1.9 ([KL12a])
Let $\psi \in L^2(\mathbb{R}^2)$ be defined by

$$\hat{\psi}(\xi_1,\xi_2) = \hat{\psi_1}(\xi_1)\hat{\psi}(\xi_1,\frac{\xi_1}{\xi_2}),$$

where ψ_1, ψ_2 satisfy the following conditions:

(i) $\sum\limits_{j\in\mathbb{Z}} |\hat{\psi_1}(2^{-j}\xi_1)|^2 = 1,$ for a.e. $\xi_1 \in \mathbb{R}$

(ii) $\hat{\psi_1} \in C^\infty(\mathbb{R})$ and supp $\psi_1 \subset [-\frac{1}{2},-\frac{1}{16}] \cup [\frac{1}{16},\frac{1}{2}]$

(iii) $\hat{\psi_1} \in C^\infty(\mathbb{R}), \hat{\psi_2} \subseteq [-1,1]$ and $\sum\limits_{k\in\{-1,0,1\}} |\hat{\psi_2}(\xi_2+k)|^2 = 1$ for a.e. $\xi_2 \in [-1,1]$

Then, we call ψ a *classical shearlet*

One of the first goals is to determine under which assumptions a shearlet system forms a frame for $L^2(\mathbb{R}^2)$. The following result shows that classical shearlets indeed generate Parseval frames for $L^2(\mathbb{R}^2)$.

Theorem 1.10 ([KL12a])
Let ψ be a classical shearlet. Then $\mathcal{SH}(\psi)$ forms a Parseval frame for $L^2(\mathbb{R}^2)$.

Basically, the right generators will determine whether or not a shearlet system forms a Parseval frame. There are two types of generators, namely *band-limited* and *compactly supported*. The classical shearlets are belong to the class of band-limited shearlets since the Fourier transform of the generator has compact support in frequency domain. However, due to the fact that the frequency tiling of classical shearlets is biased toward x_2-axis, it can lead to problems when analyzing singularities along x_1-axis. Another band-limited shearlet type named *cone-adapted shearlet system* was introduced to tackle this problem.

Definition 1.11 [KL12a]
Let $\phi, \psi, \tilde{\psi} \in L^2(\mathbb{R}^2)$ and $c = (c_1, c_2) \in (\mathbb{R}^+)^2$. The cone-adapted shearlet system associated with ϕ, ψ, is defined by

$$\mathcal{SH}(\phi, \psi, \tilde{\psi}, c) := \Phi(\phi, c_1) \cup \Psi(\psi, c) \cup \tilde{\Psi}(\tilde{\psi}, c),$$

where

$$\Phi(\phi, c_1) := \{\phi(x - c_1 m) : m \in \mathbb{Z}^2\},$$
$$\Phi(\psi, c) := \{2^{3j/4}\psi(S_k A_j x - M_c m) : j \geq 0, |k| \leq \lceil 2^{j/2} \rceil\},$$
$$\tilde{\Psi}(\tilde{\psi}, c) := \{2^{3j/4}\tilde{\psi}(\tilde{S}_k \tilde{A}_j x - \tilde{M}_c m) : j \geq 0, |k| \leq \lceil 2^{j/2} \rceil\},$$

with

$$M_c = \begin{pmatrix} c_1 & 0 \\ 0 & c_2 \end{pmatrix}, \tilde{M}_c = \begin{pmatrix} c_1 & 0 \\ 0 & c_2 \end{pmatrix}, \tilde{S}_k = \begin{pmatrix} 1 & 0 \\ k & 1 \end{pmatrix}, \tilde{A}_j = \begin{pmatrix} 2^{j/2} & 0 \\ 0 & 2^j \end{pmatrix}.$$

The following result shows how to obtain Parseval frames for a subspace of $L^2(\mathbb{R}^2)$. This result can be then extended to the entire space $L^2(\mathbb{R}^2)$ using corresponding projections in the Fourier domain.

Theorem 1.12 ([KL12a])
Let $\psi \in L^2(\mathbb{R}^2)$ be a classical shearlet. Then,the following system

$$\Psi(\psi, (1,1)) := 2^{3j/4}\psi(S_k A_j x - m) : j \geq 0, |k| \leq \lceil 2^{j/2} \rceil, m \in \mathbb{Z}^2\}$$

is a Parseval frame for

$$\left\{ f \in L^2(\mathbb{R}^2) : \operatorname{supp} \hat{f} \subset \{\xi \in \mathbb{R}^2 : |\xi_1| \geq 1, |\frac{|\xi_2|}{|\xi_1|}|\} \right\}$$

However, the construction of cone-adapted shearlets is based on projection onto subspaces of $L^2(\mathbb{R}^2)$ which need to carefully define 'boundary shearlets' to touch the seam lines in a smooth way. Those problems were exactly solved with *smooth Parseval of shearlets* in [GL13], and then was generalized in [GK14] with *universal shearlets* which we will give more detail about its construction in Chapter 4.

For the other type of shearlets, the first explicit construction of compactly supported shearlets was presented in [KKL12]. The following results show the nice error decay rate using approximations for cartoon like functions based on compactly supported shearlet frames.

Theorem 1.13 ([KL12a])
Let $\psi, \tilde{\psi} \in L^2(\mathbb{R}^2)$ be compactly supported. For $\alpha > 5, \gamma \geq 4$, and a function $h \in L^1(\mathbb{R})$, such that the followings hold

$$|\hat{\psi}(\xi_1, \xi_2) \leq C \cdot \min\{1, |\xi_1|^{\alpha}\} \min\{1, |\xi_1|^{-\gamma}\} \min\{1, |\xi_2|^{-\gamma}\},$$

and

$$\Big|\frac{\partial}{\partial\xi_2}\hat{\psi}(\xi)\Big| \leq |h(\xi_1)\Big(1+\Big|\frac{\xi_2}{\xi_1}\Big|\Big)^{-\gamma}.$$

In addition, the shearlet $\tilde{\psi}$ satisfies similar conditions as ψ with the roles of ξ_1 and ξ_2 reversed.

If $\mathcal{SH}(f,\phi,\psi,\tilde{\psi},(1,1))$ forms a frame for $L^2(\mathbb{R}^2)$, then there exists a constant $C>0$ such that the optimal rate of decay of the best N-term approximation satisfies as $N\to\infty$

$$\sigma_N(f,\mathcal{SH}(f,\phi,\psi,\tilde{\psi},(1,1))) \leq C\cdot N^{-2}(logN)^{3/2}.$$

1.2 Compressed Sensing

Compressed sensing provides a framework for simultaneous sensing and compression of finite dimensional vectors, based on the assumption that the signal possesses a sparse or nearly sparse representation in a suitable basis or frames. The technique of compressed sensing is proved to be an effective tool for acquiring signals from an underdetermined system of linear equations. The key idea of this methodology is to compress a signal of interest $x\in\mathbb{R}^n$ by very few non-adaptive linear measurements whose number is typically much smaller than the number of unknowns n. In this context, our main goal is to solve the following underdetermined system

$$Ax=b, \tag{1.4}$$

where $A\in\mathbb{R}^{m,n}, m<<n$, is so-called measurement matrix, b is a vector of size $m\times 1$. Since $m<n$, this linear system is typically under-determined with infinite number of solutions. However, according to compressed sensing theory, the exact reconstruction is possible due to the sparsity of the signal x.

In the following, we summarize several approaches of compressed sensing technique to solve the system (1.4).

1.2.1 l_0- Minimization

In many applications, the vector x is not usually supported everywhere, i.e., it has only few non-zero entries. We first recall that a vector $x=(x_1,x_2,\ldots,x_n)\in\mathbb{R}^n$ is called $k-$sparse if it has at most k non-zero entries, i.e., $\|x\|_0<k$, where

$$\|x\|_0 := \#\Big\{i\in\{1,2,\ldots,n\} : x_i\neq 0\Big\}.$$

In compressed sensing, the signal x is encoded by m linear measurement $b\in\mathbb{R}^m$, using a known measurement matrix A. The compressibility of the signal x concerns the question: How small can the number of measurements m be in order to recover the original signal x exactly from b?. A very natural approach to this question is to solve the following optimization problem:

$$\min_{x\in\mathcal{H}}\|x\|_0, \text{ subject to } Ax=b. \tag{1.5}$$

It has been shown that the number of measurements needed to recover all k-sparse vectors always satisfies $m>2k$. However, this is generally an NP-hard problem. Thus, this

raises a need for an relaxation of (1.5) which is considered in the literature.

1.2.2 Basic Pursuit

In the previous subsection, we seek for the sparsest solution of (1.4) by using (1.5). However, this problem is numerically intractable if m and n are getting larger. An alternative solution to (1.5) named as l_1- *minimization* or *basic pursuit* is to minimize the l_1 norm. Given measurement matrix $A \in \mathbb{R}^{m\times n}, m < n$, and a vector $b \in \mathbb{R}^m$, basic pursuit model considers

$$\min_{x\in\mathcal{H}} \|x\|_1, \text{ subject to } Ax = b. \tag{1.6}$$

This optimization problem is convex and can be solved by linear programming. There are many algorithms with numerous software packages implementing them, e.g., in Matlab to solve (1.6).

In next subsections, we address the conditions on measurement matrix A required to ensure that the original sparse vector x can be reconstructed through basis pursuit model (1.6).

1.2.3 Null Space Property

Let $S \subset \{1,2,\dots,n\}$ and $S^c \subset \{1,2,\dots,n\} \setminus S$ be its compliment in $\{1,2,\dots,n\}$. For a vector $v \in \mathbb{R}^n$ and a set of indexes $S \subset \{1,2,\dots,n\}$, we denote by v_S the vector in $\mathbb{R}^S$, which coincides with v on the indices in S and is extended to zero outside the set S. The so-called *null space property* is a necessary and sufficient condition for an exact recovery of sparse vectors via the basis pursuit.

Definition 1.14 ([FR13])
A matrix $A \in \mathbb{R}^{m,n}$ is said to satisfy the null space property relative to a set $S \subset \{1,2,\dots,n\}$ if the following holds

$$\|v_S\|_1 < \|v_{S^c}\|_1 \text{ for all } v \in \ker A \setminus \{0\}.$$

It is said to satisfy the null property of order k if it satisfies the null space property relative to any set $S \subset \{1,2,\dots,n\}$ with $card(S) \leq k$.

The following theorem shows that the NSP is a necessary and sufficient condition for the exact recovery of sparse vectors.

Theorem 1.15 ([FR13])
Given a matrix $A \in \mathbb{R}^{m,n}$, every vector $x \in \mathbb{R}^n$ supported on a set S is the unique solution of 1.6 with $Ax = b$ if and only if A satisfies the null space property relative to S.

This theorem implies that if A has the NSP of order k, the solution of (1.5) can be determined by (1.6) for all $k-$sparse vectors. Roughly speaking, NSP provides a necessary and sufficient condition for guaranteeing the exact recovery of (1.6), requiring that every null space vector of the measurement matrix A is not concentrating its energy on any set of entries.

By using 1.15, we have a sufficient result for unique sparse recovery via basis pursuit using notion of the *mutual coherence.*

Theorem 1.16 ([EB02; DE03])
Let $A := (A_1, A_2, \ldots, A_n)$ *be an matrix in* $\mathbb{R}^{m,n}$ *and* $x \in \mathbb{R}^n$. *If*

$$\|x\|_0 < \frac{1}{2}(1 + \frac{1}{\mu(A)}), \tag{1.7}$$

where the mutual coherence

$$\mu(A) := \max_{i \neq j} \frac{\|\langle A_i, A_j \rangle\|}{\|A_i\|_2 \|A_j\|_2}.$$

Then, x is the unique solution of (1.6).

1.2.4 Restricted Isometry Property

Compared to the Null Space Property, the condition (1.7) is just a sufficient condition for the exact recover of (1.6). We might want to construct A with small order k. For this, the *Restricted Isometry Property* (RIP) is an additional measure of the quality of the measurement matrix A.

Definition 1.17 ([FR13])
Let $A \in \mathbb{R}^{m,n}$ and $k \in \{1, 2, \ldots, n\}$. Then, the $k-$th restricted isometry constant $\delta_k = \delta_k(A)$ of a matrix $A \in \mathbb{R}^{m,n}$ is the smallest $\delta \geq 0$ such that

$$(1 - \delta)\|x\|_2^2 \leq \|Ax\|_2^2 \leq (1 + \delta)\|x\|_2^2$$

for all $k-$sparse vector $x \in \mathbb{R}^n$. We say that A satisfies the restricted isometry property of order k with the constant δ_k if $\delta_k < 1$.

The following result shows that a sufficiently small Restricted Isometric Property constant implies the Null Space Property.

Theorem 1.18 ([FR13])
Let $A \in \mathbb{R}^{m,n}$ *and* $k \in \{1, 2, \ldots, n\}$ *with* $k \leq \frac{n}{2}$. *If* $\delta_{2k}(A) < \frac{1}{3}$, *then A has the NSP of order k. Therefore, every* $k-$*sparse vector x is the unique solution of* (1.6) *with* $Ax = b$.

2

Problem of Geometric Separation

This chapter is devoted to the problem of geometric separation using compressed sensing technique and suitable chosen frames presented in the previous chapter.

Our contributions in this chapter consist of three main points. First, we present a theoretical guarantee for the problem of separating two geometric components using two frames (Theorem 2.7). Second, in Subsection 2.3.3 we construct a pair of bandlimited α-shearlet dual frames which provide an optimal sparse representation for curvilinear singularities. Finally, we derive an asymptotic geometric separation result for separating pointlike and curvelike singularities (Theorem 2.11). Also, we show that the proposed algorithm successfully reconstructs sub-images by l^1-minimization if the bandlimited α-shearlets do not coincide with wavelets in sense of isotropic fashion.

To achieve the objectives mentioned above, we organize this chapter in the following manner: First we formulate the general image separation problem in Section 2.1. Next, in Section 2.2 we provide a theoretical machinery which guarantees the success of Algorithm 1 based on notions of joint concentration and cluster coherence of two general frames. We then present the model of pointlike and curvelike singularities and construct radial wavelets as well as a pair of dual bandlimited α-shearlets in Section 2.3. In Section 2.4 we finally present an asymptotic separation result of the proposed component models by l^1-minimization. We close with a conclusion and outlook to further applications in Section 2.5.

2.1 Problem Formulation

The problem of geometric separation is presented in the introduction section, we now want to dive deeper into this problem with more precise definitions and notions.

2.1.1 General Component Separation

Given an image f, we assume that f can be composed of two geometric components, i.e.,

$$f = \mathcal{P} + \mathcal{C}, \tag{2.1}$$

where $\mathcal{P}, \mathcal{C}$ are two unknown components which we want to recover. Since the unknowns are twice as many as the equations, the task of component separation is ill-posed without additional assumptions. However, we often have more information about the components $\mathcal{P}, \mathcal{C}$. Compressed sensing techniques enable us to exactly recover these components which are sparse in appropriate dictionaries. Here, we assume that $\mathcal{P}$ is smooth away from point discontinuities and $\mathcal{C}$ is smooth away from curvilinear singularities. In our approach, we use microlocal analysis to give a heuristic understanding of

why separation might be possible. The core ingredient is based on the idea that important coefficients are clustered geometrically in phase space.

2.1.2 Recovery via l_1-Minimization

We consider the following algorithm proposed in the past which used Parseval frames for separating two components. We extend it to the case of two general frames $\{\Phi_1\}_{i\in I}, \{\Phi_2\}_{j\in J}$ with frame bounds (A_1, B_1) and (A_2, B_2) respectively.

Algorithm 2.1 (Image separation)

Input: observed image f, two frames $\{\Phi_1\}_{i\in I}, \{\Phi_2\}_{j\in J}$. **Compute:** $(\mathcal{P}^\star, \mathcal{C}^\star)$, where

$$(\mathcal{P}^\star, \mathcal{C}^\star) = \underset{f_1, f_2}{\operatorname{argmin}} \|\Phi_1^* f_1\|_1 + \|\Phi_2^* f_2\|_1, \quad \text{subject to} \quad f_1 + f_2 = f. \tag{2.2}$$

Output: recovered components. $\mathcal{P}^\star, \mathcal{C}^\star$.

We would like to remark that here we minimize the l^1 norm of the analysis coefficients when expanding the components in two frames to exploit their geometric features underlying the image. The success of the algorithm (2.2) is proven later under prior information that each geometric component is captured by the corresponding frame.

2.2 Theoretical Guarantee for Component Separation

2.2.1 Joint Concentration Analysis

The notion of *joint concentration* was first introduced in [DK13], which used Parseval frames to propose an analyzing tool for deriving the theoretical guarantee. There, the joint concentration associated with two Parseval frames Φ_1, Φ_2 and sets of indexes Λ_1, Λ_2 is defined by

$$\kappa(\Lambda_1, \Lambda_2) = \sup_{f\in\mathcal{H}} \frac{\|\mathbb{1}_{\Lambda_1}\Phi_1^* f\|_1 + \|\mathbb{1}_{\Lambda_2}\Phi_2^* f\|_1}{\|\Phi_1^* f\|_1 + \|\Phi_2^* f\|_1}.$$

For an extension, we modify the joint concentration associated with two frames instead of Parseval frames based on the idea that each frame can sparsely represent each component but can not sparsely represent the other. This philosophy plays a central role in the success of the proposed algorithm.

Definition 2.2 Let Φ_1, Φ_2 be two frames. We define the *joint concentration* $\bar{\kappa} = \bar{\kappa}(\Lambda_1, \Lambda_2)$ with respect to sets of coefficients Λ_1, Λ_2 by

$$\bar{\kappa}(\Lambda_1, \Lambda_2) = \sup_{\mathcal{P},\mathcal{C}\in\mathcal{H}} \frac{\|\mathbb{1}_{\Lambda_1}\Phi_1^* \mathcal{P}\|_1 + \|\mathbb{1}_{\Lambda_2}\Phi_2^* \mathcal{C}\|_1}{\|\Phi_1^* \mathcal{C}\|_1 + \|\Phi_2^* \mathcal{P}\|_1}.$$

Definition 2.3 Fix $\delta > 0$. Given a Hilbert space $\mathcal{H}$ with a frame $\Phi, f \in \mathcal{H}$ is *$\delta-$relatively sparse* in Φ with respect to Λ if

$$\|\mathbb{1}_{\Lambda^c}\Phi^* f\|_1 \leq \delta,$$

where Λ^c denotes $X \setminus \Lambda$.

Under the assumption of joint concentration and δ-relative sparsity of the components $\mathcal{P}$ and $\mathcal{C}$, we can guarantee the success of (2.2), as the next proposition shows.

Proposition 2.4 *Let Φ_1, Φ_2 be two frames with frame bounds $(A_1, B_1), (A_2, B_2)$, respectively. For $\delta_1, \delta_2 > 0$, we assume that $f = \mathcal{P} + \mathcal{C}$ where $\mathcal{P}, \mathcal{C}$ is δ_1, δ_2-relatively sparse in Φ_1 and Φ_2 with respect to Λ_1 and Λ_2, respectively. Let $(\mathcal{P}^\star, \mathcal{C}^\star)$ solve (2.2) and we have $\bar{\kappa}(\Lambda_1, \Lambda_2) < \frac{1}{2}$, then*

$$\|\mathcal{P}^\star - \mathcal{P}\|_2 + \|\mathcal{C}^\star - \mathcal{C}\|_2 \leq \frac{2\max\{\frac{1}{A_1}, \frac{1}{A_2}\}(\delta_1 + \delta_2)}{1 - 2\bar{\kappa}(\Lambda_1, \Lambda_2)}.$$

Proof. For convenience, we set $\bar{\kappa} := \bar{\kappa}(\Lambda_1, \Lambda_2), \delta = \delta_1 + \delta_2$, and $err := \mathcal{P}^\star - \mathcal{P} = \mathcal{C} - \mathcal{C}^\star$. Note here that we have $\mathcal{P}^\star + \mathcal{C}^\star = \mathcal{P} + \mathcal{C} = f$. By the upper frame bounds of Φ_1, Φ_2, we obtain

$$\begin{aligned}\|\mathcal{P}^\star - \mathcal{P}\|_2 + \|\mathcal{C}^\star - \mathcal{C}\|_2 &\leq \max\{\frac{1}{A_1}, \frac{1}{A_2}\}\Big(\|\Phi_1^*(\mathcal{P}^\star - \mathcal{P})\|_2 + \|\Phi_2^*(\mathcal{C}^\star - \mathcal{C})\|_2\Big) \\ &\leq \max\{\frac{1}{A_1}, \frac{1}{A_2}\}\Big(\|\Phi_1^*(err)\|_1 + \|\Phi_2^*(err)\|_1\Big). \qquad (2.3)\end{aligned}$$

Thus, we have

$$\begin{aligned} & S := \|\Phi_1^*(err)\|_1 + \|\Phi_2^*(err)\|_1 \\ \leq\ & \|\mathbb{1}_{\Lambda_1}\Phi_1^*(err)\|_1 + \|\mathbb{1}_{\Lambda_2}\Phi_2^*(err)\|_1 + \|\mathbb{1}_{\Lambda_1^c}\Phi_1^*(\mathcal{P}^\star - \mathcal{P})\|_1 + \|\mathbb{1}_{\Lambda_2^c}\Phi_2^*(\mathcal{C}^\star - \mathcal{C})\|_1 \\ \leq\ & \bar{\kappa}S + \|\mathbb{1}_{\Lambda_1^c}\Phi_1^*\mathcal{P}^\star\|_1 + \|\mathbb{1}_{\Lambda_2^c}\Phi_2^*\mathcal{C}^\star\|_1 + \|\mathbb{1}_{\Lambda_1^c}\Phi_1^*\mathcal{P}\|_1 + \|\mathbb{1}_{\Lambda_2^c}\Phi_2^*\mathcal{C}\|_1 \\ \leq\ & \bar{\kappa}S + \|\mathbb{1}_{\Lambda_1^c}\Phi_1^*\mathcal{P}^\star\|_1 + \|\mathbb{1}_{\Lambda_2^c}\Phi_2^*\mathcal{C}^\star\|_1 + \delta_1 + \delta_2 \\ =\ & \bar{\kappa}S + \delta + \|\Phi_1^*\mathcal{P}^\star\|_1 + \|\Phi_2^*\mathcal{C}^\star\|_1 - \|\mathbb{1}_{\Lambda_1}\Phi_1^*\mathcal{P}^\star\|_1 - \|\mathbb{1}_{\Lambda_2}\Phi_2^*\mathcal{C}^\star\|_1. \end{aligned}$$

We now exploit that $(\mathcal{P}^\star, \mathcal{C}^\star)$ is a minimizer of (2.2). Therefore, we obtain

$$\|\Phi_1^*\mathcal{P}^\star\|_1 + \|\Phi_2^*\mathcal{C}^\star\|_1 \quad \leq \quad \|\Phi_1^*\mathcal{P}\|_1 + \|\Phi_2^*\mathcal{C}\|_1.$$

Thus, the triangle inequality yields

$$\begin{aligned} S \ &\leq\ \bar{\kappa}S + \delta + \|\Phi_1^*\mathcal{P}\|_1 + \|\Phi_2^*\mathcal{C}\|_1 - \|\mathbb{1}_{\Lambda_1}\Phi_1^*\mathcal{P}^\star\|_1 - \|\mathbb{1}_{\Lambda_2}\Phi_2^*\mathcal{C}^\star\|_1 \\ &\leq\ \bar{\kappa}S + \delta + \|\Phi_1^*\mathcal{P}\|_1 + \|\Phi_2^*\mathcal{C}\|_1 + \|\mathbb{1}_{\Lambda_1}\Phi_1^* err\|_1 + \|\mathbb{1}_{\Lambda_2}\Phi_2^* err\|_1 - \|\mathbb{1}_{\Lambda_1}\Phi_1^*\mathcal{P}\|_1 \\ &\quad\ -\|\mathbb{1}_{\Lambda_2}\Phi_2^*\mathcal{C}\|_1 \\ &\leq\ \bar{\kappa}S + 2\delta + \bar{\kappa}S = 2\bar{\kappa}S + 2\delta. \end{aligned}$$

This implies

$$S \leq \frac{2\delta}{1-2\bar{\kappa}}$$

and the claim follows in combination with (2.3).

■

2.2.2 Theoretical Guarantee via Cluster Coherence

Typically, the information on each component is encoded by a particular choice of the clusters Λ_1, Λ_2 through the number of non-zero coefficients. By choosing such clusters we might get the successful recovery by Proposition 2.4, but it seems hard to achieve the joint concentration. The notion of *cluster coherence* was first introduced in [DK13] in an attempt to transfer the theoretical guarantee based on the notion of joint concentration to another analyzing tool that enables us to check in practice. They used Parseval frames in their definition. In our paper, we modify this ansatz and extend it to the case of generic frames instead of Parseval frames.

Definition 2.5 Given two frames $\Phi_1 = (\Phi_{1i})_{i\in I}$ and $\Phi_2 = (\Phi_{2j})_{j\in J}$ with frame bounds $(A_1, B_1), (A_2, B_2)$, the *cluster coherence* $\mu_c(\Lambda, \Phi_1; \Phi_2)$ of Φ_1 and Φ_2 with respect to the index set $\Lambda \subset I$ is defined by

$$\mu_c(\Lambda, \Phi_1; \Phi_2) = \max_{j\in J} \sum_{i\in\Lambda} |\langle \phi_{1i}, \phi_{2j}\rangle|.$$

Formulated in this way, the notion of cluster coherence encodes the geometric difference between the components in a way that can be checked in practice. The following lemma allows to bound the joint concentration from above by the cluster coherence.

Lemma 2.6 *We have*

$$\bar{\kappa}_1(\Lambda_1, \Lambda_2) \leq \inf_{\Phi_1^d \in \mathbb{D}_{\Phi_1}, \Phi_2^d \in \mathbb{D}_{\Phi_2}} \max\{\mu_c(\Lambda_1, \Phi_1; \Phi_2^d), \mu_c(\Lambda_2, \Phi_2; \Phi_1^d)\}.$$

Proof. For $\mathcal{P}, \mathcal{C} \in \mathcal{H}, \Phi_1^d \in \mathbb{D}_{\Phi_1}, \Phi_2^d \in \mathbb{D}_{\Phi_2}$, we have

$$\mathcal{P} = \sum_{j\in J} \langle \mathcal{P}, \phi_{2j}\rangle \phi_{2j}^d, \ \mathcal{C} = \sum_{i\in I} \langle \mathcal{C}, \phi_{1i}\rangle \phi_{1i}^d.$$

In the other words, $\mathcal{P} = \Phi_2^d \Phi_2^* \mathcal{P}$, $\mathcal{C} = \Phi_1^d \Phi_1^* \mathcal{C}$. Now we set $\alpha_1 = \Phi_1^* \mathcal{C}$, $\alpha_2 = \Phi_2^* \mathcal{P}$, we then obtain $\mathcal{P} = \Phi_2^d \alpha_2$, $\mathcal{C} = \Phi_1^d \alpha_1$. Therefore, we have

$$\begin{aligned}
& \|\mathbb{1}_{\Lambda_1} \Phi_1^* \mathcal{P}\|_1 + \|\mathbb{1}_{\Lambda_2} \Phi_2^* \mathcal{C}\|_1 = \|\mathbb{1}_{\Lambda_1} \Phi_1^* \Phi_2^d \alpha_2\|_1 + \|\mathbb{1}_{\Lambda_2} \Phi_2^* \Phi_1^d \alpha_1\|_1 \\
\leq & \sum_{i\in\Lambda_1} \Big(\sum_j |\langle \Phi_{1i}, \Phi_{2j}^d\rangle| |\alpha_{2j}| \Big) + \sum_{j\in\Lambda_2} \Big(\sum_i |\langle \Phi_{2j}, \Phi_{1i}^d\rangle| |\alpha_{1i}| \Big) \\
= & \sum_j \Big(\sum_{i\in\Lambda_1} |\langle \Phi_{1i}, \Phi_{2j}^d\rangle| \Big) |\alpha_{2j}| + \sum_i \Big(\sum_{j\in\Lambda_2} |\langle \Phi_{2j}, \Phi_{1i}^d\rangle| \Big) |\alpha_{1i}|
\end{aligned}$$

$$\begin{aligned} &\leq \mu_c(\Lambda_1,\Phi_1;\Phi_2^d)\|\alpha_2\|_1 + \mu_c(\Lambda_2,\Phi_2;\Phi_1^d)\|\alpha_1\|_1 \\ &\leq \max\{\mu_c(\Lambda_1,\Phi_1;\Phi_2^d),\mu_c(\Lambda_2,\Phi_2;\Phi_1^d)\}(\|\alpha_2\|_1 + \|\alpha_1\|_1) \\ &= \max\{\mu_c(\Lambda_1,\Phi_1;\Phi_2^d),\mu_c(\Lambda_2,\Phi_2;\Phi_1^d)\}(\|\Phi_2^*\mathcal{P}\|_1 + \|\Phi_1^*\mathcal{C}\|_1). \end{aligned}$$

Thus, we obtain $\bar{\kappa}_1(\Lambda_1,\Lambda_2) \leq \max\{\mu_c(\Lambda_1,\Phi_1;\Phi_2^d),\mu_c(\Lambda_2,\Phi_2;\Phi_1^d)\}$, $\forall\Phi_1^d \in \mathbb{D}_{\Phi_1}, \forall\Phi_2^d \in \mathbb{D}_{\Phi_2}$. This completes the proof. ∎

We can now present our theoretical guarantee for the procedure (2.2) to be convergent using two generic frames instead of Parseval frames.

Theorem 2.7 *Let Φ_1,Φ_2 be two frames with frame bounds $(A_1,B_1),(A_2,B_2)$, respectively. For $\delta_1,\delta_2 > 0$, we suppose that $f \in \mathcal{H}$ can be decomposed as $f = \mathcal{P} + \mathcal{C}$ so that each component $\mathcal{P},\mathcal{C}$ is δ_1,δ_2-relatively sparse in Φ_1 and Φ_2 with respect to Λ_1 and Λ_2, respectively. Let $(\mathcal{P}^\star,\mathcal{C}^\star)$ solve (2.2). If we have $\mu_c(\Lambda_1,\Lambda_2) < \frac{1}{2}$, where*

$$\mu_c(\Lambda_1,\Lambda_2) := \inf_{\Phi_1^d\in\mathbb{D}_{\Phi_1},\Phi_2^d\in\mathbb{D}_{\Phi_2}} \max\{\mu_c(\Lambda_1,\Phi_1;\Phi_2^d),\mu_c(\Lambda_2,\Phi_2;\Phi_1^d)\},$$

then we have

$$\|\mathcal{P}^\star - \mathcal{P}\|_2 + \|\mathcal{C}^\star - \mathcal{C}\|_2 \leq \frac{2\max\{\frac{1}{A_1},\frac{1}{A_2}\}(\delta_1+\delta_2)}{1-2\mu_c(\Lambda_1,\Lambda_2)}. \tag{2.4}$$

Proof. The proof follows directly from Proposition 2.4 and Lemma 2.6. ∎

We would like to remark that in case Φ_1,Φ_2 are Parseval frames we have

$$\mu_c(\Lambda_1,\Lambda_2) \leq \max\{\mu_c(\Lambda_1,\Phi_1;\Phi_2),\mu_c(\Lambda_2,\Phi_2;\Phi_1)\},$$

since $\Phi_1 \in \mathbb{D}_{\Phi_1},\Phi_2 \in \mathbb{D}_{\Phi_2}$. This consequence is exactly the result used in several papers [DK09; KKZ11; KL12b; DK13; Kut13] which chose Parseval frames as sparsifying systems. Thus, our theoretical guarantee based on the notion of cluster coherence (2.4) is more general than are shown in aforementioned papers since we can choose an other dual instead of using itself. Although it is not easy to construct a dual, this theoretical guarantee actually shows that we can use synthesis pseudo-dual's properties instead of its explicit construction. The nice property we need in our analysis is that dual frame elements have good time-frequency localization which leads to small cluster coherence.

For the construction of a shearlet dual, some works [Gro13; KL16] have shown desirable properties such as well localization and highly directional sensitivity. In the next section, we use the approach from [Gro13] to construct a dual pair of bandlimited α-shearlets for our analysis.

2.3 Component Separation

2.3.1 Mathematical Model of Components

Consider the image separation problem (2.1), we now introduce the model of components. In our analysis, we assume that the pointlike part $\mathcal{P}$ is modeled as

$$\mathcal{P}(x) = \sum_{1}^{K} c_i |x - x_i|^{-\lambda_i},$$

where two sequences of constants $\{\lambda_i\}_{i=1}^K, \{c_i\}_{i=1}^K$ satisfy $0 < \lambda_i < 2, 0 < c_i, \ \forall i = 1, 2, \ldots, K$. We choose $\lambda_i < 2$ to bound the energy of the component in frequency domain as the scale goes finer. The choice of $\{\lambda_i\}_{i=1}^K$ depends on each problem of image separation which make components comparable.

For the curvilinear singularities, we first recall the *Schwartz functions* or the *rapidly decreasing functions*

$$\mathcal{S}(\mathbb{R}^2) = \Big\{ f \in C^\infty(\mathbb{R}^2) \mid \forall K, N \in \mathbb{N}_0, \sup_{x \in \mathbb{R}^2} (1 + |x|^2)^{N/2} \sum_{|\alpha| \leq K} |D^\alpha f(x)| < \infty \Big\}.$$

Let $\sigma : [0, 1] \to \mathbb{R}^2$ be a closed C^2 curve with non vanishing curvature everywhere. We first consider the model of curvilinear singularity $\mathcal{C}$ as

$$\mathcal{C} = \int_{\mathbb{R}^2} \delta_{\sigma(t)} dt,$$

where δ_x denotes the usual Dirac delta distribution located at x. It is well known that the class of α-shearlets using α-scaling can sparsely represent such curvilinear structures [Kei12; KLL12a]. For the sake of simplicity, we restrict our model to the case of *line singularity*. The reader should be aware of the fact that by Tubular neighborhood theorem we can extend it to the general case. Intuitively, we can use the technique in [DK13] to first partition the curve σ into small pieces and then bend them to the form of a line singularity, see [DK13, Section 6] for details.

Similarly as introduced in several papers [GK14; KKZ14], we model the line distribution $w\mathcal{L}$ acting on Schwartz functions by

$$\langle w\mathcal{L}, f \rangle = \int_{\rho}^{\rho} w(x_1) f(x_1, 0) dx_1, \ f \in \mathcal{S}(\mathbb{R}^2),$$

where w is a weighted function such that $0 \not\equiv w \in C^\infty(\mathbb{R}), \operatorname{supp} w \subset [-\rho, \rho]$, for some $\rho > 0$, and $0 \leq w(x) \leq 1, \forall x \in [-\rho, \rho]$. For such a setting, we now approach the question if it possible to separate point-singularities and the line singularities using wavelets and bandlimited α-shearlet types which interpolate from wavelet type ($\alpha = 2$) to shearlet type ($\alpha = 1$). In our analysis, we prove that we can separate them as long as bandlimited α-shearlets do not coincide with the wavelet type, i.e., $2 > \alpha \geq 1$.

Among well-known systems, wavelets provide an optimal sparse representation to the pointwise singularities, whereas shearlets are efficient for curvilinear structures. In what follows, we introduce the construction of these two sparsifying systems.

2.3.2 Wavelet Frames

To sparsely present $\mathcal{P}$, we choose radial wavelets which form a Parseval frame with perfectly isotropic generating elements. We modify the construction of radial wavelets as follows.

Let Ξ be a Schwartz function on $\mathbb{R}^2$ such that $\operatorname{supp}\hat{\Xi} \subset [-\frac{1}{16}, \frac{1}{16}]$, $0 \leq \hat{\Xi}(\theta) \leq 1$ for $\theta \in \mathbb{R}$ and $\hat{\Xi}(\theta) = 1$ for $\theta \in [-\frac{1}{32}, \frac{1}{32}]$. We now define the *low-pass function* $\Omega(\xi)$ and the *window function* $W(\xi)$ for $j \in \mathbb{N}$ and $\xi = (\xi_1, \xi_2) \in \mathbb{R}^2$,

$$\hat{\Omega}(\xi) := \hat{\Xi}(\xi_1)\hat{\Xi}(\xi_2), \tag{2.5}$$

$$W(\xi) := \sqrt{\hat{\Omega}^2(2^{-2}\xi) - \hat{\Omega}^2(\xi)}, \quad W_j(\xi) := W(2^{-2j}\xi). \tag{2.6}$$

By definition, $\sup W \subset [-\frac{1}{4}, \frac{1}{4}]^2 \setminus [-\frac{1}{32}, \frac{1}{32}]^2$ and W_j is compactly supported in the corona

$$\mathcal{A}_j := [-2^{2j-2}, 2^{2j-2}]^2 \setminus [-2^{2j-5}, 2^{2j-5}]^2, \quad \forall j \geq 1.$$

In addition, we obtain the partition of unity property

$$\hat{\Omega}^2(\xi) + \sum_{j\geq 0} W_j^2(\xi) = 1, \quad \forall \xi \in \mathbb{R}^2. \tag{2.7}$$

The radial wavelets $\mathbf{\Psi} = \{\psi_{j,m}\}_{(j,m)} \cup \{\Omega(\cdot - m)\}, j \in \mathbb{N}_0, m \in \mathbb{Z}^2$ which form a Pareval frame are then defined by their Fourier transforms

$$\hat{\psi}_{j,m}(\xi) = 2^{-2j} W_j(\xi) e^{2\pi i \xi^T m / 2^{2j}}, j \in \mathbb{N}_0, m \in \mathbb{Z}^2.$$

Since the low frequency part is not of interest to us in our analysis, we therefore simply write $\mathbf{\Psi} = \{\psi_{j,m}\}_{(j,m)}$ at some points.

2.3.3 A Pair of Bandlimited α-Shearlet Dual Frames

This section is devoted to the construction of a pair of *bandlimited α-shearlet* dual frames which possess many desirable properties. We choose shearlets as it is widely accepted that shearlets in general provide optimal sparse representation for images which are governed by curvilinear structures [GL07; DK09; KL10]. Motivated by [Gro13], we modify the construction of the shearlet frame pair and extend it to the case of α-scaling instead of parabolic scaling since α-shearlet type with $\alpha = \frac{2}{\beta}$, $\alpha \in [1, 2)$, might be best adapted to C^β curvilinear singularities. In addition, we modify the Fourier domain decomposition to make it comparable to the wavelet frames.

We first define the *scaling* and *shearing matrix* by

$$A_{\alpha,\mathrm{h}} := \begin{bmatrix} 2^2 & 0 \\ 0 & 2^\alpha \end{bmatrix}, \quad S_{\mathrm{h}} := \begin{bmatrix} 1 & 1 \\ 0 & 1 \end{bmatrix},$$

$$A_{\alpha,\mathrm{v}} := \begin{bmatrix} 2^\alpha & 0 \\ 0 & 2^2 \end{bmatrix}, \quad S_{\mathrm{v}} := \begin{bmatrix} 1 & 0 \\ 1 & 1 \end{bmatrix},$$

where $\alpha \in [1, 2)$ is the *scaling parameter*. Let $v \in C^\infty(\mathbb{R})$ be a *bump function* such that

supp $v \subset [-\frac{3}{2}, \frac{3}{2}]$ and

$$\sum_{l=-2}^{2} |v(\omega - l)|^2 = 1, \text{ for } \omega \in [-\frac{3}{2}, \frac{3}{2}].$$

Consequently, the following holds for $j \geq 0, \omega \in [-\frac{3}{2}, \frac{3}{2}]$,

$$\sum_{l=-\lceil 2\cdot 2^{(2-\alpha)j}\rceil}^{\lceil 2\cdot 2^{(2-\alpha)j}\rceil} |v(2^{(2-\alpha)j}\omega - l)|^2 = 1. \tag{2.8}$$

Next, we define the *cone functions* V_1, V_2 by

$$V_{\mathrm{h}}(\xi) := v\Big(\frac{\xi_2}{\xi_1}\Big), \quad V_{\mathrm{v}}(\xi) := v\Big(\frac{\xi_1}{\xi_2}\Big).$$

horizontal frequency cone and the *vertical frequency cone*

$$\mathcal{C}_{\mathrm{h}} := \Big\{(\xi_1, \xi_2) \in \mathbb{R}^2 : |\xi_1| \geq \frac{1}{8}, \Big|\frac{\xi_2}{\xi_1}\Big| \leq \frac{3}{2}\Big\},$$

$$\mathcal{C}_{\mathrm{v}} := \Big\{(\xi_1, \xi_2) \in \mathbb{R}^2 : |\xi_2| \geq \frac{1}{8}, \Big|\frac{\xi_1}{\xi_2}\Big| \leq \frac{3}{2}\Big\},$$

and low frequency part

$$\mathcal{C}_0 := \Big\{(\xi_1, \xi_2) \in \mathbb{R}^2 : |\xi_1|, |\xi_2| \leq 1\}.$$

A system of shearlets is then defined by

$$\mathbf{\Phi} = \Big\{\phi^{\alpha,\iota}_{j,l,k}(x), \iota = \{\mathrm{h}, \mathrm{v}\}, j \in \mathbb{N}, -\lceil 2\cdot 2^{(2-\alpha)j}\rceil \leq l \leq \lceil 2\cdot 2^{(2-\alpha)j}\rceil, k \in \mathbb{Z}^2\Big\},$$

where $\hat{\phi}^{\alpha,\iota}_{j,l,k}(\xi) = W_j(\xi) V_\iota\Big(\xi^T A^{-j}_{\alpha,\iota} S^{-l}_\iota\Big) e^{2\pi i \xi^T A^{-j}_{\alpha,\iota} S^{-l}_\iota k}, \iota = \{\mathrm{h}, \mathrm{v}\}$. For an illustration, Fig. 2.1 shows the tiling of the frequency domain induced by shearlets.

By the definition $\hat{\phi}^{\alpha,\iota}_{j,l,k}$ has compact support in the trapezoidal region

$$\text{supp}\, \hat{\phi}^{\alpha,\mathrm{v}}_{j,l,k} = \Big\{\xi \in \mathbb{R}^2 \mid \xi_2 \in [-2^{2j-2}, 2^{2j-2}] \setminus [-2^{2j-5}, 2^{2j-5}], \Big|\frac{\xi_1}{\xi_2} - l2^{-(2-\alpha)j}\Big|\Big\}, \tag{2.9}$$

$$\text{supp}\, \hat{\phi}^{\alpha,\mathrm{h}}_{j,l,k} = \Big\{\xi \in \mathbb{R}^2 \mid \xi_1 \in [-2^{2j-2}, 2^{2j-2}] \setminus [-2^{2j-5}, 2^{2j-5}], \Big|\frac{\xi_2}{\xi_1} - l2^{-(2-\alpha)j}\Big|\Big\}. \tag{2.10}$$

For convenience, we also define two following compact sets

$$\mathcal{C}^*_{\mathrm{h}} := \Big\{\xi \in \mathbb{R}^2 : \frac{1}{32} \leq |\xi_1| \leq \frac{1}{4}, \Big|\frac{\xi_2}{\xi_1}\Big| \leq \frac{3}{2}\Big\} \supset \text{supp}\, \hat{\phi}^{\alpha,\mathrm{h}}_{j,l,k}(\xi^T S^l_{\mathrm{h}} A^j_{\alpha,\mathrm{h}}),$$

$$\mathcal{C}^*_{\mathrm{v}} := \Big\{\xi \in \mathbb{R}^2 : \frac{1}{32} \leq |\xi_2| \leq \frac{1}{4}, \Big|\frac{\xi_1}{\xi_2}\Big| \leq \frac{3}{2}\Big\} \supset \text{supp}\, \hat{\phi}^{\alpha,\mathrm{v}}_{j,l,k}(\xi^T S^l_{\mathrm{v}} A^j_{\alpha,\mathrm{v}}).$$

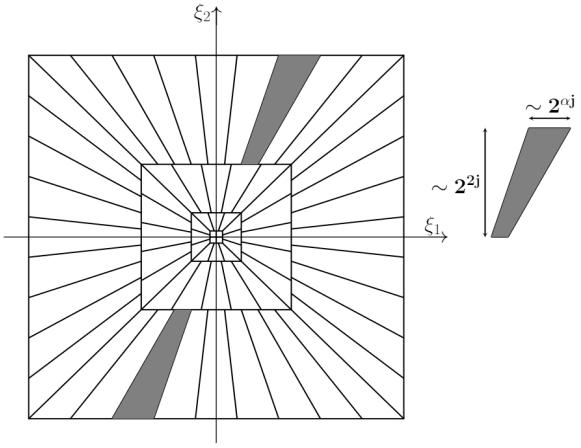

Figure 2.1: Frequency tiling of shearlets.

The key ingredient for the construction of a pair of dual shearlet frames is derived from the following Parseval frames for sub-spaces $L^2(\mathcal{C}_{\mathrm{h}})^\vee, L^2(\mathcal{C}_{\mathrm{v}})^\vee$ which can be then aggregated to form a frame for $L^2(\mathbb{R}^2)$.

Lemma 2.8 *The system* $\mathbf{\Phi}^{\iota}_{\boldsymbol{\alpha}} = \{\phi^{\alpha,\iota}_{j,l,k}, j \in \mathbb{N}_0, -\lceil 2\cdot 2^{(2-\alpha)j}\rceil \le l \le \lceil 2\cdot 2^{(2-\alpha)j}\rceil, k \in \mathbb{Z}^2\}$ *forms a Parseval frame for* $L_2(\mathcal{C}_\iota)^\vee, \iota = \{\mathrm{h},\mathrm{v}\}$ *where* $L_2(\mathcal{C}_\iota)^\vee = \{f \in L_2(\mathbb{R}^2) : \operatorname{supp}\hat{f} \subset \mathcal{C}_\iota\}$.

Proof. We only consider $\iota = \mathrm{h}$, since the other case is done similarly. Indeed, by (2.7) and (2.8) we have

$$\begin{aligned}\sum_{j\in\mathbb{N}_0}\sum_{l=-\lceil 2^{(2-\alpha)j+1}\rceil}^{\lceil 2^{(2-\alpha)j+1}\rceil} |\hat{\phi}^{\alpha,\mathrm{h}}_{j,l,k}(\xi)|^2 &= \sum_{j\in\mathbb{N}_0}|W_j(\xi)|^2 \sum_{l=-\lceil 2^{(2-\alpha)j+1}\rceil}^{\lceil 2^{(2-\alpha)j+1}\rceil} |v(2^{(2-\alpha)j}\frac{\xi_2}{\xi_1}-l)|^2\\ &= 1, \quad \forall \xi \in \mathcal{C}_{\mathrm{h}}.\end{aligned}$$

Here we note that low-pass function $\Omega(\xi) = 0,\ \forall \xi \in \mathcal{C}_{\mathrm{h}}$. By using Parseval's identity and the observation that $\operatorname{supp}\hat{\phi}^{\alpha,\mathrm{h}}_{j,l,k}(\xi^T S^l_{\mathrm{h}} A^j_{\alpha,\mathrm{h}}) \subset \mathcal{C}^*_{\mathrm{h}} \subset [-\frac{1}{2},\frac{1}{2}]^2$, we concludes the claim by standard arguments. ∎

We will construct a pair of dual shearlet frames by carefully patching together three Parseval frames $\mathbf{\Phi}^{\iota}_{\boldsymbol{\alpha}}, \iota = \{0,\mathrm{h},\mathrm{v}\}$, where the construction of translation-invariant Parseval frame $\mathbf{\Phi^0}$ for $L^2(\mathcal{C}_0)$ is well-known. We first define corresponding cones of the dual

$$\mathcal{C}^d_{\mathrm{h}} := \Big\{(\xi_1,\xi_2) \in \mathbb{R}^2 : |\xi_1| \ge \frac{1}{4}, \Big|\frac{\xi_2}{\xi_1}\Big| \le \frac{4}{3}\Big\},$$

$$\mathcal{C}^d_{\mathrm{v}} := \Big\{(\xi_1,\xi_2) \in \mathbb{R}^2 : |\xi_2| \ge \frac{1}{4}, \Big|\frac{\xi_1}{\xi_2}\Big| \le \frac{4}{3}\Big\},$$

and low frequency part

$$\mathcal{C}^d_0 := \Big\{(\xi_1,\xi_2) \in \mathbb{R}^2 : |\xi_1|, |\xi_2| \le \frac{2}{3}\}.$$

For an illustration, we refer to Figure 2.2.

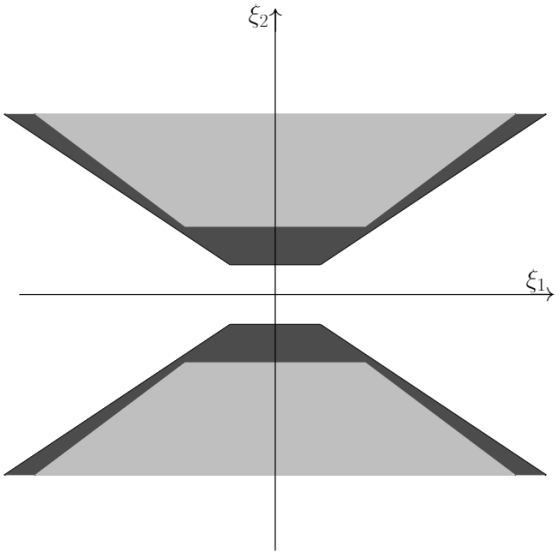

Figure 2.2: Cones $\mathcal{C}_{\mathrm{v}}$ (black) and $\mathcal{C}_{\mathrm{v}}^d$ (gray) with $\mathcal{C}_{\mathrm{v}}^d \subset \mathcal{C}_{\mathrm{v}}$ in frequency domain.

Next, we choose χ_ι, γ_ι in $C^\infty(\mathbb{R}^2), \iota = 0, \mathrm{h}, \mathrm{v}$ by the following lemma.

Lemma 2.9 *There exist χ_ι, γ_ι in $C^\infty(\mathbb{R}^2), \iota = 0, \mathrm{h}, \mathrm{v}$ such that the following properties hold:*

(i) $\operatorname{supp} \chi_\iota, \gamma_\iota \subset \mathcal{C}_\iota,\ \iota = \{0, \mathrm{h}, \mathrm{v}\}, \sum_{\iota \in \{0,\mathrm{h},\mathrm{v}\}} \chi_\iota(\xi) = 1,\ \forall \xi \in \mathbb{R}^2.$

(ii) $\chi_\iota(\xi^T S_\iota^l A_{\alpha,\iota}^j), \gamma_\iota(\xi^T S_\iota^l A_{\alpha,\iota}^j) \in C^\infty(\mathcal{C}_\iota^*)$ *with norms*

$$\|\chi_\iota((\cdot)^T S_\iota^l A_{\alpha,\iota}^j)\|_{C^N(\mathcal{C}_\iota^*)},\ \|\gamma_\iota((\cdot)^T S_\iota^l A_{\alpha,\iota}^j)\|_{C^N(\mathcal{C}_\iota^*)} \leq C_N,$$

where constants C_N are independent of j.

Proof. Let $\chi_0 \in C^\infty, \operatorname{supp} \chi = \mathcal{C}_0 = \{\xi \in \mathbb{R}^2 : |\xi| \leq 1\}$ and $\chi_0(\xi) = 1, \forall \xi = (\xi_1, \xi_2) : |\xi| \leq \frac{2}{3}$. We now define

$$\chi_{\mathrm{h}} := g_{\mathrm{h}}(\xi_1) h_{\mathrm{h}}(\frac{\xi_2}{\xi_1}), \quad \chi_{\mathrm{v}}(\xi_1, \xi_2) := \chi_{\mathrm{h}}(\xi_2, \xi_1) = g_h(\xi_2) h_{\mathrm{h}}(\frac{\xi_1}{\xi_2}),$$

where $g_{\mathrm{h}}, h_{\mathrm{h}}$ are real-valued functions such that $g_{\mathrm{h}}, h_{\mathrm{h}} \in C^\infty(\mathbb{R}), \operatorname{supp} g_{\mathrm{h}} = [\frac{1}{8}, \infty)$, $g_{\mathrm{h}}|_{[\frac{1}{2},\infty)} \equiv 1$, and $\operatorname{supp} h_{\mathrm{h}} \subset [-\frac{3}{2}, \frac{3}{2}], h_{\mathrm{h}}|_{[-\frac{4}{3},\frac{4}{3}]} \equiv 1$.

Next, we define

$$\gamma_{\mathrm{h}}(\xi) := g_{\mathrm{v}}(\xi_1) h_{\mathrm{v}}(\frac{\xi_2}{\xi_1}), \quad \gamma_{\mathrm{v}}(\xi) = g_{\mathrm{v}}(\xi_2)\Big[1 - h_{\mathrm{v}}(\frac{\xi_2}{\xi_1})\Big],$$

where $\operatorname{supp} g_{\mathrm{v}} = [\frac{1}{4}, \infty), g_{\mathrm{v}}|_{[\frac{1}{2},\infty)} \equiv 1$, and $\operatorname{supp} h_{\mathrm{v}} = [-\frac{4}{3}, \frac{4}{3}], h_{\mathrm{v}}|_{[-\frac{3}{4},\frac{3}{4}]} \equiv 1$. We now

choose $\gamma_0(\xi) = 1 - \chi_{\mathrm{h}}(\xi)\gamma_{\mathrm{h}}(\xi) - \chi_{\mathrm{v}}(\xi)\gamma_{\mathrm{v}}(\xi), \forall \xi \in \mathbb{R}^2$. We prove that χ_ι, γ_ι satisfy desired properties. Indeed,

i) Obviously, supp $\chi_\iota \subset \mathcal{C}_\iota, \iota = \{0, \mathrm{h}, \mathrm{v}\}$. By definition, supp $\gamma_{\mathrm{h}} \subset \mathcal{C}_{\mathrm{h}}^d$, and supp $\gamma_{\mathrm{v}} \subset \mathcal{C}_{\mathrm{v}}^d$ since $1 - h_{\mathrm{v}}(\frac{\xi_2}{\xi_1}) = 0$ for $\xi = (\xi_1, \xi_2) : \left|\frac{\xi_1}{\xi_2}\right| > \frac{4}{3}$.

Now it remains to show that supp $\gamma_0 \subset \mathcal{C}_0$. For this, we need to prove $\chi_{\mathrm{h}}(\xi)\gamma_{\mathrm{h}}(\xi) + \chi_{\mathrm{v}}(\xi)\gamma_{\mathrm{v}}(\xi) = 1$ for $\xi, |\xi| > \frac{2}{3}$. Indeed, we first observe

$$h_{\mathrm{h}}(\frac{\xi_2}{\xi_1}) \cdot h_{\mathrm{v}}(\frac{\xi_2}{\xi_1}) = h_{\mathrm{v}}(\frac{\xi_2}{\xi_1}),\ \forall \xi \in \mathbb{R}^2, \tag{2.11}$$

and

$$h_{\mathrm{h}}(\frac{\xi_1}{\xi_2}) \cdot \Big[1 - h_{\mathrm{v}}(\frac{\xi_2}{\xi_1})\Big] = 1 - h_{\mathrm{v}}(\frac{\xi_2}{\xi_1}),\ \forall \xi \in \mathbb{R}^2. \tag{2.12}$$

Next we consider four cases

Case 1: $|\xi_1| \geq \frac{2}{3}, |\xi_2| < \frac{1}{2}$. Since $|\xi_1| > \frac{1}{2}, \left|\frac{\xi_1}{\xi_2}\right| > \frac{4}{3}, \left|\frac{\xi_2}{\xi_1}\right| < \frac{3}{4}$, we obtain $g_{\mathrm{h}}(\xi_1) = g_{\mathrm{v}}(\xi_1) = h_{\mathrm{h}}(\frac{\xi_2}{\xi_1}) = h_{\mathrm{v}}(\frac{\xi_2}{\xi_1}) = 1$. Thus, $\chi_{\mathrm{h}}(\xi)\gamma_{\mathrm{h}}(\xi) + \chi_{\mathrm{v}}(\xi)\gamma_{\mathrm{v}}(\xi) = 1$.

Case 2: $|\xi_1| \geq \frac{2}{3}, |\xi_2| \geq \frac{1}{2}$. We have $g_{\mathrm{h}}(\xi_1) = g_{\mathrm{v}}(\xi_1) = g_{\mathrm{h}}(\xi_2) = g_{\mathrm{v}}(\xi_2) = 1$. This implies

$$\begin{aligned}\chi_{\mathrm{h}}(\xi)\gamma_{\mathrm{h}}(\xi) + \chi_{\mathrm{v}}(\xi)\gamma_{\mathrm{v}}(\xi) &= h_{\mathrm{h}}(\frac{\xi_2}{\xi_1})h_{\mathrm{v}}(\frac{\xi_2}{\xi_1}) + h_{\mathrm{h}}(\frac{\xi_1}{\xi_2})\Big[1 - h_{\mathrm{v}}(\frac{\xi_2}{\xi_1})\Big] \\ &\overset{(2.11)+(2.12)}{=} h_{\mathrm{v}}(\frac{\xi_2}{\xi_1}) + 1 - h_{\mathrm{v}}(\frac{\xi_2}{\xi_1}) = 1.\end{aligned}$$

Case 3: $|\xi_2| \geq \frac{2}{3}, |\xi_1| < \frac{1}{2}$. Since $|\xi_2| \geq \frac{1}{2}, \left|\frac{\xi_2}{\xi_1}\right| > \frac{4}{3}, \left|\frac{\xi_1}{\xi_2}\right| < \frac{3}{4}$, we obtain $g_{\mathrm{h}}(\xi_2) = g_{\mathrm{v}}(\xi_2) = 1, h_{\mathrm{h}}(\frac{\xi_1}{\xi_2}) = 1, h_{\mathrm{v}}(\frac{\xi_2}{\xi_1}) = 0$. Thus, $\chi_{\mathrm{h}}(\xi)\gamma_{\mathrm{h}}(\xi) + \chi_{\mathrm{v}}(\xi)\gamma_{\mathrm{v}}(\xi) = 0 + 1 = 1$.

Case 4: $|\xi_2| \geq \frac{2}{3}, |\xi_1| \geq \frac{1}{2}$. Since $g_{\mathrm{h}}(\xi_1) = g_{\mathrm{v}}(\xi_1) = g_{\mathrm{h}}(\xi_2) = g_{\mathrm{v}}(\xi_2) = 1$, we derive

$$\begin{aligned}\chi_{\mathrm{h}}(\xi)\gamma_{\mathrm{h}}(\xi) + \chi_{\mathrm{v}}(\xi)\gamma_{\mathrm{v}}(\xi) &= h_{\mathrm{h}}(\frac{\xi_2}{\xi_1})h_{\mathrm{v}}(\frac{\xi_2}{\xi_1}) + h_{\mathrm{h}}(\frac{\xi_1}{\xi_2})\Big[1 - h_{\mathrm{v}}(\frac{\xi_2}{\xi_1})\Big] \\ &\overset{(2.11)+(2.12)}{=} h_{\mathrm{v}}(\frac{\xi_2}{\xi_1}) + 1 - h_{\mathrm{v}}(\frac{\xi_2}{\xi_1}) = 1.\end{aligned}$$

Thus, we obtain supp $\gamma_0 \subset \mathcal{C}_0^d$.

On the other hand, by definition we have $\gamma_0(\xi) + \chi_{\mathrm{h}}(\xi)\gamma_{\mathrm{h}}(\xi) + \chi_{\mathrm{v}}(\xi)\gamma_{\mathrm{v}}(\xi) = 1, \forall \xi \in \mathbb{R}^2$. In addition, supp $\gamma_0 \subset \mathcal{C}_0^d = \{\xi \in \mathbb{R}^2 : |\xi| \leq \frac{2}{3}\}$ and $\chi_0 \equiv 1, \forall \xi \in \mathcal{C}_0^d$, we obtain $\chi_0(\xi)\gamma_0(\xi) = \gamma_0(\xi),\ \forall \xi \in \mathbb{R}^2$. Thus, $\sum_{\iota \in 0,\mathrm{h},\mathrm{v}} \chi_\iota(\xi)\gamma_\iota(\xi) = 1$. This concludes the claim.

iii) First we consider

$$\begin{aligned}\chi_{\mathrm{h}}(\xi^T S_{\mathrm{h}}^l A_{\alpha,\mathrm{h}}^j) &= \chi_{\mathrm{h}}(2^{2j}\xi_1, 2^{\alpha j}(\xi_2 + l\xi_1)) \\ &= g_{\mathrm{h}}(2^{2j}\xi_1)h_{\mathrm{h}}(2^{-(2-\alpha)j}(\frac{\xi_2}{\xi_1} + l)).\end{aligned}$$

Since we have $g_{\mathrm{h}}(2^{2j}\xi_1) \equiv 1, \forall \xi \in \mathcal{C}_{\mathrm{h}}^*$, for $j \geq 2$. Obviously, $\chi_{\mathrm{h}}(\xi^T S_{\mathrm{h}}^l A_{\alpha,\mathrm{h}}^j) \in C^\infty(\mathcal{C}_{\mathrm{h}}^*)$ with $\|\chi_{\mathrm{h}}((\cdot)^T S_{\mathrm{h}}^l A_{\alpha,\mathrm{h}}^j)\|_{C^N(\mathcal{C}_{\mathrm{h}}^*)} \leq C_N$. The proof works analogously to case of $\chi_{\mathrm{v}}(\xi^T S_{\mathrm{v}}^l A_{\alpha,\mathrm{v}}^j)$ or

$\gamma_{\mathrm{h}}(\xi^T S_{\mathrm{h}}^l A_{\alpha,\mathrm{h}}^j)$. It remains to prove for $\gamma_{\mathrm{v}}(\xi^T S_{\mathrm{v}}^l A_{\alpha,\mathrm{v}}^j)$, we have

$$\gamma_{\mathrm{v}}(\xi^T S_{\mathrm{v}}^l A_{\alpha,\mathrm{v}}^j) \quad = \quad g_{\mathrm{v}}(2^{2j}\xi_2)\Big[1 - h_{\mathrm{v}}(\frac{2^{2j}\xi_2}{2^{\alpha j}(l\xi_1+\xi_2}))\Big].$$

The observation $\operatorname{supp} h_{\mathrm{v}} = [-\frac{4}{3}, \frac{4}{3}]$ implies $h_{\mathrm{v}}(\frac{2^{2j}\xi_2}{2^{\alpha j}(l\xi_1+\xi_2}) = 0$, for $\left|\frac{2^{2j}\xi_2}{2^{\alpha j}(l\xi_1+\xi_2}\right| > \frac{4}{3}$. In the other words, for $j \geq 2, \gamma_{\mathrm{v}}(\xi^T S_{\mathrm{v}}^l A_{\alpha,\mathrm{v}}^j) \neq 1$ only for $l \gtrsim 2^{(2-\alpha)j}$. By a direct computation, for $j \geq 2, l \gtrsim 2^{(2-\alpha)j}$, we obtain $G(\xi) := 2^{(2-\alpha)j}\frac{\xi_2}{l\xi_1+\xi_2} \in C^\infty(\mathcal{C}_{\mathrm{v}}^*)$ and $\left|\frac{\partial^N}{\partial\xi_1^N}G(\xi)\right|, \left|\frac{\partial^N}{\partial\xi_2^N}G(\xi)\right| \leq C_N$, where C_N are constants independent of j. This finishes the proof. ∎

Let us now go back to the starting point of constructing a dual pair of shearlet types. We define two representation systems of bandlimited α-shearlet associated with those functions in Lemma 2.9 by

$$\mathbf{\Phi}_{\boldsymbol{\alpha}} = \Big\{\check{\chi}_\iota * \phi_{j,l,k}^{\alpha,\iota}(x), \iota = \{\mathrm{h},\mathrm{v}\}, j \in \mathbb{N}_0, -\lceil 2\cdot 2^{(2-\alpha)j}\rceil \leq l \leq \lceil 2\cdot 2^{(2-\alpha)j}\rceil, k \in \mathbb{Z}^2\Big\}$$

$$\bigcup\{\check{\chi}_0 * \phi_k^0(x), k \in \mathbb{Z}^2\},$$

and

$$\mathbf{\Phi}_{\boldsymbol{\alpha}}^{\boldsymbol{d}} = \Big\{\check{\gamma}_\iota * \phi_{j,l,k}^{\alpha,\iota}(x), \iota = \{\mathrm{h},\mathrm{v}\}, j \in \mathbb{N}_0, -\lceil 2\cdot 2^{(2-\alpha)j}\rceil \leq l \leq \lceil 2\cdot 2^{(2-\alpha)j}\rceil, k \in \mathbb{Z}^2\Big\}.$$

$$\bigcup\{\check{\gamma}_0 * \phi_k^0(x), k \in \mathbb{Z}^2\},$$

where $\mathbf{\Phi^0} = \{\phi_k^0(x)\}_{k\in\mathbb{Z}^2}$ forms a Parseval frame for $L^2(\mathcal{C}_0)$.

As mentioned before, these two systems are a natural extension of shearlets by using flexible scaling to accommodate the smoothness of the data. They consist of a countable collection of well-localized shearlet elements at various locations, scales, and orientations. In addition, we combine two Parseval frames by using χ_ι, γ_ι instead of $\gamma_\iota, \frac{\chi_\iota}{\gamma_\iota}$ used in [Gro13] which might lead to bad behavior when we consider higher derivatives of shearlet elements.

For convenience, let us use the following index set of shearlets

$$\Delta := \Big\{(j,l,k,\iota) \mid j \geq 0, l \in \mathbb{Z}, |l| \leq \lceil 2\cdot 2^{(2-\alpha)j}\rceil, k \in \mathbb{Z}^2, \iota \in \{\mathrm{h},\mathrm{v}\}\Big\}. \tag{2.13}$$

Lemma 2.10 *The systems $\mathbf{\Phi}_{\boldsymbol{\alpha}}, \mathbf{\Phi}_{\boldsymbol{\alpha}}^{\boldsymbol{d}}$ form a pair of shearlet frames for $L^2(\mathbb{R}^2)$. Consequently, we have $\mathbf{\Phi}_{\boldsymbol{\alpha}}^{\boldsymbol{d}} \in \mathbb{D}_{\mathbf{\Phi}_{\boldsymbol{\alpha}}}$.*

Proof. First we prove that $\mathbf{\Phi}_{\boldsymbol{\alpha}}$ forms a frame for $L^2(\mathbb{R}^2)$. Indeed, the observation $\operatorname{supp}\chi_\iota \in \mathcal{C}_\iota, \iota = \{0,\mathrm{h},\mathrm{v}\}$ implies $\operatorname{supp}\chi_\iota\hat{f} \in \mathcal{C}_\iota, \iota = \{0,\mathrm{h},\mathrm{v}\}$. Now we exploit that $\mathbf{\Phi^0}$ and $\mathbf{\Phi}_{\boldsymbol{\alpha}}^{\boldsymbol{\iota}} = \{\phi_{j,l,k}^{\alpha,\iota}, j \in \mathbb{N}_0, -\lceil 2\cdot 2^{(2-\alpha)j}\rceil \leq l \leq \lceil 2\cdot 2^{(2-\alpha)j}\rceil, k \in \mathbb{Z}^2\}, \iota = \{\mathrm{h},\mathrm{v}\}$ constitute Parseval frames for $\mathcal{C}_\iota, \iota = \{0,\mathrm{h},\mathrm{v}\}$ and obtain

$$\sum_{\substack{\{(j,l,k,\iota)\in\Delta\}\\ \cup\{\iota=0,k\in\mathbb{Z}^2\}}} |\langle f, \Phi_\alpha\rangle|^2 = \sum_{(j,l,k,\iota)\in\Delta} |\langle\hat{f}, \chi_\iota\hat{\phi}_{j,l,k}^{\alpha,\iota}\rangle|^2 + \sum_{k\in\mathbb{Z}^2} |\langle\hat{f}, \chi_0\hat{\phi}_k^0\rangle|^2$$

$$= \sum_{(j,l,k,\iota)\in\Delta} |\langle \chi_\iota \hat{f}, \hat{\phi}^{\alpha,\iota}_{j,l,k}\rangle|^2 + \sum_{k\in\mathbb{Z}^2} |\langle \chi_0 \hat{f}, \hat{\phi}^0_k\rangle|^2$$
$$= \sum_{\iota\in\{0,\mathrm{h},\mathrm{v}\}} \|\chi_\iota \hat{f}\|_2^2 \leq \sum_{\iota\in\{0,h,v\}} \|\chi_\iota\|_\infty^2 \cdot \|f\|_2^2. \tag{2.14}$$

In addition,

$$3 \sup_{\iota\in\{0,\mathrm{h},\mathrm{v}\}} \|\gamma_\iota\|_\infty^2 \cdot \sum_{\substack{\{(j,l,k,\iota)\in\Delta\}\\ \cup\{\iota=0,k\in\mathbb{Z}^2\}}} |\langle f, \Phi_\alpha\rangle|^2 = 3 \sup_{\iota\in\{0,\mathrm{h},\mathrm{v}\}} \|\gamma_\iota\|_\infty^2 \cdot \sum_{\iota\in\{0,\mathrm{h},\mathrm{v}\}} \|\chi_\iota \hat{f}\|_2^2$$
$$\geq \| \sum_{\iota\in\{0,h,v\}} \chi_\iota \gamma_\iota \hat{f}\|_2^2 = \|f\|_2^2. \tag{2.15}$$

Combine (2.14) and (2.15) we obtain

$$\frac{1}{3\sup_{\iota\in\{0,\mathrm{h},\mathrm{v}\}} \|\gamma_\iota\|_\infty^2} \cdot \|f\|_2^2 \leq \sum_{\substack{\{(j,l,k,\iota)\in\Delta\}\\ \cup\{\iota=0,k\in\mathbb{Z}^2\}}} |\langle f, \Phi_\alpha\rangle|^2 \leq \sum_{\iota\in\{0,h,v\}} \|\chi_\iota\|_\infty^2 \cdot \|f\|_2^2.$$

Similarly, we have

$$\frac{1}{3\sup_{\iota\in\{0,\mathrm{h},\mathrm{v}\}} \|\chi_\iota\|_\infty^2} \cdot \|f\|_2^2 \leq \sum_{\substack{\{(j,l,k,\iota)\in\Delta\}\\ \cup\{\iota=0,k\in\mathbb{Z}^2\}}} |\langle f, \Phi^d_\alpha\rangle|^2 \leq \sum_{\iota\in\{0,h,v\}} \|\gamma_\iota\|_\infty^2 \cdot \|f\|_2^2.$$

It remains to show that $\mathbf{\Phi_\alpha}, \mathbf{\Phi^d_\alpha}$ form a pair of dual frames. Due to Plancherel's theorem and $\mathbf{\Phi^0}, \mathbf{\Phi^\iota_\alpha}, \iota = \{\mathrm{h}, \mathrm{v}\}$ being Parseval frames for $L^2(\mathcal{C}_\iota)^\vee, \iota = \{0, \mathrm{h}, \mathrm{v}\}$, we have

$$\begin{aligned}
\sum_{\substack{\{(j,l,k,\iota)\in\Delta\}\\ \cup\{\iota=0,k\in\mathbb{Z}^2\}}} \langle f, \Phi_\alpha\rangle \hat{\Phi}^d_\alpha &= \sum_{(j,l,k,\iota)\in\Delta} \langle \hat{f}, \chi_\iota \hat{\phi}^{\alpha,\iota}_{j,l,k}\rangle \gamma_\iota \hat{\phi}^{\alpha,\iota}_{j,l,k} + \sum_{k\in\mathbb{Z}^2} \langle \hat{f}, \chi_0 \phi^0_k\rangle \gamma_0 \phi^0_k \\
&= \sum_{(j,l,k,\iota)\in\Delta} \langle \chi_\iota \gamma_\iota \hat{f}, \hat{\phi}^{\alpha,\iota}_{j,l,k}\rangle \hat{\phi}^{\alpha,\iota}_{j,l,k} + \sum_{k\in\mathbb{Z}^2} \langle \chi_0 \gamma_0 \hat{f}, \phi^0_k\rangle \phi^0_k \\
&= \sum_{\iota\in\{0,\mathrm{h},\mathrm{v}\}} \chi_\iota \gamma_\iota \hat{f} = \hat{f}.
\end{aligned}$$

This finishes the proof. ∎

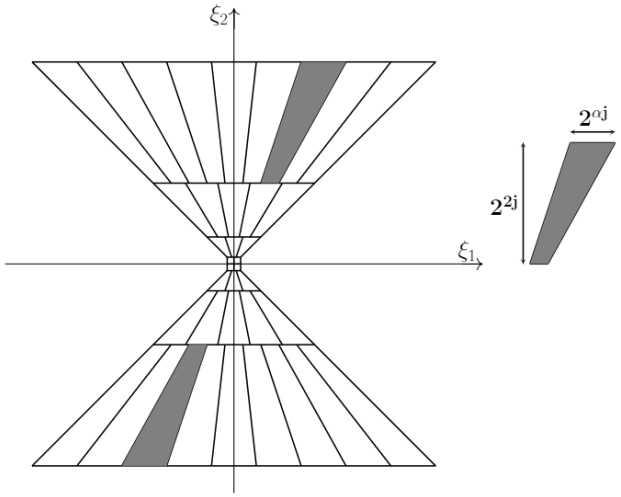

Figure 2.3: The frequency tilling of the vertical cone $\mathcal{C}_v$, with the support of one shearlet highlighted.

Shearlets have been studied extensively so far due to their highly directional performance and smooth digital grid, whereas wavelets are best adapted to anisotropic features like point singularities. Bandlimited α-shearlets allow for a unified treatment of wavelets and shearlets. If $\alpha = 1$ we obtain the bandlimited shearlet frame by using parabolic scaling. Different from the literature [Gro13], we here rescaled the parameter j to $2j$. Therefore, the spatial footprints of shearlets are of size 2^{-j} times 2^{-2j} instead of $2^{-j/2}$ times 2^{-j}. Also, if α approaches 2 the elements of α-shearlets scale in an isotropic fashion. Thus, $\mathbf{\Phi}_\alpha = \{\phi^{\alpha,\iota}_{j,l,k}\}_{(j,l,k,\iota)\in\Delta} \cup \{\phi^0_k\}_{k\in\mathbb{Z}^2}$ can be viewed as a special instance of wavelets. Consider the shearlet system $\mathbf{\Phi}_\alpha$ the tiling of the frequency domain on the vertical cone $\mathcal{C}_v$ is illustrated in Figure 2.3.

The reader should be aware of the fact that we can construct a system satisfying a milder condition (1.3), i.e., an element of $\mathbb{D}_{\mathbf{\Phi}}$, instead of forming a dual. In fact, if there exists a well-localized synthesis pseudo-dual the success of the proposed algorithm is guaranteed.

2.4 Multi-scale Component Separation

For $\alpha \in [1, 2)$, we first fix a constant ϵ such that

$$0 < \epsilon < \frac{2-\alpha}{4}. \tag{2.16}$$

Using the window function W_j by (2.6), we define a class of *frequency filters* F_j defined by its Fourier transform

$$\hat{F}_j(\xi) := W_j(\xi) = W(\xi/2^{2j}), \quad \forall j \geq 1, \xi \in \mathbb{R}^2,$$

and in low frequency part

$$\hat{F}_{low}(\xi) := \Omega(\xi), \quad \xi \in \mathbb{R}^2,$$

where Ω is defined in (2.5). Using these filters to decompose f into sub-images by $f_j = F_j * f$, the original image f is then recovered from its pieces f_j by (2.7)

$$f = F_{low} * F_{low} * f + \sum_{j \in \mathbb{N}_0} F_j * f_j. \tag{2.17}$$

We intend to apply Algorithm 1 for each sub-image f_j which is assumed to be $\mathcal{P}_j + w\mathcal{L}_j$, where $\mathcal{P}_j = F_j * \mathcal{P}, w\mathcal{L}_j = F_j * w\mathcal{L}$. The whole signal f is then reconstructed by (2.17).

These filters allow us to consider the pointlike and curvelike part at different scales. The separation problem is meaningful at each scale if the components are comparable in sense of their energy. A main issue is the balance of the energy of each component [DK13; Kut13], i.e., we may assume that $\{\gamma_i\}_{i=1}^K, \{c_i\}_{i=1}^K$ are chosen satisfying $\|\mathcal{P}_j\|_2 \approx \|\mathcal{C}_j\|_2$ at each scale j. In that case, we can choose $\max_{i=1,2,\cdots,K} \{\lambda_i\} = \frac{3}{2}$. However, we will not restrict to this energy balancing condition in our analysis. We later show that the success of the proposed algorithm is guaranteed as long as the energy of components are not too small, i.e., they satisfy a lower bound at each scale. This guarantees the performance even in case of different energies.

We would like to emphasize that there are very few elements interacting significantly with the discontinuities, i.e., few elements of the wavelet and shearlet expansions are enough to provide accurate approximations of the components. This allows us to define the following clusters which will be then exploited to derive small error approximation as well as the cluster coherence of

$$\Lambda_{1j} = \left\{(j', m) \mid j' \in \mathbb{Z}, |j' - j| \leq 1, m = (m_1, m_2) \in \mathbb{Z}^2, \sqrt{m_1^2 + m_2^2} \leq 2^{\epsilon j}\right\},$$

and

$$\Lambda_{2j} = \left\{(j', l, k, \mathrm{v}) \in \Delta \mid j', l \in \mathbb{Z}, |j' - j| \leq 1, |l| \leq 1, k = (k_1, k_2) \in \mathbb{Z}^2, |k_2 - lk_1| \leq 2^{\epsilon j}\right\},$$

where Δ is defined in (2.13). Intuitively, the geometry underlying these two components should be different so that a chosen frame pair can provide sufficient small cluster sparsity and cluster coherence, which guarantee the success of Algorithm 1. Indeed, although points and curves can overlap in spatial domain, their wavefront set might be quite different in phase space consisting of a pair of positions and directions. Here the wavefront set of a distribution f is the set of positions and orientations at which f is not smooth. This difference intuitively enables us to separate the components by microlocal analysis, see [DK13] for a more comprehensive discussion.

We now present our main separation result.

Theorem 2.11 *Consider a wavelet frame $\mathbf{\Psi} = \{\psi_{j,m}\}_{(j,m)} \cup \{\Omega(\cdot - m)\}, j \in \mathbb{N}_0, m \in \mathbb{Z}^2$ and a bandlimited α-shearlet frame $\mathbf{\Phi}_\alpha = \{\phi_{j,l,k}^{\alpha,\iota}\}_{(j,l,k,\iota)\in\Delta} \cup \{\phi_k^0\}_{k\in\mathbb{Z}^2}, \alpha \in [1,2)$. Then separation based on scale j is achieved by (2.2) in the limit of large j. Namely, we have*

$$\frac{\|\mathcal{P}_j^\star - \mathcal{P}_j\|_2}{\|\mathcal{P}_j\|_2} + \frac{\|\mathcal{C}_j^\star - w\mathcal{L}_j\|_2}{\|w\mathcal{L}_j\|_2} = o(2^{-Nj}) \to 0, \quad j \to \infty,$$

for all $N \geq 0$, where $(\mathcal{P}_j^\star, \mathcal{C}_j^\star)$ is the solution of (2.2) and $(\mathcal{P}_j, w\mathcal{L}_j)$ are purported components.

We delay the proof until later after we have introduced our main tools in Subsections 2.4.1, 2.4.2. We will use Theorem 2.7 for the proof of this theorem. For this, we need to show that clusters $\Lambda_{1,j}, \Lambda_{2,j}$ provide sparse representation of pointlike and curvelike singularities in the sense that the sparsity $\delta = \delta_{1,2} + \delta_{2,j}$ is negligible. In addition, the cluster coherence $\mu_c = \mu_c(\Lambda_{1,j}, \mathbf{\Psi}; \mathbf{\Phi}^\alpha) + \mu_c(\Lambda_{2,j}, \mathbf{\Phi}_\alpha; \mathbf{\Psi})$ is also sufficiently small. Those conditions ensure the success of Algorithm 1 as a result of Theorem 2.7. We would like to remark that in our analysis we need the fast decay of the dual frame rather than its explicit construction.

As a consequence, Theorem 2.11 implies that it is possible to separate pointlike and curvelike structures using wavelets and α-shearlets if α-shearlets do not share the isotropic feature with wavelets, i.e., $\alpha < 2$. Indeed, traditional wavelets which are based on isotropic dilations are not very effective when dealing with multivariate data. In contrast, shearlets show a greater ability to capture anisotropic features by applying a different dilation factor along the two axes. Here the parameter α measures the degree of anisotropy. If $\alpha = 2$ the scaling matrices $A_{\alpha,\iota}, \iota = \{\mathrm{h}, \mathrm{v}\}$ become isotropic dilations which show similar behavior as wavelets in the sense of directional sensitivity.

The next two subsections are dedicated to the estimate of cluster coherence and the cluster sparsity.

2.4.1 Estimate of Cluster Coherence

First, we introduce the notation which is useful in rest of the paper

$$\langle |x| \rangle = (1 + |x|^2)^{1/2}.$$

The following lemma shows that wavelet and shearlet elements are well-localized at various scales, positions and directions.

Lemma 2.12 *Consider a wavelet frame $\mathbf{\Psi}$ and a band limited α-shearlet frame $\mathbf{\Phi}_\alpha$. Then there exists a universal constant C_N independent of j such that the following estimates hold for any arbitrary integer $N = 1, 2, \ldots$*

(i) $|\psi_{j,m}(x)| \leq C_N \cdot 2^{2j} \cdot \langle |2^{2j}x_1 + m_1| \rangle^{-N} \langle |2^{2j}x_2 + m_2| \rangle^{-N}$.

(ii)
$$|\check{\chi}_\mathrm{v} * \phi^{\alpha,\mathrm{v}}_{j,l,k}(x)| \leq C_N \cdot 2^{(2+\alpha)j/2} \cdot \langle |2^{\alpha j}x_1 + k_1| \rangle^{-N} \langle |2^{2j}x_2 + l2^{\alpha j}x_1 + k_2| \rangle^{-N},$$
$$|\check{\chi}_\mathrm{h} * \phi^{\alpha,\mathrm{h}}_{j,l,k}(x)| \leq C_N \cdot 2^{(2+\alpha)j/2} \cdot \langle |2^{2j}x_1 + l2^{\alpha j}x_2 - k_1)| \rangle^{-N} \langle |2^{\alpha j}x_2 - k_2| \rangle^{-N},$$
and similarly
$$|\check{\gamma}_\mathrm{v} * \phi^{\alpha,\mathrm{v}}_{j,l,k}(x)| \leq C_N \cdot 2^{(2+\alpha)j/2} \cdot \langle |2^{\alpha j}x_1 + k_1| \rangle^{-N} \langle |2^{2j}x_2 + l2^{\alpha j}x_1 + k_2| \rangle^{-N},$$
$$|\check{\gamma}_\mathrm{h} * \phi^{\alpha,\mathrm{h}}_{j,l,k}(x)| \leq C_N \cdot 2^{(2+\alpha)j/2} \cdot \langle |2^{2j}x_1 + l2^{\alpha j}x_2 - k_1)| \rangle^{-N} \langle |2^{\alpha j}x_2 - k_2| \rangle^{-N}.$$

(iii)
$$|\langle \psi_{j,m}, \check{\chi}_\iota * \phi^{\alpha,\iota}_{j,l,k} \rangle| \leq C_N \cdot 2^{-(2-\alpha)j/2}, \quad \forall \iota \in \{\mathrm{v}, \mathrm{h}\},$$
$$|\langle \psi_{j,m}, \check{\gamma}_\iota * \phi^{\alpha,\iota}_{j,l,k} \rangle| \leq C_N \cdot 2^{-(2-\alpha)j/2}, \quad \forall \iota \in \{\mathrm{v}, \mathrm{h}\}.$$

Proof. i) With the variable $\zeta = 2^{-2j}\xi$, we have

$$\begin{aligned} |\psi_{j,m}(x)| &= \Big| \int_{\mathbb{R}^2} 2^{-2j} W_j(\xi) e^{2\pi i \xi^T m/2^{2j}} e^{2\pi i \xi^T x} d\xi \Big| \\ &= \Big| \int_{\mathbb{R}^2} 2^{2j} W(\zeta) e^{2\pi i \zeta^T (2^{2j}x+m)} d\zeta \Big|. \end{aligned}$$

By integration by parts for $N_1, N_2 = 1, 2, \ldots$, with respect to ζ_1, ζ_2, respectively, we have

$$\begin{aligned} |\psi_{j,m}(x)| &= \Big| \int_{\mathbb{R}^2} 2^{2j} (2^{2j}x_1 + m_1)^{-N_1} \frac{\partial^{N_1}}{\partial \zeta_1^{N_1}} [W(\zeta)] e^{2\pi i \zeta^T (2^{2j}x+m)} d\zeta \Big| \\ &= \Big| \int_{\mathbb{R}^2} 2^{2j} (2^{2j}x_1 + m_1)^{-N_1} (2^{2j}x_2 + m_2)^{-N_2} \frac{\partial^{N_1+N_2}}{\partial \zeta_1^{N_1} \partial \zeta_2^{N_2}} [W(\zeta)] e^{2\pi i \zeta^T (2^{2j}x+m)} d\zeta \Big| \\ &\leq 2^{2j} |2^{2j}x_1 + m_1|^{-N_1} |2^{2j}x_2 + m_2|^{-N_2} \int_{\mathbb{R}^2} \Big| \frac{\partial^{N_1+N_2}}{\partial \zeta_1^{N_1} \partial \zeta_2^{N_2}} [W(\zeta)] \Big| d\zeta, \end{aligned}$$

and similarly

$$|\psi_{j,m}(x)| \leq 2^{2j} |2^{2j}x_i + m_i|^{-N_i} \int_{\mathbb{R}^2} \Big| \frac{\partial^{N_i}}{\partial \zeta_i^{N_i}} [W(\zeta)] \Big| d\zeta,$$

for $i = 1, 2$. Note that the boundary terms vanish since $W(\zeta)$ has compact support. Thus,
$2^{-2j}\Big(1 + |2^{2j}x_1 + m_1|^{N_1} + |2^{2j}x_2 + m_2|^{N_2} + |2^{2j}x_1 + m_1|^{N_1} |2^{2j}x_2 + m_2|^{N_2}\Big) |\psi_{j,m}(x)|$

$$\begin{aligned} &= 2^{-2j} (1 + |2^{2j}x_1 + m_1|^{N_1})(1 + |2^{2j}x_2 + m_2|^{N_2}) |\psi_{j,m}(x)| \\ &\leq \int_{\mathbb{R}^2} |W(\zeta)| d\zeta + \int_{\mathbb{R}^2} \Big| \frac{\partial^{N_1}}{\partial \zeta_1^{N_1}} W(\zeta) \Big| d\zeta + \int_{\mathbb{R}^2} \Big| \frac{\partial^{N_2}}{\partial \zeta_2^{N_2}} W(\zeta) \Big| d\zeta \\ &\quad + \int_{\mathbb{R}^2} \Big| \frac{\partial^{N_1+N_2}}{\partial \zeta_1^{N_1} \partial \zeta_2^{N_2}} W(\zeta) \Big| d\zeta. \end{aligned}$$

Since $W(\zeta) \in C^\infty$, there exists a constant C'_{N_1,N_2} independent of j such that
$\int_{\mathbb{R}^2} |W(\zeta)| d\zeta + \int_{\mathbb{R}^2} \Big| \frac{\partial^{N_1}}{\partial \zeta_1^{N_1}} W(\zeta) \Big| d\zeta + \int_{\mathbb{R}^2} \Big| \frac{\partial^{N_2}}{\partial \zeta_2^{N_2}} W(\zeta) \Big| d\zeta + \int_{\mathbb{R}^2} \Big| \frac{\partial^{N_1+N_2}}{\partial \zeta_1^{N_1} \partial \zeta_2^{N_2}} W(\zeta) \Big| d\zeta \leq C'_{N_1,N_2}$.
Thus, we obtain

$$|\psi_{j,m}(x)| \leq C'_{N_1,N_2} \cdot 2^{2j} \cdot \frac{1}{1 + |2^{2j}x_1 + m_1|^{N_1}} \frac{1}{1 + |2^{2j}x_2 + m_2|^{N_2}}.$$

In addition, there exist constants C'_{N_1}, C'_{N_2} for each $N_1, N_2 = 1, 2, \ldots$ such that

$$\langle |2^{2j}x_1 + m_1| \rangle^{N_1} = (1 + |2^{2j}x_1 + m_1|^2)^{N_1/2} \leq C'_{N_1} (1 + |2^{2j}x_1 + m_1|^{N_1}),$$

and

$$\langle |2^{2j}x_2 + m_2| \rangle^{N_2} = (1 + |2^{2j}x_2 + m_2|^2)^{N_2/2} \leq C'_{N_2} (1 + |2^{2j}x_2 + m_2|^{N_2}).$$

Finally, we obtain

$$|\psi_{j,m}(x)| \leq C_{N_1,N_2} \cdot 2^{2j} \cdot \langle |2^{2j}x_1 + m_1| \rangle^{-N_1} \langle |2^{2j}x_2 + m_2| \rangle^{-N_2}.$$

This shows the first claim.
ii) With the variable $\zeta^T = \xi^T A_{\alpha,\iota}^{-j} S_\iota^{-l}$, we obtain

$$\begin{aligned} & |\check{\chi}_\iota(x) * \phi_{j,l,k}^{\alpha,\iota}(x)| = \Big| \int_{\mathbb{R}^2} \chi_\iota(\xi) \hat{\phi}_{j,l,k}^{\alpha,\iota}(\xi) e^{2\pi i \xi^T x} d\xi \Big| \\ = & \Big| \int_{\mathbb{R}^2} 2^{-(2+\alpha)j/2} \chi_\iota(\xi) W_j(\xi) V_\iota\Big(\xi^T A_{\alpha,\iota}^{-j} S_\iota^{-l}\Big) e^{2\pi i \xi^T (x + A_{\alpha,\iota}^{-j} S_\iota^{-l} k)} d\xi \Big| \\ = & \Big| \int_{\mathbb{R}^2} 2^{(2+\alpha)j/2} \chi_\iota(\xi) W_j((S_\iota^l A_{\alpha,\iota}^j)^T \zeta) V_\iota(\zeta) e^{2\pi i \zeta^T (S_\iota^l A_{\alpha,\iota}^j x + k)} d\zeta \Big|. \end{aligned}$$

By a similar approach as in i) the decay of each shearlet element is then estimated by

$$|\check{\chi}_{\mathrm{v}} * \phi_{j,l,k}^{\alpha,\mathrm{v}}(x)| \le C_N \cdot 2^{(2+\alpha)j/2} \cdot \langle |2^{\alpha j} x_1 - k_1| \rangle^{-N} \langle |2^{2j} x_2 + l 2^{\alpha j} x_1 - k_2| \rangle^{-N},$$

$$|\check{\chi}_{\mathrm{h}} * \phi_{j,l,k}^{\alpha,\mathrm{h}}(x)| \le C_N \cdot 2^{(2+\alpha)j/2} \cdot \langle |2^{2j} x_1 + l 2^{\alpha j} x_2 - k_1)| \rangle^{-N} \langle |2^{\alpha j} x_2 - k_2| \rangle^{-N}.$$

The same fact is true with the roles of χ_ι and γ_ι interchanged. It should be mentioned that here we use Lemma 2.9, ii) to estimate the constant C_N.
iii) By using i) and ii) the change of variables $(y_1, y_2) = 2^{2j}(x_1, x_2)$ we easily verify the claim. Indeed, for $\iota = \mathrm{v}$ we have

$$\begin{aligned} |\langle \psi_{j,m}, \check{\chi}_{\mathrm{v}} * \phi_{j,l,k}^{\alpha,\mathrm{v}} \rangle| &\le \int_{\mathbb{R}^2} |\psi_{j,m}(x)| |\check{\chi}_{\mathrm{v}} * \phi_{j,l,k}^{\alpha,\mathrm{v}}(x)| dx \\ &\le C_N 2^{2j} 2^{(2+\alpha)j/2} \int_{\mathbb{R}^2} \langle |2^{2j} x_1 + m_1| \rangle^{-N} \langle |2^{2j} x_2 + m_2| \rangle^{-N} \\ &\quad \cdot \langle |2^{\alpha j} x_1 + k_1| \rangle^{-N} \langle |2^{2j} x_2 + l 2^{\alpha j} x_1 + k_2| \rangle^{-N} dx \\ &\le C_N 2^{-(2-\alpha)j/2} \int_{\mathbb{R}^2} \langle |y_1 + m_1| \rangle^{-N} \langle |y_2 + m_2| \rangle^{-N} dy_1 dy_2 \\ &\le C'_N 2^{-(2-\alpha)j/2}. \end{aligned}$$

■

For the other cases, the proofs are similar.

Such decay estimates in Lemma 2.12 are particularly useful for estimating the cluster coherence introduced next as well as the cluster sparsity in Subsection 2.4.2.

Proposition 2.13 *Consider wavelet frame $\mathbf{\Psi}$ and bandlimited α-shearlet frame $\mathbf{\Phi}_{\boldsymbol{\alpha}}$, we have*

$$\mu_c(\Lambda_{1j}, \mathbf{\Psi}; \mathbf{\Phi}_{\boldsymbol{\alpha}}) \to 0, \ j \to +\infty.$$

Proof. By definition, we have

$$\mu_c(\Lambda_{1j}, \mathbf{\Psi}; \mathbf{\Phi}_{\boldsymbol{\alpha}}) = \max_{(\bar{j},l,k,\iota) \in \Delta} \sum_{(j',m) \in \Lambda_{1,j}} |\langle \psi_{j',m}, \check{\chi}_\iota(x) * \phi_{\bar{j},l,k}^{\alpha,\iota} \rangle|.$$

Without loss of generality, we assume that the maximum is attained at $\check{\chi}_{\mathrm{v}}(x) * \phi_{j,l',k'}^{\alpha,\mathrm{v}}$. Cases $\iota = \mathrm{h}, \bar{j} = \{j-1, j+1\}$ are done similarly. By Lemma 2.12, iii), there exist a

constant $C > 0$ such that

$$\begin{aligned}\mu_c(\Lambda_{1j}, \boldsymbol{\Psi}; \boldsymbol{\Phi}_{\boldsymbol{\alpha}}) &\leq \#\{(j,m) \in \Lambda_{1,j}\} \cdot C \cdot 2^{-(2-\alpha)j/2} \\ &\leq C \cdot 2^{2\epsilon j} \cdot 2^{-(2-\alpha)j/2} \\ &= C \cdot 2^{-(2-\alpha-4\epsilon)j/2} \xrightarrow[j\to+\infty]{} 0,\end{aligned}$$

where the last estimate is due to $2 - \alpha - 4\epsilon > 0$ by (2.16). This finishes the proof. ∎

Proposition 2.14 *Consider wavelet frame $\boldsymbol{\Psi} = \{\psi_{j,k}\}_{(j,k)}$ and band limited α-shearlet frame $\boldsymbol{\Phi}_{\boldsymbol{\alpha}} = \{\phi^{\alpha,\iota}_{j,l,k}\}_{(j,l,k,\iota)\in\Delta}$, we have*

$$\mu_c(\Lambda_{2j}, \boldsymbol{\Phi}_{\boldsymbol{\alpha}}; \boldsymbol{\Psi}) \to 0,\ j \to +\infty.$$

Proof. By definition, we have

$$\mu_c(\Lambda_{2j}, \boldsymbol{\Phi}_{\boldsymbol{\alpha}}; \boldsymbol{\Psi}) = \max_{\bar{j}\in\mathbb{N}, m\in\mathbb{Z}^2} \sum_{(j',l,k,\mathrm{v})\in\Lambda_{2,j}} |\langle \check{\chi}_\iota(x) * \phi^{\alpha,\mathrm{v}}_{j',l,k}, \psi_{\bar{j},m}\rangle|.$$

We assume that the maximum is attained at $\psi_{j,m'}$. By Lemma 2.12, i) and ii), we have

$$\begin{aligned}\mu_c(\Lambda_{2j}, \boldsymbol{\Phi}_{\boldsymbol{\alpha}}; \boldsymbol{\Psi}) \leq C_N 2^{(6+\alpha)j/2} \sum_{\substack{|l|\leq 1, |j'-j|\leq 1 \\ k\in\mathbb{Z}^2, |k_2 - lk_1| < 2^{\epsilon j'}}} \int_{\mathbb{R}^2} \langle |2^{2j}x_1 + m_1'| \rangle^{-N} \cdot \\ \langle |2^{2j}x_2 + m_2'| \rangle^{-N} \langle |2^{\alpha j'}x_1 + k_1| \rangle^{-N} \langle |2^{2j'}x_2 + l2^{\alpha j'}x_1 + k_2| \rangle^{-N} dx.\end{aligned}$$

Without loss of generality, we consider only the case $j' = j$, the cases $j' = j-1, j+1$ follow similarly.

Indeed, by the change of variable $(y_1, y_2) = (2^{2j}x_1, 2^{2j}x_2)$, we obtain

$$\begin{aligned}\mu_c(\Lambda_{2j}, \boldsymbol{\Phi}_{\boldsymbol{\alpha}}; \boldsymbol{\Psi}) \leq C_N 2^{-(2-\alpha)j/2} \sum_{\substack{l\in\{-1,0,1\}, k\in\mathbb{Z}^2 \\ |k_2 - lk_1| < 2^{\epsilon j'}}} \int_{\mathbb{R}^2} \langle |y_1 + m_1'| \rangle^{-N} \langle |y_2 + m_2'| \rangle^{-N} \\ \cdot \langle |2^{-(2-\alpha)j}y_1 + k_1| \rangle^{-N} \langle |y_2 + l2^{\alpha j}x_1 + k_2| \rangle^{-N} dy. \qquad (2.18)\end{aligned}$$

In addition, there exists a constant C' such that

$$\sum_{k\in\mathbb{Z}^2} \langle |2^{-(2-\alpha)j}y_1 + k_1| \rangle^{-N} \langle |y_2 + l2^{\alpha j}x_1 + k_2| \rangle^{-N} \leq C'. \qquad (2.19)$$

Combining (2.18) with (2.19), we obtain

$$\begin{aligned}\mu_c(\Lambda_{2j}, \boldsymbol{\Phi}_{\boldsymbol{\alpha}}; \boldsymbol{\Psi}) &\leq C'_N \cdot 2^{-(2-\alpha)j/2} \int_{\mathbb{R}^2} \langle |y_1 + m_1'| \rangle^{-N} \langle |y_2 + m_2'| \rangle^{-N} dy \\ &\leq C''_N \cdot 2^{-(2-\alpha)j/2} \xrightarrow{j\to+\infty} 0.\end{aligned}$$

This concludes the claim.

∎

2.4.2 Sparse Representation Error

Proposition 2.15 *For all $N = 1, 2, \ldots$, we have $\delta_{1j} = \circ(2^{-Nj})$.*

Proof. We remark that it is sufficient to consider $\mathcal{P}(x) = \frac{1}{|x|^\lambda}, \lambda \in (0, 2)$. The general case is then done by combining all single cases and triangle inequality.

We first observe that $\hat{\mathcal{P}}(\xi) = \frac{1}{|\xi|^{2-\lambda}}$. Thus,

$$\begin{aligned}\delta_{1,j} &= \sum_{(j',m)\notin\Lambda_{1,j}} \langle \psi_{j',m}, \mathcal{P}_j \rangle \\ &= \sum_{|j'-j|\le 1, |m|>2^{\epsilon j}} \int_{\mathbb{R}^2} 2^{-2j} W_{j'}(\xi) e^{2\pi i \xi^T \frac{m}{2^{2j}}} W_j(\xi) \frac{1}{|\xi|^{2-\lambda}} d\xi.\end{aligned}$$

Since $W_{j'}(\xi) W_j(\xi) = 0$ for $|j' - j| > 1$ due to their supports. Without loss of generality we can assume that $j' = j$, the other cases are estimated analogously.

By the change of variables $\eta = (\eta_1, \eta_2) = 2^{-2j}(\xi_1, \xi_2)$, we obtain

$$\delta_{1,j} \lesssim 2^{2(\lambda-1)j} \sum_{|m|>2^{\epsilon j}} \int_{\mathbb{R}^2} \frac{1}{|\eta|^{2-\lambda}} W^2(\eta) e^{2\pi i \eta^T m} d\eta.$$

Using integration by parts for $N = 1, 2, \ldots$, with respect to η_1, η_2, respectively, yields

$$\begin{aligned}\delta_{1,j} &\lesssim 2^{2(\lambda-1)j} \sum_{\substack{m_1,m_2\neq 0,\\ |m|>2^{\epsilon j}}} \Big| \int_{\mathbb{R}^2} |m_1|^{-N} |m_2|^{-N} \frac{\partial^{2N}}{\partial \eta_1^N \partial \eta_2^N} \Big[\frac{1}{|\eta|^{2-\lambda}} W(\eta) \Big] e^{2\pi i \eta^T m} d\eta \Big| \\ &\le C_N 2^{2(\lambda-1)j} \sum_{|m|>2^{\epsilon j}} |m_1|^{-N} |m_2|^{-N} \\ &\le C_N 2^{2(\lambda-1)j} \sum_{m_1\in\mathbb{Z}} \sum_{|m_2|\ge \frac{2^{\epsilon j}}{2}} |m_1|^{-N} |m_2|^{-N} \\ &\le C_N 2^{2(\lambda-1)j} 2^{-(N-1)(\epsilon j - 1)},\end{aligned}$$

for any arbitrary number $N \in \mathbb{N}$. Note that the boundary terms vanish due to the compact support of $W(\zeta)$. This concludes the claim. ∎

Proposition 2.16 *We have $\delta_{2j} = \circ(2^{-Nj})$, for $\forall N = 1, 2, \ldots$*

Proof. By definition, we have

$$\begin{aligned}\delta_{2,j} &= \sum_{(j',l,k,\iota)\notin\Lambda_{2,j}} |\langle w\mathcal{L}_j, \check{\chi}_\iota * \phi^{\alpha,\iota}_{j',l,k} \rangle| \\ &= \sum_{\substack{\{(j',l,k,\mathrm{h})\in\Delta\}\cup\\ \{(j',l,k,\mathrm{v})\in\Delta, |l|>1\}}} |\langle \widehat{w\mathcal{L}_j}, \chi_\iota \hat{\phi}^{\alpha,\iota}_{j',l,k} \rangle| + \sum_{\substack{(j',l,k,\mathrm{v})\in\Delta,\\ |l|\le 1, |k_2 - lk_1|>2^{\epsilon j}}} |\langle w\mathcal{L}_j, \check{\chi}_\mathrm{v} * \phi^{\alpha,\mathrm{v}}_{j',l,k} \rangle| \\ &= I_1 + I_2, \end{aligned} \tag{2.20}$$

where

$$I_1 = \sum_{\substack{\{(j',l,k,\mathrm{h})\in\Delta\}\cup \\ \{(j',l,k,\mathrm{v})\in\Delta,|l|>1\}}} |\langle \widehat{w\mathcal{L}_j}, \chi_\iota \hat{\phi}^{\alpha,\iota}_{j',l,k}\rangle|, \; I_2 = \sum_{\substack{(j',l,k,\mathrm{v})\in\Delta, \\ |l|\le 1, |k_2 - lk_1|>2^{\epsilon j}}} |\langle w\mathcal{L}_j, \check{\chi}_{\mathrm{v}} * \phi^{\alpha,\mathrm{v}}_{j',l,k}\rangle|.$$

Since $W_j(\xi)W_{j'}(\xi) = 0$ for $|j'-j|>1$ due to the different support we only consider $j' = j$ without loss of generality. Before starting with I_1, we put

$$t^{\mathrm{v}} = (t^{\mathrm{v}}_1, t^{\mathrm{v}}_2) := A^{-j}_{\alpha,\mathrm{v}} S^{-l}_{\mathrm{v}} k = (2^{-\alpha j}k_1, 2^{-2j}(k_2 - lk_1)),$$

$$t^{\mathrm{h}} = (t^{\mathrm{h}}_1, t^{\mathrm{h}}_2) := A^{-j}_{\alpha,\mathrm{h}} S^{-l}_{\mathrm{h}} k = (2^{-2j}(k_1 - lk_2), 2^{-\alpha j}k_2).$$

We have

$$\begin{aligned}
\left|\langle w\mathcal{L}_j, \check{\chi}_\iota * \phi^{\alpha,\iota}_{j,l,k}\rangle\right| &= \left|\langle \widehat{w\mathcal{L}_j}, \chi_\iota \hat{\phi}^{\alpha,\iota}_{j,l,k}\rangle\right| = \left| \int_{\mathbb{R}^2} \hat{w}(\xi_1)\chi_\iota(\xi) W_j(\xi) \overline{\hat{\phi}^{\alpha,\iota}_{j,l,k}(\xi)}\right| \\
&= \left| \int_{\mathbb{R}} e^{2\pi i t^\iota_2 \xi_2} \int_{\mathbb{R}} \hat{w}(\xi_1)\chi_\iota(\xi) W_j(\xi) \hat{\phi}^{\alpha,\iota}_{j,l,0}(\xi) e^{2\pi i t^\iota_1 \xi_1} d\xi_1 d\xi_2 \right| \\
&= \left| \int_{\mathbb{R}} e^{2\pi i t^\iota_2 \xi_2} \int_{\mathbb{R}} \hat{w}(\xi_1)\Theta^\iota_{j,l}(\xi) e^{2\pi i t^\iota_1 \xi_1} d\xi_1 d\xi_2 \right|,
\end{aligned}$$

where $\Theta^\iota_{j,l}(\xi) := \chi_\iota(\xi) W_j(\xi) \hat{\phi}^{\alpha,\iota}_{j,l,0}(\xi)$.

Applying repeated integration by parts twice with respect to $\xi_i, i = 1, 2$, we have

$$\begin{aligned}
\left|\langle w\mathcal{L}_j, \phi^{\alpha,\iota}_{j,l,k}\rangle\right| &= \left| \int_{\mathbb{R}} e^{2\pi i t^\iota_2 \xi_2} \Big[\int_{\mathbb{R}} \frac{\partial^2}{\partial \xi_1^2} [\hat{w}(\xi_1)\Theta^\iota_{j,l}(\xi)] \frac{1}{(2\pi i t^\iota_1)^2} e^{2\pi i t^\iota_1 \xi_1} d\xi_1 \Big] d\xi_2 \right| \\
&\le \frac{C}{|t^\iota_1|^2} \left| \int_{\mathbb{R}} e^{2\pi i t^\iota_2 \xi_2} \int_{\mathbb{R}} \frac{\partial^2}{\partial \xi_1^2} [\hat{w}(\xi_1)\Theta^\iota_{j,l}(\xi)] e^{2\pi i t^\iota_1 \xi_1} d\xi_1 d\xi_2 \right| \\
&\le C|t^\iota_1|^{-2} \int_{\mathbb{R}} \int_{\mathbb{R}} \left| \frac{\partial^2}{\partial \xi_1^2} [\hat{w}(\xi_1)\Theta^\iota_{j,l}(\xi)] \right| d\xi_1 d\xi_2. \qquad (2.21)
\end{aligned}$$

Similarly, we obtain

$$\left|\langle w\mathcal{L}_j, \phi^{\alpha,\iota}_{j,l,k}\rangle\right| \le C|t^\iota_2|^{-2} \int_{\mathbb{R}} \int_{\mathbb{R}} \left| \frac{\partial^2}{\partial \xi_2^2} [\hat{w}(\xi_1)\Theta^\iota_{j,l}(\xi)] \right| d\xi_1 d\xi_2 \qquad (2.22)$$

$$\left|\langle w\mathcal{L}_j, \phi^{\alpha,\iota}_{j,l,k}\rangle\right| \le C|t^\iota_1|^{-2}|t^\iota_2|^{-2} \int_{\mathbb{R}} \int_{\mathbb{R}} \left| \frac{\partial^4}{\partial \xi_1^2 \partial \xi_2^2} [\hat{w}(\xi_1)\Theta^\iota_{j,l}(\xi)] \right| d\xi_1 d\xi_2. \qquad (2.23)$$

Therefore, we have

$$|t^\iota_1|^2 \left|\langle w\mathcal{L}_j, \phi^{\alpha,\iota}_{j,l,k}\rangle\right| \overset{(2.21)}{\le} C \int_{\mathbb{R}} \int_{\mathbb{R}} \left| \frac{\partial^2}{\partial \xi_1^2} [\hat{w}(\xi_1)\Theta^\iota_{j,l}(\xi)] \right| d\xi_1 d\xi_2$$

$$|t^\iota_2|^2 \left|\langle w\mathcal{L}_j, \phi^{\alpha,\iota}_{j,l,k}\rangle\right| \overset{(2.22)}{\le} C \int_{\mathbb{R}} \int_{\mathbb{R}} \left| \frac{\partial^2}{\partial \xi_2^2} [\hat{w}(\xi_1)\Theta^\iota_{j,l}(\xi)] \right| d\xi_1 d\xi_2$$

$$|t_1^\iota|^2|t_2^\iota|^2\left|\langle w\mathcal{L}_j, \phi_{j,l,k}^{\alpha,\iota}\rangle\right| \overset{(2.23)}{\leq} C\int_{\mathbb{R}}\int_{\mathbb{R}}\left|\frac{\partial^4}{\partial\xi_1^2\partial\xi_2^2}[\hat{w}(\xi_1)\Theta_{j,l}^\iota(\xi)]\right|d\xi_1 d\xi_2.$$

These imply

$$(1+|t_1^\iota|^2+|t_2^\iota|^2+|t_1^\iota|^2|t_2^\iota|^2)\left|\langle w\mathcal{L}_j, \phi_{j,l,k}^{\alpha,\iota}\rangle\right| = \langle|t_1^\iota|\rangle^2\langle|t_2^\iota|\rangle^2\left|\langle w\mathcal{L}_j, \phi_{j,l,k}^{\alpha,\iota}\rangle\right|$$

$$\begin{aligned}\leq\ & C\int_{\mathbb{R}^2}\left|\hat{w}(\xi_1)\Theta_{j,l}^\iota(\xi)\right| + \left|\frac{\partial^2}{\partial\xi_1^2}[\hat{w}(\xi_1)\Theta_{j,l}^\iota(\xi)]\right| + \left|\frac{\partial^2}{\partial\xi_2^2}[\hat{w}(\xi_1)\Theta_{j,l}^\iota(\xi)]\right| \\ & + \left|\frac{\partial^4}{\partial\xi_1^2\partial\xi_2^2}[\hat{w}(\xi_1)\Theta_{j,l}^\iota(\xi)]\right|d\xi = C\int_{\mathbb{R}}\Gamma(\xi_2)d\xi_2,\end{aligned}$$

where $\Gamma(\xi_2) :=$
$\int_{\mathbb{R}}\left|\hat{w}(\xi_1)\Theta_{j,l}^\iota(\xi)\right| + \left|\frac{\partial^2}{\partial\xi_1^2}[\hat{w}(\xi_1)\Theta_{j,l}^\iota(\xi)]\right| + \left|\frac{\partial^2}{\partial\xi_2^2}[\hat{w}(\xi_1)\Theta_{j,l}^\iota(\xi)]\right| + \left|\frac{\partial^4}{\partial\xi_1^2\partial\xi_2^2}[\hat{w}(\xi_1)\Theta_{j,l}^\iota(\xi)]\right|d\xi_1.$

Now we investigate the term Γ further. By the definition, we have $\hat{\psi}_{j,l,k}^{\alpha,\iota}$ has compact support in the trapezoidal regions by (2.9), (2.10). This implies that for any $\xi \in \operatorname{supp}\Theta_{j,l}^\iota$, with $\iota = \mathrm{v}$, or $\iota = \mathrm{h}$, $|l| > 1$, there exist constants $C_1, C_2 > 0$ such that

$$\xi_1 \in I_{j,l} := [-C_2 l 2^{\alpha j}, -C_1 l 2^{\alpha j}] \cup [C_2 l 2^{\alpha j}, C_1 l 2^{\alpha}].$$

Thus, we obtain the decay estimate of $\hat{w}^{(n)}(\xi_1), \xi_1 \in I_{j,l}, n = 0, 1, 2$, by

$$|\hat{w}^{(n)}(\xi_1)| \leq C_N\langle|2^{\alpha j}|\rangle^{-N},\ \forall N \in \mathbb{N}_0. \tag{2.24}$$

For an illustration, we refer to Fig. 2.4

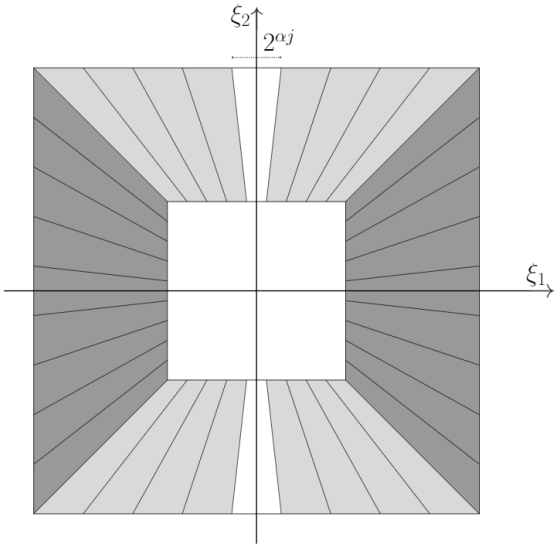

Figure 2.4: Frequency support of shearlets with $\iota = \mathrm{v}, |l| > 1$ (gray) and shearlets with $\iota = \mathrm{h}$ (black).

By a direct computation, we also have ${\Theta^{\iota}_{j,l}}^{(n)} \leq C_n, n = 0,1,2$. Combining this with (2.24), we obtain $\int_{\mathbb{R}} \Gamma(\xi_2) d\xi_2 \leq C_N \langle |2^{\alpha j}| \rangle^{-N}$, $\forall N \in \mathbb{N}_0$. Thus,

$$\left| \langle w\mathcal{L}_j, \phi^{\alpha,\iota}_{j,l,k} \rangle \right| \leq C_N \langle |2^{\alpha j}| \rangle^{-N} \langle |t^{\iota}_1| \rangle^2 \langle |t^{\iota}_2| \rangle^2.$$

This implies

$$I_1 \leq C_N \langle |2^{\alpha j}| \rangle^{-N} \sum_{\substack{(j,l,k,\mathrm{h}) \cup \\ \{\iota = \mathrm{v}, |l|>1\}}} \langle |t^{\iota}_1| \rangle^{-2} \langle |t^{\iota}_2| \rangle^{-2}. \tag{2.25}$$

In addition, we have

$$\begin{aligned} \sum_{k_1,k_2 \in \mathbb{Z}} \langle |t^{\mathrm{h}}_1| \rangle^{-2} \langle |t^{\mathrm{h}}_2| \rangle^{-2} &= \sum_{k_1,k_2 \in \mathbb{Z}} \langle |2^{-2j}(k_1 - lk_2)| \rangle^{-2} \langle |2^{-\alpha j} k_2| \rangle^2 \\ &= \sum_{k_1,k_2 \in \mathbb{Z}} \langle |2^{-2j} k_1| \rangle^{-2} \langle |2^{-\alpha j} k_2| \rangle^{-2} \\ &\leq \int_{\mathbb{R}} \langle |2^{-2j} t_1| \rangle^{-2} dt_1 \int_{\mathbb{R}} \langle |2^{-\alpha j} t_2| \rangle^{-2} dt_2 \\ &\leq C 2^{(2+\alpha)2j}. \end{aligned} \tag{2.26}$$

Similarly, we obtain

$$\sum_{k_1,k_2 \in \mathbb{Z}} \langle |t^{\mathrm{v}}_1| \rangle^{-2} \langle |t^{\mathrm{v}}_2| \rangle^{-2} \leq C 2^{(2+\alpha)2j}. \tag{2.27}$$

In addition, we have

$$|l| \leq \lceil 2 \cdot 2^{(2-\alpha)j} \rceil. \tag{2.28}$$

Combining (2.25), (2.26), (2.27), and (2.28) we obtain

$$I_1 \leq C_N \lceil 2 \cdot 2^{(2-\alpha)j} \rceil \langle |2^{\alpha j}| \rangle^{-N}. \tag{2.29}$$

We now turn our attention to the term I_2. We have

$$\begin{aligned} |w\mathcal{L}_j(x)| &= \left| \int_{\mathbb{R}} w(y_1) F_j(x - (y_1, 0)) dy_1 \right| \\ &\leq \left| \int_{\mathbb{R}} |w(y_1)| \cdot 2^{4j} |\check{W}(2^{2j}(x - (y_1, 0)))| dy_1 \right| \\ &\leq \int_{\mathbb{R}} |w(y_1)| \cdot C_N 2^{4j} \langle |2^{2j} x_2| \rangle^{-N} \langle |2^{2j}(y_1 - x_1)| \rangle^{-N} dy_1 \\ &= C_N 2^{4j} \langle |2^{2j} x_2| \rangle^{-N} [|w * \langle 2^{2j}[\cdot]| \rangle^{-N}](x_1) \\ &= C_N 2^{4j} \langle |2^{2j} x_2| \rangle^{-N} \tau_{N,j}(x_1), \end{aligned} \tag{2.30}$$

where $\tau_{N,j}(x_1) := [|w * \langle 2^{2j}[\cdot]| \rangle^{-N}](x_1)$, $x = (x_1, x_2) \in \mathbb{R}^2$. Combining (2.30) with Lemma 2.12, we obtain

$$I_2 \leq C_N \sum_{\substack{l \in \{-1,0,1\}, \\ |k_2 - lk_1| > 2^{\epsilon j}}} \int_{\mathbb{R}^2} 2^{4j} \langle |2^{2j} x_2| \rangle^{-N} \tau_{N,j}(x_1) 2^{(\alpha+2)j/2} \langle |2^{\alpha j} x_1 - k_1| \rangle^{-N}$$

$$
\begin{aligned}
&\cdot\langle|l2^{\alpha j}x_1+2^{2j}x_2-k_2|\rangle^{-N}dx\\
=\;& C_N 2^{(6-\alpha)j/2}\sum_{\substack{l\in\{-1,0,1\},\\ |k_2-lk_1|>2^{\epsilon j}}}\int_{\mathbb{R}^2}\langle|x_2|\rangle^{-N}\tau_{N,j}(2^{-\alpha j}(x_1+k_1))\langle|x_1|\rangle^{-N}\\
&\cdot\langle|lx_1+lk_1+x_2-k_2|\rangle^{-N}dx\\
\le\;& C_N 2^{(6-\alpha)j/2}\sum_{\substack{l\in\{-1,0,1\},\\ |k_2-lk_1|>2^{\epsilon j}}}\int_{\mathbb{R}}\tau_{N,j}(2^{-\alpha j}(x_1+k_1))\langle|x_1|\rangle^{-N}\cdot\\
&\langle|lx_1+lk_1-k_2|\rangle^{-N}dx_1.
\end{aligned}
$$

The last equality comes from the fact that there exists a constant $C_N>0$ satisfying

$$
\int_{\mathbb{R}}\langle|x|\rangle^{-N}\langle|x+a|\rangle^{-N}dx\le C_N\langle|a|\rangle^{-N},\quad\forall a\in\mathbb{R}. \tag{2.31}
$$

In addition, we have

$$
\begin{aligned}
\sum_{k_1\in\mathbb{Z}}\tau_{N,j}(2^{-\alpha j}(x_1+k_1)) &= \sum_{k_1\in\mathbb{Z}}\int_{\mathbb{R}}|w(y_1)|\langle|2^{2j}(y_1-2^{-\alpha j}(x_1+k_1))|\rangle^{-N}dy_1\\
&= \sum_{k_1\in\mathbb{Z}}\int_{\mathbb{R}}|w(y_1)|\langle|2^{(2-\alpha)j}(k_1+x_1-2^{\alpha j}y_1)|\rangle^{-N}dy_1\\
&\overset{\alpha\le 2}{\le} \int_{\mathbb{R}}|w(y_1)|\Big(\sum_{k_1\in\mathbb{Z}}\langle|k_1+x_1-2^{\alpha j}y_1|\rangle^{-N}\Big)dy_1\\
&\le C\int_{\mathbb{R}}|w(y_1)|\Big(\int_{\mathbb{R}}\langle|t+x_1-2^{\alpha j}y_1|\rangle^{-N}dt\Big)dy_1\\
&= C\int_{\mathbb{R}}|w(y_1)|\Big(\int_{\mathbb{R}}\langle|t|\rangle^{-N}dt\Big)dy_1\le C_N.
\end{aligned}
$$

Therefore, we obtain

$$
\begin{aligned}
I_2 &\le C_N 2^{(6-\alpha)j/2}\sum_{\substack{l\in\{-1,0,1\},k_2\in\mathbb{Z}\\ |k_2|>2^{\epsilon j}}}\int_{\mathbb{R}}\langle|x_1|\rangle^{-N}\langle|lx_1+k_2|\rangle^{-N}dx_1\\
&\overset{\text{by (2.31)}}{\le} C_N 2^{(-\alpha)j/2}\sum_{k_2\in\mathbb{Z},|k_2|>2^{\epsilon j}}\langle|k_2|\rangle^{-N}dx_1\\
&\le C_N 2^{(6-\alpha)j/2}\int_{t>2^{\epsilon j}}\langle|t|\rangle^{-N}\le C_N 2^{(6-\alpha)j/2}2^{-(N-1)\epsilon j},\quad\forall N\in\mathbb{N}_0.
\end{aligned} \tag{2.32}
$$

Finally, combining (2.29), (2.32) with (2.20) concludes the claim.

■

2.4.3 Proof of Main Theorem

Now we are well prepared to provide a proof for Theorem 2.11.

Proof. Applying Theorem 2.7 and Propositions 2.13, 2.14, 2.15, 2.16, we obtain

$$\|\mathcal{P}_j^\star - \mathcal{P}_j\|_2 + \|\mathcal{C}_j^\star - w\mathcal{L}_j\|_2 = o(2^{-Nj}) \to 0, \quad j \to \infty. \tag{2.33}$$

Since (2.33) holds for arbitrarily large number $N \in \mathbb{N}$ we are left to estimate the lower bounds of $\|\mathcal{P}_j\|_2$ and $\|w\mathcal{L}_j\|_2$. Without loss of generality, we assume that $\mathcal{P} = \frac{1}{|x|^\lambda}, 0 < \lambda < 2$. The more general case follows by combining translation invariance with many uses of the triangle inequality. By Plancherel's theorem and $\widehat{(\frac{1}{|x|^\lambda})} = \frac{1}{|\xi|^{2-\lambda}}$, we have

$$\begin{aligned} \|\mathcal{P}_j\|_2^2 = \|F_j * \frac{1}{|x|^\lambda}\|_2^2 &= \int_{\mathcal{A}_j} W_j^2(\xi) \frac{1}{|\xi|^{2(2-\lambda)}} d\xi \\ &\gtrsim c \cdot 2^{(2-2\lambda)2j}. \end{aligned}$$

In addition,

$$\begin{aligned} \|w\mathcal{L}_j\|_2^2 &= \int_{\mathcal{A}_j} \hat{w}^2(\xi_1) W_j^2(\xi) d\xi \\ &\gtrsim \int_{\xi_1 \in \mathbb{R}} \hat{w}^2(\xi_1) d\xi_1 \int_{2^{2j-5}}^{2^{2j-2}} C d\xi_2 \\ &\gtrsim C 2^{2j}. \end{aligned}$$

This finishes the proof. ∎

2.5 Conclusions and Further Discussion

Our main results, Theorem 2.7 and Theorem 2.11, show that the ground truth components are under reasonable assumptions perfectly recovered at fine scales by Algorithm 1. For a practical multiscale approach, we first apply the proposed algorithm for each filtered subband image at each scale and then recover the whole signal using the reconstruction formula (2.17). These theorems might be extended in several ways. Here we focus on separating pointlike and curvelike structures, but our approach holds for other types of geometric components as well as any frames providing sparse representation. We can therefore use wavelets, curvelets, Gabor frames, as well as other sparsifying systems for representing components to be separated. A similar asymptotic separation result can be achieved by using such sparsifying systems if they provide sufficient small cluster sparsity and cluster coherence.

In our later chapters, we will extend our theory to the case of multiple-component separation. Our results might also be applicable to images that are corrupted by noise. In addition, other algorithms such as thresholding methods [Kut14] or l_1-minimization with an additional regularization term [KL12b] which is effective for image separation in empirical work can be considered in our future study.

3

Problem of Image Inpainting

This chapter is devoted to problem of recovering missing content in images. As presented in the introduction section, texture is a ubiquitous visual phenomenon in many machine vision as well as medical imaging applications, see Fig. 3.1 for some examples of texture. We therefore restrict our focus on texture images in our analysis after introducing the general problem of image inapainting.

The rest of this chapter is organized as follows. We first start with a quick overview of results in [KKZ14], the authors presented there asymptotic results for inpainting images governed by edges. Motivated from [KKZ14], we formulate the problem of image inpainting and propose an algorithm for solving this task in Section 3.2. We then provide a theoretical guarantee for the abstract model of image inpainting. Next, we introduce the model of texture and missing space in Section 3.3. Based on that setting, we transfer the theory to prove the success of texture inpainting and derive an L^2-error estimate of the reconstruction for the whole signal in Section 3.4.

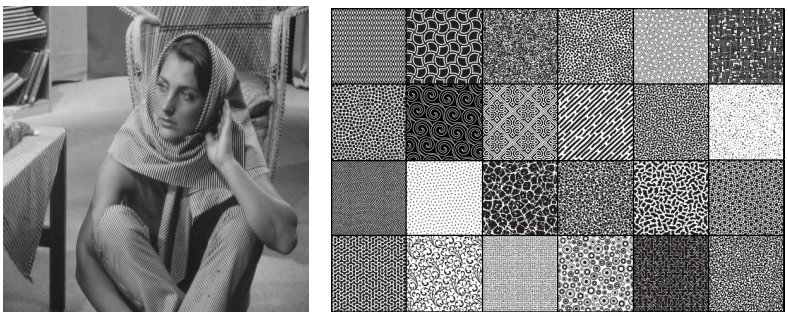

Figure 3.1: Left: Barbara image. Right: Some popular texture samples.

3.1 Results on Images Governed by Edges

In order to recover the missing parts in an image, various strategies have been applied in the past, with recovery performance varying considerably depending on the image type and geometry of the missing data. King et. al. introduced in [KKZ14] a multiscale analysis framework to provide a deeper understanding of such an image restoration challenge and showed that a shearlet based inpainting approach outperforms wavelets where the line singularities is considered as the main image model. There, the original image is decomposed into sub-images using filtered sub-bands at each scale. Then the main result shows that at fine scales precise inpainting can be obtained for the line singularity provided that the size of the missing strip is asymptotically comparable to the size of the

analyzing functions. Theoretically, under some suitable assumptions we have

$$\frac{\|L_j - w\mathcal{L}_j\|_2}{\|w\mathcal{L}_j\|_2} \longrightarrow 0, \quad j \to \infty,$$

where L_j denotes the recovered image of the l_1 minimization algorithm and $w\mathcal{L}_j$ denotes the line singularity. Another remarkable result is about thresholding algorithm where shearlets are shown to better inpaint missing part for the line singularity, we would like to refer the reader to see [KKZ14] for more details.

3.2 Texture Inpainting- a Global Approach

Motivated from previous section's results, we present in this section the general theory for the problem of image inpainting and propose a theoretical guarantee for the success of the l_1 minimization algorithm as the recover strategy. A key point we want to focus on in our analysis is that real images often contain noise. This therefore requires a need for denoising methods which will also be included in this section. We first start with the following problem statement.

3.2.1 Formulation of Image Inpainting

Given an image that is corrupted or incomplete, we aim to reconstruct the groundtruth signal in a plausible way with the knowledge of the known part. Namely, let f be the signal of interest we assume that the known part $P_K f$ is given to us. For a noise-free situation, the problem of image inpainting is formulated as follows

$$\text{Find } f^* \in \mathcal{H} \text{ to minimize } \|f^* - f\|_{\mathcal{H}}, \text{ subject to } P_K f^* = P_K f. \tag{3.1}$$

For images with additive noise, we assume that the observed part is given by $\tilde{f} = P_K f + \eta$, where η is unknown and characterized by noise. The formulation of the inpainting problem is given by

$$\text{Find } f^* \in \mathcal{H} \text{ to minimize } \|f^* - f\|_{\mathcal{H}}, \text{ subject to } P_K f^* = P_K f + \eta. \tag{3.2}$$

In this situation, noise is often assumed to be small.

We consider the inpainting problem of model (3.2) in our analysis and later assume that f is a pure texture image. It should be also mentioned that for corrupted images which are composed of several different structures, first step is to separate them into their underlying components before analyzing each component separately. For instance, this task can be done by geometric separation techniques [Kut13; FHMZ17] or texture extraction methods [Rod12; VP19].

3.2.2 Recovery Algorithm

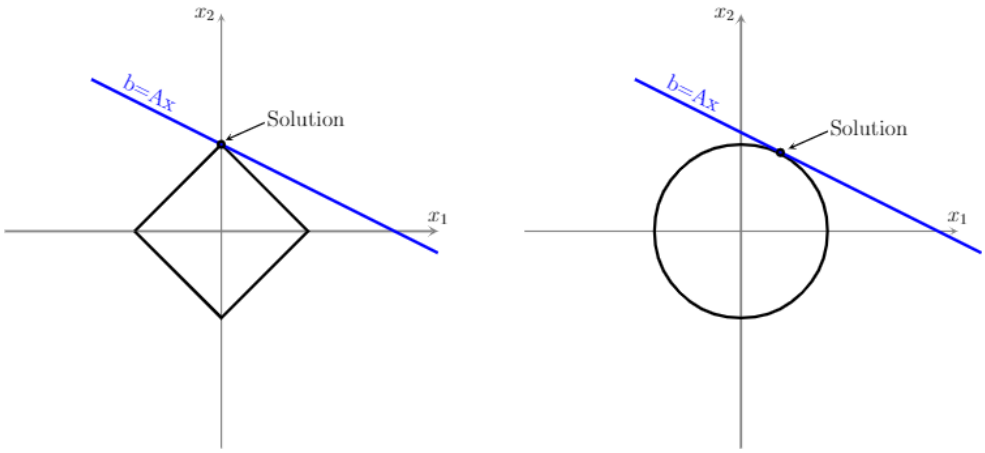

Figure 3.2: Difference between l_1 and l_2 minimization for finding sparse solutions.

Inpainting techniques are often to exploit significant information surrounding the region to be inpainted. Many algorithms have been introduced in the past to perform inpainting task automatically. Among them, *basic pursuit* model has been widely used in applications. In this compressed sensing approach, the sparsity of the signal under a certain sparsifying system is utilized to recover lost information. Given $b \in \mathbb{R}^m$ and measurement matrix $A \in \mathbb{R}^{m\times n}$, $m < n$, basic pursuit model is given by

$$\min_{x\in\mathcal{H}} \|x\|_1, \text{ subject to } Ax = b.$$

This model is particularly suited to solve the problem (3.1) and it also refers to the compressibility of the signal x since l_1 minimization tends to find sparse solutions. For an illustration, Fig. 3.2 shows how basic pursuit provides sparse solutions rather than l_2 minimization.

Another approach known as *basic pursuit denoising* is to deal with (3.2) for the reduction of noise or reconstruction of lossy data. This model has the form of

$$\min_{x\in\mathcal{H}} \|x\|_1 + \lambda\|Ax - b\|_2^2.$$

In our study, we introduce the following algorithm with a theoretical guarantee for the success of the reconstruction.

Algorithm 3.1 Image inpainting

Input: an observed image f, a frame $\Phi = \{\phi_i\}_{i\in I}$. **Compute:**

$$f^\star = \underset{u\in L^2(\mathbb{R}^2)}{\operatorname{argmin}} \|\Phi^* u\|_1 + \lambda\|P_K(u - f)\|_2. \tag{3.3}$$

Output: reconstructed image $f^\star$.

We also intend to apply compressed sensing technique in order to utilize the sparsity of the signal to be inpainted. One of the advantages of this algorithm is that it is capable of handling additive noise. In addition, we would like to remark that if λ is sufficiently large, for instance $\lambda = +\infty$, the optimization problem (3.3) becomes (0.1) which appeared in some papers in the literature where a multi-scale approach was used [KKZ14; KDJ20].

3.2.3 Theoretical Analysis Tools

Cluster coherence was introduced in [DK13] to solve the geometric separation problem. This notion is then applied to image inpainting in [KKZ14]. There, given a Parseval frame $\Phi = \{\phi\}_{i\in I}$ for a Hilbert space $\mathcal{H}$ and set of indexes Λ the cluster coherence is defined by $\max_{j\in I} \sum_{i\in\Lambda} |\langle P_M\phi_i, \phi_j\rangle|$. Motivated by the triangle inequality which leads to

$$\max_{j\in I} |\langle \sum_{i\in\Lambda} P_M\phi_i, \phi_j\rangle| \leq \max_{j\in I} \sum_{i\in\Lambda} |\langle P_M\phi_i, \phi_j\rangle|,$$

we generalize this notion to the use of general frames and modify it by putting the absolute value into the inner product to make the cluster coherence smaller. Here we would like to emphasize that the smaller cluster coherence we have the better error bound is derived which will be later shown in Proposition 3.4.

Definition 3.2 Let $\Phi = \{\phi\}_{i\in I}$ be a frame. The *cluster coherence* associated with the set of indexes $\Lambda \subset I$ is defined by

$$\mu_c(\Lambda, P_M\Phi; \Phi) = \max_{j\in I} |\langle \sum_{i\in\Lambda} P_M\phi_i, \phi_j\rangle|.$$

Lemma 3.3 *We have* $\kappa := \sup_{f\in L^2(\mathbb{R}^2)} \frac{\|\mathbb{1}_\Lambda \Phi^*(P_M f)\|_1}{\|\Phi^* f\|_1} \leq \inf_{\Phi^d\in\mathbb{D}_\Phi} \mu_c(\Lambda, P_M\Phi; \Phi^d)$.

Proof. For $f \in L^2(\mathbb{R}^2), \Phi^d = \{\phi_i^d\}_{i\in I} \in \mathbb{D}_\Phi$, by definition we have $f = \sum_{i\in I}\langle f, \phi_i\rangle\phi_i^d$. In the other words, $f = \Phi^d\Phi^* f = \Phi^d\alpha$, where $\alpha := \Phi^* f$. This leads to

$$\begin{aligned}
\|\mathbb{1}_\Lambda\Phi^* P_M f\|_1 &= \|\mathbb{1}_\Lambda\Phi^* P_M\Phi^d\alpha\|_1 = \|\mathbb{1}_\Lambda(P_M\Phi)^*\Phi^d\alpha\|_1 \\
&\leq \sum_{i\in\Lambda}\Big(\sum_{j\in I} |\langle P_M\Phi_i, \Phi_j^d\rangle||\alpha_j|\Big) \\
&= \sum_{j\in I}\Big(\sum_{i\in\Lambda} |\langle P_M\Phi_i, \Phi_j^d\rangle|\Big)|\alpha_j| \leq \mu_c(\Lambda, P_M\Phi; \Phi^d)\|\alpha\|_1 \\
&= \mu_c(\Lambda, P_M\Phi; \Phi^d)\|\Phi^* f\|_1. \qquad (3.4)
\end{aligned}$$

Since (3.4) holds for $\forall\Phi^d \in \mathbb{D}_\Phi$ this concludes the claim. ∎

Proposition 3.4 *Let $\Phi = \{\phi_i\}_{i\in I}$ be a frame for $\mathcal{H} = L^2(\mathbb{R}^2)$ with frame bounds (A, B), and f be the groundtruth signal. Given $\delta > 0$, we assume that there exists $\Lambda \subset I$ such*

that $\|\mathbb{1}_{\Lambda^c}\Phi^*\|_1 \leq \delta$. *If* $\mu_c := \min_{\phi^d \in \mathbb{D}_\Phi} \mu_c(\Lambda, P_h\Phi; \Phi^d) < 1/2$ *and* $\sum_{i\in\Lambda} \|\phi_i\|_2 \leq \frac{\lambda}{2}$, *then the minimizer* f^* *of* (3.3) *satisfies*

$$\|f^* - f\|_2 \leq \frac{2\delta}{A(1-2\mu_c)}. \tag{3.5}$$

Proof. We first observe that

$$\|f^\star - f\|_2 \leq \frac{1}{A}\|\Phi^*(f^\star - f)\|_2 \leq \frac{1}{A}\|\Phi_1^*(f^\star - f)\|_1.$$

For convenience, we set $z = P_K(f^\star - f)$. By definition and triangle inequality, we have

$$\begin{aligned}
\|\Phi^*(f^\star - f)\|_1 &= \|\mathbb{1}_\Lambda\Phi^*(f^\star - f)\|_1 + \|\mathbb{1}_{\Lambda^c}\Phi^*(f^\star - f)\|_1 \\
&\leq \|\mathbb{1}_\Lambda\Phi^* z\|_1 + \|\mathbb{1}_\Lambda\Phi^* P_M(f^\star - f)\|_1 + \|\mathbb{1}_{\Lambda^c}\Phi^* f^\star\|_1 + \delta \\
&\leq \|\mathbb{1}_\Lambda\Phi^* z\|_1 + \kappa\|\Phi^*(f^\star - f)\|_1 + \|\mathbb{1}_{\Lambda^c}\Phi^* f^\star\|_1 + \delta \\
&= \|\mathbb{1}_\Lambda\Phi^* z\|_1 + \kappa\|\Phi^*(f^\star - f)\|_1 + \|\Phi^* f^\star\|_1 - \|\mathbb{1}_\Lambda\Phi^* f^*\|_1 + \delta \\
&\leq \|\mathbb{1}_\Lambda\Phi^* z\|_1 + \kappa\|\Phi^*(f^\star - f)\|_1 + \|\Phi^* f^\star\|_1 + \|\mathbb{1}_\Lambda\Phi^*(f^* - f)\|_1 \\
&\quad - \|\mathbb{1}_\Lambda\Phi^* f\|_1 + \delta \\
&\leq 2\|\mathbb{1}_\Lambda\Phi^* z\|_1 + 2\kappa\|\Phi^*(f^\star - f)\|_1 + \|\Phi^* f^\star\|_1 - \|\mathbb{1}_\Lambda\Phi^* f\|_1 + \delta \\
&\leq 2\|\mathbb{1}_\Lambda\Phi^* z\|_1 + 2\kappa\|\Phi^*(f^\star - f)\|_1 - \lambda\|z\|_2 + 2\delta.
\end{aligned} \tag{3.6}$$

where the last inequality follows from the fact that $f^\star$ is a solution of (3.3). In addition, we have

$$\|\mathbb{1}_\Lambda\Phi^* z\|_1 = \sum_{i\in\Lambda} |\langle \Phi_i, z\rangle| \leq \Big(\sum_{i\in\Lambda} \|\Phi_i\|_2\Big)\|z\|_2. \tag{3.7}$$

Combining (3.6), (3.7) and the assumption $\sum_{i\in\Lambda} \|\phi_i\|_2 \leq \frac{\lambda}{2}$, we obtain

$$\|\Phi^*(f^\star - f)\|_1 \quad \leq \quad 2\kappa\|\Phi^*(f^\star - f)\|_1 + 2\delta.$$

This leads to

$$\|\Phi^*(f^\star - f)\|_1 \leq \frac{2\delta}{1-2\kappa}.$$

The claim follows by Lemma 3.3. ∎

Let us now see how this proposition can be used in applications. As a result, the estimates of δ and $\mu_c(\Lambda, P_h\Phi, \Phi)$ measure whether a Parseval frame Φ should be used in Algorithm 3.1. If we can choose the set of significant coefficients Λ such as both the approximation error and the cluster coherence are negligible, we derive a success of our algorithm by (3.5). Clearly, the correct choice of Λ plays a vital role in this approach. If we choose Λ too large we will get very small δ but we might loose control over the cluster coherence. In contrast, if we choose Λ too small we might get very good cluster coherence but the approximation error can be large in this case. This implies that the chosen frames should be well adapted to represent the signal of interest, i.e., a relatively small set Λ can be used to well approximate f. This is therefore possible to make both δ and

$\mu_c(\Lambda, P_h\Phi; \Phi)$ small.

3.3 Image Model Settings

3.3.1 Model of Texture

Despite the fact that texture is an important component of real world images it is still a challenging area of research to define this notion precisely. A major reason for this is that natural textures often exhibit contradictory features, such as regularity versus randomness, uniformity versus distortion, which are difficult to describe in a unified way. Since the definition of texture varies among researchers, it is important to imply the characteristics of texture such as regularity, directionality, coarseness, roughness, and density. Motivated from [Kut13; DLK22], we present the following model of texture.

Definition 3.5 Let $0 \not\equiv \tilde{g} \in L^2(\mathbb{R}^2)$ be a window satisfying $\hat{\tilde{g}} \in C^\infty(\mathbb{R}^2)$, $\operatorname{supp} \hat{\tilde{g}} \in [-1/2, 1/2]^2$. For the subset of Fourier elements $I_T \subseteq \mathbb{Z}^2$, a model of texture is then defined by

$$\mathcal{T}(x) = \sum_{n \in I_T} d_n \tilde{g}(x) e^{2\pi i x^\top n}, \tag{3.8}$$

where $(d_n)_{n\in\mathbb{Z}^2}, d_n \neq 0$ denotes a bounded sequence of complex numbers.

In our analysis, we assume that the size of the index set I_T is not too large and comparable with the size of the missing part by

$$\# I_T \leq h^{-\epsilon/3}. \tag{3.9}$$

Intuitively, if the size gap h is large the inpainting task is more challenging so we simplify the model of texture to guarantee the success of the reconstruction. In contrast, if the size gap h goes finer we can successfully inpaint the missing content of a more complex texture model. The next lemma shows that the energy of texture is not too small.

Lemma 3.6 *There exists a constant $C > 0$ such that the following holds*

$$\|\mathcal{T}\|_2 \geq C.$$

Proof. By Plancherel's theorem, we have

$$\begin{aligned} \|\mathcal{T}\|_2^2 &= \langle \hat{\mathcal{T}}(x), \hat{\mathcal{T}}(x) \rangle \\ &= \Big\langle \sum_{n\in I_T} d_n \hat{\tilde{g}}(\xi - n), \sum_{n'\in I_T} d_{n'} \hat{\tilde{g}}(\xi - n') \Big\rangle \\ &= \int_{\mathbb{R}^2} \sum_{n\in I_T} |d_n|^2 \hat{\tilde{g}}^2(\xi - n) d\xi. \end{aligned}$$

Here the last equality is due to the fact that $\operatorname{supp} \hat{\tilde{g}} = [-1/2, 1/2]^2$. By applying the

change of variable $\eta = \xi - n$, there exists a constant $C > 0$ such that

$$\|\mathcal{T}\|_2^2 = \sum_{n \in I_T} |d_n|^2 \cdot \int_{\mathbb{R}^2} \hat{\mathcal{G}}^2(\eta) d\eta \geq C.$$

This finishes the proof. ∎

3.3.2 Missing Part Model

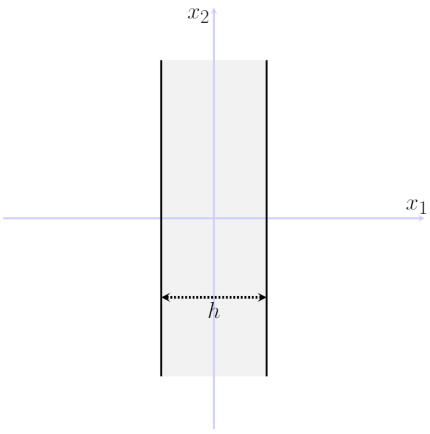

Figure 3.3: Model of the missing trip at scale j.

In many applications, image data is not densely sampled in all coordinates, which might be due to changes in environmental factors, missing sensors or economic limitations. For instance, seismic data [HH08; HFH10] in situation of missing sensor or land development leads to white trips at places corresponding with missing data in the output images.

In contrast to blind inpainting where it does not require the position of the missing regions, we assume that the missing part is known to us. Motivated from seismic data, we choose the model of missing space to be

$$\mathcal{M}_h = \{x = (x_1, x_2) \in \mathbb{R}^2 \mid |x_1| \leq h\}.$$

Associated with this missing space, we define by $P_h = \mathbb{1}_{\{|x_1| \leq h\}}$ the orthogonal projection on $\mathcal{M}_h$, where $\mathbb{1}_A(x) = \begin{cases} 0, & x \notin A \\ 1 & x \in A \end{cases}$ for a measurable subset $A \subset \mathbb{R}^2$. We refer to Fig. 3.3 for an illustration. Given the observed signal $(1 - P_h)f$, we now aim to recover f.

3.4 Main Result

3.4.1 Set of Significant Gabor Coefficients

In what follows, we fix a constant $\epsilon > 0$ and the set of significant Gabor coefficients is chosen to be

$$\Lambda = B_h \times I_T^{\pm},$$

where $B_r = \{m \in \mathbb{Z}^2 \mid |m| \leq r^{-\epsilon/4}\}$, $I_T^{\pm} = \{n \in \mathbb{Z}^2 \mid \exists n' \in I_T, |n - n'| \leq 1\}$. We would like to remark that the key ingredient of our theoretical analysis is the choice of this set and it is just an analyzing tool which allows us to derive an error estimate of the reconstruction by Algorithm 3.1. Roughly speaking, we intend to use the theoretical guarantee (3.5) in Proposition 3.4. For this, first step is to choose the set of significant coefficients which allows us to give an estimate of the right hand side of (3.5).

3.4.2 A Convergence for Image Inpainting

We now present our main result.

Theorem 3.7 *Let $\mathcal{T}$ be texture of definition (3.8), and $\mathcal{T}^*$ solve (3.3) with $\Phi = \mathcal{G}$ and $\lambda = h^{-\epsilon}$. For each $N = 1, 2, \ldots$, there exists a constant C_N independent of h such that*

$$\frac{\|\mathcal{T}^* - \mathcal{T}\|_2}{\|\mathcal{T}\|_2} \leq C_N h^{\epsilon N}, \tag{3.10}$$

for the sufficiently small gap size h.

The reader should be aware of the fact that the error of the reconstruction should be much smaller than the size of the missing strip to make meaningful inpainting. Since (3.10) holds for any $N \in \mathbb{N}$ we indeed achieve perfect inpainting provided that the gap size h is sufficiently small. The rest of this paper is devoted to the proof of this main theorem.

3.4.3 Proof of Theorem 3.7

We first introduce the following short hand notation in the rest of this paper

$$\langle |x| \rangle = (1 + |x|^2)^{1/2}.$$

The main idea of the proof can be briefly described as follows. We aim to apply the theoretical guarantee as shown in Proposition 3.4. In this sense, we need provide estimates of the error approximation δ and the cluster coherence $\mu_c(\Lambda, P_h\mathcal{G}; \mathcal{G})$. To motivate the idea, let us start with the following lemma.

Lemma 3.8 *There exists a constant C_N for each $N = 1, 2, \ldots$ such that the following holds*

$$|g_{m,n}(x)| \leq C_N \langle |x_1 + \frac{m_1}{2}| \rangle^{-N} \langle |x_2 + \frac{m_2}{2}| \rangle^{-N}, \quad \forall m, n \in \mathbb{Z},$$

and similarly

$$|\tilde{g}(x)| \leq C_N \langle |x_1| \rangle^{-N} \langle |x_2| \rangle^{-N}, .$$

Proof. We first apply the change of variable $\zeta = \xi - n$, we obtain

$$\begin{aligned} |g_{m,n}(x)| &= \left| \int_{\mathbb{R}^2} \hat{g}_{m,n}(\xi) e^{2\pi i \xi^T x} d\xi \right| = \left| \int_{\mathbb{R}^2} \hat{g}(\xi - n) e^{2\pi i \xi^T (x + \frac{m}{2})} d\xi \right| \\ &= \left| e^{2\pi i n^T (x + \frac{m}{2})} \int_{\mathbb{R}^2} \hat{g}(\zeta) e^{2\pi i \zeta^T (x + \frac{m}{2})} d\zeta \right| \end{aligned}$$

$$\leq \Big| \int_{\mathbb{R}^2} \hat{g}(\zeta) e^{2\pi i \zeta^T (x+\frac{m}{2})} d\zeta \Big|.$$

Using integration by parts for $N = 1, 2, \ldots$, with respect to ζ_1, ζ_2, respectively, we have

$$\begin{aligned}
|g_{m,n}(x)| &= \Big| \int_{\mathbb{R}^2} (x_1 + \frac{m_1}{2})^{-N} \frac{\partial^N}{\partial \zeta_1^N} [\hat{g}(\zeta)] e^{2\pi i \zeta^T (x+\frac{m}{2})} d\zeta \Big| \\
&= \Big| \int_{\mathbb{R}^2} (x_1 + \frac{m_1}{2})^{-N} (x_2 + \frac{m_2}{2})^{-N} \frac{\partial^{2N}}{\partial \zeta_1^N \partial \zeta_2^N} [\hat{g}(\zeta)] e^{2\pi i \zeta^T (x+\frac{m}{2})} d\zeta \Big| \\
&\leq |x_1 + \frac{m_1}{2}|^{-N} |x_2 + \frac{m_2}{2}|^{-N} \int_{\mathbb{R}^2} \Big| \frac{\partial^{2N}}{\partial \zeta_1^N \partial \zeta_2^N} [\hat{g}(\zeta)] \Big| d\zeta. \qquad (3.11)
\end{aligned}$$

By the same arguments, we obtain

$$|g_{m,n}(x)| \leq |x_1 + \frac{m_1}{2}|^{-N} \int_{\mathbb{R}^2} \Big| \frac{\partial^N}{\partial \zeta_1^N} [\hat{g}(\zeta)] \Big| d\zeta \qquad (3.12)$$

and

$$|g_{m,n}(x)| \leq |x_2 + \frac{m_2}{2}|^{-N} \int_{\mathbb{R}^2} \Big| \frac{\partial^N}{\partial \zeta_2^N} [\hat{g}(\zeta)] \Big| d\zeta. \qquad (3.13)$$

Note that the boundary terms vanish due to the compact support of $\hat{g}_{m,n}(\zeta)$. Combining (3.11), (3.12), and (3.13), we obtain

$$\begin{aligned}
&\Big(1 + |x_1 + \tfrac{m_1}{2}|^N + |x_2 + \tfrac{m_2}{2}|^N + |x_1 + \tfrac{m_1}{2}|^N |x_2 + \tfrac{m_2}{2}|^N \Big) |g_{m,n}(x)| \\
&= (1 + |x_1 + \frac{m_1}{2}|^N)(1 + |x_2 + \frac{m_2}{2}|^N) |g_{m,n}(x)| \\
&\leq \int_{\mathbb{R}^2} |\hat{g}(\zeta)| + \Big| \frac{\partial^N}{\partial \zeta_1^N} [\hat{g}(\zeta)] \Big| + \Big| \frac{\partial^N}{\partial \zeta_2^N} [\hat{g}(\zeta)] \Big| + \Big| \frac{\partial^{2N}}{\partial \zeta_1^N \partial \zeta_2^N} [\hat{g}(\zeta)] \Big| d\zeta.
\end{aligned}$$

On the other hand, there exists a constant C'_N independent of j such that

$$\int_{\mathbb{R}^2} |\hat{g}(\zeta)| + \Big| \frac{\partial^N}{\partial \zeta_1^N} [\hat{g}(\zeta)] \Big| + \Big| \frac{\partial^N}{\partial \zeta_2^N} [\hat{g}(\zeta)] \Big| + \Big| \frac{\partial^{2N}}{\partial \zeta_1^N \partial \zeta_2^N} [\hat{g}(\zeta)] \Big| d\zeta \leq C'_N.$$

This leads to

$$|g_{m,n}(x)| \leq C'_N \cdot \frac{1}{1 + |x_1 + \frac{m_1}{2}|^N} \frac{1}{1 + |x_2 + \frac{m_2}{2}|^N}.$$

We now observe that there exist C'_N for each $N = 1, 2, \ldots$ satisfying

$$\langle |x_1 + \frac{m_1}{2}| \rangle^N = (1 + |x_1 + \frac{m_1}{2}|^2)^{N/2} \leq C'_N (1 + |x_1 + \frac{m_1}{2}|)^N,$$

$$\langle |x_2 + \frac{m_2}{2}| \rangle^N = (1 + |x_2 + \frac{m_2}{2}|^2)^{N/2} \leq C'_N (1 + |x_2 + \frac{m_2}{2}|)^N.$$

Thus, we obtain

$$|g_{m,n}(x)| \leq C_N \langle |x_1 + \frac{m_1}{2}| \rangle^{-N} \langle |x_2 + \frac{m_2}{2}| \rangle^{-N}.$$

This concludes the claim. ∎

Next, we establish some estimates of the error approximation and the cluster coherence.

Lemma 3.9 *For each $N = 1, 2, \ldots$, there exists C_N such that*

$$\delta := \sum_{(m',n') \notin B_h \times I_T^{\pm}} |\langle \mathcal{T}, g_{m',n'} \rangle| \leq C_N h^N, \forall N \in \mathbb{N}.$$

Proof. Indeed, we first observe that if $n' \notin I_T^{\pm}$, we obtain

$$\begin{aligned} |\langle \mathcal{T}_j, g_{m',n'} \rangle| &= |\langle \hat{\mathcal{T}}_j, \hat{g}_{m',n'} \rangle| \\ &= \int \Big| \sum_{n \in I_T} d_n \hat{\tilde{g}}(\xi - n) \overline{\hat{g}(\xi - n')} e^{-2\pi i \xi^\top \frac{m'}{2}} \Big| \\ &= 0, \end{aligned}$$

where the last equality is due to the different supports of $\hat{g}$ and $\hat{\tilde{g}}$. Therefore, we just need to consider $n' \in I_T^{\pm}, m' \notin B_h$. Lemma 3.8 yields

$$\begin{aligned} \delta &= \sum_{\substack{m' \notin B_h \\ n' \in I_T^{\pm}}} |\langle \mathcal{T}_j, g_{m',n'} \rangle| \leq \sum_{\substack{|m'| > h^{-\epsilon/4} \\ n' \in I_T^{\pm}}} \int_{\mathbb{R}^2} \sum_{n \in I_T} |d_n \tilde{g}(x) e^{2\pi i x^T n}| \cdot |g_{m',n'}(x)| dx \\ &\leq \sum_{\substack{|m'| > h^{-\epsilon j/4} \\ n' \in I_T^{\pm}}} \int_{\mathbb{R}^2} C_N \langle |x_1| \rangle^{-N} \langle |x_2| \rangle^{-N} \langle |x_1 + \frac{m_1'}{2}| \rangle^{-N} \langle |x_1 + \frac{m_2'}{2}| \rangle^{-N} dx \end{aligned}$$

In addition, for each $N = 1, 2, \cdots$, there exists a constant $C_N > 0$ satisfying

$$\int_{\mathbb{R}} \langle |t| \rangle^{-N} \langle |t + a| \rangle^{-N} dt \leq C_N \langle |a| \rangle^{-N}, \quad \forall a \in \mathbb{R}.$$

Thus, we obtain

$$\begin{aligned} \delta &\leq C_N \cdot \#\{n \in I_T^{\pm}\} \cdot \sum_{|m'| > h^{-\epsilon/4}} \langle |\frac{m_1'}{2}| \rangle^{-N} \langle |\frac{m_2'}{2}| \rangle^{-N} \\ &\overset{\text{by (3.9)}}{\leq} C_N \cdot h^{-\epsilon/3} \cdot \int_{\mathbb{R}} \int_{\frac{1}{2} h^{-\epsilon/4}}^{+\infty} \langle |\frac{t_1}{2}| \rangle^{-N} \langle |\frac{t_2}{2}| \rangle^{-N} dt_1 dt_2 \\ &\leq C_N' \cdot h^{-\epsilon/3} \cdot h^{(N-1)\epsilon/4}. \end{aligned}$$

This finishes the proof since the last estimate holds for an arbitrarily large $N \in \mathbb{N}$. ∎

We now turn our attention to the cluster coherence $\mu_c(\Lambda, P_h \mathcal{G}; \mathcal{G})$. An estimate of this term is given by the following lemma.

Lemma 3.10 *We have*

$$\mu_c(\Lambda, P_h \mathcal{G}; \mathcal{G}) = O(h).$$

Proof. Indeed, we assume that the maximum is attained at $(m', n') \in \Lambda$. This leads to

$$\begin{aligned}\mu_c(\Lambda, P_h\mathcal{G}; \mathcal{G}) &= \sum_{(m,n)\in B_h\times I_T^{\pm}} |\langle P_h g_{m,n}, g_{m',n'}\rangle| \\ &= \sum_{(m,n)\in B_h\times I_T^{\pm}} \Big| \int_{-h}^{h}\int_{\mathbb{R}} g_{m,n}(x)\overline{g_{m',n'}(x)}dx\Big| \\ &\leq \sum_{(m,n)\in B_h\times I_T^{\pm}} \int_{-h}^{h}\int_{\mathbb{R}} |g_{m,n}(x)||g_{m',n'}(x)|dx. \end{aligned} \tag{3.14}$$

By Lemma 3.8, we have

$$|g_{m,n}(x)| \leq C_N \cdot \langle|x_1 + \frac{m_1}{2}|\rangle^{-N}\langle|x_2 + \frac{m_2}{2}|\rangle^{-N}, \forall m, n \in \mathbb{Z}^2.$$

Thus, we obtain

$$\begin{aligned}&\int_{-h}^{h}\int_{\mathbb{R}} |g_{m,n}(x)||g_{m',n'}(x)|dx \\ &\leq \int_{-h}^{h}\int_{\mathbb{R}} C_N^2\langle|x_1 + \frac{m_1}{2}|\rangle^{-N}\langle|x_2 + \frac{m_2}{2}|\rangle^{-N}\langle|x_1 + \frac{m_1'}{2}|\rangle^{-N}\langle|x_2 + \frac{m_2'}{2}|\rangle^{-N}dx \\ &= C_N^2\int_{-h}^{h}\int_{\mathbb{R}} \langle|y_1 + \frac{m_1}{2}|\rangle^{-N}\langle|y_2 + \frac{m_2}{2}|\rangle^{-N}\langle|y_1 + \frac{m_1'}{2}|\rangle^{-N}\langle|y_2 + \frac{m_2'}{2}|\rangle^{-N}dy. \end{aligned} \tag{3.15}$$

On the other hand, for each $N = 1, 2, \ldots$ there exist $\tilde{C}_N$ satisfying

$$\sum_m \langle|y_1 + \frac{m_1}{2}|\rangle^{-N}\langle|y_2 + \frac{m_2}{2}|\rangle^{-N} \leq \tilde{C}_N, \text{ and } \int_{\mathbb{R}} \langle|y_2 + \frac{m_2'}{2}|\rangle^{-N}dy_2 \leq \tilde{C}_N. \tag{3.16}$$

Combining (3.14), (3.15), and (3.16), we obtain

$$\begin{aligned}\mu_c(\Lambda_{2,j}, P_j\mathbf{G}; \mathbf{G}) &\leq \sum_{n\in I_T} C_N'' \cdot h \\ &\leq C_N''' \cdot h. \end{aligned}$$

■

Lemma 3.11 *We have* $\sum_{(m,n)\in\Lambda} \|g_{m,n}\|_2 \leq \frac{\lambda}{2} = \frac{1}{2}h^{-\epsilon}$.

Proof. By Lemma 3.8, we have

$$\begin{aligned}\|g_{m,n}\|_2 &= \Big(\int_{\mathbb{R}^2} g_{m,n}^2(x)dx\Big)^{1/2} \\ &\leq C_N\Big(\int_{\mathbb{R}^2}\langle|x_1 + \frac{m_1}{2}|\rangle^{-2N}\langle|x_2 + \frac{m_2}{2}|\rangle^{-2N}dx\Big)^{1/2} \\ &\leq C_N', \quad \forall m, n \in \mathbb{Z}^2. \end{aligned}$$

In addition, by (3.9) we have

$$\#\{(m,n) \in B_h \times I_T^{\pm}\} \leq (h^{-\epsilon/4})^2 \cdot 9h^{-\epsilon/3} = 9h^{-5\epsilon/6}.$$

Thus, we obtain

$$\sum_{(m,n)\in\Lambda} \|g_{(m,n)}\|_2 \leq C_N h^{-5\epsilon/6} \leq \frac{1}{2} h^{-\epsilon},$$

for sufficiently small h. ∎

We are now ready to provide a proof of Theorem 3.7. Indeed, by Proposition 3.4 we obtain

$$\|\mathcal{T}^* - \mathcal{T}\|_2 \leq \frac{2\delta}{1 - 2\mu_c(\Lambda, P_h\mathcal{G}; \mathcal{G})}.$$

Here we have $\sum_{(m,n)\in\Lambda} \|g_{m,n}\|_2 \leq \frac{\lambda}{2} = \frac{1}{2}h^{-\epsilon}$ by Lemma 3.11, and $\mu_c(\Lambda, P_h\mathcal{G}; \mathcal{G}) < 1/2$ for sufficiently small h by Lemma 3.10. In addition, by Lemma 3.9 we have

$$\delta \leq C_N h^N, \quad \forall N \in \mathbb{N}.$$

Combining this with Lemma 3.6 we obtain the statement (3.10). This finishes the proof.

4

Simultaneous Separation and Inpainting

The purpose of this chapter is to deal with the question that: Is it still possible to use one algorithm for both image inpainting and image separation ?. This chapter is a slightly modified version of the paper [DLK22]:

VT. Do, R. Levie, G. Kutyniok, "Analysis of simultaneous inpainting and geometric separation based on sparse decomposition" , Analysis and Applications, Vol. 20, No. 02, pp. 303-352, 2022.

4.1 Motivation

A digital image typically has two or more distinct constituents, e.g., it might contain a cartoon and texture components. A key question is whether we can separate the image into its two components. This task is of interest in many applications, such as compression and restoration [ZP01; SMRR04; SED05]. The separation problem is underdetermined and seems to be impossible to stably solve. However, if we have prior knowledge about the types of geometric components underlying the image, the separation task is possible, as shown in previous papers [DH01; GB03; SED04; SMBED05; BGN08]. Some approaches commonly used in this context for image separation are variational methods, e.g., [VO03; SED05] and PDE-based separation methods [VO03].

More recently, compressed sensing approaches showed that l_1 minimization can stably and precisely solve this problem both theoretically [EB02; DE03; GN03; DET06; DK09; DK13] and empirically [GB03; SMBED05]. The core idea is to use multiple dictionaries, each sparsely representing one geometric part of the image. As opposed to thresholding approaches like [Tro04a], which are harder to analyze, the l_1 minimization approach comes with strong theoretical results.

Another classical problem in imaging science is to restore corrupted or missing parts of images, namely *image inpainting*. Images are often damaged due to different factors including improper storage, chemical processing, or losses of image data during transmission. The problem of image inpainting is of interest in numerous applications, from the restoration of scratched photos and corrupted images, to the removal of selected objects. Image inpainting is an ill-posed problem, so some prior information on the missing part is required here as well. One approach that has been effectively applied to this problem is total variational [BSCB00; BBCSV01; BBS01; CS02]. Variational approaches work well on piecewise smooth images, but generally perform poorly on images that contain a superposition of cartoon and texture. On the other hand, local statistical analysis and prediction have been shown to perform well at inpainting the texture content [EL99; Tro04b]. Another class of methods for image inpainting (and denoising) are transform-based methods. The key idea is to use sparse representation systems such as wavelets,

curvelets, shearlets, and framlets, to solve optimization problem in the transform domain. Among these methods, iterative thresholding algorithms have shown good performance for image inpainting [ESQD05; SHB17; HMZZ19]. In our analysis, we focus on a compressed sensing driven approach via l_1 minimization, based on the prior information that the components of the image are sparsely represented by two representation systems.

For an illustration of texture and cartoon parts of an image, we present in Figure 4.1 a corrupted photo with missing part and region covered by texture.

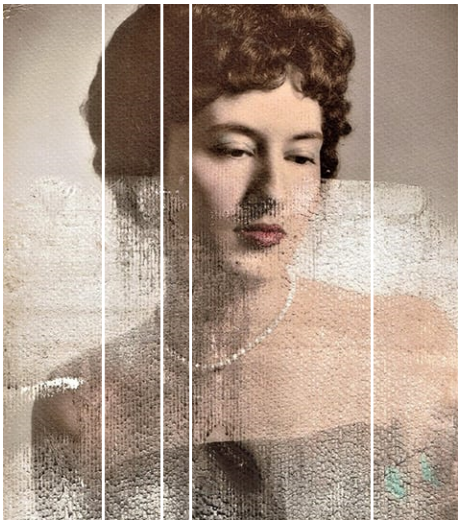

Figure 4.1: A corrupted photo, where the noise is a texture part together with missing stripes, and the clean image is the cartoon part.

4.2 Simultaneous Inpainting and Separation Approach

In this section we summarize our general theory of simultaneous inpainting and separation.

4.2.1 The Separation Problem

The task is to extract the two components $\mathcal{C}$ and $\mathcal{T}$ from the observed image f, where we assume that

$$f = \mathcal{C} + \mathcal{T}. \tag{4.1}$$

Here, only f is given, and the components $\mathcal{C}$ and $\mathcal{T}$ are unknown to us.

To solve this underdetermined problem, we assume that each component can be sparsely represented by some dictionary, that cannot sparsely represent the other component. In our theory, dictionaries are modeled as frames [DS52].

In our context, the Hilbert space $\mathcal{H}$ is the space of signals/images, and Φ is the dictionary. By abusing notion, we recall that we also denote by Φ the *synthesis operator*

$$\Phi : l_2(I) \to \mathcal{H}, \quad \Phi(\{a_i\}_{i\in I}) = \sum_{i\in I} a_i \phi_i,$$

which synthesizes an image $f \in \mathcal{H}$ from given coefficients $\{a_i\}_{i\in I}$. We denote by Φ^* the *analysis operator*

$$\Phi^* : \mathcal{H} \to l_2(I), \quad \Phi^*(f) = (\langle f, \phi_i \rangle)_{i\in I}.$$

The analysis operator is interpreted as the transform that computed the different dictionary coefficients of images f.

4.2.2 The Inpainting Problem

To model the inpainting problem, we suppose that there is some missing data in the image f. Given the Hilbert space $\mathcal{H}$, we assume that $\mathcal{H} = \mathcal{H}_K \oplus \mathcal{H}_M$, where the subspaces $\mathcal{H}_K, \mathcal{H}_M$ denote the *known part* and *missing part* respectively. Let P_M and P_K denote the orthogonal projection of $\mathcal{H}$ upon these two subspaces, respectively. In the inpainting problem, we assume that we are only given the image in the known part $P_K f$, and the goal is to reconstruct f. The inpainting problem is solved by considering a dictionary $\{\phi_i\}_{i\in I}$ that sparsely represents f using a known subset of indices $\Lambda \subset I$, but does not sparsely represent $P_M f$ using the indices Λ. This idea is formalized in Definition 4.2.

4.2.3 The Simultaneous Separation and Inpainting problem

In the simultaneous problem, the goal is to extract $\mathcal{C}$ and $\mathcal{T}$, satisfying (4.1), given only the image in the known part $P_K f$. In our approach, we consider two Parseval frames Φ_1 and Φ_2 in $\mathcal{H}$ that sparsely represent their respective component $\mathcal{C}$ and $\mathcal{T}$, but do not sparsely represent the other component. This is formalized through Definitions 4.3 and 4.1 for the joint concentration approach, and 4.3 and 4.5 for the cluster coherence approach. We moreover suppose that the index subsets Λ_1 and Λ_2 of Φ_1 and Φ_2 respectively can sparsely represent $\mathcal{C}$ and $\mathcal{T}$, but cannot sparsely represent $P_M\mathcal{T}$ and $P_M\mathcal{C}$. This is formalized through Definitions 4.3 and 4.2 for the joint concentration approach, and 4.3 and 4.5 for the cluster coherence approach.

We consider the following algorithm, for simultaneously inpaint and separate (INP-SEP) geometric components, based on l_1 minimization.

Algorithm (INP-SEP)

INPUT: corrupted signal $P_K f \in \mathcal{H}_K$, two Parseval frames $\{\Phi_1\}_{i\in I}$ and $\{\Phi_2\}_{j\in J}$.

COMPUTE: $f^\star = (\mathcal{C}^\star, \mathcal{T}^\star)$ where

$$(\mathcal{C}^\star, \mathcal{T}^\star) = \underset{x_1,x_2}{\operatorname{argmin}} \|\Phi_1^* x_1\|_1 + \|\Phi_2^* x_2\|_1, \quad s.t. \quad P_K(x_1 + x_2) = P_K(f). \tag{4.2}$$

OUTPUT: recovered components $\mathcal{C}^\star, \mathcal{T}^\star$.

In Section 4.3, we provide a theoretical analysis for the success of algorithm (4.2).

4.3 General Separation and Inpainting Theory

In this section, we introduce a theory in which we can prove the success of Algorithm (INP-SEP) for a general separation and inpainting problem.

4.3.1 Joint Concentration

We propose a sufficient condition for the success of the (INP-SEP) algorithm, based on the notion of joint concentration. Joint concentration was first introduced in [DK13]. We present two slightly different notions of joint concentration, modified for our needs.

Definition 4.1 Let Φ_1, Φ_2 be two Parseval frames. Given two sets of coefficients Λ_1, Λ_2, define the *mixed joint concentration* $\kappa_1 = \kappa_1(\Lambda_1, \Lambda_2)$ by

$$\kappa_1 = \kappa_1(\Lambda_1, \Lambda_2) = \sup_{x,y \in \mathcal{H}} \frac{\|\mathbb{1}_{\Lambda_1} \Phi_1^* x\|_1 + \|\mathbb{1}_{\Lambda_2} \Phi_2^* y\|_1}{\|\Phi_1^* y\|_1 + \|\Phi_2^* x\|_1}.$$

Given an l_2 normalized signal f, it is common to interpret the l_1 norm of f as a measure of spread (opposite of sparsity). Thus, the mixed joint concentration with respect to the coefficient sets Λ_1 and Λ_2 quantifies the extent to which signals can have most of their energy supported and well spread in Λ_j while being sparsely concentrated in the other frame Φ_k, for $j \neq k$. Bounding κ_1 from above is one of the conditions that ensure that Algorithm (INP-SEP) succeeds in the separation task. Next, we introduce another joint concentration notion which will be used to prove the success of the inpainting method.

Definition 4.2 Let Φ_1, Φ_2 be two Parseval frames. Given two sets of coefficients Λ_1, Λ_2, define the *joint concentration of the missing part* $\kappa_2 = \kappa_2(\Lambda_1, \Lambda_2)$ by

$$\kappa_2 = \kappa_2(\Lambda_1, \Lambda_2) = \sup_{\substack{x,y \in \mathcal{H}; \\ P_K x = P_K y}} \frac{\|\mathbb{1}_{\Lambda_1} \Phi_1^*(x-y)\|_1 + \|\mathbb{1}_{\Lambda_2} \Phi_2^*(x-y)\|_1}{\|\Phi_1^* x\|_1 + \|\Phi_2^* y\|_1}.$$

The joint concentration of the missing part quantifies the extent to which signals which coincide on the known part can have most of the energy of their difference supported and well spread in Λ_1, Λ_2 while begin sparse in Φ_1 and Φ_2. The joint concentration κ_2 is thus used to encode the geometric relation between the missing part $\mathcal{H}_M$ and expansions in Φ_1 and Φ_2. Bounding κ_2 from above is another one of the conditions that ensure the success of Algorithm (INP-SEP).

4.3.2 Recovery Guarantee Through Joint Concentration

The sufficient condition for recovery is based on finding sets of coefficients Λ_1 and Λ_2 for which the joint concentrations are small, and Λ_1 and Λ_2 capture most of the energy of the ground truth separated components $\mathcal{C}$ and $\mathcal{T}$. For this, we recall the following definition from [KKZ14].

Definition 4.3 Fix $\delta > 0$. Given a Hilbert space $\mathcal{H}$ with a Parseval frame Φ, $f \in \mathcal{H}$ is *$\delta-$relatively sparse* in Φ with respect to Λ if $\|\mathbb{1}_{\Lambda^c} \Phi^* f\|_1 \leq \delta$, where Λ^c denotes $X \setminus \Lambda$.

We now prove our first separation result.

Proposition 4.4 *For $\delta_1, \delta_2 > 0$, fix $\delta = \delta_1 + \delta_2$, and suppose that $f \in \mathcal{H}$ can be decomposed as $f = \mathcal{C} + \mathcal{T}$ so that each component $\mathcal{C}, \mathcal{T}$ is δ_1, δ_2-relatively sparse in Φ_1 and Φ_2 with respect to Λ_1 and Λ_2, respectively. Let $(\mathcal{C}^\star, \mathcal{T}^\star)$ solve* (INP-SEP). *If we have $\kappa_1 + \kappa_2 < \frac{1}{2}$, then*

$$\|\mathcal{C}^\star - \mathcal{C}\|_2 + \|\mathcal{T}^\star - \mathcal{T}\|_2 \leq \frac{2\delta}{1 - 2(\kappa_1 + \kappa_2)}. \tag{4.3}$$

Proof. First, we set

$$\kappa = \kappa(\Lambda_1, \Lambda_2) := \sup_{P_K u = P_K v} \frac{\|\mathbb{1}_{\Lambda_1} \Phi_1^* u\|_1 + \|\mathbb{1}_{\Lambda_2} \Phi_2^* v\|_1}{\|\Phi_1^* u\|_1 + \|\Phi_2^* v\|_1},$$

and $x = \mathcal{C}^\star - \mathcal{C}$, $y = \mathcal{T} - \mathcal{T}^\star$. Since Φ_1 and Φ_2 are two Parseval frames, thus

$$\begin{aligned} \|\mathcal{C}^\star - \mathcal{C}\|_2 + \|\mathcal{T}^\star - \mathcal{T}\|_2 &= \|\Phi_1^*(\mathcal{C}^\star - \mathcal{C})\|_2 + \|\Phi_2^*(\mathcal{T}^\star - \mathcal{T})\|_2 \\ &\leq \|\Phi_1^*(\mathcal{C}^\star - \mathcal{C})\|_1 + \|\Phi_2^*(\mathcal{T}^\star - \mathcal{T})\|_1 \\ &= \|\Phi_1^*(x)\|_1 + \|\Phi_2^*(y)\|_1 := S. \end{aligned}$$

Now we invoke the relation $P_K(\mathcal{C}^\star + \mathcal{T}^\star) = P_K(f) = P_K(\mathcal{C} + \mathcal{T})$ and hence $P_K(x) = P_K(y)$. By the definition of κ, we have

$$\begin{aligned} S &= \|\mathbb{1}_{\Lambda_1} \Phi_1^* x\|_1 + \|\mathbb{1}_{\Lambda_2} \Phi_2^* y\|_1 + \|\mathbb{1}_{\Lambda_1^c} \Phi_1^*(\mathcal{C}^\star - \mathcal{C})\|_1 + \|\mathbb{1}_{\Lambda_2^c} \Phi_2^*(\mathcal{T}^\star - \mathcal{T})\|_1 \\ &\leq \kappa S + \|\mathbb{1}_{\Lambda_1^c} \Phi_1^* \mathcal{C}^\star\|_1 + \|\mathbb{1}_{\Lambda_1^c} \Phi_1^* \mathcal{C}\|_1 + \|\mathbb{1}_{\Lambda_2^c} \Phi_2^* \mathcal{T}^\star\|_1 + \|\mathbb{1}_{\Lambda_2^c} \Phi_2^* \mathcal{T}\|_1 \\ &\leq \kappa S + \|\mathbb{1}_{\Lambda_1^c} \Phi_1^* \mathcal{C}^\star\|_1 + \|\mathbb{1}_{\Lambda_2^c} \Phi_2^* \mathcal{T}^\star\|_1 + \delta \\ &= \kappa S + \delta + \|\Phi_1^* \mathcal{C}^\star\|_1 + \|\Phi_2^* \mathcal{T}^\star\|_1 - \|\mathbb{1}_{\Lambda_1} \Phi_1^* \mathcal{C}^\star\|_1 - \|\mathbb{1}_{\Lambda_2} \Phi_2^* \mathcal{T}^\star\|_1. \end{aligned}$$

We note that $(\mathcal{C}^\star, \mathcal{T}^\star)$ is a minimizer of (INP-SEP). Thus,

$$\|\Phi_1^* \mathcal{C}^\star\|_1 + \|\Phi_2^* \mathcal{T}^\star\|_1 \leq \|\Phi_1^* \mathcal{C}\|_1 + \|\Phi_2^* \mathcal{T}\|_1.$$

Therefore,

$$\begin{aligned} S &\leq \kappa S + \delta + \|\Phi_1^* \mathcal{C}\|_1 + \|\Phi_2^* \mathcal{T}\|_1 - \|\mathbb{1}_{\Lambda_1} \Phi_1^* \mathcal{C}^\star\|_1 - \|\mathbb{1}_{\Lambda_2} \Phi_2^* \mathcal{T}^\star\|_1 \\ &\leq \kappa S + \delta + \|\Phi_1^* \mathcal{C}\|_1 + \|\Phi_2^* \mathcal{T}\|_1 + \|\mathbb{1}_{\Lambda_1} \Phi_1^* x\|_1 + \|\mathbb{1}_{\Lambda_2} \Phi_2^* y\|_1 - \|\mathbb{1}_{\Lambda_1} \Phi_1^* \mathcal{C}\|_1 \\ &\quad - \|\mathbb{1}_{\Lambda_2} \Phi_2^* \mathcal{T}\|_1 \\ &\leq \kappa S + 2\delta + \kappa S = 2\kappa S + 2\delta. \end{aligned}$$

Thus,

$$S \leq \frac{2\delta}{1 - 2\kappa}.$$

The last inequality comes from the fact that

$$\begin{aligned} \frac{\|\mathbb{1}_{\Lambda_1} \Phi_1^* x\|_1 + \|\mathbb{1}_{\Lambda_2} \Phi_2^* y\|_1}{\|\Phi_1^* x\|_1 + \|\Phi_2^* y\|_1} \leq\ & \frac{\|\mathbb{1}_{\Lambda_1} \Phi_1^* y\|_1 + \|\mathbb{1}_{\Lambda_2} \Phi_2^* x\|_1}{\|\Phi_1^* x\|_1 + \|\Phi_2^* y\|_1} + \\ & \frac{\|\mathbb{1}_{\Lambda_1} \Phi_1^*(x - y)\|_1 + \|\mathbb{1}_{\Lambda_2} \Phi_2^*(x - y)\|_1}{\|\Phi_1^* x\|_1 + \|\Phi_2^* y\|_1}. \end{aligned}$$

This leads to $\kappa \leq \kappa_1 + \kappa_2$. Finally, we obtain (4.3)

$$\|\mathcal{C}^\star - \mathcal{C}\|_2 + \|\mathcal{T}^\star - \mathcal{T}\|_2 \leq \frac{2\delta}{1 - 2(\kappa_1 + \kappa_2)}.$$

■

We note that [KM18, Theorem 1] also proposed a theoretical guarantee for the inpainting and separation problem based on joint concentration and relative sparsity. However, while the derived theorem is mathematically sound, we did not find any way to use it in practice. The reconstruction bound in [KM18, Theorem 1] appears artificially similar to our Proposition 4.4, but the components x and y are analyzed via the frames that sparsify them in the denominator of the mixed joint concentration, so the denominator is small. Hence, the formulation in [KM18, Theorem 1] goes against the philosophy of finding a frame that sparsely describes one part and not the other. In contrast, in our formulation, each x and y is analyzed via the frame that sparsifies the other component, and the denominator can be made large by choosing appropriate frames.

4.3.3 Recovery Guarantee Through Cluster Coherence

Deriving bounds for joint concentrations can be difficult in practice. Our goal in this subsection is to replace the joint concentrations by easier to compute terms. For that, we recall the notion of cluster coherence. We then prove that joint concentrations can be bounded by cluster coherence terms. Deriving bounds to cluster coherence terms is generally easier than bounding joint concentrations. The following definition is taken from [DK13].

Definition 4.5 Given two Parseval frames $\Phi_1 = (\Phi_{1i})_{i\in I}$ and $\Phi_2 = (\Phi_{2j})_{j\in J}$. Then the *cluster coherence* $\mu_c(\Lambda, \Phi_1; \Phi_2)$ of Φ_1 and Φ_2 with respect to the index set $\Lambda \subset I$ is defined by

$$\mu_c(\Lambda, \Phi_1; \Phi_2) = \max_{j\in J} \sum_{i\in\Lambda} |\langle \phi_{1i}, \phi_{2j}\rangle|$$

in case this maximum exists.

We allow applying a projection P_M on one or both of the frames in Definition 4.5. For example, similarly to [KKZ14], we use the notation $\mu_c(\Lambda, P_M\Phi_1; P_M\Phi_2)$ to denote

$$\mu_c(\Lambda, P_M\Phi_1; P_M\Phi_2) = \max_{j\in J} \sum_{i\in\Lambda} |\langle P_M\phi_{1i}, P_M\phi_{2j}\rangle|.$$

Next, we present two lemmas which bound the joint concentrations by corresponding cluster coherences.

Lemma 4.6 *We have*

$$\kappa_1(\Lambda_1, \Lambda_2) \leq \max\{\mu_c(\Lambda_1, \Phi_1; \Phi_2), \mu_c(\Lambda_2, \Phi_2; \Phi_1)\}.$$

Proof. For $x, y \in \mathcal{H}$, we set $\alpha_1 = \Phi_1^* y, \alpha_2 = \Phi_2^* x$. Then invoking the fact that Φ_1 and Φ_2

are two Parseval frames, hence $x = \Phi_2\Phi_2^* x = \Phi_2\alpha_2$ and $y = \Phi_1\Phi_1^* y = \Phi_1\alpha_1$, we have

$$\begin{aligned}
& \|\mathbb{1}_{\Lambda_1}\Phi_1^* x\|_1 + \|\mathbb{1}_{\Lambda_2}\Phi_2^* y\|_1 \\
= \; & \|\mathbb{1}_{\Lambda_1}\Phi_1^*\Phi_2\alpha_2\|_1 + \|\mathbb{1}_{\Lambda_2}\Phi_2^*\Phi_1\alpha_1\|_1 \\
\leq \; & \sum_{i\in\Lambda_1}\Big(\sum_j |\langle\Phi_{1i},\Phi_{2j}\rangle||\alpha_{2j}|\Big) + \sum_{j\in\Lambda_2}\Big(\sum_i |\langle\Phi_{1i},\Phi_{2j}\rangle||\alpha_{1i}|\Big) \\
= \; & \sum_j\Big(\sum_{i\in\Lambda_1} |\langle\Phi_{1i},\Phi_{2j}\rangle|\Big)|\alpha_{2j}| + \sum_i\Big(\sum_{j\in\Lambda_2} |\langle\Phi_{1i},\Phi_{2j}\rangle|\Big)|\alpha_{1i}| \\
\leq \; & \mu_c(\Lambda_1,\Phi_1;\Phi_2)\|\alpha_2\|_1 + \mu_c(\Lambda_2,\Phi_2;\Phi_1)\|\alpha_1\|_1 \\
\leq \; & \max\{\mu_c(\Lambda_1,\Phi_1;\Phi_2),\mu_c(\Lambda_2,\Phi_2;\Phi_1)\}(\|\alpha_2\|_1 + \|\alpha_1\|_1) \\
= \; & \max\{\mu_c(\Lambda_1,\Phi_1;\Phi_2),\mu_c(\Lambda_2,\Phi_2;\Phi_1)\}(\|\Phi_2^* x\|_1 + \|\Phi_1^* y\|_1).
\end{aligned}$$

Thus, we obtain $\kappa_1(\Lambda_1,\Lambda_2) \leq \max\{\mu_c(\Lambda_1,\Phi_1;\Phi_2),\mu_c(\Lambda_2,\Phi_2;\Phi_1)\}$. ∎

Lemma 4.7 *We have*

$$\begin{aligned}
\kappa_2(\Lambda_1,\Lambda_2) \; \leq \; & \max\{\mu_c(\Lambda_1,P_M\Phi_1;P_M\Phi_1) + \mu_c(\Lambda_2,P_M\Phi_2;P_M\Phi_1), \\
& \mu_c(\Lambda_2,P_M\Phi_2;P_M\Phi_2) + \mu_c(\Lambda_1,P_M\Phi_1;P_M\Phi_2)\} \\
= \; & \max\{\mu_c(\Lambda_1,P_M\Phi_1;\Phi_1) + \mu_c(\Lambda_2,P_M\Phi_2;\Phi_1), \\
& \mu_c(\Lambda_2,P_M\Phi_2;\Phi_2) + \mu_c(\Lambda_1,P_M\Phi_1;\Phi_2)\}.
\end{aligned}$$

Proof. For each $h \in \mathcal{H}_M$ and $x \in \mathcal{H}$, set $\alpha = \Phi_1^*(x+h)$ and $\beta = \Phi_2^* x$ then we have

$$\begin{aligned}
h &= x + h - x \\
&= \Phi_1\Phi_1^*(x+h) - \Phi_2\Phi_2^*(x) \\
&= \Phi_1\alpha - \Phi_2\beta.
\end{aligned}$$

Note that P_K is an orthogonal projection, and hence $h = P_M^* P_M h = P_M^* P_M\Phi_1\alpha - P_M^* P_M\Phi_2\beta$. Therefore, we obtain

$$\begin{aligned}
\|\mathbb{1}_{\Lambda_1}\Phi_1^* h\|_1 &= \|\mathbb{1}_{\Lambda_1}\Phi_1^* P_M^* P_M\Phi_1\alpha - \mathbb{1}_{\Lambda_1}\Phi_1^* P_M^* P_M\Phi_2\beta\|_1 \\
&= \|\mathbb{1}_{\Lambda_1}(P_M\Phi_1)^*(P_M\Phi_1)\alpha - \mathbb{1}_{\Lambda_1}(P_M\Phi_1)^*(P_M\Phi_2)\beta\|_1 \\
&\leq \|\mathbb{1}_{\Lambda_1}(P_M\Phi_1)^*(P_M\Phi_1)\alpha\|_1 + \|\mathbb{1}_{\Lambda_1}(P_M\Phi_1)^*(P_M\Phi_2)\beta\|_1 \\
&\leq \sum_{i\in\Lambda_1}\Big(\sum_j |\langle P_M\Phi_{1i},P_M\Phi_{1j}\rangle||\alpha_j|\Big) + \\
&\quad \sum_{i\in\Lambda_1}\Big(\sum_j |\langle P_M\Phi_{1i},P_M\Phi_{2j}\rangle||\beta_j|\Big) \\
&\leq \sum_j\Big(\sum_{i\in\Lambda_1} |\langle P_M\Phi_{1i},P_M\Phi_{1j}\rangle|\Big)|\alpha_j| + \\
&\quad \sum_j\Big(\sum_{i\in\Lambda_1} |\langle P_M\Phi_{1i},P_M\Phi_{2j}\rangle|\Big)|\beta_j| \\
&\leq \mu_c(\Lambda_1,P_M\Phi_1;P_M\Phi_1)\|\alpha\|_1 + \mu_c(\Lambda_1,P_M\Phi_1;P_M\Phi_2)\|\beta\|_1
\end{aligned}$$

$$= \mu_c(\Lambda_1, P_M\Phi_1; P_M\Phi_1)\|\Phi_1^*(x+h)\|_1 + \mu_c(\Lambda_1, P_M\Phi_1; P_M\Phi_2)\|\Phi_2^*(x)\|_1.$$

Similarly, we have

$$\|\mathbb{1}_{\Lambda_2}\Phi_2^* h\|_1 \leq \mu_c(\Lambda_2, P_M\Phi_2; P_M\Phi_1)\|\Phi_1^*(x+h)\|_1 + \mu_c(\Lambda_2, P_M\Phi_2; P_M\Phi_2)\|\Phi_2^*(x)\|_1.$$

This leads to

$$\begin{aligned}\|\mathbb{1}_{\Lambda_1}\Phi_1^* h\|_1 + \|\mathbb{1}_{\Lambda_2}\Phi_2^* h\|_1 \quad \leq \quad & \max\{\mu_c(\Lambda_1, P_M\Phi_1; P_M\Phi_1) + \mu_c(\Lambda_2, P_M\Phi_2; P_M\Phi_1),\\ & \mu_c(\Lambda_2, P_M\Phi_2; P_M\Phi_2) + \mu_c(\Lambda_1, P_M\Phi_1; P_M\Phi_2)\}\\ & (\|\Phi_1^*(x+h)\|_1 + \|\Phi_2^*(x)\|_1).\end{aligned}$$

Finally,

$$\begin{aligned}\kappa_2(\Lambda_1, \Lambda_2) \quad \leq \quad & \max\{\mu_c(\Lambda_1, P_M\Phi_1; P_M\Phi_1) + \mu_c(\Lambda_2, P_M\Phi_2; P_M\Phi_1),\\ & \mu_c(\Lambda_2, P_M\Phi_2; P_M\Phi_2) + \mu_c(\Lambda_1, P_M\Phi_1; P_M\Phi_2)\}\\ = \quad & \max\{\mu_c(\Lambda_1, P_M\Phi_1; \Phi_1) + \mu_c(\Lambda_2, P_M\Phi_2; \Phi_1),\\ & \mu_c(\Lambda_2, P_M\Phi_2; \Phi_2) + \mu_c(\Lambda_1, P_M\Phi_1; \Phi_2)\}.\end{aligned}$$

■

We can now formulate a general guarantee for the success of Algorithm (INP-SEP), based on cluster coherence.

Theorem 4.8 *Let Φ_1, Φ_2 be two Parseval frames for a Hilbert space $\mathcal{H}$. For $\delta_1, \delta_2 > 0$, fix $\delta = \delta_1 + \delta_2$, and suppose that $f \in \mathcal{H}$ can be decomposed as $f = \mathcal{C} + \mathcal{T}$ so that each component $\mathcal{C}, \mathcal{T}$ is δ_1, δ_2-relatively sparse in Φ_1 and Φ_2 with respect to Λ_1, Λ_2 respectively. Let $(\mathcal{C}^\star, \mathcal{T}^\star)$ solve* (INP-SEP). *If we have $\mu_c < \frac{1}{2}$, then*

$$\|\mathcal{C}^\star - \mathcal{C}\|_2 + \|\mathcal{T}^\star - \mathcal{T}\|_2 \leq \frac{2\delta}{1-2\mu_c}, \tag{4.4}$$

where $\mu_c = \max\{\mu_c(\Lambda_1, P_M\Phi_1; \Phi_1) + \mu_c(\Lambda_2, P_M\Phi_2; \Phi_1), \mu_c(\Lambda_2, P_M\Phi_2; \Phi_2) + \mu_c(\Lambda_1, P_M\Phi_1; \Phi_2)\} + \max\{\mu_c(\Lambda_1, \Phi_1; \Phi_2), \mu_c(\Lambda_2, \Phi_2; \Phi_1)\}$.

Proof. The bound (4.4) holds as a consequence of Lemmas 4.6, 4.7 and Proposition 4.4. ■

Let us interpret this estimate. The relative sparsity δ and the cluster coherence μ_c depend on the geometric sets of indices Λ_1, Λ_2, which are not used at all in Algorithm (INP-SEP). Hence, Λ_1, Λ_2 are analytic tools that we can choose arbitrarily, and are used only for deriving theoretical bounds. If we choose very large Λ_1, Λ_2, we get very small relative sparsities δ_1, δ_2, but we might loose control over the cluster coherence μ_c. Therefore, choosing appropriate Λ_1 and Λ_2 is an important step when applying our theory in concrete examples.

4.4 Mathematical Models of Texture and Cartoon

We now focus on the specific problem of inpainting and separating texture from cartoon. In this section we define our models of texture and cartoon parts, and of the missing part.

4.4.1 Model of Texture

One of the earliest qualitative texture description that corresponds to human visual perception is: coarseness, contrast, directionality, line-likeness, regularity, roughness [TMY78]. From a mathematical modeling point of view, many definitions of texture were proposed in the past, for instance [Mey01; BZ03; OSV03; Kut13]. Our model for texture is inspired by [Kut13], and based on an expansion of Gabor frame elements. To motivate our definition of texture we offer the following discussion. A very restrictive definition of texture would be a periodical signal with a short period. The Fourier transform of a periodical signal is a signal supported on a delta train on a regular grid in the frequency domain. To relax the hard periodicity condition, suppose that we allow to perturb the locations of the points of the regular frequency grid. This would result in a signal supported on a sparse set of Fourier coefficients, which is exactly our definition of texture. Such a definition indeed produces images that look like a repeating pattern, but not in a strictly periodical fashion (see Figure 4.2 for example).

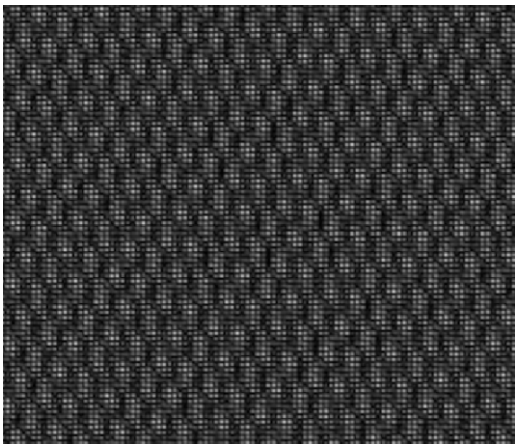

Figure 4.2: Real valued texture sample produced by randomly choosing a sparse set of Fourier coefficients with random values and an appropriate symmetry in the frequency domain, with the rest of the Fourier coefficients set to zero.

Before formally defining texture, we recall the *Schwartz functions* or the *rapidly decreasing functions*

$$\mathbb{S}(\mathbb{R}^2) := \left\{ f \in C^\infty(\mathbb{R}^2) \mid \forall K, N \in \mathbb{N}_0 : \sup_{x \in \mathbb{R}^2} (1 + |x|^2)^{N/2} \sum_{|\alpha| \leq K} |D^\alpha f(x)| < \infty \right\}.$$

We define the Fourier transform and inverse Fourier transform for $f, F \in \mathbb{S}(\mathbb{R}^2)$ by

$$\hat{f}(\xi) = \mathcal{F}[f](\xi) = \int_{\mathbb{R}^2} f(x) e^{-2\pi i x^T \xi} dx,$$

$$\check{F}(x) = \mathcal{F}^{-1}[F](x) = \int_{\mathbb{R}^2} F(\xi) e^{2\pi i \xi^T x} dx,$$

which can be extended to a well defined Fourier transform and inverse Fourier transform for functions in $L^2(\mathbb{R}^2)$ (cf. [Gra08]). Using a window function $g : \mathbb{R}^2 \to \mathbb{R}$ which localizes a texture patch in the spatial domain, we now introduce our model for texture.

Definition 4.9 Let $g \in L^2(\mathbb{R}^2)$ be a window with $\hat{g} \in C^\infty(\mathbb{R}^2)$, and frequency support $\operatorname{supp} \hat{g} \in [-1,1]^2$ satisfying the partition of unity condition

$$\sum_{n \in \mathbb{Z}^2} |\hat{g}(\xi + n)|^2 = 1, \quad \xi \in \mathbb{R}^2. \tag{4.5}$$

For $s > 0$, we define the L^2- normalized scaled version of g by $g_s(x) = s \cdot g(sx)$. Let $I_T \subseteq \mathbb{Z}^2$, be a subset of Fourier elements. A texture is defined by

$$\mathcal{T}_s(x) = \sum_{n \in I_T} d_n g_s(x) e^{2\pi i x^T s n}, \tag{4.6}$$

where $(d_n)_{n \in \mathbb{Z}^2}$ denotes a sequence of complex numbers.

A real valued texture image can be generated via Definition 4.9 by choosing complex coefficients $(d_n)_{n \in \mathbb{Z}^2}$ with the appropriate symmetry in the frequency domain ($\bar{d}_n = d_{-n}$).

In Subsection 4.6.3 we add a restriction on the size of the index set I_T. For now, we just mention that I_T is a small/sparse set in some sense. We also remark that by Definition 4.9, we have $\hat{g}_s(\xi) = s^{-1} \cdot \hat{g}(s^{-1}\xi)$, $\operatorname{supp} \hat{g}_s \subseteq [-s,s]^2$ and the partition of unity condition (4.5) now reads

$$\sum_{n \in \mathbb{Z}^2} |\hat{g}_s(\xi + sn)|^2 = s^{-2}, \quad \xi \in \mathbb{R}^2.$$

4.4.2 The Local Cartoon Patch

In [GKKS16; Sch16], cartoon functions are defined as

$$\mathcal{C} = f_0 + f_1 \cdot \mathbb{1}_{B_\tau}, \tag{4.7}$$

where $f_0, f_1 \in L^2(\mathbb{R}^2) \cap C^\beta(\mathbb{R}^2), \beta \in (0, +\infty)$, with compact support and B_τ denotes the interior of a closed, non-intersecting curve τ in $C^\beta(\mathbb{R}^2)$. In the separation algorithm of cartoon and texture, we analyze the input image using a *Gabor frame* and the so-called *universal shearlet frame* (see Subsection 4.5). Both of these frames analyze images on local patches. Thus, for the sake of simplicity, we also reduce our model of the cartoon part to a local cartoon model. This is done in two steps.

Cartoon images are locally close to piecewise constant functions with discontinuity along an edge curve, which is locally close to a line. We thus consider the *windowed step function*

$$w\mathcal{S}_0(x) = \begin{cases} w(x_1) & x_2 \leq 0 \\ 0 & x_2 > 0, \end{cases} \tag{4.8}$$

where $w \in C^\infty(\mathbb{R})$ is a *weighted function* satisfying $w \not\equiv 0, 0 \leq w(u) \leq 1$ and $\operatorname{supp} w \subset$

$[-\rho, \rho]$. In our work, the cartoon part is analyzed using universal shearlets, which is a shear invariant system up to the cone adaptation. Since shearing is a way of changing orientation, our analysis also applies to the more general case where the discontinuity in (4.8) is along a general line in any orientation. We note that it is possible to extend our results from the local cartoon model (4.8) to the global cartoon model (4.7) by using a *tubular neighborhood* argument as shown in [Kut13].

The cartoon part (4.8) can be seen as a *tempered distribution* acting on *Schwartz functions* by

$$\langle w\mathcal{S}_0, f\rangle = \int_{-\rho}^{\rho} w(x_1) \int_{-\infty}^{0} f(x_1, x_2) dx_2 dx_1, f \in \mathbb{S}(\mathbb{R}^2).$$

By the fact that $\widehat{\mathbb{1}_{(-\infty,0]}} = \frac{1}{2}\left[\delta(\omega) + \frac{i}{\pi\omega}\right]$, we have $\widehat{w\mathcal{S}_0}(\xi) = \hat{w}(\xi_1)\left(\delta(\xi_2) + \frac{i}{\pi\xi_2}\right)$.

Now, we modify the local cartoon part to get an image in $L_2(\mathbb{R}^2)$. We note that we are interested in the local behaviour of $w\mathcal{S}_0$ about $(x_1, x_2) = 0$. Thus, the "DC part" of $\widehat{w\mathcal{S}_0}$ is not of interest to us, as it models some global asymptotic behaviour of the patch in $\mathbb{R}^2$. We thus filter our the band $|\xi_2| < r$ from $\widehat{w\mathcal{S}_0}(\xi_1, \xi_2)$ for some arbitrarily small $r > 0$, to obtain

$$\widehat{w\mathcal{S}} = \mathbb{1}_{\{|\xi_2| \geq r\}} \widehat{w\mathcal{S}_0}. \tag{4.9}$$

It is easy to see that

$$\begin{aligned}\widehat{w\mathcal{S}} &= \mathbb{1}_{\{|\xi_2| \geq r\}}(\xi_2)\widehat{\mathbb{1}_{(-\infty,0]}}(\xi_2)\hat{w}(\xi_1) \\ &= \frac{i}{2\pi\xi_2}\mathbb{1}_{\{|\xi_2| \geq r\}}(\xi_2)\hat{w}(\xi_1).\end{aligned}$$

The main change incurred by this filtering of $w\mathcal{S}_0$ is a "translation along the y axis $w\mathcal{S}_0 \mapsto w\mathcal{S}_0 - \mathrm{DC}$", which does not affect the analysis via shearlet frames. This filtering changes the behaviour of $w\mathcal{S}_0$ about $(x_1, x_2) = 0$ negligibly, since r is small, and retains the quality of $w\mathcal{S}_0$ being approximately piecewise constant locally with a line discontinuity (see Figure 4.3).

To give more intuition about how to interpret the model as local, we note that in the multi-scale approach of Subsection 4.6.1, the resulting models of cartoon are indeed spatially localized. This can be seen through Lemma 4.21, where the shearlet coefficients of the cartoon models are shown to decay fast in the spatial parameter.

Henceforth, we call the local cartoon part $w\mathcal{S}$ simply a cartoon part.

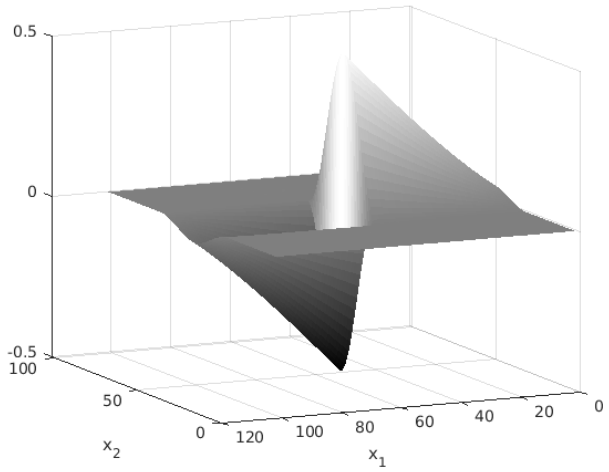

Figure 4.3: A local cartoon patch.

4.4.3 The Missing Part

In our analysis, the shape of the missing region is chosen to be

$$\mathcal{M}_h = \{x = (x_1, x_2) \in \mathbb{R}^2 \mid |x_1| \leq h\}, \quad \text{for } h > 0, \tag{4.10}$$

and the orthogonal projection associated with this missing part is $P_M = \mathbb{1}_{\mathcal{M}_h}$.

Note that this models a local and axis aligned missing part, corresponding to the local model of texture (4.6) and the local and axis aligned cartoon model (4.9). When combining and re-orienting the local patches, we can obtain many missing stripes at various orientations. Moreover, in practice, the missing part can be any domain contained in $\mathcal{M}_h$ of (4.10).

One practical example where the missing part is of the form (4.10) is seismic data, where the image is commonly incomplete due to missing or faulty sensor or land development causing white strips [HH08; HFH10].

4.5 Sparsifying Systems for Texture and Cartoon

In this section, we choose frames that sparsely represent the texture and cartoon parts. To represent texture, it is clear from Definition 4.9 that a Gabor frame is a natural choice. For the cartoon part, among popular sparsifying representation systems such as wavelets, curvelets, and shearlets, it was shown in [KLR15] that shearlets outperform not only wavelets, but also most other directional sparsifying systems for inpainting larger gap size [GK14; KKZ14].

We hence choose the following sparse representation systems.

- Gabor frame - a tight frame with time-frequency balanced elements
- Universal shearlet frame - a directional tight frame.

4.5.1 Gabor Frame

We first recall some basic facts about Gabor frames.

Definition 4.10 Denote for $x, y \in \mathbb{R}^2$ and $g \in L^2(\mathbb{R}^2)$

$$g(x,y)(t) = g(t-x)e^{2\pi i t^T y}.$$

For $a, b > 0$ we call the collection of functions $\{g(ma, nb) \mid m, n \in \mathbb{Z}^2\}$ a *Gabor system*. Such a system is called a *Gabor frame* if it forms a frame.

For our Gabor system, we use a window $\tilde{g}$ that satisfies the assumptions of the window g of texture (Definition 4.9). We note that $\tilde{g}$ and g may be different in general. However, the analysis for $\tilde{g} \neq g$ is almost identical to the analysis in case $g = \tilde{g}$. Without loss of generality, we assume henceforth that both Definitions 4.9 and 4.10 are based on the same window g, satisfying the assumptions of Definition 4.9.

For each scaling factor $s > 0$, we consider the Gabor tight frame $\mathbf{G_s} = \{(g_s)_\lambda(x)\}_\lambda$. This frame is represented in the frequency domain as

$$(\hat{g})_\lambda(\xi) = \hat{g}_s(\xi - sn)e^{2\pi i \xi^T \frac{m}{2s}},$$

where $\lambda = (m, n)$ is the spatial and frequency position and the parameter s denotes the band-size. This system constitutes a tight frame for $L^2(\mathbb{R}^2)$, see [DGM86] for more details.

4.5.2 The Universal-scaling Shearlet Frame

Shearlets were first introduced in [GKL06] as a representation system extending the wavelet framework. They are a directional representation system with similar optimal approximation properties as curvelets, but with the advantage of allowing for a unified treatment of the continuum and digital domains. Extending the shearlet system, α-shearlets, first introduced in [KLL12a], can be regarded as a parametrized family ranging from wavelets to shearlets. In [GKKS16; Sch16] it was shown that $\alpha-$shearlets provide optimally sparse approximations for cartoon images defined as piecewise $C^{1/\alpha}-$functions, separated by a $C^{1/\alpha}$ singularity curve. A further extension is universal shearlets [GK14], which is motivated by [GL13], with the aim at constructing a type of $\alpha-$shearlets that forms a Parseval frame. In our setting we choose universal shearlets as the sparsifying system of the cartoon part, since they form a Parseval frame, a necessary condition in our theory.

Let ϕ be a function in $\mathbb{S}(\mathbb{R})$ satisfying $0 \leq \hat{\phi}(u) \leq 1$ for $u \in \mathbb{R}$, $\hat{\phi}(u) = 1$ for $u \in [-1/16, 1/16]$ and $\operatorname{supp}\hat{\phi} \subset [-1/8, 1/8]$. Define the *low pass function* $\Phi(\xi)$ and the *corona scaling functions* for $j \in \mathbb{N}$ and $\xi = (\xi_1, \xi_2) \in \mathbb{R}^2$,

$$\hat{\Phi}(\xi) := \hat{\phi}(\xi_1)\hat{\phi}(\xi_2),$$

$$W(\xi) := \sqrt{\hat{\Phi}^2(2^{-2}\xi) - \hat{\Phi}^2(\xi)}, \quad W_j(\xi) := W(2^{-2j}\xi). \tag{4.11}$$

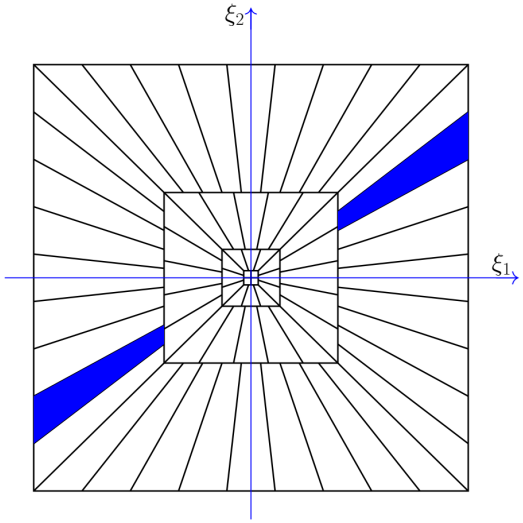

Figure 4.4: Frequency tiling of a cone-adapted shearlet.

It is easy to see that we have the partition of unity property

$$\hat{\Phi}^2(\xi) + \sum_{j\geq 0} W_j^2(\xi) = 1, \quad \xi \in \mathbb{R}^2. \tag{4.12}$$

Next, we use a bump-like function $v \in C^\infty(\mathbb{R})$ to produce the directional scaling feature of the system. Suppose $\operatorname{supp}(v) \subset [-1,1]$ and $|v(u-1)|^2 + |v(u)|^2 + |v(u+1)|^2 = 1$ for $u \in [-1,1]$. Define the *horizontal frequency cone* and the *vertical frequency cone*

$$\mathcal{C}_{(\mathrm{h})} := \left\{(\xi_1,\xi_2) \in \mathbb{R}^2 \mid \left|\frac{\xi_2}{\xi_1}\right| \leq 1\right\}$$

and

$$\mathcal{C}_{(\mathrm{v})} := \left\{(\xi_2,\xi_1) \in \mathbb{R}^2 \mid \left|\frac{\xi_1}{\xi_2}\right| \leq 1\right\}.$$

Define the cone functions $V_{(\mathrm{h})}, V_{(\mathrm{v})}$ by

$$V_{(\mathrm{h})}(\xi) := v\Big(\frac{\xi_2}{\xi_1}\Big), \quad V_{(\mathrm{v})}(\xi) := v\Big(\frac{\xi_1}{\xi_2}\Big).$$

The *shearing* and *scaling matrix* are defined by

$$A_{\alpha,(\mathrm{h})} := \begin{bmatrix} 2^2 & 0 \\ 0 & 2^\alpha \end{bmatrix}, \quad S_{(\mathrm{h})} := \begin{bmatrix} 1 & 1 \\ 0 & 1 \end{bmatrix},$$

$$A_{\alpha,(\mathrm{v})} := \begin{bmatrix} 2^\alpha & 0 \\ 0 & 2^2 \end{bmatrix}, \quad S_{(\mathrm{v})} := \begin{bmatrix} 1 & 0 \\ 1 & 1 \end{bmatrix},$$

where $\alpha \in (-\infty, 2)$ is the *scaling parameter*. The following two definitions are taken from [GK14].

Definition 4.11 Let Φ, W, v be defined as above. For $\alpha \in (-\infty, 2), k \in \mathbb{Z}^2$, we define

1. *Coarse scaling functions*: $\psi_{-1,k}(x) := \Phi(x-k), k \in \mathbb{Z}^2, x \in \mathbb{R}^2$.
2. *Interior shearlets*: let $j \in \mathbb{N}_0, l \in \mathbb{Z}$ such that $|l| < 2^{(2-\alpha)j}, k \in \mathbb{Z}^2$ and $(\iota) \in \{(\mathrm{h}), (\mathrm{v})\}$. Then we define $\psi^{\alpha,(\iota)}_{j,l,k}(x)$ by its Fourier transform

$$\hat{\psi}^{\alpha,(\iota)}_{j,l,k}(\xi) := 2^{-(2+\alpha)j/2} W_j(\xi) V_{(\iota)}\left(\xi^T A^{-j}_{\alpha,(\iota)} S^{-l}_{(\iota)}\right) e^{-2\pi i \xi^T A^{-j}_{\alpha,(\iota)} S^{-l}_{(\iota)} k}, \xi \in \mathbb{R}^2.$$

3. *Boundary shearlets*: let $j \in \mathbb{N}$, and $l = \pm\lceil 2^{(2-\alpha)j} \rceil$ we define

$$\hat{\psi}^{\alpha,(\mathrm{b})}_{j,l,k}(\xi) := \begin{cases} 2^{-(2+\alpha)j/2-1/2} W_j(\xi) V_{(\mathrm{h})}\left(\xi^T A^{-j}_{\alpha,(\mathrm{h})} S^{-l}_{(\mathrm{h})}\right) e^{-\pi i \xi^T A^{-j}_{\alpha,(\mathrm{h})} S^{-l}_{(\mathrm{h})} k}, & \xi \in \mathcal{C}_{(\mathrm{h})} \\ 2^{-(2+\alpha)j/2-1/2} W_j(\xi) V_{(\mathrm{v})}\left(\xi^T A^{-j}_{\alpha,(\mathrm{v})} S^{-l}_{(\mathrm{v})}\right) e^{-\pi i \xi^T A^{-j}_{\alpha,(\mathrm{v})} S^{-l}_{(\mathrm{v})} k}, & \xi \in \mathcal{C}_{(\mathrm{v})} \end{cases}$$

and in the case $j = 0, l = \pm 1$, we define

$$\hat{\psi}^{\alpha,(\mathrm{b})}_{0,l,k}(\xi) := \begin{cases} W(\xi) V_{(\mathrm{h})}\left(\xi^T S^{-l}_{(\mathrm{h})}\right) e^{-2\pi i \xi^T k}, & \xi \in \mathcal{C}_{(\mathrm{h})} \\ W(\xi) V_{(\mathrm{v})}\left(\xi^T S^{-l}_{(\mathrm{v})}\right) e^{-2\pi i \xi^T k}, & \xi \in \mathcal{C}_{(\mathrm{v})}. \end{cases}$$

Definition 4.12 Let $(\alpha_j)_{j \in \mathbb{N}_0} \subset \mathbb{R}$ be a *scaling sequence*, i.e,

$$\alpha_j \in Z_j := \left\{ \frac{m}{j} \mid m \in \mathbb{Z}, m \leq 2j-1 \right\}.$$

We define the associated *universal-scaling shearlet system*, or shorter, *universal shearlet system*, by

$$\mathbf{\Psi} = \mathrm{SH}(\phi, v, (\alpha_j)_j) := \mathrm{SH}_{\mathrm{Low}}(\phi) \cup \mathrm{SH}_{\mathrm{Int}}(\phi, v, (\alpha_j)_j) \cup \mathrm{SH}_{\mathrm{Bound}}(\phi, v, (\alpha_j)_j),$$

where

$$\begin{aligned} \mathrm{SH}_{\mathrm{Low}}(\phi) &:= \{\psi_{-1,k}(x) \mid k \in \mathbb{Z}^2\} \\ \mathrm{SH}_{\mathrm{Int}}(\phi, v, (\alpha_j)_j) &:= \left\{ \psi^{\alpha_j,(\iota)}_{j,l,k}(x) \mid j \in \mathbb{N}, l \in \mathbb{Z}, |l| < 2^{(2-\alpha_j)j}, k \in \mathbb{Z}^2, \iota \in \{\mathrm{h}, \mathrm{v}\} \right\} \\ \mathrm{SH}_{\mathrm{Bound}}(\phi, v, (\alpha_j)_j) &:= \left\{ \psi^{\alpha_j,(\mathrm{b})}_{j,l,k}(x) \mid j \in \mathbb{N}, l \in \mathbb{Z}, |l| = \pm 2^{(2-\alpha_j)j}, k \in \mathbb{Z}^2 \right\}. \end{aligned}$$

In [GK14, Theorem 2.4] it was shown that $\{\mathbf{\Psi}\}_\eta$, $\eta = (j, l, k; \alpha_j, (\iota))$ constitutes a Parseval frame for $L^2(\mathbb{R}^2)$, and all shearlets (coarse scaling functions, interior shearlets, and boundary shearlets) are smooth in the frequency domain. The universal shearlet system is restricted to discrete $\alpha_j \in Z_j$ in order for the set of sheared cone functions to exactly cover the horizontal and vertical frequency cones, and for the boundary shearlet to be smooth in the frequency domain. For a real $\alpha \in (-\infty, 2)$, we can choose $(\alpha_j)_j$ that pro-

vide the best possible approximation of α, i.e,

$$\alpha_j := \underset{\tilde{\alpha}_j \in Z_j}{\operatorname{argmin}} |\tilde{\alpha}_j - \alpha|, \quad j \geq 1. \tag{4.13}$$

This implies that $2^{\alpha_j j} = \Theta(2^{\alpha j})$ and $\lim \alpha_j = \alpha$ as $j \to \infty$. Indeed, we can show that

$$\alpha_j = \frac{\lfloor j\alpha + 0.5 \rfloor}{j}. \tag{4.14}$$

For our model, we consider universal shearlets with an arbitrary scaling sequence $(\alpha_j)_{j \in \mathbb{N}_0}$ chosen as in (4.14) with $\alpha \in (0, 2)$.

4.6 Inpainting and Separation of Cartoon and Texture

In this section we formulate our main result on inpainting and separation of cartoon and texture.

4.6.1 Multi-scale Separation and Inpainting

In our analysis, the separation problem is analyzed in a multi-scale setting. What we show is that the inpainting and separation method is more accurate for smaller scale components of the image, as long as the size of the missing part gets smaller in scale. Here, we adopt the multi-scale asymptotic analysis approach which was introduced in [DK13] for the problem of image separation. This approach was then adopted in [KKZ14] for image inpainting. The premise is that in the separation and inpainting problem there is no direct way to do asymptotic analysis, as the problem is fixed. One simple way to do asymptotic analysis is letting the missing band become smaller, and computing the rate of convergence of the reconstructed parts to the ground true parts. However, such a setting is somewhat trivial. The idea in [KKZ14] is to modify the model by breaking the cartoon part (and also the texture part in our case) to different scale components. By considering this sequence of models, we can formulate the accuracy of the problem as a function of the scale, thus deriving an asymptotic analysis. This approach was also adopted in [GK14; KDJ20].

Since texture is a stationary phenomenon, it mainly has middle and high frequency components. Thus, in our approach, the low frequency part of the signal is directly assigned to the cartoon part. Namely, for the low frequency band, we only use the shearlet frame in the l_1 minimization problem, and treat the resulting signal as a cartoon part. This is essentially the problem which is solved in [GK14], where the only difference there is that instead of cartoon the paper studies curve singularities. Note that our analysis extends to the one component analysis.

Consider the window function W defined in (4.11). We construct a family of *frequency filters* F_j with the Fourier representation

$$\hat{F}_j(\xi) := W_j(\xi) = W(\xi/2^{2j}), \quad \forall j \geq 1, \xi \in \mathbb{R}^2,$$

and in the case $j = 0$

$$\hat{F}_0(\xi) := \Phi(\xi), \quad \xi \in \mathbb{R}^2.$$

Notice that W_j is compactly supported in the corona

$$\mathcal{A}_j := [-2^{2j-1}, 2^{2j-1}]^2 \setminus [-2^{2j-4}, 2^{2j-4}]^2, \quad \forall j \geq 1. \tag{4.15}$$

We now consider the texture and cartoon parts at different scales by filtering them with F_j. For the patch size of texture, we typically use a fixed size s for all scales j. However, we also allow s to depend on the scale j to make the setting more flexible. We hence consider a variable s_j, and associated with s_j the domain $\mathcal{A}_{s,j}, \forall j \geq 1$, defined by

$$\mathcal{A}_{s,j} = \{\xi \in \mathbb{R}^2 : s_j \xi \in \mathcal{A}_j\}.$$

We split the components $w\mathcal{S}$ and $\mathcal{T}_s$ into pieces of different scales $w\mathcal{S}_j = F_j * w\mathcal{S}$ and $\mathcal{T}_{s,j} = F_j * \mathcal{T}_s$, where $\mathcal{T}_s$ is the texture of patch size $s = s_j$. The total signal at scale j is defined to be

$$f_j = w\mathcal{S}_j + \mathcal{T}_{s,j}.$$

As mentioned above, we typically pick a constant $s_j = s$. In the constant s case, the pieces f_j can be filtered directly from f, namely, $f_j = F_j * f$. We moreover have by (4.12)

$$f = \sum_j F_j * f_j.$$

In the general case, the Fourier transform $\hat{f}_j$ of f_j is supported in the annulus with inner radius 2^{2j-4} and outer radius 2^{2j-1}. Now, at each scale j we consider the simultaneous inpainting and separation problem of extracting $w\mathcal{S}_j$ and $\mathcal{T}_{s,j}$ from

$$(1 - P_j) f_j = (1 - P_j) w\mathcal{S}_j + (1 - P_j)\mathcal{T}_{s,j}. \tag{4.16}$$

As in [GK14], we assume that at scale j the size of the missing part h_j depends on j. Denote by P_j the characteristic function of the missing part at scale j, i.e,

$$P_j = \mathbb{1}_{\{|x_1| \leq h_j\}}. \tag{4.17}$$

Since generally $s = s_j$ depends on j, we use different Gabor frames to solve (4.16) for different scales. We denote by $\mathbf{G_j}$ the Gabor tight frame associated with $s = s_j$, i.e,

$$\mathbf{G_j} := \mathbf{G_{s_j}} = \{(g_{s_j})_{(m,n)}(x)\}_{(m,n)\in\mathbb{Z}^2}. \tag{4.18}$$

Under the above construction, in Theorem 4.16 we show that algorithm (INP-SEP), applied to each scale model (4.16), is asymptotically accurate as $j \to \infty$.

In the analysis of the next subsections, we need the following representation of P_j in the frequency domain.

Lemma 4.13 *We have* $\hat{P}_j(\xi) = 2h_j sinc(2h_j\xi_1)\delta(\xi_2)$.

Proof. By definition, we have

$$\hat{P}_j(\xi) = \int_{\mathbb{R}^2} P_j(x) e^{-2\pi i x^T \xi} dx$$

$$= \Big(\int_{-h_j}^{h_j} e^{-2\pi i x_1 \xi_1} dx_1\Big)\Big(\int_{\mathbb{R}} e^{-2\pi i x_2 \xi_2} dx_2\Big)$$
$$= 2h_j sinc(2h_j\xi_1)\delta(\xi_2).$$

■

4.6.2 Balancing the Texture and Cartoon Parts

It is important to avoid the trivial case where one of the parts, cartoon or texture, is much larger than the other. This would lead to the trivial separation outcome in which the whole image is taken as the estimation of the larger part, and the smaller part is estimated as zero. We thus suppose that the filtered components $w\mathcal{S}_j$ and $\mathcal{T}_{s,j}$ have comparable magnitudes at each scale.

Consider the sub-band components

$$w\mathcal{S}_j = F_j * w\mathcal{S}, \tag{4.19}$$

and

$$\mathcal{T}_{s,j} = F_j * \mathcal{T}_s, \tag{4.20}$$

where $w\mathcal{S}$ is defined in (4.9) and texture is in Definition 4.9 . The following lemma formulates the *energy balancing condition*.

Lemma 4.14 *Consider the cartoon patch and texture with sub-bands defined in* (4.19), (4.20)*, respectively. We have*

$$\|w\mathcal{S}_j\|_2^2 \sim 2^{-2j}, \quad j \to \infty,$$

and

$$\|\mathcal{T}_{s,j}\|_2^2 \sim \sum_{n \in \mathbb{Z}^2 \cap \mathcal{A}_{s,j}} |d_n|^2.$$

Therefore, energy balance is achieved for

$$c_0 2^{-2j} \leq \sum_{n \in I_T \cap \mathcal{A}_{s,j}} |d_n|^2 \leq c_1 2^{-2j}, \quad c_0, c_1 > 0. \tag{4.21}$$

Proof. We present the following sketch of the proof. For W sufficient nice we have

$$\begin{aligned}
\|w\mathcal{S}_j\|_2^2 &= \int_{\substack{\xi \in \mathbb{R}^2, \\ |\xi_2| \geq r}} |\hat{w}(\xi_1)|^2 \cdot W^2(2^{-2j}\xi) \cdot \frac{1}{4}\Big|\delta(\xi_2) + \frac{i}{\pi\xi_2}\Big|^2 d\xi \\
&\sim \int_{\substack{\xi \in \mathcal{A}_j, \\ |\xi_2| \geq r}} \frac{1}{\xi_2^2} \cdot |\hat{w}(\xi_1)|^2 d\xi \\
&\sim \int_{\substack{\xi \in \mathcal{A}_j, \\ |\xi_2| \geq 2^{2j-5}}} \frac{1}{\xi_2^2} |\hat{w}(\xi_1)|^2 d\xi + \int_{\substack{\xi \in \mathcal{A}_j, \\ 2^{2j-5} \geq |\xi_2| \geq r}} \frac{1}{\xi_2^2} |\hat{w}(\xi_1)|^2 d\xi.
\end{aligned}$$

Note that by (4.15), $\mathcal{A}_j = [-2^{2j-1}, 2^{2j-1}]^2 \setminus [-2^{2j-4}, 2^{2j-4}]^2$. Thus, $\{\xi \in \mathcal{A}_j, 2^{2j-5} \geq |\xi_2| \geq$

$r\} \subset \{\xi \in \mathcal{A}_j, |\xi_1| \geq 2^{2j-4}\}$. We now use the rapid decay of $\hat{w}$

$$\sup_{|\xi_1|\geq 2^{2j-5}} |\hat{w}(\xi_1)| \leq C_N \langle |2^{2j}| \rangle^{-N}, \quad \forall N \in \mathbb{N}.$$

This leads to

$$\int_{\substack{\xi\in\mathcal{A}_j,\\ 2^{2j-5}\geq|\xi_2|\geq r}} \frac{1}{\xi_2^2}|\hat{w}(\xi_1)|^2 d\xi_2 \leq C_N \cdot \frac{2^{2j}}{r^2} \cdot 2^{2j}\langle |2^{2j}| \rangle^{-N}, \quad \forall N \in \mathbb{N}. \tag{4.22}$$

Since $\xi \in \mathcal{A}_j = [-2^{2j-1}, 2^{2j-1}]^2 \setminus [-2^{2j-4}, 2^{2j-4}]^2$, we have

$$C2^{-2j} = \int_{2^{2j-4}}^{2^{2j-1}} \frac{1}{\xi_2^2} d\xi_2 \cdot \int_{-2^{2j-1}}^{2^{2j-1}} |\hat{w}(\xi_1)|^2 d\xi_1 \leq \int_{\substack{\xi\in\mathcal{A}_j,\\ |\xi_2|\geq 2^{2j-5}}} \frac{1}{\xi_2^2}|\hat{w}(\xi_1)|^2 d\xi.$$

Thus,

$$\int_{\substack{\xi\in\mathcal{A}_j,\\ |\xi_2|\geq 2^{2j-5}}} \frac{1}{\xi_2^2}|\hat{w}(\xi_1)|^2 d\xi_2 \sim C \cdot 2^{-2j}. \tag{4.23}$$

Combining (4.22) and (4.23), we finally obtain

$$\|w\mathcal{S}_j\|_2^2 \sim 2^{-2j}. \tag{4.24}$$

On the other hand, we have

$$\mathcal{T}_s = \sum_{n\in I_T} d_n g_{s_j}(x) e^{2\pi i \langle s_j n, x\rangle}.$$

This leads to

$$\hat{\mathcal{T}}_s = \sum_{n\in I_T} d_n \hat{g}_{s_j}(\xi - s_j n).$$

Now, using the change of variable $\omega = \frac{\xi}{s_j}$ we get

$$\begin{aligned}
\|\mathcal{T}_{s,j}\|_2^2 &= \|\hat{\mathcal{T}}_{s,j}\|_2^2 = \sum_{n,\tilde{n}\in I_T} \int d_n \overline{d_{\tilde{n}}} W^2(\xi/2^{2j}) \hat{g}_{s_j}(\xi - s_j n)\hat{g}_{s_j}(\xi - s_j\tilde{n}) d\xi \\
&= s_j^2 \cdot \sum_{\substack{|n-\tilde{n}|\leq 1\\ n,\tilde{n}\in I_T}} \int d_n \overline{d_{\tilde{n}}} W^2(s_j\omega/2^{2j}) \hat{g}_{s_j}(s_j(\omega - n))\hat{g}_{s_j}(s_j(\omega - \tilde{n})) d\omega \\
&= \sum_{\substack{|n-\tilde{n}|\leq 1\\ n,\tilde{n}\in I_T}} \int d_n \overline{d_{\tilde{n}}} W^2(s_j\omega/2^{2j}) \hat{g}(\omega - n)\hat{g}(\omega - \tilde{n}) d\omega.
\end{aligned}$$

Note that for each n, there exist a finite number of $\tilde{n}$'s independent of j satisfying $|n - \tilde{n}| \leq 1$, and since W is sufficiently nice,

$$\int W^2(s_j\omega/2^{2j}) \hat{g}(\omega - n)\hat{g}(\omega - \tilde{n}) d\omega \sim \int_{\mathcal{A}_{s,j}} \hat{g}(\omega - n)\hat{g}(\omega - \tilde{n}) d\omega.$$

Thus, we obtain

$$\begin{aligned}\|\mathcal{T}_{s,j}\|_2^2 &\sim \sum_{\substack{|n-\tilde{n}|\le 1\\ n\in I_T\cap\mathcal{A}_{s,j}}} \int_{\mathcal{A}_{s,j}} d_n\overline{d_{\tilde{n}}}\hat{g}(\omega-n)\overline{\hat{g}(\omega-\tilde{n})}d\omega\\ &\sim \sum_{n\in I_T\cap\mathcal{A}_{s,j}} \int_{\mathcal{A}_{s,j}} |d_n|^2|\hat{g}(\omega-n)|^2 d\omega.\end{aligned}$$

Up to a small set of coefficients, we assume that the support of $\hat{g}$ is always entirely contained in $\mathcal{A}_{s,j}$. Hence,

$$\begin{aligned}\|\mathcal{T}_{s,j}\|_2^2 &\sim \sum_{n\in I_T\cap\mathcal{A}_{s,j}} \int_{\mathbb{R}^2} |d_n|^2|\hat{g}(\omega-n)|^2 d\omega\\ &= \sum_{n\in I_T\cap\mathcal{A}_{s,j}} |d_n|^2 \int_{\mathbb{R}^2} |\hat{g}(\omega)|^2 d\omega \sim \sum_{n\in I_T\cap\mathcal{A}_{s,j}} |d_n|^2.\end{aligned} \tag{4.25}$$

Combining (4.24) and (4.25), we finish the proof. ∎

For later analysis, we also need an energy estimate of the cartoon patch in the missing region. We use the following useful notation in the whole paper

$$\langle|x|\rangle = (1+|x|^2)^{1/2}. \tag{4.26}$$

Lemma 4.15 *For $h_j = o(2^{-\alpha_j j})$, $\alpha_j \in (0,2)$, and $\omega(0)\neq 0$, there exists a constant $C_1>0$ such that*

$$\|P_j w\mathcal{S}_j\|_2^2 \ge C_1\cdot h_j^2 2^{-2j}$$

Proof. By Plancherel's theorem and Lemma 4.13, we have

$$\begin{aligned}\|P_j w\mathcal{S}_j\|_2^2 &= \int_{\substack{\xi\in\mathbb{R}^2\\ |\xi_2|\ge r}} \Big|\int_{\mathbb{R}^2} \hat{P}_j(t)\widehat{w\mathcal{S}_j}(\xi-t)dt\Big|^2 d\xi\\ &= \int_{\substack{\xi\in\mathbb{R}^2\\ |\xi_2|\ge r}} \Big|\int_{\mathbb{R}} 2h_j sinc(2h_j t_1)\hat{w}(\xi_1-t_1)\frac{1}{(\pi\xi_2)}W_j(\xi_1-t_1,\xi_2)dt_1\Big|^2 d\xi\\ &= \frac{4h_j^2}{\pi^2}\int_{\substack{\xi\in\mathbb{R}^2\\ |\xi_2|\ge r}} \frac{1}{\xi_2^2}\Big|\int_{\mathbb{R}} sinc(2h_j t_1)\hat{w}(\xi_1-t_1)W_j(\xi_1-t_1,\xi_2)dt_1\Big|^2 d\xi.\end{aligned} \tag{4.27}$$

Next, recalling the definition of $W_j(\xi)$ in (4.11), we have

$$W_j(\xi)=1,\quad \forall\xi \text{ such that } \xi\in[-2^{2j-2},2^{2j-2}]^2\setminus[-2^{2j-3},2^{2j-3}]^2. \tag{4.28}$$

For ξ in the corona-shape $\{\xi\in\mathbb{R}^2 \mid \xi\in[-2^{2j-2},2^{2j-2}]^2\setminus[-2^{2j-3},2^{2j-3}]^2\}$, if ξ_1 is small then ξ_2 must be large. More accurately, for ξ with $|\xi_1|\le 1$, we are guaranteed to have $\xi\in[-2^{2j-2},2^{2j-2}]^2\setminus[-2^{2j-3},2^{2j-3}]^2$ in case $\xi_2\in(2^{2j-3},2^{2j-2})$. Combining this observation

with (4.27), the following holds

$$\|P_j\omega\mathcal{S}_j\|_2^2 \geq Ch_j^2 \int_{2^{2j-3}}^{2^{2j-2}} \frac{1}{\xi_2^2} \int_{-1}^{1} \Big| \int_{\mathbb{R}} sinc(2h_jt_1)\hat{\omega}(\xi_1 - t_1)W_j(\xi_1 - t_1, \xi_2)dt_1\Big|^2 d\xi_1 d\xi_2. \quad (4.29)$$

Next, we study the term $I_j(\xi) := \Big| \int_{\mathbb{R}} sinc(2h_jt_1)\hat{\omega}(\xi_1 - t_1)W_j(\xi_1 - t_1, \xi_2)dt_1\Big|$. By the triangle inequality, we have

$$\begin{aligned} I_j(\xi) \geq & \Big| \int_{|t_1|\leq 2^{\alpha_j j-4}} sinc(2h_jt_1)\hat{\omega}(\xi_1 - t_1)W_j(\xi_1 - t_1, \xi_2)dt_1\Big| - \\ & \Big| \int_{|t_1|\geq 2^{\alpha_j j-4}} sinc(2h_jt_1)\hat{\omega}(\xi_1 - t_1)W_j(\xi_1 - t_1, \xi_2)dt_1\Big|. \end{aligned} \quad (4.30)$$

We now use the rapid decay of $\hat{w}$ to obtain

$$\sup_{|t_1|\geq 2^{\alpha_j j}} |\hat{w}(\xi_1 - t_1)| \leq C_N\langle|2^{\alpha_j j}|\rangle^{-N}, \quad \forall\xi_1 \in [-1, 1], \forall N \in \mathbb{N}. \quad (4.31)$$

This leads to

$$\Big| \int_{|t_1|\geq 2^{\alpha_j j-4}} sinc(2h_jt_1)\hat{\omega}(\xi_1 - t_1)W_j(\xi_1 - t_1, \xi_2)dt_1\Big| \leq C'_N\langle|2^{\alpha_j j}|\rangle^{-N}. \quad (4.32)$$

For the other term, we observe that for fine scale j, we have $(\xi_1 - t_1, \xi_2) \in [-2^{2j-2}, 2^{2j-2}]^2 \setminus [-2^{2j-3}, 2^{2j-3}]^2$ for $\xi_1 \in [-1, 1], |t_1| \leq 2^{\alpha_j j-4}, \alpha_j \in (0, 2)$ and $\xi_2 \in (2^{2j-3}, 2^{2j-2})$. Combining this with (4.28), we derive $W_j(\xi_1 - t_1, \xi_2) = 1$. Thus, we obtain

$$\begin{aligned} \int_{|t_1|\leq 2^{\alpha_j j-4}} sinc(2h_jt_1)\hat{\omega}(\xi_1 - t_1)W_j(\xi_1 - t_1, \xi_2)dt_1 \quad = \quad & \int_{|t_1|\leq 2^{\alpha_j j-4}} sinc(2h_jt_1) \\ & \cdot\hat{\omega}(\xi_1 - t_1)dt_1. \end{aligned}$$

We now prove that there exists a constant $C' > 0$ such that for sufficiently large j, we have

$$\Big| \int_{|t_1|\leq 2^{\alpha_j j-4}} sinc(2h_jt_1)\hat{\omega}(\xi_1 - t_1)dt_1\Big| \geq C', \quad \forall\xi_1 \in [-1, 1]. \quad (4.33)$$

By triangle inequality, we obtain

$$\begin{aligned} & \Big| \int_{|t_1|\leq 2^{\alpha_j j-4}} sinc(2h_jt_1)\hat{\omega}(\xi_1 - t_1)dt_1\Big| \geq \\ & \Big| \int_{|t_1|\leq 2^{\alpha_j j-4}} \hat{w}(\xi_1 - t_1)dt_1\Big| - \Big| \int_{|t_1|\leq 2^{\alpha_j j-4}} \Big(sinc(2h_jt_1) - 1\Big)\hat{w}(\xi_1 - t_1)dt_1\Big|. \end{aligned} \quad (4.34)$$

For the first term, the following holds for $\forall\xi_1 \in [-1, 1]$

$$\begin{aligned} \Big| \int_{|t_1|\leq 2^{\alpha_j j-4}} \hat{w}(\xi_1 - t_1)dt_1\Big| \geq & \Big| \int_{\mathbb{R}} \hat{w}(t_1)dt_1\Big| - \Big| \int_{|t_1|\geq 2^{\alpha_j j-4}} \hat{w}(\xi_1 - t_1)dt_1\Big| \\ & \overset{\text{by (4.31)}}{\approx} |w(0)| = \text{const} > 0. \end{aligned} \quad (4.35)$$

For the second term of the right hand side of (4.34), by the assumption $h_j 2^{\alpha_j j} \xrightarrow{j\to+\infty} 0$, we have

$$\begin{aligned}
&\Big| \int_{|t_1|\le 2^{\alpha_j j-4}} (sinc(2h_j t_1) - 1)\hat{w}(\xi_1 - t_1)dt_1 \Big| \\
&\le \sup_{|t_1|\le 2^{\alpha_j j-4}} |sinc(2h_j t_1) - 1| \int_{\mathbb{R}} |\hat{w}(t_1|dt_1 \\
&\le C \cdot \sup_{|t_1|\le 2^{\alpha_j j-4}} |sinc(2h_j t_1) - 1| \xrightarrow{j\to+\infty} 0. \qquad (4.36)
\end{aligned}$$

Thus, by (4.34), (4.36) and (4.35), we conclude the proof of (4.33).

Now, by (4.30), (4.32), and (4.33), we have $I_j(\xi) \ge C' = \text{const}$. Combining this with (4.29), we finally obtain

$$\begin{aligned}
\|P_j \omega \mathcal{S}_j\|_2^2 &\ge C h_j^2 \Big(\int_{2^{2j-3}}^{2^{2j-\frac{5}{2}}} \frac{1}{\xi_2^2} d\xi_2 \Big) \Big(\int_{-1}^{1} C'^2 d\xi_1 \Big) \\
&= C_1 \cdot h_j^2 2^{-2j},
\end{aligned}$$

which concludes the proof. ∎

4.6.3 Sparsity Assumptions on Texture

Next, we restrict the definition of texture by bounding the size of the index set I_T of Definition 4.9. Define the domain

$$M_{j,l,(\iota)} := \Big[s_j^{-1} \cdot S_{(\iota)}^{-l} \cdot (\operatorname{supp} \hat{\psi}_{j,0,0}^{\alpha_j,(\iota)} + B_1(0,1)) \Big] \cap \mathbb{Z}^2,$$

where $A + B := \{a + b \mid a \in A, b \in B\}$ is the Minkowski sum, and multiplication of a set of vectors by a matrix is done elementwise. We assume that at every scale j, the number of non-zero Gabor elements with the same position, generating $\mathcal{T}_{s,j}$, is not too large. More accurately, denote $|A| = \#\{n \in \mathbb{Z}^2 \cap A\}$, and define the neighborhood set $I_T^{\pm}$ of the index set I_T by

$$I_T^{\pm} = \{n' \in \mathbb{Z}^2 \mid \exists n \in I_T : |n' - n| \le 1\}.$$

What we assume is that at every scale j, for all $l \in \mathbb{Z}$ satisfying $|l| \le 2^{(2-\alpha_j)j}$ we have

$$|I_T \cap M_{j,l,(\iota)}| \le 2^{(2-\alpha_j-\epsilon)j/2} = o(2^{(2-\alpha_j)j/2}), \quad \forall (\iota) \in \{(\mathrm{h}), (\mathrm{v}), (\mathrm{b})\}, \qquad (4.37)$$

and

$$|I_T^{\pm} \cap \mathcal{A}_{s,j}| \le \frac{2^{\alpha_j j}}{s_j} \quad \text{as } j \to \infty. \qquad (4.38)$$

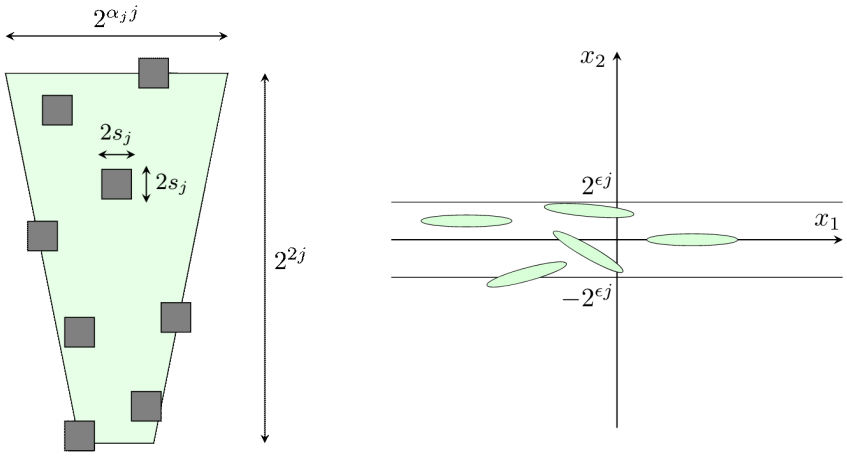

Figure 4.5: Left: Interaction between a cluster of Gabor elements (black small squares) and a shearlet (gray) in the frequency domain; Right: Some shearlet elements (gray) associated with $\Lambda_{1,j}$ in the spatial domain for $l = 0$.

4.6.4 Cluster Sets for Texture and Cartoon

We define the cluster for texture at scale j to be

$$\Lambda_{2,j} := \left(\mathbb{Z}^2 \cap B(0, M_j)\right) \times \left(I_T^{\pm} \cap \mathcal{A}_{s,j}\right), \tag{4.39}$$

where $M_j := 2^{\epsilon j/6}$ and $B(0,r)$ denotes the closed l_2 ball around the origin in $\mathbb{R}^2$. The term $M_j = 2^{\epsilon j/6}$ controls the trade-off between the relative sparsity and cluster coherence of the Gabor systems.

To represent the cartoon part, consider a universal shearlet system with α_j from (4.13), where $\alpha \in (0,2)$ is a global constant. To define the cluster sets, we fix a constant ϵ satisfying

$$0 < \epsilon < \frac{2-\alpha}{3}.$$

Since α_j satisfies $\lim_{j\to\infty} \alpha_j = \alpha$, we have $\lim_{j\to+\infty} \alpha_j \leq 2 - 3\epsilon$ and

$$0 < \epsilon < \frac{2-\alpha_j}{3}, \tag{4.40}$$

at fine enough scales j. For the cartoon model $w\mathcal{S}_j$ we define the set of significant coefficients of universal shearlet system by

$$\Lambda_{1,j}^{\pm} := \Lambda_{1,j-1} \cup \Lambda_{1,j} \cup \Lambda_{1,j+1}, \quad \forall j \geq 2, \tag{4.41}$$

where $\Lambda_{1,j} := \left\{(j,l,k;\alpha_j,\mathrm{v}) \mid |l| \leq 1, k = (k_1,k_2) \in \mathbb{Z}^2, |k_2 - lk_1| \leq 2^{\epsilon j}\right\}$.

4.6.5 The Separation and Inpainting Theorem for Cartoon and Texture

We now present our main result. In the following theorem, we prove the success of separation and inpaining via Algorithm (INP-SEP). Since we inpaint a band of width h_j for each scale j, it is important to show that the inpainting error is asymptotically smaller than the energy that typical cartoon and texture parts have in the missing band. For the cartoon part, we can prove that the relative reconstruction error, restricted to the missing part, goes to zero as $j \to \infty$. For texture, we note that it is possible for $\mathcal{T}_{s,j}$ to be close to zero in the missing part, and thus the relative error restricted to the missing part need not go to zero in the general case. However, generic texture parts are not close to zero in the missing band, and typically

$$\|P_j \mathcal{T}_{s,j}\|_2 \propto h_j \|\mathcal{T}_{s,j}\|_2 \propto h_j 2^{-j}.$$

We thus consider for texture a relative error of the form

$$\frac{\|P_j \mathcal{T}_j^\star - P_j \mathcal{T}_{s,j}\|_2}{h_j 2^{-j}}.$$

Theorem 4.16 *Consider the cartoon patch and texture with $w\mathcal{S}_j$ and $\mathcal{T}_{s,j}$ defined in (4.19) and (4.20) respectively. Suppose that the energy matching (4.21) holds. Suppose that the index set of the texture $\mathcal{T}_{s,j}$ satisfies (4.37) and (4.38). Then, for $0 < h_j = o(2^{-(\alpha_j+\epsilon)j})$ with $\alpha_j \in (0,2), \liminf \alpha_j > 0$ and ϵ satisfying (4.40), the recovery error provided by Algorithm (INP-SEP) decays rapidly and we have asymptotically perfect simultaneous separation and inpainting. Namely, for all $N \in \mathbb{N}_0$,*

$$\frac{\|\mathcal{C}_j^\star - w\mathcal{S}_j\|_2 + \|\mathcal{T}_j^\star - \mathcal{T}_{s,j}\|_2}{\|w\mathcal{S}_j\|_2 + \|\mathcal{T}_{s,j}\|_2} = o(2^{-Nj}) \to 0, \quad j \to \infty,$$

where $(\mathcal{C}_j^\star, \mathcal{T}_j^\star)$ is the solution of (INP-SEP) and $(w\mathcal{S}_j, \mathcal{T}_{s,j})$ are ground truth components. In addition, if $\omega(0) \neq 0$, we have asymptotically accurate relative reconstruction error in the missing part

$$\frac{\|P_j \mathcal{C}_j^\star - P_j \omega \mathcal{S}_j\|_2}{\|P_j \omega \mathcal{S}_j\|_2} \xrightarrow{j\to+\infty} 0 \quad \text{and} \quad \frac{\|P_j \mathcal{T}_j^\star - P_j \mathcal{T}_{s,j}\|_2}{h_j 2^{-j}} \xrightarrow{j\to+\infty} 0.$$

We postpone the proof of Theorem 4.16 to Section 4.10, after we discuss preliminary material.

Note that in Theorem 4.16 there is no direct restriction on the texture patch sizes s_j^{-1}, and the theorem works even when the texture patch at each scale is smaller than the scale 2^{-j}. However, the most useful case of Theorem 4.16, which appropriately models the relation between texture and cartoon, is when $s_j = s$ is constant for all j. This is formulated in the following corollary.

Corollary 4.17 *Consider the conditions of Theorem 4.16, and suppose that the texture part $\mathcal{T}_{s,j}$ is based on a constant $s_j = s$. Then, we have asymptotically perfect separation and*

inpainting, i.e, for $\forall N \in \mathbb{N}_0$,

$$\frac{\|\mathcal{C}_j^\star - \mathcal{C}_j\|_2 + \|\mathcal{T}_j^\star - \mathcal{T}_{s,j}\|_2}{\|\mathcal{C}_j\|_2 + \|\mathcal{T}_{s,j}\|_2} = o(2^{-Nj}) \to 0, \quad j \to \infty,$$

where $(\mathcal{C}_j^\star, \mathcal{T}_j^\star)$ *is the solution of* (INP-SEP) *and* $(\mathcal{C}_j, \mathcal{T}_{s,j})$ *are ground truth components. In addition, if* $\omega(0) \neq 0$, *we have*

$$\frac{\|P_j\mathcal{C}_j^\star - P_j\omega\mathcal{S}_j\|_2}{\|P_j\omega\mathcal{S}_j\|_2} \xrightarrow{j\to+\infty} 0 \quad \textit{and} \quad \frac{\|P_j\mathcal{T}_j^\star - P_j\mathcal{T}_{s,j}\|_2}{h_j 2^{-j}} \xrightarrow{j\to+\infty} 0.$$

4.7 Extensions and Future Directions

In this section, we present potential extensions and future directions of our approach.

1. **Global cartoon model**. Using the technique introduced in [DK13] and [Kut13], we can localize a global cartoon part $\mathcal{C}_j$ by a *partition of unity* $(w_Q)_{Q\in\mathcal{Q}}$. Denoting $\mathcal{C}_{j,Q} = \mathcal{C}_j \cdot w_Q$, we have
$$\sum_Q \mathcal{C}_{j,Q} = \mathcal{C}_j.$$
In this approach, using a *tubular neighborhood theorem* ([DK13, Sect. 6] and [Kut13]), we apply a diffeomorphism Φ_Q to each piece $\mathcal{C}_{j,Q}$ to straighten out the local curve discontinuity. By combining the different neighborhoods, we can derive a convergence results for a global cartoon part.

2. **Other types of components**. Our theoretical analysis holds for general representation systems which form Parseval frames. Thus, our general technique can be applied to problems of image separation and image ipainting of other types of image parts.

3. **Noisy case**. In future work we will extend our theory to the case where the image contains noise.

4. **More components**. In our analysis we consider the case where there are two components. In future work we will extend our theoretical guarantee for separation and inpainting of more than two geometric components.

In the rest of the paper we prove Theorem 4.16. For that, in section 4.8 we study the relative sparsity of texture and cartoon, and in Section 4.9 we study the cluster coherence of the sparsifying systems.

4.8 Relative Sparsity of Texture and Cartoon

In this section, we bound the relative sparsity of texture with respect to shearlet frame (Subsection 4.8.2) and texture with respect to Gabor frame (Subsection 4.8.3).

4.8.1 Decay Estimates of Shearlet and Gabor Elements

First, we provide decay estimates of shearlet and Gabor elements.

Lemma 4.18 *Consider the shearlet frame $\mathbf{\Psi}$ of Definition 4.12 and the Gabor frame of scale j, $\mathbf{G_j}$ defined in (4.18). For any arbitrary integer $N = 1, 2, \dots$ there exists a constant C_N depending on j such that the following estimates hold*

1. $|(g_{s_j})_{m,n}(x)| \leq C_N \cdot s_j \cdot \langle |s_j x_1 + \frac{m_1}{2}| \rangle^{-N} \langle |s_j x_2 + \frac{m_2}{2}| \rangle^{-N}$,
2. $|\psi^{\alpha_j,(\mathrm{v})}_{j,l,k}(x)| \leq C_N \cdot 2^{(2+\alpha_j)j/2} \cdot \langle |2^{\alpha_j j} x_1 - k_1| \rangle^{-N} \langle |2^{2j} x_2 + l 2^{\alpha_j j} x_1 - k_2| \rangle^{-N}$,
   $|\psi^{\alpha_j,(\mathrm{h})}_{j,l,k}(x)| \leq C_N \cdot 2^{(2+\alpha_j)j/2} \cdot \langle |2^{2j} x_1 + l 2^{\alpha_j j} x_2 - k_1)| \rangle^{-N} \langle |2^{\alpha_j j} x_2 - k_2| \rangle^{-N}$,
3. $|\langle (g_{s_j})_{m,n}, \psi^{\alpha_j,(\iota)}_{j,l,k} \rangle| \leq C_N \cdot 2^{-(2-\alpha_j)j/2}, \quad \forall (\iota) \in \{(\mathrm{v}), (\mathrm{h}), (\mathrm{b})\}$.

Proof. 1) By the change of variable $\zeta = s_j^{-1}\xi - n$, we have

$$\begin{aligned} |(g_{s_j})_{m,n}(x)| &= \Big| \int_{\mathbb{R}^2} (\hat{g}_{s_j})_{m,n}(\xi) e^{2\pi i \xi^T x} d\xi \Big| = \Big| \int_{\mathbb{R}^2} s_j^{-1} \hat{g}(s_j^{-1}\xi - n) e^{2\pi i \xi^T (x + \frac{m}{2s_j})} d\xi \Big| \\ &= \Big| s_j e^{2\pi i n^T (s_j x + \frac{m}{2})} \int_{\mathbb{R}^2} \hat{g}(\zeta) e^{2\pi i \zeta^T (s_j x + \frac{m}{2})} d\zeta \Big| \\ &\leq \Big| s_j \int_{\mathbb{R}^2} \hat{g}(\zeta) e^{2\pi i \zeta^T (s_j x + \frac{m}{2})} d\zeta \Big|. \end{aligned}$$

We now apply integration by parts for $N_1, N_2 = 1, 2, \dots$, with respect to ζ_1, ζ_2, respectively, we obtain

$$\begin{aligned} & |(g_{s_j})_{m,n}(x)| \\ = & \Big| \int_{\mathbb{R}^2} s_j (s_j x_1 + \frac{m_1}{2})^{-N_1} \frac{\partial^{N_1}}{\partial \zeta_1^{N_1}} [\hat{g}(\zeta)] e^{2\pi i \zeta^T (s_j x + \frac{m}{2})} d\zeta \Big| \\ = & \Big| \int_{\mathbb{R}^2} s_j (s_j x_1 + \frac{m_1}{2})^{-N_1} (s_j x_2 + \frac{m_2}{2})^{-N_2} \frac{\partial^{N_1+N_2}}{\partial \zeta_1^{N_1} \partial \zeta_2^{N_2}} [\hat{g}(\zeta)] e^{2\pi i \zeta^T (s_j x + \frac{m}{2})} d\zeta \Big| \\ \leq & s_j |s_j x_1 + \frac{m_1}{2}|^{-N_1} |s_j x_2 + \frac{m_2}{2}|^{-N_2} \int_{\mathbb{R}^2} \Big| \frac{\partial^{N_1+N_2}}{\partial \zeta_1^{N_1} \partial \zeta_2^{N_2}} [\hat{g}(\zeta)] \Big| d\zeta, \end{aligned}$$

and similarly

$$|(g_{s_j})_{m,n}(x)| \leq s_j |s_j x_k + \frac{m_k}{2}|^{-N_k} \int_{\mathbb{R}^2} \Big| \frac{\partial^{N_k}}{\partial \zeta_k^{N_k}} [\hat{g}(\zeta)] \Big| d\zeta$$

for $k = 1, 2$. Here, the boundary terms vanish due to the compact support of $(\hat{g}_{s_j})_{m,n}(\zeta)$. Thus,

$$\begin{aligned} & s_j^{-1} \Big(1 + |s_j x_1 + \tfrac{m_1}{2}|^{N_1} + |s_j x_2 + \tfrac{m_2}{2}|^{N_2} + |s_j x_1 + \tfrac{m_1}{2}|^{N_1} |s_j x_2 + \tfrac{m_2}{2}|^{N_2} \Big) |(g_{s_j})_{m,n}(x)| \\ = & \; s_j^{-1} (1 + |s_j x_1 + \frac{m_1}{2}|^{N_1})(1 + |s_j x_2 + \frac{m_2}{2}|^{N_2}) |(g_{s_j})_{m,n}(x)| \end{aligned}$$

$$\leq \int_{\mathbb{R}^2} |\hat{g}(\zeta)| d\zeta + \int_{\mathbb{R}^2} \Big| \frac{\partial^{N_1}}{\partial \zeta_1^{N_1}} [\hat{g}(\zeta)] \Big| d\zeta + \int_{\mathbb{R}^2} \Big| \frac{\partial^{N_2}}{\partial \zeta_2^{N_2}} [\hat{g}(\zeta)] \Big| d\zeta + \int_{\mathbb{R}^2} \Big| \frac{\partial^{N_1+N_2}}{\partial \zeta_1^{N_1} \partial \zeta_2^{N_2}} [\hat{g}(\zeta)] \Big| d\zeta.$$

By the smoothness of $\hat{g}(\zeta)$ and $\operatorname{supp} \hat{g} = [-1, 1]$, there exists a constant C'_{N_1,N_2} independent of j such that
$\int_{\mathbb{R}^2} |\hat{g}(\zeta)| d\zeta + \int_{\mathbb{R}^2} \Big| \frac{\partial^{N_1}}{\partial \zeta_1^{N_1}} [\hat{g}(\zeta)] \Big| d\zeta + \int_{\mathbb{R}^2} \Big| \frac{\partial^{N_2}}{\partial \zeta_2^{N_2}} [\hat{g}(\zeta)] \Big| d\zeta + \int_{\mathbb{R}^2} \Big| \frac{\partial^{N_1+N_2}}{\partial \zeta_1^{N_1} \partial \zeta_2^{N_2}} [\hat{g}(\zeta)] \Big| d\zeta \leq C'_{N_1,N_2}.$

We obtain

$$|(g_{s_j})_{m,n}(x)| \leq C'_{N_1,N_2} \cdot s_j \cdot \frac{1}{1 + |s_j x_1 + \frac{m_1}{2}|^{N_1}} \frac{1}{1 + |s_j x_2 + \frac{m_2}{2}|^{N_2}}.$$

Moreover, for each $N_1, N_2 = 1, 2, \ldots$ there exist C'_{N_1}, C'_{N_2} such that

$$\langle |s_j x_1 + \frac{m_1}{2}| \rangle^{N_1} = (1 + |s_j x_1 + \frac{m_1}{2}|^2)^{N_1/2} \leq C'_{N_1} (1 + |s_j x_1 + \frac{m_1}{2}|)^{N_1},$$

$$\langle |s_j x_2 + \frac{m_2}{2}| \rangle^{N_2} = (1 + |s_j x_2 + \frac{m_2}{2}|^2)^{N_2/2} \leq C'_{N_2} (1 + |s_j x_2 + \frac{m_2}{2}|)^{N_2}.$$

Thus,

$$|(g_{s_j})_{m,n}(x)| \leq C_{N_1,N_2} \cdot s_j \cdot \langle |s_j x_1 + \frac{m_1}{2}| \rangle^{-N_1} \langle |s_j x_2 + \frac{m_2}{2}| \rangle^{-N_2}.$$

This proves the claim for any arbitrary integer N.
2) By the change of variable $\zeta^T = \xi^T A^{-j}_{\alpha_{j'}(\iota)} S^{-l}_{(\iota)}$, we have

$$\begin{aligned} |\psi^{\alpha_{j'}(\iota)}_{j,l,k}(x)| &= \Big| \int_{\mathbb{R}^2} \hat{\psi}^{\alpha_{j'}(\iota)}_{j,l,k}(\xi) e^{2\pi i \xi^T x} d\xi \Big| \\ &= \Big| \int_{\mathbb{R}^2} 2^{-(2+\alpha_j)j/2} W_j(\xi) V_{(\iota)} \Big(\xi^T A^{-j}_{\alpha_{j'}(\iota)} S^{-l}_{(\iota)} \Big) e^{2\pi i \xi^T (x - A^{-j}_{\alpha_{j'}(\iota)} S^{-l}_{(\iota)} k)} d\xi \Big| \\ &= \Big| \int_{\mathbb{R}^2} 2^{(2+\alpha_j)j/2} W_j((S^l_{(\iota)} A^j_{\alpha_{j'}(\iota)})^T \zeta) V_{(\iota)}(\zeta) e^{2\pi i \zeta^T (S^l_{(\iota)} A^j_{\alpha_{j'}(\iota)} x - k)} d\zeta \Big|. \end{aligned}$$

Similarly to in 1) we apply integration by parts for $N_1, N_2 = 1, 2, \ldots$ with respect to ζ_1, ζ_2. We obtain the decay estimate of universal shearlets

$$|\psi^{\alpha_{j'}(\mathrm{v})}_{j,l,k}(x)| \leq C_N \cdot 2^{(2+\alpha_j)j/2} \cdot \langle |2^{\alpha_j j} x_1 - k_1| \rangle^{-N} \langle |2^{2j} x_2 + l 2^{\alpha_j j} x_1 - k_2| \rangle^{-N},$$

$$|\psi^{\alpha_{j'}(\mathrm{h})}_{j,l,k}(x)| \leq C_N \cdot 2^{(2+\alpha_j)j/2} \cdot \langle |2^{2j} x_1 + l 2^{\alpha_j j} x_2 - k_1)| \rangle^{-N} \langle |2^{\alpha_j j} x_2 - k_2| \rangle^{-N}.$$

3) We consider three cases.
Case 1: $(\iota) = (\mathrm{v})$. Applying 1) and 2) and the change of variables $(y_1, y_2) = (s_j x_1, 2^{2j} x_2 + l 2^{\alpha_j j} x_1)$, we obtain

$$|\langle (g_{s_j})_{m,n}, \psi^{\alpha_{j'}(\mathrm{v})}_{j,l,k} \rangle| = \Big| \int_{\mathbb{R}^2} (g_{s_j})_{m,n}(x) \overline{\psi^{\alpha_{j'}(\mathrm{v})}_{j,l,k}(x)} dx \Big|$$

$$\begin{aligned} &\leq C'_N \cdot 2^{-(2-\alpha_j)j/2} \int_{\mathbb{R}^2} \langle |y_1 + \frac{m_1}{2}| \rangle^{-N} \langle |y_2 - k_2| \rangle^{-N} dy_1 dy_2 \\ &\leq C_N \cdot 2^{-(2-\alpha_j)j/2}. \end{aligned}$$

Case 2: $(\iota) = (\mathrm{h})$. Similarly, we can use 1), 2) and the change of varibles $(y_1, y_2) = (2^{2j}x_1 + l2^{\alpha_j j}x_2, s_j x_2)$ to obtain $|\langle (g_{s_j})_{m,n}, \psi_{j,l,k}^{\alpha_j,(\mathrm{v})} \rangle| \leq C_N \cdot 2^{-(2-\alpha_j)j/2}$.
Case 3: $(\iota) = (\mathrm{b})$. By the definition of boundary shearlets, we can verify this estimate by combining two cases above. ∎

Next, we prove a useful lemma for estimating bounds of the type of Proposition 4.20 and Proposition 4.23.

Lemma 4.19 *For each $N \in \mathbb{N}$ there exists a constant $C_N > 0$ such that*

$$\int_{\mathbb{R}} \langle |z| \rangle^{-N} \langle |z+t| \rangle^{-N} dz \leq C_N \langle |t| \rangle^{-N}, \quad \forall t \in \mathbb{R}.$$

Proof. We have

$$\begin{aligned} \int_{\mathbb{R}} \langle |z| \rangle^{-N} \langle |z+t| \rangle^{-N} dz &= \int_{\mathbb{R}} \max\{\langle |z| \rangle^{-N}, \langle |z+t| \rangle^{-N}\} \min\{\langle |z| \rangle^{-N}, \langle |z+t| \rangle^{-N}\} dz \\ &\leq \int_{\mathbb{R}} \left(\langle |z| \rangle^{-N} + \langle |z+t| \rangle^{-N} \right) \cdot \langle |t/2| \rangle^{-N} dz \\ &\leq C_N \langle |t| \rangle^{-N}. \end{aligned}$$

∎

4.8.2 Cartoon Patch

For the sake of brevity, we use some indexing sets for universal shearlets

$$\begin{aligned} \Delta &:= \left\{ (j,l,k;\alpha_j,(\iota)) \mid j \geq 0, |l| < 2^{(2-\alpha_j)j}, k \in \mathbb{Z}^2, (\iota) \in \{(\mathrm{h}),(\mathrm{v})\} \right\} \\ &\quad \bigcup \left\{ (j,l,k;\alpha_j,(\mathrm{b})) \mid j \geq 0, |l| = 2^{(2-\alpha_j)j}, k \in \mathbb{Z}^2 \right\}, \\ \Delta_j &:= \{(j',k,l;\alpha_j,(\iota)) \in \Delta \mid j' = j\}, \quad j \geq 0, \\ \Delta_j^{\pm} &:= \Delta_{j-1} \cup \Delta_j \cup \Delta_{j+1}, \end{aligned}$$

where $\Delta_{-1} = \emptyset$. We now have the following result.

Proposition 4.20 *Consider the shearlet frame $\mathbf{\Psi}$ of Definition 4.12 and the cartoon patch $w\mathcal{S}_j$ as defined in (4.19). We assume that $\liminf_{j\to\infty} \alpha_j > 0$. Then, we have the following decay estimate of the cluster approximate error $\delta_{1,j}$*

$$\delta_{1,j} := \sum_{\eta \in \Delta, \eta \notin \Lambda_{1,j}^{\pm}} |\langle \psi_{j',l,k}^{\alpha_{j'},(\iota)}, w\mathcal{S}_j \rangle| = o(2^{-Nj}), \quad \forall N \in \mathbb{N},$$

where $\eta = (j', l, k; \alpha_{j'}, (\iota))$.

The proof of this proposition roughly follows the lines of the Proposition 5.2 in [GK14]. For the sake of brevity we denote

$$t^{(\mathrm{v})} = (t_1^{(\mathrm{v})}, t_2^{(\mathrm{v})}) := A_{\alpha_{j,(\mathrm{v})}}^{-j} S_{(\mathrm{v})}^{-l} k = (2^{-\alpha_j j} k_1, 2^{-2j}(k_2 - l k_1)),$$

$$t^{(\mathrm{h})} = (t_1^{(\mathrm{h})}, t_2^{(\mathrm{h})}) := A_{\alpha_{j,(\mathrm{h})}}^{-j} S_{(\mathrm{h})}^{-l} k = (2^{-2j}(k_1 - l k_2), 2^{-\alpha_j j} k_2).$$

The proof also relies on the following two lemmas.

Lemma 4.21 *Consider the shearlet frame* $\boldsymbol{\Psi}$ *of Definition 4.12 and the cartoon patch with sub-band* $w\mathcal{S}_j$ *defined in (4.19). Then, for* $\alpha_j \in (0,2), j' \in \{j-1, j, j+1\}, j \geq 2$, *the following estimates hold for arbitrary integers* $M \geq 0$

1. *If* $(\iota) = (\mathrm{v})$ *and* $|l| > 1$, *we have*

$$\left|\langle w\mathcal{S}_j, \psi_{j',l,k}^{\alpha_{j'},(\mathrm{v})}\rangle\right| \leq C_M \cdot 2^{-(2+\alpha_{j'})j'/2} \cdot \langle |t_1^{(\mathrm{v})}|\rangle^{-2} \langle |t_2^{(\mathrm{v})}|\rangle^{-2} \langle |2^{\alpha_{j'} j'}|\rangle^{-M}.$$

2. *If* $(\iota) = (\mathrm{h})$, *we have*

$$\left|\langle w\mathcal{S}_j, \psi_{j',l,k}^{\alpha_{j'},(\mathrm{h})}\rangle\right| \leq C_M \cdot \frac{2^{2j'}}{r^3} \cdot \langle |t_1^{(\mathrm{h})}|\rangle^{-2} \langle |t_2^{(\mathrm{h})}|\rangle^{-2} \langle |2^{2j'}|\rangle^{-M},$$

   where r *is defined in (4.9).*

3. *If* $(\iota) = (\mathrm{b})$ *and* $|l| = 2^{(2-\alpha_{j'})j'}$, *we have*

$$\left|\langle w\mathcal{S}_j, \psi_{j',l,k}^{\alpha_{j'},(\mathrm{b})}\rangle\right| = C_M \cdot 2^{-(2+\alpha_{j'})j'/2} \cdot \langle |t_1^{(\mathrm{b})}|\rangle^{-2} \langle |t_2^{(\mathrm{b})}|\rangle^{-2} \langle |2^{\alpha_{j'} j'}|\rangle^{-M}.$$

Proof. Without loss of generality, we prove for $j' = j$. The other cases are treated similarly.

1) By the definition of $w\mathcal{S}_j$ and Plancherel's theorem, we obtain

$$\begin{aligned}
\left|\langle w\mathcal{S}_j, \psi_{j,l,k}^{\alpha_j,(\mathrm{v})}\rangle\right| &= \left|\langle \widehat{w\mathcal{S}_j}, \hat{\psi}_{j,l,k}^{\alpha_j,(\mathrm{v})}\rangle\right| = \left|\int_{\mathbb{R}^2} \hat{w}(\xi_1) \frac{1}{2\pi\xi_2} W_j(\xi) \overline{\hat{\psi}_{j,l,k}^{\alpha_j,(\mathrm{v})}(\xi)}\right| \\
&= \frac{1}{2\pi}\left|\int_{\mathbb{R}} e^{2\pi i t_2^{(\mathrm{v})}\xi_2} \int_{\mathbb{R}} \hat{w}(\xi_1) \frac{1}{\xi_2} W_j(\xi) \hat{\psi}_{j,l,0}^{\alpha_j,(\mathrm{v})}(\xi) e^{2\pi i t_1^{(\mathrm{v})}\xi_1} d\xi_1 d\xi_2\right| \\
&= \frac{1}{2\pi}\left|\int_{\mathbb{R}} e^{2\pi i t_2^{(\mathrm{v})}\xi_2} \int_{\mathbb{R}} \hat{w}(\xi_1) \tau_{j,l}(\xi) e^{2\pi i t_1^{(\mathrm{v})}\xi_1} d\xi_1 d\xi_2\right|,
\end{aligned}$$

where $\tau_{j,l}(\xi) := \frac{1}{\xi_2} W_j(\xi) \hat{\psi}_{j,l,0}^{\alpha_j,(\mathrm{v})}(\xi)$.

We now apply repeated integration by parts with respect to ξ_i, $i = 1, 2,$. We get

$$\left|\langle w\mathcal{S}_j, \psi_{j,l,k}^{\alpha_j,(\mathrm{v})}\rangle\right| = \frac{1}{2\pi}\left|\int_{\mathbb{R}} e^{2\pi i t_2^{(\mathrm{v})}\xi_2} \int_{\mathbb{R}} \frac{\partial^2}{\partial \xi_1^2}[\hat{w}(\xi_1)\tau_{j,l}(\xi)] \frac{1}{(2\pi i t_1^{(\mathrm{v})})^2} e^{2\pi i t_1^{(\mathrm{v})}\xi_1} d\xi_1\right] d\xi_2\right|$$

$$\leq \frac{1}{|t_1^{(\mathrm{v})}|^2}\Big|\int_{\mathbb{R}} e^{2\pi i t_2^{(\mathrm{v})}\xi_2}\int_{\mathbb{R}}\frac{\partial^2}{\partial\xi_1^2}[\hat{w}(\xi_1)\tau_{j,l}(\xi)]e^{2\pi i t_1^{(\mathrm{v})}\xi_1}d\xi_1 d\xi_2\Big|$$
$$\leq |t_1^{(\mathrm{v})}|^{-2}\int_{\mathbb{R}}\int_{\mathbb{R}}\Big|\frac{\partial^2}{\partial\xi_1^2}[\hat{w}(\xi_1)\tau_{j,l}(\xi)]\Big|d\xi_1 d\xi_2 \tag{4.42}$$

and similarly

$$\Big|\langle w\mathcal{S}_j, \psi_{j,l,k}^{\alpha_j,(\mathrm{v})}\rangle\Big| \leq |t_2^{(\mathrm{v})}|^{-2}\int_{\mathbb{R}}\int_{\mathbb{R}}\Big|\frac{\partial^2}{\partial\xi_2^2}[\hat{w}(\xi_1)\tau_{j,l}(\xi)]\Big|d\xi_1 d\xi_2 \tag{4.43}$$

$$\Big|\langle w\mathcal{S}_j, \psi_{j,l,k}^{\alpha_j,(\mathrm{v})}\rangle\Big| \leq |t_1^{(\mathrm{v})}|^{-2}|t_2^{(\mathrm{v})}|^{-2}\int_{\mathbb{R}}\int_{\mathbb{R}}\Big|\frac{\partial^4}{\partial\xi_1^2\partial\xi_2^2}[\hat{w}(\xi_1)\tau_{j,l}(\xi)]\Big|d\xi_1 d\xi_2. \tag{4.44}$$

Thus,

$$|t_1^{(\mathrm{v})}|^2\Big|\langle w\mathcal{S}_j, \psi_{j,l,k}^{\alpha_j,(\mathrm{v})}\rangle\Big| \overset{(4.42)}{\leq} \int_{\mathbb{R}}\int_{\mathbb{R}}\Big|\frac{\partial^2}{\partial\xi_1^2}[\hat{w}(\xi_1)\tau_{j,l}(\xi)]\Big|d\xi_1 d\xi_2$$
$$|t_2^{(\mathrm{v})}|^2\Big|\langle w\mathcal{S}_j, \psi_{j,l,k}^{\alpha_j,(\mathrm{v})}\rangle\Big| \overset{(4.43)}{\leq} \int_{\mathbb{R}}\int_{\mathbb{R}}\Big|\frac{\partial^2}{\partial\xi_2^2}[\hat{w}(\xi_1)\tau_{j,l}(\xi)]\Big|d\xi_1 d\xi_2$$
$$|t_1^{(\mathrm{v})}|^2|t_2^{(\mathrm{v})}|^2\Big|\langle w\mathcal{S}_j, \psi_{j,l,k}^{\alpha_j,(\mathrm{v})}\rangle\Big| \overset{(4.44)}{\leq} \int_{\mathbb{R}}\int_{\mathbb{R}}\Big|\frac{\partial^4}{\partial\xi_1^2\partial\xi_2^2}[\hat{w}(\xi_1)\tau_{j,l}(\xi)]\Big|d\xi_1 d\xi_2.$$

This leads to

$$(1+|t_1^{(\mathrm{v})}|^2+|t_2^{(\mathrm{v})}|^2+|t_1^{(\mathrm{v})}|^2|t_2^{(\mathrm{v})}|^2)\Big|\langle w\mathcal{S}_j, \psi_{j,l,k}^{\alpha_j,(\mathrm{v})}\rangle\Big| = \langle|t_1^{(\mathrm{v})}|\rangle^2\langle|t_2^{(\mathrm{v})}|\rangle^2\Big|\langle w\mathcal{S}_j, \psi_{j,l,k}^{\alpha_j,(\mathrm{v})}\rangle\Big|$$

$$\leq \int_{\mathbb{R}^2}\Big|\hat{w}(\xi_1)\tau_{j,l}(\xi)\Big| + \Big|\frac{\partial^2}{\partial\xi_1^2}[\hat{w}(\xi_1)\tau_{j,l}(\xi)]\Big| + \Big|\frac{\partial^2}{\partial\xi_2^2}[\hat{w}(\xi_1)\tau_{j,l}(\xi)]\Big|$$
$$+\Big|\frac{\partial^4}{\partial\xi_1^2\partial\xi_2^2}[\hat{w}(\xi_1)\tau_{j,l}(\xi)]\Big|d\xi \tag{4.45}$$
$$= \int_{\mathbb{R}}\Gamma(\xi_2)d\xi_2,$$

where $\Gamma(\xi_2) :=$
$\int_{\mathbb{R}}\Big|\hat{w}(\xi_1)\tau_{j,l}(\xi)\Big| + \Big|\frac{\partial^2}{\partial\xi_1^2}[\hat{w}(\xi_1)\tau_{j,l}(\xi)]\Big| + \Big|\frac{\partial^2}{\partial\xi_2^2}[\hat{w}(\xi_1)\tau_{j,l}(\xi)]\Big| + \Big|\frac{\partial^4}{\partial\xi_1^2\partial\xi_2^2}[\hat{w}(\xi_1)\tau_{j,l}(\xi)]\Big|d\xi_1$. Next, we bound Γ. By the definition of the universal shearlets, $\hat{\psi}_{j,l,k}^{\alpha_j,(\mathrm{v})}$ has compact support in the trapezoidal region

$$supp(\hat{\psi}_{j,l,k}^{\alpha_j,(\mathrm{v})}) = \Big\{\xi\in\mathbb{R}^2 \mid \xi_2\in[-2^{2j-1},2^{2j-1}]\setminus[-2^{2j-4},2^{2j-4}], \Big|\frac{\xi_1}{\xi_2} - l2^{-(2-\alpha_j)j}\Big|\Big\}. \tag{4.46}$$

This implies that for any $\xi\in$ supp $\tau_{j,l}$ we have

$$(l-1)2^{(\alpha_j-2)j} \leq \frac{\xi_1}{\xi_2} \leq (l+1)2^{(\alpha_j-2)j} \text{ and } 2^{2j-4}\leq|\xi_2|\leq 2^{2j-1}.$$

Using the assumption $|l| > 1$ follows that there exist constants $C_1, C_2 > 0$ such that

$$\xi_1 \in I_{j,l} := [-C_2 l 2^{\alpha_j j}, -C_1 l 2^{\alpha_j j}] \cup [C_2 l 2^{\alpha_j j}, C_1 l 2^{\alpha_j j}].$$

We now give some further estimates. By the fact that $\tau_{j,l}(\xi)$ is zero for $\xi_2 < 2^{2j-4}$, we obtain

$$\begin{aligned} 2^{(2+\alpha_j)j/2}\Big|\frac{\partial \tau_{j,l}}{\partial \xi_1}(\xi)\Big| &= \Big|\frac{\partial}{\partial \xi_1}\Big[\frac{1}{\xi_2} W_j^2(\xi) v\Big(2^{(2-\alpha_j)j}\frac{\xi_1}{\xi_2} - l\Big)\Big]\Big| \\ &\leq \frac{1}{2^{2j-4}}\Big[\frac{2}{2^{2j}} W(\frac{\xi_1}{2^{2j}}, \frac{\xi_2}{2^{2j}}) \frac{\partial W}{\partial \xi_1}(\frac{\xi_1}{2^{2j}}, \frac{\xi_2}{2^{2j}}) v\Big(2^{(2-\alpha_j)j}\frac{\xi_1}{\xi_2} - l\Big) + \\ &\quad \frac{2^{(2-\alpha_j)j}}{\xi_2}\frac{\partial v}{\partial \xi_1}\Big(2^{(2-\alpha_j)j}\frac{\xi_1}{\xi_2} - l\Big) W^2(\frac{\xi_1}{2^{2j}}, \frac{\xi_2}{2^{2j}})\Big] \\ &\leq \frac{1}{2^{2j-4}}\Big(C_1 2^{-2j} + C_2 \frac{2^{(2-\alpha_j)j}}{|\xi_2|}\Big) \overset{0<\alpha_j\leq 2}{\leq} C 2^{-2j}. \end{aligned} \tag{4.47}$$

Furthermore, we have

$$2^{(2+\alpha_j)j/2}\Big|\frac{\partial \tau_{j,l}}{\partial \xi_2}(\xi)\Big| = 2^{(2+\alpha_j)j/2}\Big|\frac{\partial \frac{\sigma_{j,l}}{\xi_2}}{\partial \xi_2}\Big|,$$

where $\sigma_{j,l} := W_j^2(\xi) v\Big(2^{(2-\alpha_j)j}\frac{\xi_1}{\xi_2} - l\Big)$. Thus, in the support (4.46) we have

$$\begin{aligned} & 2^{(2+\alpha_j)j/2}\Big|\frac{\partial \sigma_{j,l}}{\partial \xi_2}\Big| = \Big|\frac{\partial}{\partial \xi_2}\Big[W_j^2(\xi) v\Big(2^{(2-\alpha_j)j}\frac{\xi_1}{\xi_2} - l\Big)\Big]\Big| \\ = \;& \frac{2}{2^{2j}} W(\frac{\xi_1}{2^{2j}}, \frac{\xi_2}{2^{2j}}) \frac{\partial W}{\partial \xi_2}(\frac{\xi_1}{2^{2j}}, \frac{\xi_2}{2^{2j}}) v\Big(2^{(2-\alpha_j)j}\frac{\xi_1}{\xi_2} - l\Big) - \frac{2^{(2-\alpha_j)j}\xi_1}{\xi_2^2}\frac{\partial v}{\partial \xi_1} W^2(\frac{\xi_1}{2^{2j}}, \frac{\xi_2}{2^{2j}}) \\ \leq \;& C_1 2^{-2j} + C_2 \frac{2^{(2-\alpha_j)j}|\xi_1|}{|\xi_2|^2} \overset{\alpha_j\leq 2}{\leq} C 2^{-\alpha_j j}. \end{aligned}$$

Consequently, we get

$$2^{(2+\alpha_j)j/2}\Big|\frac{\partial \tau_{j,l}}{\partial \xi_2}(\xi)\Big| = 2^{(2+\alpha_j)j/2}\Big|\frac{\partial \sigma_{j,l}}{\partial \xi_2}\frac{1}{\xi_2} - \frac{\sigma_{j,l}(\xi)}{\xi_2^2}\Big| \leq \frac{C 2^{-\alpha_j j}}{2^{2j-4}} + \frac{C'}{2^{2j-4}} \leq C'' 2^{-2j}. \tag{4.48}$$

Similarly, we obtain

$$2^{(2+\alpha_j)j/2}\Big|\frac{\partial^2 \tau_{j,l}}{\partial \xi_1^2}(\xi)\Big| \leq C 2^{-2j}, \tag{4.49}$$

and

$$2^{(2+\alpha_j)j/2}\Big|\frac{\partial^2 \tau_{j,l}}{\partial \xi_2^2}(\xi)\Big| \leq C 2^{-2j}. \tag{4.50}$$

We now exploit the specific form of $I_{j,l}$ as well as the rapid decay of $\hat{w}$ to study $\hat{w}^{(n)}$ for

$n = 0, 1, 2$. These lead to (see Figure 4.6 for illustration)

$$\begin{aligned}\|\hat{w}^{(n)}\|_{L^1(I_{j,l})} &\leq vol(I_{j,l}) \sup_{\xi_1 \in I_{j,l}} |\hat{w}^{(n)}(\xi_1)| \leq C_{M,n} |l2^{\alpha_j j}| \langle |l2^{\alpha_j j}| \rangle^{-(M+1)} \\ &\leq C_{M,n} \langle |l2^{\alpha_j j}| \rangle^{-M} \overset{l>1}{\leq} C_{M,n} \langle |2^{\alpha_j j}| \rangle^{-M}, \ \forall M \in \mathbb{N}, \forall n = 1, 2, \dots \end{aligned} \tag{4.51}$$

Combining (4.47), (4.48), (4.49), (4.50), (4.51), with (4.45), we have

$$\begin{aligned}\Gamma(\xi_2) &\leq C \cdot 2^{-(2+\alpha_j)j/2} \cdot 2^{-2j} \max\left\{ \|\hat{w}\|_{L^1(I_{j,l})}, \|\frac{\partial \hat{w}}{\partial \xi_1}\|_{L^1(I_{j,l})}, \|\frac{\partial^2 \hat{w}}{\partial \xi_1^2}\|_{L^1(I_{j,l})} \right\} \\ &\leq C_M \cdot 2^{-(2+\alpha_j)j/2} \cdot 2^{-2j} \cdot \langle |2^{\alpha_j j}| \rangle^{-M}.\end{aligned}$$

In addition, since $\operatorname{supp} \Gamma(\xi_2) = [2^{2j-4}, 2^{2j-1}]$, we finally obtain

$$\left| \langle w\mathcal{S}_j, \psi_{j,l,k}^{\alpha_{j'},(\mathrm{v})} \rangle \right| \leq C_M \cdot 2^{-(2+\alpha_j)j/2} \cdot \langle |t_1^{(\mathrm{v})}| \rangle^{-2} \langle |t_2^{(\mathrm{v})}| \rangle^{-2} \langle |2^{\alpha_j j}| \rangle^{-M}.$$

2) This claim is similar to 1) but we need to modify the intervals $I_{j,l}$ to be $[-C_2 2^{2j}, -C_1 2^{2j}] \cup [C_1 2^{2j}, C_2 2^{2j}]$, where $C_1, C_2 > 0$. This leads to the additional terms $\langle |2^{2j}| \rangle^{-M}$ and r in 2) when comparing with 1). Next, we use $r \leq |\xi_2| \leq 2^{2j-1}$ instead of using $2^{2j-4} \leq |\xi_2| \leq 2^{2j-1}$ for the support of $\tau_{j,l}$. Thus, redefining $\tau_{j,l}(\xi) = \frac{1}{\xi_2} W_j(\xi) \hat{\psi}_{j,l,0}^{\alpha_{j'},(\mathrm{h})}(\xi)$, we modify (4.47), (4.48), (4.49),(4.50) as follows.

$$\begin{aligned}2^{(2+\alpha_j)j/2} \left| \frac{\partial \tau_{j,l}}{\partial \xi_1}(\xi) \right| &= \left| \frac{\partial}{\partial \xi_1} \left[\frac{1}{\xi_2} W_j^2(\xi) v\left(2^{(2-\alpha_j)j} \frac{\xi_2}{\xi_1} - l \right) \right] \right| \\ &\leq \frac{1}{r} \left| \frac{2}{2^{2j}} W(\frac{\xi_1}{2^{2j}}, \frac{\xi_2}{2^{2j}}) \frac{\partial W}{\partial \xi_1}(\frac{\xi_1}{2^{2j}}, \frac{\xi_2}{2^{2j}}) v\left(2^{(2-\alpha_j)j} \frac{\xi_2}{\xi_1} - l \right) \right| + \\ &\quad \left| \frac{2^{(2-\alpha_j)j}}{\xi_1^2} \frac{\partial v}{\partial \xi_1} W^2(\frac{\xi_1}{2^{2j}}, \frac{\xi_2}{2^{2j}}) \right| \\ &\leq \frac{1}{r} \left(C_1 2^{-2j} + C_2 \frac{2^{(2-\alpha_j)j}}{|\xi_1|^2} \right) \overset{0<\alpha_j \leq 2}{\leq} \frac{C}{r \cdot 2^{2j}}.\end{aligned}$$

Furthermore, we have

$$2^{(2+\alpha_j)j/2} \left| \frac{\partial \tau_{j,l}}{\partial \xi_2}(\xi) \right| = 2^{(2+\alpha_j)j/2} \left| \frac{\partial \frac{\sigma_{j,l}}{\xi_2}}{\partial \xi_2} \right|,$$

where $\sigma_{j,l} := W_j^2(\xi) v\left(2^{(2-\alpha_j)j} \frac{\xi_2}{\xi_1} - l \right)$. Thus,

$$\begin{aligned}&2^{(2+\alpha_j)j/2} \left| \frac{\partial \sigma_{j,l}}{\partial \xi_2} \right| = \left| \frac{\partial}{\partial \xi_2} \left[W_j^2(\xi) v\left(2^{(2-\alpha_j)j} \frac{\xi_2}{\xi_1} - l \right) \right] \right| \\ \leq\ & \left| \frac{2}{2^{2j}} W(\frac{\xi_1}{2^{2j}}, \frac{\xi_2}{2^{2j}}) \frac{\partial W}{\partial \xi_2}(\frac{\xi_1}{2^{2j}}, \frac{\xi_2}{2^{2j}}) v\left(2^{(2-\alpha_j)j} \frac{\xi_2}{\xi_1} - l \right) \right| + \left| \frac{2^{(2-\alpha_j)j}}{\xi_1} \frac{\partial v}{\partial \xi_1} W^2(\frac{\xi_1}{2^{2j}}, \frac{\xi_2}{2^{2j}}) \right|\end{aligned}$$

$$\leq \quad C_1 2^{-2j} + C_2 \frac{2^{(2-\alpha_j)j}}{|\xi_1|} \quad \overset{0<\alpha_j\leq 2}{\leq} \quad C.$$

Consequently, we have

$$\left|\frac{\partial \tau_{j,l}}{\partial \xi_2}(\xi)\right| = \left|\frac{\partial \sigma_{j,l}}{\partial \xi_2}\frac{1}{\xi_2} - \frac{\sigma_{j,l}(\xi)}{\xi_2^2}\right| \leq \frac{C'}{r^2}.$$

Similarly, we obtain

$$2^{(2+\alpha_j)j/2}\left|\frac{\partial^2 \tau_{j,l}}{\partial \xi_1^2}(\xi)\right| \leq \frac{C}{r\cdot 2^{2j}},$$

and

$$\left|\frac{\partial^2 \tau_{j,l}}{\partial \xi_2^2}(\xi)\right| \leq \frac{C'}{r^3}.$$

These bounds lead to

$$\Gamma(\xi_2) \leq \frac{C}{r^3}\cdot \max\left\{\|\hat{w}\|_{L^1(I_{j,l})}, \|\frac{\partial \hat{w}}{\partial \xi_1}\|_{L^1(I_{j,l})}, \|\frac{\partial^2 \hat{w}}{\partial \xi_1^2}\|_{L^1(I_{j,l})}\right\}.$$

Thus, by the rapid decay of $\hat{w}$, as before,

$$\left|\langle w\mathcal{S}_j, \psi_{j,l,k}^{\alpha_j,(\mathrm{v})}\rangle\right| \quad \leq \quad C_M \cdot \frac{2^{2j}}{r^3}\cdot \langle |t_1^{(\mathrm{v})}|\rangle^{-2}\langle |t_2^{(\mathrm{v})}|\rangle^{-2}\langle |2^{2j}|\rangle^{-M}.$$

For an illustration, we refer to Figure 4.6. Finally, we obtain 3). Recalling the definition of the shearlets, we can easily verify this estimate since boundary shearlets is just a particular case of horizontal and vertical shearlets. ∎

Lemma 4.22 *Consider the shearlet frame $\mathbf{\Psi}$ of Definition 4.12 and the cartoon patch with sub-band $w\mathcal{S}_j$ defined in (4.19). For $j \in \{j-1, j, j+1\}, j \geq 2$, and for any arbitrary $N \geq 2$, there exists a constant $C_N > 0$ such that*

$$\begin{aligned}\left|\langle w\mathcal{S}_j, \psi_{j',l,k}^{\alpha_{j'},(\mathrm{v})}\rangle\right| \quad &\leq \quad C_N 2^{(2-\alpha_{j'})j'/2}\int_{\mathbb{R}} \tilde{w}_{N,j}(2^{-\alpha_{j'}j'}(x_1+k_1))\langle |x_1|\rangle^{-N} \\ &\qquad \langle |lx_1 + lk_1 - k_2|\rangle^{-N} dx_1,\end{aligned}$$

where $\tilde{w}_{N,j'} := |w| * \langle |2^{2j'}[\cdot]|\rangle^{-N}$, and $\langle |\cdot| \rangle$ is defined from (4.26) .

Proof. Without loss of generality, we can prove only for $j' = j$. We first note that in $\operatorname{supp} \psi_{j,l,k}^{\alpha_{j'},(\mathrm{v})}$ we have $w\mathcal{S}_0 \equiv w\mathcal{S}$, where $w\mathcal{S}$ is defined in (4.9). We now consider the line distribution $w\mathcal{L}$ introduced in [GK14] by

$$\langle w\mathcal{L}, f\rangle = \int_{-\rho}^{\rho} w(x_1) f(x_1, 0) dx_1, \quad f \in \mathbb{S}(\mathbb{R}^2),$$

with Fourier transform

$$\langle \widehat{w\mathcal{L}}, f\rangle = \int_{\mathbb{R}^2} \hat{w}(\xi_1) f(\xi) d\xi.$$

Next, we observe that

$$\begin{aligned}\langle w\mathcal{L}, f\rangle &= \int_{-\rho}^{\rho} w(x_1) f(x_1, 0) dx_1 = \int_{-\rho}^{\rho} w(x_1) \int_{\mathbb{R}} f(x_1, x_2)\delta(x_2) dx_2 dx_1 \\ &= \iint_{\mathbb{R}^2} w(x_1)\delta(x_2) f(x_1, x_2) dx_1 dx_2 = \langle w(x_1)\delta(x_2), f\rangle,\end{aligned}$$

where $\delta(x)$ denotes the usual Dirac delta functional. Thus,

$$w\mathcal{L}(x) = w(x_1)\delta(x_2).$$

In addition,

$$\begin{aligned}\langle w\mathcal{S}, f\rangle &= \int_{-\rho}^{\rho} w(x_1) \int_{-\infty}^{0} f(x) dx_2 dx_1 = \int_{-\rho}^{\rho} w(x_1) \int_{-\infty}^{+\infty} f(x) \mathbb{1}_{\{0 \geq x_2\}}(0) dx_2 dx_1 \\ &= \int_{-\rho}^{\rho} w(x_1) \int_{\mathbb{R}} f(x) \Big(\int_{\mathbb{R}} \mathbb{1}_{\{y \geq x_2\}}(y)\delta(y) dy \Big) dx_2 dx_1 \\ &= \int_{-\rho}^{\rho} w(x_1) \int_{\mathbb{R}} f(x) \Big(\int_{x_2}^{+\infty} \delta(y) dy \Big) dx_2 dx_1 = \Big\langle \int_{x_2}^{+\infty} w(x_1)\delta(y) dy, f(x) \Big\rangle.\end{aligned}$$

Hence, we obtain

$$w\mathcal{S}(x) = \int_{x_2}^{+\infty} w\mathcal{L}(x_1, y) dy.$$

Since integration commutes with convolution, we also have

$$w\mathcal{S}_j = w\mathcal{S} * F_j = \int_{x_2}^{+\infty} w\mathcal{L}_j(x_1, y) dy.$$

where $w\mathcal{L}_j$ is defined by $w\mathcal{L} * F_j$. In addition, by integration by parts with respect to variable x_2, we obtain

$$\langle w\mathcal{S}_j, \psi_{j,l,k}^{\alpha_j,(\mathrm{v})}\rangle = \langle \int_{x_2}^{+\infty} w\mathcal{L}_j(x_1, y) dy, \psi_{j,l,k}^{\alpha_j,(\mathrm{v})}\rangle\rangle = \langle w\mathcal{L}_j(x), \int_{x_2}^{+\infty} \psi_{j,l,k}^{\alpha_j,(\mathrm{v})}(x_1, y) dy\rangle,$$

where the boundary terms vanish due to the compact support of $\psi_{j,l,k}^{\alpha_j,(\mathrm{v})}$. Now we put

$$\Xi_{j,l,k}^{\alpha_j,(\mathrm{v})}(x) := \int_{x_2}^{+\infty} \psi_{j,l,k}^{\alpha_j,(\mathrm{v})}(x_1, y) dy,$$

and note that $\hat{\Xi}_{j,l,k}^{\alpha_j,(\mathrm{v})}(\xi) = \frac{i}{2\pi\xi_2} \cdot \hat{\psi}_{j,l,k}^{\alpha_j,(\mathrm{v})}(\xi)$. Similarly to Lemma 4.18, which was based on $\psi_{j,l,k}^{\alpha_j,(\mathrm{v})}$, we can prove a lemma for $\Xi_{j,l,k}^{\alpha_j,(\mathrm{v})}$, and prove the rapid decay property

$$\begin{aligned}|\Xi_{j,l,k}^{\alpha_j,(\mathrm{v})}(x)| &\leq C'_N \cdot \frac{1}{2^{2j-4}} \cdot 2^{(2+\alpha_j)j/2} \cdot \langle |2^{\alpha_j j} x_1 - k_1|\rangle^{-N} \langle |l2^{\alpha_j j} x_1 + 2^{2j} x_2 - k_2|\rangle^{-N} \\ &\leq C_N \cdot 2^{(\alpha_j - 2)j/2} \cdot \langle |2^{\alpha_j j} x_1 - k_1|\rangle^{-N} \langle |l2^{\alpha_j j} x_1 + 2^{2j} x_2 - k_2|\rangle^{-N}. \qquad (4.52)\end{aligned}$$

Now we can use the decay estimate of the line singularities $w\mathcal{L}_j$ to obtain

$$\begin{aligned}
|w\mathcal{L}_j(x)| &= |[w\mathcal{L} * F_j](x)| = \Big| \int_{\mathbb{R}} w(y_1) F_j(x-(y_1,0)) dy_1 \Big| \\
&\leq \Big| \int_{\mathbb{R}} |w(y_1)| 2^{4j} |\check{W}(2^{2j}(x-(y_1,0)))| dy_1 \Big| \\
&\leq \int_{\mathbb{R}} |w(y_1)| 2^{4j} C_N \langle |2^{2j} x_2| \rangle^{-N} \langle |2^{2j}(y_1 - x_1)| \rangle^{-N} dy_1 \\
&= C_N 2^{4j} \langle |2^{2j} x_2| \rangle^{-N} [|w * \langle 2^{2j}[\cdot]| \rangle^{-N}](x_1) \\
&= C_N 2^{4j} \langle |2^{2j} x_2| \rangle^{-N} \tilde{w}_{N,j}(x_1),
\end{aligned}$$

where $\tilde{w}_{N,j}(x_1) := [|w * \langle 2^{2j}[\cdot]| \rangle^{-N}](x_1), \quad x = (x_1, x_2) \in \mathbb{R}^2$. Combining this with the rapid decay properties of $\Xi_{j,l,k}^{\alpha_j,(\mathrm{v})}(x)$ from (4.52) and Lemma 4.19, we have

$$\begin{aligned}
&\Big| \langle w\mathcal{S}_j, \psi_{j,l,k}^{\alpha_j,(\mathrm{v})} \rangle \Big| \\
\leq\ & C_N \int_{\mathbb{R}^2} 2^{2j} \langle |2^{2j} x_2| \rangle^{-N} \tilde{w}_{N,j}(x_1) 2^{(\alpha_j+2)j/2} \langle |2^{\alpha_j j} x_1 - k_1| \rangle^{-N} \\
&\qquad \cdot \langle |l 2^{\alpha_j j} x_1 + 2^{2j} x_2 - k_2| \rangle^{-N} dx \\
=\ & C_N 2^{(2-\alpha_j)j/2} \int_{\mathbb{R}^2} \langle |x_2| \rangle^{-N} \tilde{w}_{N,j}(2^{-\alpha_j j}(x_1 + k_1)) \langle |x_1| \rangle^{-N} \\
&\qquad \cdot \langle |l x_1 + l k_1 + x_2 - k_2| \rangle^{-N} dx \\
\leq\ & C_N 2^{(2-\alpha_j)j/2} \int_{\mathbb{R}} \tilde{w}_{N,j}(2^{-\alpha_j j}(x_1 + k_1)) \langle |x_1| \rangle^{-N} \langle |l x_1 + l k_1 - k_2| \rangle^{-N} dx_1.
\end{aligned}$$

■

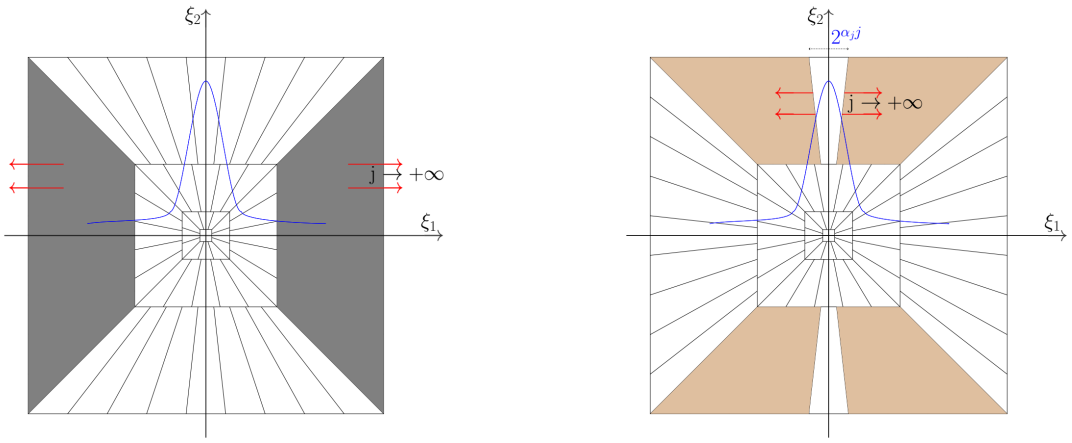

Figure 4.6: Interactions between horizontal shearlets, vertical shearlets and the sub-image of cartoon part $w\mathcal{S}_j$. Left: Frequency support of horizontal shearlets at scale j (gray), $w\mathcal{S}_j$ (bold). Right: Frequency support of vertical shearlets with $|l| > 1$ (gray), $w\mathcal{S}_j$ (bold).

Now we are ready to prove Proposition 4.20

Proof of Proposition 4.20. By the definition of $\delta_{1,j}$ and the support of the window function

F_j, only shearlet coefficients in $\Delta_j^{\pm}$ have nonzero inner products with wS_j, so we have

$$\begin{aligned}
\delta_{1,j} &= \sum_{\eta\in\Delta,\eta\notin\Lambda_{1,j}^{\pm}} |\langle \psi_{j',l,k}^{\alpha_{j'},(\iota)}, wS_j\rangle| = \sum_{\eta\in\Delta_j^{\pm},\eta\notin\Lambda_{1,j}^{\pm}} |\langle \psi_{j',l,k}^{\alpha_{j'},(\iota)}, wS_j\rangle| \\
&= \sum_{\substack{k\in\mathbb{Z}^2,|l|\le 1\\ |k_2-lk_1|>2^{\epsilon j'}}} |\langle \psi_{j',l,k}^{\alpha_{j'},(\mathrm{v})}, wS_j\rangle| + \sum_{k\in\mathbb{Z}^2,|l|>1} |\langle \psi_{j',l,k}^{\alpha_{j'},(\mathrm{v})}, wS_j\rangle| \\
&\quad + \sum_{k\in\mathbb{Z}^2,l\in\mathbb{Z}} |\langle \psi_{j',l,k}^{\alpha_{j'},(\mathrm{h})}, wS_j\rangle| + \sum_{k\in\mathbb{Z}^2} |\langle \psi_{j',\pm 2^{(2-\alpha_{j'})j'},k}^{\alpha_{j'},(\mathrm{b})}, wS_j\rangle| \\
&= T_1 + T_2 + T_3 + T_4,
\end{aligned}$$

where

$$T_1 := \sum_{\substack{k\in\mathbb{Z}^2,|l|\le 1\\ |k_2-lk_1|>2^{\epsilon j'}}} |\langle \psi_{j',l,k}^{\alpha_{j'},(\mathrm{v})}, wS_j\rangle|, \quad T_2 := \sum_{k\in\mathbb{Z}^2,|l|>1} |\langle \psi_{j',l,k}^{\alpha_{j'},(\mathrm{v})}, wS_j\rangle|,$$

$$T_3 = \sum_{k\in\mathbb{Z}^2,l\in\mathbb{Z}} |\langle \psi_{j',l,k}^{\alpha_{j'},(\mathrm{h})}, wS_j\rangle|, \quad T_4 := \sum_{k\in\mathbb{Z}^2} |\langle \psi_{j',\pm 2^{(2-\alpha_{j'})j'},k}^{\alpha_{j'}}, wS_j\rangle|.$$

Without loss of generality we restrict to the scale index $j' = j$. The respective arguments for the other cases $j' = j \pm 1$ are similar.

We start with an estimation of T_1. By Lemma 4.22, for $N \ge 2$, we obtain

$$\begin{aligned}
T_1 &= \sum_{\substack{k\in\mathbb{Z}^2,|l|\le 1\\ |k_2-lk_1|>2^{\epsilon j}}} |\langle \psi_{j,l,k}^{\alpha_j,(\mathrm{v})}, wS_j\rangle| \\
&\le C_N 2^{(2-\alpha_j)j/2} \sum_{\substack{k\in\mathbb{Z}^2,|l|\le 1\\ |k_2-lk_1|>2^{\epsilon j}}} \int_{\mathbb{R}} \tilde{w}_{N,j}(2^{-\alpha_j j}(x_1+k_1))\langle |x_1|\rangle^{-N}\langle |lx_1+lk_1-k_2|\rangle^{-N} dx_1 \\
&= C_N 2^{(2-\alpha_j)j/2} \sum_{\substack{k\in\mathbb{Z}^2,|l|\le 1\\ |k_2|>2^{\epsilon j}}} \int_{\mathbb{R}} \tilde{w}_{N,j}(2^{-\alpha_j j}(x_1+k_1))\langle |x_1|\rangle^{-N}\langle |lx_1+k_2|\rangle^{-N} dx_1 \\
&= C_N 2^{(2-\alpha_j)j/2} \sum_{\substack{k_2\in\mathbb{Z},|l|\le 1\\ |k_2|>2^{\epsilon j}}} \int_{\mathbb{R}} \Big(\sum_{k_1\in\mathbb{Z}} \tilde{w}_{N,j}(2^{-\alpha_j j}(x_1+k_1))\Big)\langle |x_1|\rangle^{-N}\langle |lx_1+k_2|\rangle^{-N} dx_1.
\end{aligned}$$

Furthermore, we have

$$\begin{aligned}
\sum_{k_1\in\mathbb{Z}} \tilde{w}_{N,j}(2^{-\alpha_j j}(x_1+k_1)) &= \sum_{k_1\in\mathbb{Z}} \int_{\mathbb{R}} |w(y_1)|\langle |2^{2j}(y_1 - 2^{-\alpha_j j}(x_1+k_1))|\rangle^{-N} dy_1 \\
&= \sum_{k_1\in\mathbb{Z}} \int_{\mathbb{R}} |w(y_1)|\langle |2^{(2-\alpha_j)j}(k_1+x_1-2^{\alpha_j j}y_1)|\rangle^{-N} dy_1 \\
&\overset{\alpha_j\le 2}{\le} \int_{\mathbb{R}} |w(y_1)|\Big(\sum_{k_1\in\mathbb{Z}} \langle |k_1+x_1-2^{\alpha_j j}y_1|\rangle^{-N}\Big) dy_1 \\
&\le C' \int_{\mathbb{R}} |w(y_1)|\Big(\int_{\mathbb{R}} \langle |t+x_1-2^{\alpha_j j}y_1|\rangle^{-N} dt\Big) dy_1
\end{aligned}$$

$$= C' \int_{\mathbb{R}} |w(y_1)| \Big(\int_{\mathbb{R}} \langle |t| \rangle^{-N} dt \Big) dy_1 \leq C_N.$$

This implies

$$\begin{aligned} T_1 &\leq C_N 2^{(2-\alpha_j)j/2} \sum_{\substack{k_2 \in \mathbb{Z}, |l| \leq 1 \\ |k_2| > 2^{\epsilon j'}}} \int_{\mathbb{R}} \langle |x_1| \rangle^{-N} \langle |l x_1 + k_2| \rangle^{-N} dx_1. \\ &\overset{\text{Lemma 4.19}}{\leq} C_N 2^{(2-\alpha_j)j/2} \sum_{k_2 \in \mathbb{Z}, |k_2| > 2^{\epsilon j'}} \langle |k_2| \rangle^{-N} dx_1. \\ &\leq C_N 2^{(2-\alpha_j)j/2} \int_{t > 2^{\epsilon j}} \langle |t| \rangle^{-N} \leq C_N 2^{(2-\alpha_j)j/2} 2^{-(N-1)\epsilon j}. \end{aligned}$$

We now bound the decay rate for the term T_2. First we fix $j \geq 0$ and $|l| > 1$. For $N \geq 2$, we obtain

$$\begin{aligned} \sum_{k \in \mathbb{Z}^2} \langle |t_1^{(\mathrm{v})}| \rangle^{-2} |t_2^{(\mathrm{v})}|^{-N} &= \sum_{k \in \mathbb{Z}^2} \langle |2^{-\alpha_J j} k_1| \rangle^{-2} \langle |2^{-2j}(k_2 - l k_1)| \rangle^{-2} \\ &\leq C' 2^{(2+\alpha_j)2j} \int_{\mathbb{R}} \int_{\mathbb{R}} \langle |x_1| \rangle^{-2} \langle |x_2| \rangle^{-2} dx_1 dx_2 \leq C 2^{(2+\alpha_j)2j}. \end{aligned} \tag{4.53}$$

Now, by Lemma 4.21, we have

$$\begin{aligned} T_2 &= \sum_{\substack{k \in \mathbb{Z}^2 \\ 1 < |l| \leq 2^{(2-\alpha_j)j}}} |\langle \psi_{j,l,k}^{\alpha_j,(\mathrm{v})}, w \mathcal{S}_j \rangle| \\ &\leq C_M \sum_{\substack{k \in \mathbb{Z}^2 \\ 1 < |l| \leq 2^{(2-\alpha_j)j}}} 2^{-(2+\alpha_j)j/2} \cdot \langle |t_1^{(\mathrm{v})}| \rangle^{-2} \langle |t_2^{(\mathrm{v})}| \rangle^{-2} \langle |2^{\alpha_j j}| \rangle^{-M} \\ &\leq C_M \cdot 2^{(2-3\alpha_j)j/2} \cdot \langle |2^{\alpha_j j}| \rangle^{-M} \sum_{k \in \mathbb{Z}^2} \langle |t_1^{(\mathrm{v})}| \rangle^{-2} \langle |t_2^{(\mathrm{v})}| \rangle^{-2} \\ &\overset{(4.53)}{\leq} C'_M \cdot 2^{(2-3\alpha_j)j/2} \cdot 2^{(2+\alpha_j)2j} \cdot \langle |2^{\alpha_j j}| \rangle^{-M}. \end{aligned}$$

Using the assumption $\liminf_{j \to \infty} \alpha_j > 0$ and choosing M sufficiently large we obtain the desired decay rates. By using 2) and 3) of the Lemma 4.21 the estimates for T_3 and T_4 are done similarly. Here, note that $\frac{1}{r^3} \cdot o(2^{-Nj}) = o(2^{-Nj})$ for fixed $r > 0$. For an illustration of Lemmas 4.21, 4.22, and the main proposition, we refer to Figure 4.6. ∎

4.8.3 Texture

We now provide a relative sparsity error (Definition 4.3) for the texture part.

Proposition 4.23 *Consider the Gabor frame of scale j, $\mathbf{G_j}$, defined in (4.18), and the texture defined in Definition 4.9. Then, for every $N \in \mathbb{N}$ the sequence $(\delta_{2,j})_{j \in \mathbb{N}}$ decays rapidly in*

the sense

$$\delta_{2,j} := \sum_{\lambda \notin B(0,M_j)\times I_T^{\pm}} |\langle \mathcal{T}_{s,j}, (g_{s_j})_\lambda \rangle| = o(2^{-Nj}).$$

Proof. First, note that

$$\hat{\mathcal{T}}_s = \int_{\mathbb{R}^2} \sum_{n\in I_T} d_n g_{s_j}(x) e^{-2\pi i \langle \xi - s_j n, x\rangle} dx = \sum_{n\in I_T} d_n \hat{g}_{s_j}(\xi - s_j n).$$

Using the support condition of $\hat{g}$, denoting $\lambda = (\tilde{m}, \tilde{n})$, we obtain

$$\begin{aligned} |\langle \mathcal{T}_{s,j}, (g_{s_j})_\lambda \rangle| &= |\langle \hat{\mathcal{T}}_{s,j}, (\hat{g}_{s_j})_\lambda \rangle| \\ &= \Big| \sum_{n\in I_T} d_n \int W_j(\xi) \hat{g}_{s_j}(\xi - s_j n) \cdot \overline{\hat{g}_{s_j}(\xi - s_j \tilde{n})} e^{-2\pi i \frac{\langle \tilde{m}, \xi\rangle}{2 s_j}} d\xi \Big| \\ &= \Big| \sum_{\substack{n\in I_T, \\ |n-\tilde{n}|\le 1}} d_n \int W_j(\xi) \hat{g}_{s_j}(\xi - s_j n) \cdot \overline{\hat{g}_{s_j}(\xi - s_j \tilde{n})} e^{-\pi i \frac{\langle \tilde{m}, \xi\rangle}{s_j}} d\xi \Big|. \end{aligned}$$

Indeed, $|\langle \mathcal{T}_{s,j}, (g_{s_j})_\lambda \rangle| = |\langle \hat{\mathcal{T}}_{s,j}, (\hat{g}_{s_j})_\lambda \rangle| = 0$, for $\tilde{n} \notin I_T^{\pm} \cap \mathcal{A}_{s,j}$. Moreover, we have $\{(\tilde{m}, \tilde{n}) \notin B(0,M) \times I_T^{\pm}\} = \{(\tilde{m}, \tilde{n}) \in \mathbb{Z}^2 \times \mathbb{Z}^2, |\tilde{m}| > M_j\} \cup \{(\tilde{m}, \tilde{n}) \in \mathbb{Z}^2 \times \mathbb{Z}^2, \tilde{n} \notin I_T^{\pm}\}$. Thus, since the Gabor coefficients of $\mathcal{T}_{s,j}$ are zero for frequencies outside $I_T^{\pm}$,

$$\begin{aligned} \delta_{2,j} &= \sum_{\lambda \notin B(0,M_j)\times I_T^{\pm}} |\langle \mathcal{T}_{s,j}, (g_{s_j})_\lambda \rangle| = \sum_{|\tilde{m}|\ge M_j, \tilde{n}\in I_T^{\pm}\cap \mathcal{A}_{s,j}} |\langle \mathcal{T}_{s,j}, (g_{s_j})_\lambda \rangle| \\ &= \sum_{|\tilde{m}|\ge M_j, \tilde{n}\in I_T^{\pm}\cap \mathcal{A}_{s,j}} \Big| \int_{\mathbb{R}^2} \sum_{\substack{n\in I_T, \\ |n-\tilde{n}|\le 1}} d_n (g_{s_j})_{(0,n)}(x) \overline{(g_{s_j})_{(\tilde{m},\tilde{n})}(x)} dx \Big| \\ &\le C \sum_{|\tilde{m}|\ge M_j, \tilde{n}\in I_T^{\pm}\cap \mathcal{A}_{s,j}} |d_{\tilde{n}}| \int_{\mathbb{R}^2} |(g_{s_j})_{(0,\tilde{n})}(x)| \cdot |(g_{s_j})_{(\tilde{m},\tilde{n})}(x)| dx, \end{aligned}$$

where $d_{\tilde{n}} = \max\{|d_n| \mid n \in I_T, |n - \tilde{n}| \le 1\}$. Note that the last inequality holds since for each $\tilde{n}$, there exist a finite number of n satisfying $|n - \tilde{n}| \le 1$. Moreover, by (4.37), there are $o(2^{(2-\alpha_j)j/2})$ points of $I_T^{\pm}$ in each support of a shearlet and there are $o(2^{(2-\alpha_j)j})$ shearlets in A_j, so

$$\#\{n \in I_T^{\pm} \cap \mathcal{A}_{s,j}\} \le 9\#\{n \in I_T \cap \mathcal{A}_{s,j}\} = o(2^{(2-\alpha_j)j/2}) \cdot 2^{(2-\alpha_j)j} = o(2^{(2-\alpha_j)3j/2}).$$

Combining this with the energy matching condition

$$\sum_{n\in I_T\cap \mathcal{A}_{s,j}} |d_n|^2 \le c_1 2^{-2j},$$

which implies $d_n \le \sqrt{c_1}, \forall n \in I_T \cap \mathcal{A}_{s,j}$, we have

$$\delta_{2,j} \le C \cdot o(2^{(2-\alpha_j)3j/2}) \sum_{|\tilde{m}|>M_j} \int_{\mathbb{R}^2} |(g_{s_j})_{(0,\tilde{n})}(x)| \cdot |(g_{s_j})_{\tilde{m},\tilde{n}}(x)| dx.$$

$$\overset{\text{Lemma 4.18}}{\leq} C_N \cdot o(2^{(2-\alpha_j)3j/2}) \int_{\mathbb{R}^2} \sum_{|\tilde{m}|>M_j} s_j^2 \cdot \langle |s_j x_1| \rangle^{-2N} \langle |s_j x_2| \rangle^{-2N} \langle |s_j x_1 + \frac{\tilde{m}_1}{2}| \rangle^{-N} \cdot \langle |s_j x_2 + \frac{\tilde{m}_2}{2}| \rangle^{-N} dx.$$

By Lemma 4.19, we now obtain

$$\begin{aligned} \delta_{2,j} &\leq C_N \cdot o(2^{(2-\alpha_j)3j/2}) \cdot \sum_{|\tilde{m}|>M_j} \langle |\frac{\tilde{m}_1}{2}| \rangle^{-N} \langle |\frac{\tilde{m}_2}{2}| \rangle^{-N} \\ &\leq C_N \cdot o(2^{(2-\alpha_j)3j/2}) \cdot \int_{\mathbb{R}} \int_{\frac{1}{2}M_j} \langle \frac{t_1}{2} \rangle^{-N} \langle |\frac{t_2}{2}| \rangle^{-N} dt_1 dt_2 \\ \overset{M_j=2^{\epsilon j/6}}{\leq} & C_N \cdot o(2^{(2-\alpha_j)3j/2}) \cdot 2^{-(N-1)\epsilon j/6}. \end{aligned}$$

This proves the claim since we can choose an arbitrarily large $N \in \mathbb{N}$. ∎

4.9 Cluster Coherence for Cartoon and Texture

In the previous section we proved relative sparsity for the texture and cartoon parts. For the success of separation and inpainting, by Theorem 4.8, we need to prove that the cluster coherence terms are less than $1/2$ when summed together. To guarantee this asymptotically, we prove that the cluster coherence terms decay to zero when the scale goes to infinity.

4.9.1 Cluster Coherence of the Un-projected Frames

We now analyze the cluster coherence of the un-projected frames $\mu_c(\Lambda_{1,j}^{\pm}, \mathbf{\Psi}; \mathbf{G_j})$ and $\mu_c(\Lambda_{2,j}, \mathbf{G_j}; \mathbf{\Psi})$.

Proposition 4.24 *Consider the shearlet frame $\mathbf{\Psi}$ of Definition 4.12 and the Gabor frame of scale j, $\mathbf{G_j}$, defined in (4.18). We have*

$$\mu_c(\Lambda_{1,j}^{\pm}, \mathbf{\Psi}; \mathbf{G_j}) \to 0, \quad j \to \infty.$$

where $\Lambda_{1,j}^{\pm}$ is defined in (4.41).

Proof. Let us recall the definition of the cluster of shearlets

$$\Lambda_{1,j} = \left\{ (j, l, k; \alpha_j, (\mathrm{v})) \mid |l| \leq 1, k \in \mathbb{Z}^2, |k_2 - lk_1| \leq 2^{\epsilon j} \right\},$$

and $\Lambda_{1,j}^{\pm} = \Lambda_{1,j-1} \cup \Lambda_{1,j} \cup \Lambda_{1,j+1}$ as defined in (4.41). Without loss of generality, we prove only $\mu_c(\Lambda_{1,j}, \mathbf{\Psi}; \mathbf{G_j}) \to 0$ as $j \to \infty$, and note that summing over $j' = j-1, j, j+1$ does not change the asymptotics. By the definition of the cluster coherence, we have

$$\mu_c(\Lambda_{1,j}, \mathbf{\Psi}; \mathbf{G_j}) = \max_{(m,n)} \sum_{\eta \in \Lambda_{1,j}} |\langle \psi_{j,l,k}^{\alpha_j,(\iota)}, (g_{s_j})_{m,n} \rangle|,$$

where $\eta = (j, l, k; \alpha_j, (\iota))$. Suppose that the maximum is attained for $\bar{m}, \bar{n} \in \mathbb{Z}^2$ (the maximum exists, since both frames are translation invariant, and the shearlet elements at scale j are compactly supported in frequency). Applying the change of variables $(y_1, y_2) = (s_j x_1, 2^{2j} x_2 + l 2^{\alpha_j j} x_1 - l k_1)$ and Lemma 4.18 1) and 2) , we obtain

$$
\begin{aligned}
&\mu_c(\Lambda_{1,j}, \mathbf{\Psi}; \mathbf{G_j}) = \sum_{\eta \in \Lambda_{1,j}} |\langle \psi_{j,l,k}^{\alpha_j,(\iota)}, (g_{s_j})_{\bar{m},\bar{n}} \rangle| \\
\leq & \sum_{\substack{|l|\leq 1, k\in\mathbb{Z}^2 \\ |k_2 - l k_1| \leq 2^{\epsilon j}}} \int_{\mathbb{R}^2} C_N \cdot s_j \cdot 2^{(2+\alpha_j)j/2} \cdot \langle |2^{\alpha_j j} x_1 - k_1| \rangle^{-N} \langle |2^{2j} x_2 + l 2^{\alpha_j j} x_1 - k_2| \rangle^{-N} \\
& \qquad \cdot \langle |s_j x_1 + \frac{m_1}{2}| \rangle^{-N} \langle |s_j x_2 + \frac{m_2}{2}| \rangle^{-N} dx_1 dx_2. \\
= & \sum_{\substack{|l|\leq 1, k\in\mathbb{Z}^2 \\ |k_2 - l k_1| \leq 2^{\epsilon j}}} \int_{\mathbb{R}^2} C_N \cdot 2^{-(2-\alpha_j)j/2} \cdot \langle |\frac{2^{\alpha_j j}}{s_j} y_1 - k_1| \rangle^{-N} \langle |y_2 + l k_1 - k_2| \rangle^{-N} \\
& \qquad \cdot \langle |y_1 + \frac{m_1}{2}| \rangle^{-N} \langle |\frac{s_j}{2^{2j}} y_2 - l 2^{-(2-\alpha_j)j} y_1 + s_j 2^{-2j} l k_1 + \frac{m_2}{2}| \rangle^{-N} dy_1 dy_2 \\
\leq & \sum_{\substack{|l|\leq 1, k\in\mathbb{Z}^2 \\ |k_2| \leq 2^{\epsilon j}}} \int_{\mathbb{R}^2} C_N \cdot 2^{-(2-\alpha_j)j/2} \langle |\frac{2^{\alpha_j j}}{s_j} y_1 - k_1| \rangle^{-N} \langle |y_2 - k_2| \rangle^{-N} \\
& \qquad \cdot \langle |y_1 + \frac{m_1}{2}| \rangle^{-N} dy_1 dy_2 \\
= & \sum_{\substack{|l|\leq 1, k_2\in\mathbb{Z} \\ |k_2| \leq 2^{\epsilon j}}} \int_{\mathbb{R}^2} C_N 2^{-(2-\alpha_j)j/2} \Big(\sum_{k_1 \in \mathbb{Z}} \langle |\frac{2^{\alpha_j j}}{s_j} y_1 - k_1| \rangle^{-N} \Big) \langle |y_2 - k_2| \rangle^{-N} \\
& \qquad \cdot \langle |y_1 + \frac{m_1}{2}| \rangle^{-N} dy_1 dy_2 \\
\leq & \; C_N \cdot 2^{-(2-\alpha_j)j/2} \cdot 2^{\epsilon j} = C_N \cdot 2^{-(2-\alpha_j - 2\epsilon)j/2} \xrightarrow{j\to+\infty} 0,
\end{aligned}
$$

where $(2 - \alpha_j - 2\epsilon) > \epsilon$ at each scale j by (4.40). ∎

Next, we prove the following cluster coherence decays.

Proposition 4.25 *Consider the shearlet frame $\mathbf{\Psi}$ of Definition 4.12 and the Gabor frame of scale j, $\mathbf{G_j}$, defined in (4.18). We have*

$$\mu_c(\Lambda_{2,j}, \mathbf{G_j}; \mathbf{\Psi}) \to 0, \quad j \to \infty,$$

where $\Lambda_{2,j}$ is defined in (4.39).

Proof. Suppose that the maximum in the mutual coherence is attained at $\bar{l} \in \mathbb{Z}, \bar{k} \in \mathbb{Z}^2$ and $(\iota) \in \{(\mathrm{h}), (\mathrm{v}), (\mathrm{b})\}$ (there is a maximum since the systems are translation invariant and the inner product goes to zero as n goes to infinity). For each $N = 1, 2 \ldots$ using (4.37)

and Lemma 4.18 3), we have

$$\begin{aligned}\mu_c(\Lambda_{2,j}, \mathbf{G_j}; \mathbf{\Psi}) &= \sum_{m\in B(0,M_j), n\in I_T^{\pm}} |\langle (g_{s_j})_{m,n}, \psi_{j,\bar{l},\bar{k}}^{\alpha_j,\iota}\rangle| \\ &\leq C_N \cdot 2^{-(2-\alpha_j)j/2} \#\{m \in B(0,M_j)\} \cdot \#\{n \in I_T^{\pm} \cap M_{j,l,(\iota)}\} \\ &\leq C_N \cdot 2^{-(2-\alpha_j)j/2} \cdot M_j^2 \cdot 2^{(2-\alpha_j-\epsilon)j/2} \\ \overset{M_j=2^{\epsilon j/6}}{=} & C_N \cdot 2^{-\epsilon j/6} \xrightarrow{j\to+\infty} 0.\end{aligned}$$

■

4.9.2 Cluster Coherence of the Projected Frames

In this subsection we compute the cluster coherence terms corresponding to the missing stripe. To be able to inpaint the missing part, the following propositions rely of the fact that the gap size h_j at each scale j is smaller than the essential length of the shearlet elements in this scale. For illustration, see Figure 4.7.

In [GK14] the problem of inpainting a missing strip from a line singularity via shearlet frames was studied. As part of their construction, they prove the following proposition.

Proposition 4.26 ([GK14], Prop. 5.6) *Consider the shearlet frame $\mathbf{\Psi}$ of Definition 4.12. For $h_j = o(2^{(\alpha_j+\epsilon)j})$ with $\alpha_j \in (0,2)$, $\liminf \alpha_j > 0$ and ϵ satisfying (4.40), we have*

$$\mu_c(\Lambda_{1,j}^{\pm}, P_j\mathbf{\Psi}; \mathbf{\Psi}) \to 0, \quad j \to \infty,$$

where $\Lambda_{1,j}^{\pm}$ is defined in (4.41), P_j is defined in (4.17).

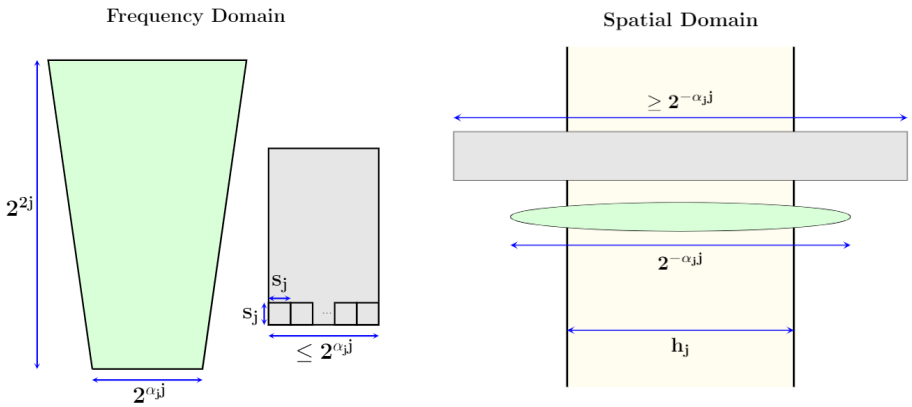

Figure 4.7: Left: Frequency support of a shearlet (trapezoidal) and Gabor elements (small squares). Right: Missing part (vertical band), essential spatial support of a shearlet (ellipse) and a cluster of Gabor elements (rectangle). The gap width does not exceed the essential length of the shearlet.

Next, we prove the following result.

Proposition 4.27 *Consider the the Gabor frame of scale j, $\mathbf{G_j}$ defined in (4.18). Suppose that $h_j = o(2^{-\alpha_j j})$ with $\alpha_j \in (0,2)$, $\liminf \alpha_j > 0$, and I_T satisfies (4.37) and (4.38). Then we have*

$$\mu_c(\Lambda_{2,j}, P_j\mathbf{G_j}; \mathbf{G_j}) \to 0, \quad j \to \infty,$$

where $\Lambda_{2,j}$ is defined in (4.39) and P_j is defined in (4.17).

For an illustration of this Proposition, we refer to Figure 4.7 (gray part). Next, we prove the following result.

Proof. First, from the definition of the cluster, we may assume that the maximum is attained for $(m', n') \in \Lambda_{2,j}$. Namely, we have

$$\begin{aligned}
\mu_c(\Lambda_{2,j}, P_j\mathbf{G_j}; \mathbf{G_j}) &= \sum_{(m,n)\in M_j\times(I_T^{\pm}\cap\mathcal{A}_{s,j})} |\langle P_j(g_{s_j})_{m,n}, (g_{s_j})_{m',n'}\rangle| \\
&= \sum_{(m,n)\in M_j\times(I_T^{\pm}\cap\mathcal{A}_{s,j})} \Big| \int_{-h_j}^{h_j}\int_{\mathbb{R}} (g_{s_j})_{m,n}(x)\overline{(g_{s_j})_{m',n'}(x)}dx\Big| \\
&\le \sum_{(m,n)\in M_j\times(I_T^{\pm}\cap\mathcal{A}_{s,j})} \int_{-h_j}^{h_j}\int_{\mathbb{R}} |(g_{s_j})_{m,n}(x)||(g_{s_j})_{m',n'}(x)|dx. \qquad (4.54)
\end{aligned}$$

By Lemma 4.18, we obtain the following decay estimate of $(g_{s_j})_{m,n}(x)$ for any $N \in \mathbb{N}$

$$|(g_{s_j})_{m,n}(x)| \le C_N \cdot s_j \cdot \langle |s_j x_1 + \frac{m_1}{2}|\rangle^{-N} \langle |s_j x_2 + \frac{m_2}{2}|\rangle^{-N}.$$

Thus, by changing variable $y = s_j x$, we have

$$\begin{aligned}
&\int_{-h_j}^{h_j}\int_{\mathbb{R}} |(g_{s_j})_{m,n}(x)||(g_{s_j})_{m',n'}(x)|dx \\
&\le \int_{-h_j}^{h_j}\int_{\mathbb{R}} C_N s_j^2 \langle |s_j x_1 + \frac{m_1}{2}|\rangle^{-N} \langle |s_j x_2 + \frac{m_2}{2}|\rangle^{-N} \langle |s_j x_1 + \frac{m_1'}{2}|\rangle^{-N} \\
&\qquad \cdot \langle |s_j x_2 + \frac{m_2'}{2}|\rangle^{-N} dx \\
&= \int_{-h_j s_j}^{h_j s_j}\int_{\mathbb{R}} C_N \langle |y_1 + \frac{m_1}{2}|\rangle^{-N} \langle |y_2 + \frac{m_2}{2}|\rangle^{-N} \langle |y_1 + \frac{m_1'}{2}|\rangle^{-N} \langle |y_2 + \frac{m_2'}{2}|\rangle^{-N} dy.
\end{aligned} \qquad (4.55)$$

Next,

$$\sum_m \langle |y_1 + \frac{m_1}{2}|\rangle^{-N} \langle |y_2 + \frac{m_2}{2}|\rangle^{-N} \le C_N', \text{ and } \int_{\mathbb{R}} \langle |y_2 + \frac{m_2'}{2}|\rangle^{-N} dy_2 \le C_N''. \qquad (4.56)$$

Thus, by (4.38) and (4.54) combined with (4.55) and (4.56) , we obtain

$$\mu_c(\Lambda_{2,j}, P_j\mathbf{G_j}; \mathbf{G_j}) \le \sum_{n\in I_T^{\pm}\cap\mathcal{A}_{s,j}} C_N \cdot h_j s_j$$

$$\leq \quad C_N \cdot \frac{2^{\alpha_j j}}{s_j} h_j s_j = C_N \cdot 2^{\alpha_j j} h_j \xrightarrow{j\to+\infty} 0.$$

■

Proposition 4.28 *Consider the shearlet frame $\mathbf{\Psi}$ of Definition 4.12 and the Gabor frame of scale j, $\mathbf{G_j}$, defined in (4.18). Assuming that I_T satisfies (4.37) and (4.38), we have*

$$\mu_c(\Lambda_{2,j}, P_j\mathbf{G_j}, \mathbf{\Psi}) \to 0, \quad j \to \infty,$$

where $\Lambda_{2,j}$ is defined in (4.39) and P_j is defined in (4.17).

Proof. The maximum of the cluster coherence is attained for some $(j, \bar{l}, \bar{k}; \alpha_j, (\iota)) \in \Delta_j$. Thus,

$$\begin{aligned}
\mu_c(\Lambda_{2,j}, P_j\mathbf{G_j}, \mathbf{\Psi}) &= \sum_{(m,n)\in M_j\times(I_T^{\pm}\cap\mathcal{A}_{s,j})} |\langle P_j(g_{s_j})_{m,n}, \psi_{j,\bar{l},\bar{k}}^{\alpha_j,(\iota)}\rangle| \\
&= \sum_{(m,n)\in M_j\times(I_T^{\pm}\cap\mathcal{A}_{s,j})} \Big| \int_{-h_j}^{h_j}\int_{\mathbb{R}} (g_{s_j})_{m,n}(x)\overline{\psi_{j,\bar{l},\bar{k}}^{\alpha_j,(\iota)}(x)}dx\Big| \\
&\leq \sum_{(m,n)\in M_j\times(I_T^{\pm}\cap\mathcal{A}_{s,j})} \int_{-h_j}^{h_j}\int_{\mathbb{R}} |(g_{s_j})_{m,n}(x)||\psi_{j,\bar{l},\bar{k}}^{\alpha_j,(\iota)}(x)|dx.
\end{aligned}$$

Now we consider three cases

1) Case $(\iota) = (\mathrm{v})$. For each $N = 1, 2, \ldots$, by Lemma 4.18, we derive the following decay estimates of $(g_{s_j})_{m,n}(x)$ and $\psi_{j,\bar{l},\bar{k}}^{\alpha_j,(\iota)}(x)$

$$|(g_{s_j})_{m,n}(x)| \leq C_N \cdot s_j \cdot \langle |s_j x_1 + \frac{m_1}{2}|\rangle^{-N} \langle |s_j x_2 + \frac{m_2}{2}|\rangle^{-N},$$

$$|\psi_{j,\bar{l},\bar{k}}^{\alpha_j,(\mathrm{v})}(x)| \leq C_N \cdot 2^{(2+\alpha)j/2} \cdot \langle |2^{\alpha_j j}x_1 - \bar{k}_1|\rangle^{-N} \langle |2^{2j}x_2 + \bar{l}2^{\alpha_j j}x_1 - \bar{k}_2|\rangle^{-N}.$$

Thus, by the change of variable $y = S_{(\mathrm{v})}^{\bar{l}} A_{\alpha_j,(\mathrm{v})}^{j} x = (2^{\alpha_j j}x_1, 2^{2j}x_2 + \bar{l}2^{\alpha_j j}x_1)$, we have

$$\begin{aligned}
&\int_{-h_j}^{h_j}\int_{\mathbb{R}} |(g_{s_j})_{m,n}(x)||\psi_{j,\bar{l},\bar{k}}^{\alpha_j,(\mathrm{v})}(x)|dx \\
&\leq C_N \cdot 2^{-(2+\alpha_j)j/2} \cdot s_j \int_{-2^{\alpha_j j}h_j}^{2^{\alpha_j j}h_j}\int_{\mathbb{R}} \langle |s_j 2^{-\alpha_j j}y_1 + \frac{m_1}{2}|\rangle^{-N} \\
&\quad \cdot \langle |s_j 2^{-2j}(y_2 - \bar{l}y_1) + \frac{m_2}{2}|\rangle^{-N} \langle |y_1 - \bar{k}_1|\rangle^{-N} \langle |y_2 - \bar{k}_2|\rangle^{-N} dy_1 dy_2 \\
&\leq C_N \cdot 2^{-(2+\alpha_j)j/2} \cdot s_j \int_{\mathbb{R}}\int_{\mathbb{R}} \langle |s_j 2^{-\alpha_j j}y_1 + \frac{m_1}{2}|\rangle^{-N} \langle |s_j 2^{-2j}(y_2 - \bar{l}y_1) + \frac{m_2}{2}|\rangle^{-N} \\
&\quad \cdot \langle |y_1 - \bar{k}_1|\rangle^{-N} \langle |y_2 - \bar{k}_2|\rangle^{-N} dy_1 dy_2. \qquad (4.57)
\end{aligned}$$

Furthermore,

$$\sum_m \langle |s_j 2^{-\alpha_j j} y_1 + \frac{m_1}{2}| \rangle^{-N} \langle |s_j 2^{-2j}(y_2 - \bar{l} y_1) + \frac{m_2}{2}| \rangle^{-N} \leq C'_N \tag{4.58}$$

and

$$\int_{\mathbb{R}} \langle |y_1 - \bar{k}_1| \rangle^{-N} dy_1 \leq C''_N, \quad \int_{\mathbb{R}} \langle |y_2 - \bar{k}_2| \rangle^{-N} dy_2 \leq C'''_N. \tag{4.59}$$

Thus, by (4.57), (4.58), (4.59) and (4.38), we obtain

$$\begin{aligned} \mu_c(\Lambda_{2,j}, P_j \mathbf{G_j}; \mathbf{\Psi}) &\leq \sum_{n \in I_T^{\pm} \cap \mathcal{A}_{s,j}} C_N \cdot 2^{-(2+\alpha_j)j/2} \cdot s_j \\ &\leq C_N \cdot 2^{-(2+\alpha_j)j/2} \cdot s_j \cdot \frac{2^{\alpha_j j}}{s_j} = C_N \cdot 2^{-(2-\alpha_j)j/2} \xrightarrow{j \to +\infty} 0. \end{aligned}$$

2) Case $(\iota) = (\mathrm{h})$. Similarly, by the change of variable $y = S^{\bar{l}}_{(\mathrm{h})} A^j_{\alpha_j,(\mathrm{h})} x = (2^{2j} x_1 + \bar{l} 2^{\alpha_j j} x_2, 2^{\alpha_j j} x_2)$, we have

$$\begin{aligned} & 2^{(2+\alpha_j)j/2} \cdot s_j^{-1} \cdot \int_{-h_j}^{h_j} \int_{\mathbb{R}} |(g_{s_j})_{m,n}(x)| |\psi^{\alpha_j,(\mathrm{h})}_{j,\bar{l},\bar{k}}(x)| dx \\ \leq\ & C_N \int_{\mathbb{R}^2} \langle |s_j 2^{-2j}(y_1 - \bar{l} y_2) + \frac{m_1}{2}| \rangle^{-N} \langle |s_j 2^{-\alpha_j j} y_2 + \frac{m_2}{2}| \rangle^{-N} \\ & \cdot \langle |y_1 - \bar{k}_1| \rangle^{-N} \langle |y_2 - \bar{k}_2| \rangle^{-N} dy. \end{aligned}$$

By using similar argument as in case $(\iota) = (\mathrm{v})$, we finally obtain

$$\begin{aligned} \mu_c(\Lambda_{2,j}, P_j \mathbf{G_j}; \mathbf{\Psi}) &\leq \sum_{n \in I_T^{\pm} \cap \mathcal{A}_{s,j}} C_N \cdot 2^{-(2+\alpha_j)j/2} \cdot s_j \\ &\overset{(4.38)}{\leq} C_N \cdot 2^{-(2-\alpha_j)j/2} \xrightarrow{j \to +\infty} 0. \end{aligned}$$

1) Case $(\iota) = (\mathrm{b})$. Recalling the definition of boundary shearlets, the decay estimate can be done similarly. ∎

Proposition 4.29 *Consider the shearlet frame $\mathbf{\Psi}$ of Definition 4.12 and the Gabor frame of scale j, $\mathbf{G_j}$, defined in (4.18). Suppose that $s_j \leq 2^{\alpha_j j}$, $h_j = o(2^{\alpha_j j})$, and $\alpha_j \in (0,2)$, $\liminf \alpha_j > 0$. Then we have*

$$\mu_c(\Lambda^{\pm}_{1,j}, P_j \mathbf{\Psi}; \mathbf{G_j}) \to 0, \quad j \to \infty,$$

where $\Lambda^{\pm}_{1,j}$ is defined in (4.41) and P_j is defined in (4.17).

Proof. Without loss of generality, we prove only $\mu_c(\Lambda_{1,j}, P_j \mathbf{\Psi}; \mathbf{G_j}) \to 0$, $j \to \infty$. First, we assume that the maximum in the definition of the cluster is attained for some $(\bar{m}, \bar{n}) \in \mathbb{Z}^2 \times \mathbb{Z}^2$. We have

$$\mu_c(\Lambda_{1,j}, P_j \mathbf{\Psi}; \mathbf{G_j}) = \sum_{(j,l,k;\alpha_j,\iota) \in \Lambda_{1,j}} |\langle P_j \psi^{\alpha_j,(\iota)}_{j,l,k}, (g_{s_j})_{\bar{m},\bar{n}} \rangle|$$

$$
\begin{aligned}
&= \sum_{\substack{|l|\le 1,k\in\mathbb{Z}^2\\ |k_2-lk_1|\le 2^{\epsilon j}}} \Big| \int_{-h_j}^{h_j}\int_{\mathbb{R}} \psi_{j,l,k}^{\alpha_{j'},(\mathrm{v})}(x)\overline{(g_{s_j})_{\bar m,\bar n}(x)}dx\Big| \\
&\le \sum_{\substack{|l|\le 1,k\in\mathbb{Z}^2\\ |k_2-lk_1|\le 2^{\epsilon j}}} \int_{-h_j}^{h_j}\int_{\mathbb{R}} |\psi_{j,l,k}^{\alpha_{j'},(\mathrm{v})}(x)||(g_{s_j})_{\bar m,\bar n}(x)|dx|.
\end{aligned}
$$

For each $N = 1,2,\dots,$ by Lemma 4.18, we derive the following decay estimates of $\psi_{j,l,k}^{\alpha_{j'},(\mathrm{v})}(x)$ and $(g_{s_j})_{\bar m,\bar n}(x)$

$$
|\psi_{j,l,k}^{\alpha_{j'},(\mathrm{v})}(x)| \le C_N\cdot 2^{(2+\alpha)j/2}\cdot \langle|2^{\alpha_j j}x_1-k_1|\rangle^{-N}\langle|2^{2j}x_2+l2^{\alpha_j j}x_1-k_2|\rangle^{-N},
$$

$$
|(g_{s_j})_{\bar m,\bar n}(x)| \le C_N\cdot s_j\cdot \langle|s_jx_1+\frac{\bar m_1}{2}|\rangle^{-N}\langle|s_jx_2+\frac{\bar m_2}{2}|\rangle^{-N}.
$$

Thus, by changing variable $y = S_{(\mathrm{v})}^l A_{\alpha_{j'},(\mathrm{v})}^j x = (2^{\alpha_j j}x_1, 2^{2j}x_2+l2^{\alpha_j j}x_1)$, we have

$$
\begin{aligned}
&\int_{-h_j}^{h_j}\int_{\mathbb{R}} |\psi_{j,l,k}^{\alpha_{j'},(\mathrm{v})}(x)|\cdot|(g_{s_j})_{\bar m,\bar n}(x)|dx \\
&\le C_N\cdot 2^{-(2+\alpha_j)j/2}\cdot s_j\cdot \int_{-2^{\alpha_j j}h_j}^{2^{\alpha_j j}h_j}\int_{\mathbb{R}} \langle|y_1-k_1|\rangle^{-N}\langle|y_2-k_2|\rangle^{-N} \\
&\quad\cdot\langle|s_j2^{-\alpha_j j}y_1+\frac{\bar m_1}{2}|\rangle^{-N}\langle|s_j2^{-2j}(y_2-ly_1)+\frac{\bar m_2}{2}|\rangle^{-N}dy_1dy_2. \qquad (4.60)
\end{aligned}
$$

Next,

$$
\langle|s_j2^{-\alpha_j j}y_1+\frac{\bar m_1}{2}|\rangle^{-N}\langle|s_j2^{-2j}(y_2-ly_1)+\frac{\bar m_2}{2}|\rangle^{-N} \le 1 \qquad (4.61)
$$

and

$$
\begin{aligned}
&\int_{\mathbb{R}}\Big(\sum_{\substack{|l|\le 1,k\in\mathbb{Z}^2\\ |k_2-lk_1|\le 2^{\epsilon j}}} \langle|y_1-k_1|\rangle^{-N}\langle|y_2-k_2|\rangle^{-N}\Big)dy_2 \\
&= \sum_{\substack{|l|\le 1,k_1,k_3\in\mathbb{Z}\\ |k_3|\le 2^{\epsilon j}}} \langle|y_1-k_1|\rangle^{-N}\cdot\Big(\int_{\mathbb{R}}\langle|y_2-k_3-lk_1|\rangle^{-N}dy_2\Big) \\
&\le C_N\cdot 2^{\epsilon j}\cdot\int_{\mathbb{R}}\langle|t-y_1|\rangle^{-N}dt \le C_N'2^{\epsilon j}. \qquad (4.62)
\end{aligned}
$$

Thus, by (4.60), (4.61), (4.62), we obtain

$$
\begin{aligned}
\mu_c(\Lambda_{1,j},P_j\mathbf{\Psi};\mathbf{G_j}) &\le C_N'\cdot 2^{-(2+\alpha_j)j/2}\cdot s_j\cdot 2^{\alpha_j j}h_j\cdot 2^{\epsilon j} \\
&\overset{s_j\le 2^{\alpha_j j}}{\le} C_N'\cdot 2^{-(2-\alpha_j-2\epsilon)j/2}\cdot 2^{\alpha_j j}h_j \xrightarrow{j\to+\infty} 0.
\end{aligned}
$$

■

4.10 Proof of Theorem 4.16

We are now ready to present the proof of Theorem 4.16.

Proof. By Theorem 4.8, we have

$$\|P_j\mathcal{C}_j^\star - P_j w\mathcal{S}_j\|_2 + \|P_j\mathcal{T}_j^\star - P_j\mathcal{T}_{s,j}\|_2 \leq \frac{2\delta_j}{1-2\mu_{c,j}}, \tag{4.63}$$

where $\delta_j = \delta_{1,j} + \delta_{2,j}$ and $\mu_{c,j} =$
$\max\{\mu_c(\Lambda_{1,j}^{\pm}, P_j\mathbf{\Psi}; \mathbf{\Psi}) + \mu_c(\Lambda_{2,j}, P_j\mathbf{G_j}; \mathbf{\Psi}), \mu_c(\Lambda_{2,j}, P_j\mathbf{G_j}; \mathbf{G_j}) + \mu_c(\Lambda_{1,j}^{\pm}, P_j\mathbf{\Psi}; \mathbf{G_j})\}$
$+ \max\{\mu_c(\Lambda_{1,j}^{\pm}, \Phi_1; \mathbf{G_j}), \mu_c(\Lambda_2, \mathbf{G_j}; \mathbf{\Psi})\}$.
Moreover, it follows from Propositions 4.20 and 4.23 that

$$\delta_j = \delta_1 + \delta_2 = o(2^{-Nj}),\ \forall N \in \mathbb{N}. \tag{4.64}$$

For the other term, the following estimate holds as a consequence of Propositions 4.24, 4.25, 4.26, 4.27, 4.28 and 4.29

$$\mu_{c,j} \longrightarrow 0, \quad j \to +\infty. \tag{4.65}$$

Combining (4.63), (4.64), and (4.65), we get

$$\|\mathcal{C}_j^\star - w\mathcal{S}_j\|_2 + \|\mathcal{T}_j^\star - \mathcal{T}_{s,j}\|_2 = o(2^{-Nj}), \quad \forall N \in \mathbb{N}.$$

This proves the first claim of the theorem.

The second claim is obtained since the following estimate holds for any arbitrarily large number $N \in \mathbb{N}$

$$\|P_j\mathcal{C}_j^\star - P_j w\mathcal{S}_j\|_2 + \|P_j\mathcal{T}_j^\star - P_j\mathcal{T}_{s,j}\|_2 \leq \|\mathcal{C}_j^\star - \mathcal{C}_j\|_2 + \|\mathcal{T}_j^\star - \mathcal{T}_{s,j}\|_2 \leq 2^{-Nj}. \tag{4.66}$$

By Lemma 4.15 and (4.66), for $N \in \mathbb{N}$ chosen sufficiently large, we obtain

$$\frac{\|P_j\mathcal{C}_j^\star - P_j w\mathcal{S}_j\|_2}{\|P_j w\mathcal{S}_j\|_2} \leq \frac{o(2^{-Nj})}{h_j 2^{-j}} \xrightarrow{j\to+\infty} 0,$$

and

$$\frac{\|P_j\mathcal{T}_j^\star - P_j\mathcal{T}_{s,j}\|_2}{h_j 2^{-j}} = \frac{o(2^{-Nj})}{h_j 2^{-j}} \xrightarrow{j\to+\infty} 0,$$

which concludes the proof. ∎

5

Multiple Component Separation and Inpainting

In practical applications, many problems in signal or image processing involve the task of separating two or more components from a given image. This problem is of interest in many applications [CCS10; Kut13], for instance, astronomers may desire to decompose the observed image into pointlike, curvelike, and texture structures. This raises a need to separate various components from the original image in order to effectively analyze them. This chapter is devoted to deal with such a situation.

The remainder of this chapter is organized as follows. We first start with some basic definitions, notions, and the formulation of inpainting and geometric separation problems in Section 5.1. Next, we modify the notions of joint concentration and cluster coherence to adapt to our need in Section 5.2. We then derive a general theoretical guarantee in Theorem 5.8 using general frames for separating $N-$ component signals based on l_1 minimization. In section 5.3, a similar theoretical guarantee is concluded in Theorem 5.11 to deal with noisy images. We finally transfer the abstract theory to derive Theorem 5.16 and 5.17 which prove that our algorithms are capable of denoising, inpainting, and separating points from curves and texture in Section 5.4. The paper ends with a summary and conclusion in Section 5.5.

5.1 Mathematical Formulation

We start with some notions and basic definitions.

5.1.1 Notations and Definitions

Let us first recall the *Schwartz space* of *rapidly decreasing functions* or *Schwartz functions*

$$\mathcal{S}(\mathbb{R}^2) := \Big\{ f \in C^\infty(\mathbb{R}^2) \mid \forall K, N \in \mathbb{N}_0, \sup_{x\in\mathbb{R}^2} (1+|x|^2)^{\frac{N}{2}} \sum_{|\alpha|\leq K} |D^\alpha f(x)| < \infty \Big\}.$$

Next, we recall some needed definitions and facts from frame theory, more details can be found in [DS52; Chr03]. We call a family of vector $\Phi = \{\phi_i\}_{i\in I}$ in a separable Hilbert space $\mathcal{H}$ a *frame* for $\mathcal{H}$ if there are constants $A, B > 0$ so that for all $f \in \mathcal{H}$ we have

$$A\|f\|_2^2 \leq \sum_{i\in I} |\langle f, \phi_i\rangle|^2 \leq B\|f\|_2^2, \tag{5.1}$$

where A, B are called the *lower* and *upper frame bound*. We call it $A-$*tight frame* in case $A = B$ and a *Parseval frame* or *tight frame* in case $A = B = 1$.

By abuse of notation we write Φ again to denote the *synthesis operator*

$$\Phi : l_2(I) \to \mathcal{H}, \quad \Phi(\{c_i\}_{i\in I}) = \sum_{i\in I} c_i \phi_i.$$

We define the *analysis operator* Φ^* by

$$\Phi^* : \mathcal{H} \to l_2(I), \quad \Phi^*(f) = (\langle f, \phi_i \rangle)_{i\in I}.$$

Associated with a frame $\Phi = \{\phi_i\}_{i\in I}$, we define the *frame operator* $\mathbb{S}$ by

$$\mathbb{S} = \Phi\Phi^* : \mathcal{H} \to \mathcal{H}, \quad \mathbb{S}f = \sum_{i\in I} \langle f, \phi_i \rangle \phi_i.$$

Given a frame $\Phi = \{\phi_i\}_{i\in I}$ for $\mathcal{H}$, a sequence $\Phi^d = \{\phi_i^d\}_{i\in I}$ in $\mathcal{H}$ is called
- an *analysis pseudo-dual* if the following holds

$$f = \Phi(\Phi^d)^* f = \sum_{i\in I} \langle f, \phi_i^d \rangle \phi_i, \ \forall f \in \mathcal{H}; \tag{5.2}$$

- a *synthesis pseudo-dual* if we have

$$f = (\Phi^d)\Phi^* f = \sum_{i\in I} \langle f, \phi_i \rangle \phi_i^d, \ \forall f \in \mathcal{H}; \tag{5.3}$$

- a *dual frame* of Φ if both (5.2) and (5.3) hold. By (5.1), the corresponding frame operator $\mathbb{S}$ is self-adjoint, invertible on $\mathcal{H}$. As a result, there exists a dual frame $\{\mathbb{S}^{-1}\phi_i\}_{i\in I}$ called the *canonical dual frame* of $\Phi = \{\phi_i\}_{i\in I}$ with frame bounds (B^{-1}, A^{-1}).

Let $\mathbb{D}_\Phi$ denote the set of all synthesis pseudo-dual of the frame Φ

$$\mathbb{D}_\Phi = \{\Phi^d = \{\phi_i^d\}_{i\in I} \in \mathcal{H} \mid f = \Phi^d\Phi^* f = \sum_{i\in I} \langle f, \phi_i \rangle \phi_i^d, \ \forall f \in \mathcal{H}\}.$$

Clearly, $\mathbb{D}_\Phi \neq \emptyset$ since $\mathbb{S}^{-1}\Phi \in \mathbb{D}_\Phi$. In addition, in case Φ forms a Parseval frame we have $\Phi \in \mathbb{D}_\Phi$.

5.1.2 Problem of Multiple Component Image Separation

In image processing, the image to be analyzed is often composed of multiple components. Given an image f, we assume that f can be decomposed of N components, i.e.,

$$f = \sum_m f_m,$$

where each f_m corresponds to a geometric feature contained in f. It would be ideal to extract all of these parts from the original image for analyzing them separately. For practical purposes, we later assume that these components contain texture and jumps or changes in behavior along point, curvilinear discontinuities. The prior information on underlying components is important to capture the geometry of the discontinuities by choosing suitable dictionaries, each sparsely representing its intended content type.

5.1.3 Problem of Image Inpainting

Image inpainting is the task of filling in holes or removing selected objects contained in an image using information from the surrounding area. Given a Hilbert space $\mathcal{H}$, we assume that $\mathcal{H}$ can be decomposed into a direct sum of missing subspace and known subspace, i.e., $\mathcal{H} = \mathcal{H}_K \oplus \mathcal{H}_M$. Let P_M and P_K denote the orthogonal projection of $\mathcal{H}$ onto the missing part and the known part, respectively. Our goal is to reconstruct the original image f from knowledge of the known part $P_K f$.

5.1.4 Recovery via l_1-Minimization

Among existing methods, l_1 minimization has been widely used for recovering sparse solutions. One appeared in several papers [DK09; Kut13] for separating two geometric components of a given image. There, the following procedure was proposed for an observed signal f and two Parseval frames $\{\Phi_1\}_{i\in I}, \{\Phi_2\}_{j\in J}$,

$$(f_1^\star, f_2^\star) = \underset{f_1,f_2}{\operatorname{argmin}} \|\Phi_1^* f_1\|_1 + \|\Phi_2^* f_2\|_1, \quad \text{subject to} \quad f_1 + f_2 = f. \tag{5.4}$$

The theoretical guarantee for (5.4) presented in the aforementioned papers was based on notions of joint concentration and cluster coherence. In our analysis, we consider the following algorithm for simultaneously inpainting and separating N distinct constituents from an observed image.

Algorithm 5.1 (Constrained optimization)

Input: observed image f, N frames $\{\Phi_{1i_1}\}_{i_1\in I_1}, \ldots, \{\Phi_{Ni_N}\}_{i_N\in I_N}$ with frame bounds $(A_1, B_1), (A_2, B_2), \ldots, (A_N, B_N)$.

Compute: $(f_1^\star, f_2^\star, \ldots, f_N^\star)$, where

$$\begin{aligned}(f_1^\star, f_2^\star, \ldots, f_N^\star) \quad = \quad & \underset{(f_1,\ldots,f_N)}{\operatorname{argmin}} \|\Phi_1^* f_1\|_1 + \|\Phi_2^* f_2\|_1 + \ldots \|\Phi_N^* f_N\|_1, \\ & \text{subject to} \quad P_K(f_1 + f_2 + \cdots + f_N) = P_K f.\end{aligned}$$

Output: recovered components $f_1^\star, f_2^\star, \ldots, f_N^\star$.

We then provide a theoretical guarantee for the success of the algorithm in the next section.

5.2 Theoretical Guarantee for Multiple Component Separation Problems

5.2.1 Joint Concentration Analysis

The notion of joint concentration was first introduced in [DK13] for separating two geometric components using Parseval frames. There, the joint concentration associated with two Parseval frames Φ_1, Φ_2 and sets of indexes Λ_1, Λ_2 was defined by

$$\kappa(\Lambda_1, \Lambda_2) = \sup_{x\in\mathcal{H}} \frac{\|\mathbb{1}_{\Lambda_1}\Phi_1^\star x\|_1 + \|\mathbb{1}_{\Lambda_2}\Phi_2^\star x\|_1}{\|\Phi_1^\star x\|_1 + \|\Phi_2^\star x\|_1}. \tag{5.5}$$

In our situation, we are now given the known part $P_K f$ of a signal f where f is a superposition of N geometric constituents. An approach was proposed in [KKZ11] to deal with separating tasks, i.e., $P_K f = f$, there

$$\kappa = \sup_{x \in \mathcal{H}} \frac{\|\mathbb{1}_{\Lambda_1} \Phi_1^* x\|_1 + \|\mathbb{1}_{\Lambda_2} \Phi_2^* x\|_1 + \cdots + \|\mathbb{1}_{\Lambda_N} \Phi_N^* x\|}{\|\Phi_1^* x\|_1 + \|\Phi_2^* x\|_1 + \cdots + \|\Phi_N^* x\|_1}. \tag{5.6}$$

Let us now have a closer look to these definitions. Let $(f_1^*, f_2^*, \ldots, f_N^*)$ be the solution of Algorithm 5.1 with $P_K = Id$, and $(f_1, f_2, \ldots, f_N)$ be the truly underlying components. In case $N = 2$, the underlying reason for the definition (5.5) lies in the fact that $f_1^* - f_1 = -(f_2^* - f_2)$ and the absolute value of the error is then encoded into variable x in (5.5). It seems plausible that (5.6) is a generalized version of (5.5). However, the approach can be problematic for more components since from assumption $f_1^\star + f_2^\star + f \cdots + f_N^\star = f_1 + f_2 + \cdots + f_N, N \geq 3$ we can not invoke a similar relation to encode with the same variable x as in (5.6).

In our study, we modify the definition of joint concentration and cluster coherence to adapt to the situation of simultaneous separation and inpainting. Obviously, the separation problem is a trivial case of simultaneous separation and inpainting problem as we can set missing space $\mathcal{H}_M = \emptyset$. Since we just know the known part, i.e., $P_K f = P_K(f_1^\star + f_2^\star + f \cdots + f_N^\star) = P_K(f_1 + f_2 + \cdots + f_N)$ we will encode with different terms corresponding with component errors $f_i^* - f_i, 1 \leq i \leq N$. This will be now made precise.

Definition 5.2 Let $\Phi_1, \Phi_2, \ldots, \Phi_N$ be a set of frames with frame bounds (A_1, B_1), $(A_2, B_2), \ldots, (A_N, B_N)$, and $\Lambda_1, \Lambda_2, \cdots, \Lambda_N$ be index sets. We define

(i) the *N-joint concentration* $\kappa := \kappa(\Lambda_1, \Phi_1; \ldots; \Lambda_N, \Phi_N)$ by

$$\kappa_N = \sup_{\sum_{n=1}^N f_N \in \mathcal{H}_M} \frac{\sum_m \left(\|\mathbb{1}_{\Lambda_m} \Phi_m^* P_K f_m\|_1 + \|\mathbb{1}_{\Lambda_m} \Phi_m^* P_M f_m\|_1 \right)}{\|\Phi_1^* f_1\|_1 + \cdots + \|\Phi_N^* f_N\|_1},$$

(ii) the *separation N-joint concentration* $\kappa_N^{sep} := \kappa(\Lambda_1, P_K\Phi_1; \ldots; P_K\Lambda_N, \Phi_N)$ by

$$\kappa_N^{sep} = \sup_{\sum_{n=1}^N f_n \in \mathcal{H}_M} \frac{\|\mathbb{1}_{\Lambda_1} \Phi_1^* P_K f_1\|_1 + \cdots + \|\mathbb{1}_{\Lambda_N} \Phi_N^* P_K f_N\|_1}{\|\Phi_1^* f_1\|_1 + \cdots + \|\Phi_N^* f_N\|_1},$$

(iii) the *inpainting N-joint concentration* $\kappa_N^{inp} := \kappa(\Lambda_1, P_M\Phi_1; \ldots; \Lambda_N, P_M\Phi_N)$ by

$$\kappa_N^{inp} = \sup_{(f_1, f_2, \ldots, f_N)} \frac{\|\mathbb{1}_{\Lambda_1} \Phi_1^* P_M f_1\|_1 + \cdots + \|\mathbb{1}_{\Lambda_N} \Phi_N^* P_M f_N\|_1}{\|\Phi_1^* f_1\|_1 + \cdots + \|\Phi_N^* f_N\|_1}.$$

These notions enable us to provide a theoretical for the success of Algorithm 5.1. Let us dive deeper into these notations by considering some special cases. If we consider each problem separately, for instance, in case of only separation problem, i.e., $\mathcal{H}_M = \emptyset$, the joint concentration $\kappa_N \equiv \kappa_N^{sep}$, κ_N^{sep} is therefore used to be responsible for the separation task. In this case, if $N = 2$, the term κ_2^{sep} is coincided with (5.5) which guarantees the

success of separating two components. In case of without separating, only inpainting, i.e., $\kappa \equiv \kappa_1^{inp} = \sup_{f_1} \frac{\|\mathbb{1}_{\Lambda_1}\Phi_1^* P_M f_1\|_1}{\|\Phi_1^* f_1\|_1}$, this notation is slightly different from one that appeared in [KKZ14] where f_1 was assumed to be in missing space $\mathcal{H}_M$, but they are bounded by the same cluster coherence which is later shown in Lemma 5.7 and they therefore play a similar role in the theoretical analysis of inpainting. Obviously, $\kappa_N \leq \kappa_N^{sep} + \kappa_N^{inp}$. Bounding each term ensures the successful algorithm for the corresponding task.

Next, we also extend a definition from [KKZ14] to the case of general frames instead of Parseval frames.

Definition 5.3 Fix $\delta > 0$. Given a Hilbert space $\mathcal{H}$ with a frame $\Phi, f \in \mathcal{H}$ is $\delta-$relatively sparse in Φ with respect to Λ if $\|\mathbb{1}_{\Lambda^c}\Phi^\star f\|_1 \leq \delta$, where A^c denotes $X \setminus A$.

The following result gives an estimate for the L_2 error of the reconstructed signals by Algorithm 5.1.

Proposition 5.4 *Let $\Phi_1, \Phi_2, \ldots, \Phi_N$ be a set of frames with pairs of frame bounds (A_1, B_1), $(A_2, B_2), \ldots, (A_N, B_N)$. For $\delta_1, \delta_2, \ldots, \delta_N > 0$, we fix $\delta = \sum_{m=1}^N \delta_m$, and suppose that $f \in \mathcal{H}$ can be decomposed as $x = \sum_{m=1}^N f_m$ so that each component $f_1, f_2, \ldots, f_N$ is $\delta_1, \delta_2, \ldots, \delta_N$-relatively sparse in $\Phi_1, \Phi_2, \ldots, \Phi_N$ with respect to $\Lambda_1, \Lambda_2, \cdots, \Lambda_N$, respectively.*
Let $(f_1^\star, f_2^\star, \ldots, f_N^\star)$ solve Algorithm 5.1. If we have $\kappa_N < \frac{1}{2}$, then

$$\sum_{m=1}^N \|f_m^\star - f_m\|_2 \leq \frac{2\max\{\frac{1}{A_1}, \frac{1}{A_2} \ldots \frac{1}{A_N}\}\delta}{1 - 2\kappa_N}.$$

Proof. First, we set $z_m = f_m^\star - f_m$, for $1 \leq m \leq N$. Since Φ_m is a frame with frame bound (A_m, B_m) for each $m \in \{1, 2, \ldots, N\}$, thus

$$\begin{aligned}\sum_{m=1}^N \|f_m^\star - f_m\|_2 &\leq \max\{\frac{1}{A_1}, \frac{1}{A_2}, \ldots, \frac{1}{A_N}\} \sum_{m=1}^N \|\Phi_m^*(f_m^\star - f_m)\|_2 \\ &= \max\{\frac{1}{A_1}, \frac{1}{A_2}, \ldots, \frac{1}{A_N}\}\mathbb{T},\end{aligned}$$

where we put $\sum_{i=1}^N \|\Phi_m^*(z_m)\|_1 := \mathbb{T}$.

We observe that $P_K(\sum_{m=1}^N f_m^\star) = P_K(\sum_{i=1}^N f_m) = P_K f$, this leads to

$$\sum_{i=1}^N z_m \in \mathcal{H}_M. \tag{5.7}$$

By (5.7) and triangle inequality, we have

$$\sum_{m=1}^N \|\mathbb{1}_{\Lambda_m}\Phi_m^* z_m\|_1 \leq \sum_{m=1}^N \|\mathbb{1}_{\Lambda_m}\Phi_m^* P_K z_m\|_1 + \sum_{m=1}^N \|\mathbb{1}_{\Lambda_m}\Phi_m^* P_M z_m\|_1 \leq \kappa_N \mathbb{T}. \tag{5.8}$$

Thus, we obtain

$$\begin{aligned}\mathbb{T} &= \sum_{m=1}^{N} \|\mathbb{1}_{\Lambda_m}\Phi_m^* z_m\|_1 + \sum_{m=1}^{N} \|\mathbb{1}_{\Lambda_m^c}\Phi_m^*(f_m^\star - f_m)\|_1 \\ &\overset{\text{By (5.8)}}{\leq} \kappa_N \mathbb{T} + \sum_{m=1}^{N} \|\mathbb{1}_{\Lambda_m^c}\Phi_m^* f_m^\star\|_1 + \delta \\ &= \kappa_N \mathbb{T} + \sum_{i=1}^{N} (\|\Phi_m^* f_m^\star\|_1 - \|\mathbb{1}_{\Lambda_m}\Phi_m^* f_m^\star\|_1) + \delta. \end{aligned} \tag{5.9}$$

We note that $(f_1^\star, f_2^\star, \ldots, f_N^\star)$ is a minimizer of Algorithm 5.1. Thus

$$\sum_{m=1}^{N} \|\Phi_m^* f_m^\star\|_1 \leq \sum_{m=1}^{N} \|\Phi_m^* f_m\|_1. \tag{5.10}$$

Using (5.8), (5.9), (5.10) and triangle inequality, we have

$$\begin{aligned}\mathbb{T} &\leq \kappa_N \mathbb{T} + \sum_{i=1}^{N} \|\Phi_m^* f_m\| + \sum_{i=1}^{N} (\|\mathbb{1}_{\Lambda_m}\Phi_m^* z_m\|_1 - \|\mathbb{1}_{\Lambda_m}\Phi_m^* f_m\|_1) + \delta \\ &\leq \kappa_N \mathbb{T} + \sum_{i=1}^{N} \|\mathbb{1}_{\Lambda_m}\Phi_m^* z_m\|_1 + 2\delta \\ &\leq 2\kappa_N \mathbb{T} + 2\delta. \end{aligned}$$

Thus, we finally obtain

$$\mathbb{T} \leq \frac{2\delta}{1 - 2\kappa_N}.$$

This concludes the claim. ∎

For real world images, geometric constituents of the image f can be supported at different places. We often deal with the case in which a component does not have missing values. This appears more clearly from the following remark.

Remark 5.5 For fixed $i \in \{1, 2, \ldots, N\}$ if there is no missing at component f_i, the definition of the joint concentration is modified corresponding to $P_K f_i = f_i, P_M f_i = 0$, i.e.,

$$\kappa_N = \sup_{\substack{\sum_{n=1}^{N} f_N \in \mathcal{H}_M}} \frac{\|\mathbb{1}_{\Lambda_i}\Phi_i^* f_i\|_1 + \sum_{m \neq i} \left(\|\mathbb{1}_{\Lambda_m}\Phi_m^* P_K f_m\|_1 + \|\mathbb{1}_{\Lambda_m}\Phi_m^* P_M f_m\|_1 \right)}{\|\Phi_1^* f_1\|_1 + \cdots + \|\Phi_N^* f_N\|_1},$$

$$\kappa_N^{sep} = \sup_{\substack{\sum_{n=1}^{N} f_N \in \mathcal{H}_M}} \frac{\|\mathbb{1}_{\Lambda_1}\Phi_i^* f_i\|_1 + \sum_{m \neq i} \|\mathbb{1}_{\Lambda_m}\Phi_m^* P_K f_m\|_1}{\|\Phi_1^* f_1\|_1 + \cdots + \|\Phi_N^* f_N\|_1},$$

$$\kappa_N^{inp} = \sup_{(f_1, f_2, \ldots, f_N)} \frac{\sum_{m \neq i} \|\mathbb{1}_{\Lambda_N}\Phi_N^* P_M f_N\|_1}{\|\Phi_1^* f_1\|_1 + \cdots + \|\Phi_N^* f_N\|_1}.$$

And similar modification if there are more components without missing parts. ◊

5.2.2 Cluster Coherence Analysis

Although Proposition 5.4 ensures the success of Algorithm 5.1, it is not obvious and may be difficult to verify when the bound is achieved. This raises a need to create a new tool to analyze the bound in practice. For this purpose, the notion of cluster coherence was first introduced in [DK13] to replace the notion of joint concentration, it was then followed by many authors [GK14; KKZ14; KDJ20; DLK22]. There, the cluster was defined by

$$\mu_c(\Lambda, \Phi_1; \Phi_2) := \max_{j\in J} \sum_{i\in\Lambda} |\langle \phi_{1i}, \phi_{2j}\rangle|.$$

For our analysis, we optimize the definition in [DK13] by putting the sum inside the inner product to make the cluster coherence smaller which therefore offers more advantages in proving the success of the proposed algorithm. We also extend it to the case of general frames instead of Parseval frames.

Definition 5.6 Given two frames $\Phi_1 = (\Phi_{1i})_{i\in I}$ and $\Phi_2 = (\Phi_{2j})_{j\in J}$. Then the cluster coherence $\mu_c(\Lambda, \Phi_1; \Phi_2)$ of Φ_1 and Φ_2 with respect to the index set $\Lambda \subset I$ is defined by

$$\mu_c(\Lambda, \Phi_1; \Phi_2) := \max_{j\in J} |\langle \sum_{i\in\Lambda} \phi_{1i}, \phi_{2j}\rangle|$$

and the cluster coherence associated with missing subspace

$$\mu_c(\Lambda, P_M\Phi_1; P_M\Phi_2) := \max_{j\in J} |\langle \sum_{i\in\Lambda} P_M\phi_{1i}, P_M\phi_{2j}\rangle|.$$

Obviously, by triangle inequality we have

$$\max_{j\in J} \left|\langle \sum_{i\in\Lambda} \phi_{1i}, \phi_{2j}\rangle\right| \le \max_{j\in J} \sum_{i\in\Lambda} |\langle \phi_{1i}, \phi_{2j}\rangle|,$$

and

$$\max_{j\in J} \left|\langle \sum_{i\in\Lambda} P_M\phi_{1i}, P_M\phi_{2j}\rangle\right| \le \max_{j\in J} \sum_{i\in\Lambda} |\langle P_M\phi_{1i}, P_M\phi_{2j}\rangle|.$$

To derive a new theoretical guarantee that is useful in practice, our goal is to bound the joint concentration from above by the cluster coherence. For this, we use the following lemma.

Lemma 5.7 *Consider N frames $\Phi_1, \Phi_2, \ldots, \Phi_N$ associated with index sets $\Lambda_1, \Lambda_2, \ldots, \Lambda_N$, respectively. The followings hold*

(i)

$$\kappa_N^{sep} \le \max_{1\le m\le N} \inf_{\Phi_m^d \in \mathbb{D}_{\Phi_m}} \sum_{\substack{n\neq m \\ 1\le n\le N}} \mu_c(\Lambda_n, P_K\Phi_n; \Phi_m^d) \le \mu_{c,N}^{sep},$$

where

$$\mu_{c,N}^{sep} := \max_{1\le m\le N} \inf_{\Phi_m^d\in\mathbb{D}_{\Phi_m}} \sum_{\substack{n\neq m\\ 1\le n\le N}} \Big(\mu_c(\Lambda_n,\Phi_n;\Phi_m^d)+\mu_c(\Lambda_n,P_M\Phi_n;\Phi_m^d)\Big).$$

(ii)

$$\kappa_N^{inp} \le \mu_{c,N}^{inp} := \max_{1\le m\le N} \inf_{\Phi_m^d\in\mathbb{D}_{\Phi_m}} \mu_c(\Lambda_m,P_M\Phi_m;\Phi_m^d).$$

(iii)

$$\begin{aligned}\kappa_N &\le \mu_{c,N} := \max_{1\le m\le N}\Big(\mu_c(\Lambda_m,P_M\Phi_m;\Phi_m^d)+\sum_{\substack{n\neq m\\ 1\le n\le N}}\mu_c(\Lambda_n,P_K\Phi_n;\Phi_m^d)\Big)\\ &\le \mu_{c,N}^{sep}+\mu_{c,N}^{inp}.\end{aligned}$$

Proof. (i) First, we set $\alpha_m := \Phi_m^* f_m$, and $\alpha_m = (\alpha_{m1},\alpha_{m2},\cdots,) \in l_2, \forall m \in \{1,2,\dots N\}$. This leads to $f_m = \Phi_m^d\Phi_m^* f_m = \Phi_m^d\alpha_m$. Since $\sum_{m=1}^N f_m \in \mathcal{H}_M$ yields $\sum_{m=1}^N P_K f_n = 0$. Thus, we have

$$\begin{aligned}\|\mathbb{1}_{\Lambda_m}\Phi_m^* P_K f_m\|_1 &= \|\sum_{n\neq m}\mathbb{1}_{\Lambda_m}\Phi_m^* P_K f_n\|_1 = \|\sum_{n\neq m}\mathbb{1}_{\Lambda_m}\Phi_m^* P_K\Phi_n^d\alpha_n\|_1\\ &\le \sum_{n\neq m}\sum_{i\in\Lambda_m}\Big(\sum_j |\langle P_K\Phi_{mi},\Phi_{nj}^d\rangle||\alpha_{nj}|\Big)\\ &= \sum_{n\neq m}\sum_j\Big(\sum_{i\in\Lambda_m}|\langle P_K\Phi_{mi},\Phi_{nj}^d\rangle|\Big)|\alpha_{nj}|\\ &\le \sum_{n\neq m}\mu_c(\Lambda_m,\Phi_m;\Phi_n^d)\|\alpha_n\|_1 = \sum_{n\neq m}\mu_c(\Lambda_m,\Phi_m;\Phi_n^d)\|\Phi_n^* f_n\|_1.\end{aligned}$$

Thus,

$$\sum_{m=1}^N \|\mathbb{1}_{\Lambda_m}\Phi_m^* P_K f_m\|_1 \le \max_{1\le m\le N}\Big\{\sum_{n\neq m}\mu_c(\Lambda_m,\Phi_m;\Phi_n^d)\Big\}\cdot\sum_{m=1}^N\|\Phi_m^* f_m\|_1.$$

This finishes the proof.

(ii) We set $\alpha_m := \Phi_m^* f_m$ for each $m \in \{1,2,\dots,N\}$. By dual frame property, we have $f_m = \Phi_m^d\Phi_m^* f_m = \Phi_m^d\alpha_m,\ m = 1,2\dots,N$. Thus, we obtain

$$\begin{aligned}\|\mathbb{1}_{\Lambda_m}\Phi_m^* P_M f_m\|_1 &= \|\mathbb{1}_{\Lambda_m}\Phi_m^* P_M\Phi_m^d\Phi_m^* f_m\|_1 = \|\mathbb{1}_{\Lambda_m}(P_M\Phi_m)^*\Phi_m^d\alpha_m\|_1\\ &\le \sum_{i\in\Lambda_m}\Big(\sum_j|\langle P_M\Phi_{mi},\Phi_{mj}^d\rangle||(\alpha_m)_j|\Big)\\ &= \sum_j\Big(\sum_{i\in\Lambda_m}|\langle P_M\Phi_{mi},\Phi_{mj}^d\rangle|\Big)|(\alpha_m)_j|\\ &\le \mu_c(\Lambda_m,P_M\Phi_m;\Phi_m^d)\|\alpha_m\|_1 = \mu_c(\Lambda_m,P_M\Phi_m;\Phi_m^d)\|\Phi_m^* f_m\|_1,\end{aligned}$$

where $\Phi_m = \{\Phi_{mj}\}_{j\in I_m}, \alpha_n = (\alpha_{n1}, \alpha_{n2}, \dots ...) \in l_2$. Thus, we have

$$\sum_{1\le m\le N} \|\mathbb{1}_{\Lambda_m}\Phi_m^* P_M f_m\|_1 \le \max_{1\le m\le N} \mu_c(\Lambda_m, P_M\Phi_m; \Phi_m^d) \cdot \sum_{1\le m\le N} \|\Phi_m^* f_m\|_1.$$

This concludes

$$\kappa_N^{inp} \le \max_{1\le m\le N} \mu_c(\Lambda_m, P_M\Phi_m; \Phi_m^d).$$

■

(iii) Similar approach to (i) and (ii) we obtain

$$\kappa_N \le \max_{1\le m\le N} \Big(\mu_c(\Lambda_m, P_M\Phi_m; \Phi_m^d) + \sum_{\substack{n\ne m\\ 1\le n\le N}} \mu_c(\Lambda_n, P_K\Phi_n; \Phi_m^d)\Big).$$

We now present our first theoretical guarantee for the success of Algorithm 5.1 based on the notion of cluster coherence.

Theorem 5.8 *Let $\Phi_1, \Phi_2, \dots, \Phi_N$ be a set of frames with pairs of frame bounds (A_1, B_1), $(A_2, B_2), \cdots, (A_N, B_N)$, respectively. For $\delta_1, \delta_2, \dots, \delta_N > 0$, we fix $\delta = \sum_{m=1}^N \delta_m$, and suppose that $f \in \mathcal{H}$ can be decomposed as $f = \sum_{m=1}^N f_m$ so that each component $f_1, f_2, \dots, f_N$ is $\delta_1, \delta_2, \dots, \delta_N$−relatively sparse in $\Phi_1, \Phi_2, \dots, \Phi_N$, respectively. Let $(f_1^\star, f_2^\star, \dots, f_N^\star)$ solve Algorithm 5.1. If we have $\mu_{c,N} < \frac{1}{2}$, then*

$$\sum_{m=1}^N \|f_m^\star - f_m\|_2 \le \frac{2\max\{\frac{1}{A_1}, \frac{1}{A_2}, \dots, \frac{1}{A_N}\}\delta}{1 - 2\mu_{c,N}}, \tag{5.11}$$

where $\mu_{c,N} \le \mu_{c,N}^{inp} + \mu_{c,N}^{sep}$ defined in Lemma 5.7.

Proof. The claim holds by Proposition 5.4 and Lemma 5.7 (iii). ■

Let us now discuss, in particular, some special cases of the theoretical guarantee. If $\Phi_1, \Phi_2, \cdots, \Phi_N$ form Parseval frames we obtain

$$\mu_{c,N} \le \max_{1\le m\le N} \Big(\mu_c(\Lambda_m, P_M\Phi_m; \Phi_m) + \sum_{\substack{n\ne m\\ 1\le n\le N}} \mu_c(\Lambda_n, P_K\Phi_n; \Phi_m)\Big)$$

$$\le \max_{1\le m\le N} \Big(\mu_c(\Lambda_m, P_M\Phi_m; \Phi_m) + \sum_{\substack{n\ne m\\ 1\le n\le N}} \mu_c(\Lambda_n, P_M\Phi_n; \Phi_m) + \mu_c(\Lambda_n, \Phi_n; \Phi_m)\Big). \tag{5.12}$$

Here we exploit the fact that $\Phi_m^d \in \mathbb{D}_{\Phi_m}$, $1 \le m \le N$. Now in case $m = 1$ we have $\mu_{c,1} \le \mu_c(\Lambda_1, P_M\Phi_1; \Phi_1)$. Thus, choosing a correct set of significant coefficients which provides small cluster sparsity and cluster coherence guarantees the success of inpainting a single component image which was studied in [GK14; KKZ14; KDJ20]. In addition, in case $m = 2, P_M = 0$ both small $\delta, \mu_{c,2}$ guarantee the success of two-component image separation as studied in [DK13; DG21], or $m = 2$ for the simultaneous separation and inpainting [DLK22]. To gain a better understanding, we present the following remark.

Remark 5.9 By (5.11), we say that we can separate f_m from f_n if the cluster coherence $\inf_{\Phi_m^d \in \mathbb{D}_{\Phi_m}, \Phi_n^d \in \mathbb{D}_{\Phi_n}} \max\{\mu_c(\Lambda_m, \Phi_m; \Phi_n^d), \mu_c(\Lambda_n, \Phi_n; \Phi_m^d)\}$ and $\delta_m + \delta_n$ are sufficiently small and we can inpaint the component f_n if both $\mu_c(\Lambda_n, P_M\Phi_n; \Phi_n^d)$ and δ_n are sufficiently small. In that sense, a few remarks are made as follows.

1. We can separate each pair of f_m and f_n, $1 \leq m \neq n \leq N$, if and only if we can separate all these N components from $f = f_1 + f_2 + \cdots + f_N$.

2. We can inpaint each single componentf_n, $1 \leq n \leq N$, if and only if we can inpaint $f = f_1 + f_2 + \cdots + f_N$.

3. We can separate f_m from f_n and inpaint each of them if and only if we can simultaneously separate and inpaint these two components.

4. We can simultaneously separate and inpaint N components if and only if we can simultaneously separate and inpaint each pair of N components.

5. For the case f_i has no missing part as referred in Remark 5.5, the cluster in (5.11) is modified with the replacement of $P_M\Phi_i, P_K\Phi_i$ by 0 and Φ_i, respectively.

$\Diamond$

5.3 l_1 Optimization of Image Denoising

In practice, the original signal f often contains noise, this therefore requires an adaption of Algorithm 5.1. For constrained optimization approach, we assume that we know $P_K f + \eta$, where noise $\eta \in \mathcal{H}_K$ such that there exists m_0, $\|\Phi_{m_0}^* \eta\|_1 < \epsilon$, for small ϵ. Our goal now is to reconstruct f. In this situation, we can modify Algorithm 5.1 by

$$(f_1^\star, f_2^\star, \ldots, f_N^\star) = \underset{(f_1,\ldots,f_N)}{\operatorname{argmin}} \|\Phi_1^* f_1\|_1 + \|\Phi_2^* f_2\|_1 + \ldots \|\Phi_N^* f_N\|_1,$$
$$\text{subject to} \quad P_K(f_1 + f_2 + \cdots + f_N) = P_K f + \eta.$$

For this, we can easily verify the following bound up to a constant similarly as in (5.11) by modifying $z_{m_0} = f_{m_0} - f_{m_0} - \eta$,

$$\sum_{m=1}^{N} \|f_m^\star - f_m\|_2 \leq \frac{2\delta + 2\kappa_N \epsilon}{1 - 2\kappa_N} \leq \frac{2\delta + 2\mu_{c,N}\epsilon}{1 - 2\mu_{c,N}}.$$

Another idea to solve this problem is to use a regularization term. In this approach, we propose the following algorithm to solve an unconstrained minimization problem using a regularizer $\mathcal{R}(x) > 0, \forall x \in \mathcal{H}, \lambda = const > 0$. Here the constant λ controls the trade-off between the l_1 norm minimization of analysis coefficients and the prior information. We will later prove that separation, inpainting, and denoising can be all included as one unified task by the following algorithm.

Algorithm 5.10 (Unconstrained optimization)

Input: observed image f, a constant $\lambda > 0$, a regularizer $\mathcal{R}$, N Parseval frames $\{\Phi_1\}_{i\in I_1}, \ldots, \{\Phi_N\}_{j\in I_N}$.

Compute: $(f_1^\star, f_2^\star, \ldots, f_N^\star)$, where

$$\begin{aligned}(f_1^\star, f_2^\star, \ldots, f_N^\star) &= \underset{(f_1,\ldots,f_N)}{\operatorname{argmin}} \|\Phi_1^* f_1\|_1 + \|\Phi_2^* f_2\|_1 + \ldots \|\Phi_N^* f_N\|_1 + \\ &\quad \lambda\mathcal{R}(P_K(f_1 + f_2 + \cdots + f_N) - P_K f).\end{aligned}$$

Output: recovered components $f_1^\star, f_2^\star, \ldots, f_N^\star$.

For a special case of our algorithm, one without theoretical analysis proposed in [KL12b] which used an L_2 regularization term

$$(f_1^\star, f_2^\star) = \underset{f_1,f_2}{\operatorname{argmin}} \|\Phi_1^* f_1\|_1 + \|\Phi_2^* f_2\|_1 + \lambda\|f - f_1 - f_2\|_2^2.$$

This empirical work using Basic pursuit exhibited very good results for separating point-like and curvelike parts. By utilizing the notions of cluster coherence, we also have a theoretical guarantee for the success of Algorithm 5.10 by the following result.

Theorem 5.11 *Let $\Phi_1, \Phi_2, \ldots, \Phi_N$ be a set frames with frame bounds $(A_1, B_1), (A_2, B_2), \cdots, (A_N, B_N)$, respectively. For $\delta_1, \delta_2, \ldots, \delta_N > 0$, fix $\delta = \sum_{m=1}^N \delta_m$, and suppose that $f \in \mathcal{H}$ can be decomposed as $f = \sum_{m=1}^N f_m$ so that each component $f_1, f_2, \ldots, f_N$ is $\delta_1, \delta_2, \ldots, \delta_N$-relatively sparse in $\Phi_1, \Phi_2, \ldots, \Phi_N$, respectively. We assume that $\Lambda_1, \Lambda_2, \ldots, \Lambda_N$ satisfy*

$$\sum_{1\le m\le N} \|\mathbb{1}_{\Lambda_m}\Phi_m z\|_1 \le \frac{\lambda}{2}\mathcal{R}(z),\ \forall z \in \mathcal{H}, \tag{5.13}$$

and $\mu_{c,N} < \frac{1}{2}$. Let $(f_1^\star, f_2^\star, \ldots, f_N^\star)$ solve Algorithm 5.10, then we have

$$\sum_{m=1}^N \|f_m^\star - f_m\|_2 \le \frac{2\max\{\frac{1}{A_1}, \frac{1}{A_2}, \ldots, \frac{1}{A_N}\}\delta}{1 - 2\mu_{c,N}}.$$

Proof. For $1 \le m, n \le N$, we set $z_m = f_m^\star - f_m, z = \sum_{m=1}^N z_m$ and $\alpha_m := \Phi_m^* z_m$. For $\Phi_m^d \in \mathbb{D}_\Phi$, we have

$$\Phi_m^d \alpha_m = \Phi_m^d \Phi_m^* z_m = z_m, \tag{5.14}$$

and

$$\begin{aligned}\sum_{m=1}^N \|f_m^\star - f_m\|_2 &\le \max\{\frac{1}{A_1}, \frac{1}{A_2}, \ldots, \frac{1}{A_N}\} \sum_{m=1}^N \|\Phi_m^*(f_m^\star - f_m)\|_2 \\ &\le \max\{\frac{1}{A_1}, \frac{1}{A_2}, \ldots, \frac{1}{A_N}\}\mathbb{T},\end{aligned}$$

where we put $\sum_{i=1}^N \|\Phi_m^*(z_m)\|_1 := \mathbb{T}$.

For each $m \in \{1, 2, \ldots, N\}$, we observe that

$$\begin{aligned}\|\mathbb{1}_{\Lambda_m}\Phi_m^* z_m\|_1 &\le \|\mathbb{1}_{\Lambda_m}\Phi_m^* P_K z_m\|_1 + \|\mathbb{1}_{\Lambda_m}\Phi_m^* P_M z_m\|_1 \\ &\le \sum_{n\neq m} \|\mathbb{1}_{\Lambda_m}\Phi_m^* P_K z_n\|_1 + \|\mathbb{1}_{\Lambda_m}\Phi_m^* P_K z\|_1 + \|\mathbb{1}_{\Lambda_m}\Phi_m^* P_M z_m\|_1.\end{aligned} \tag{5.15}$$

By (5.14), we have

$$\begin{aligned}\|\mathbb{1}_{\Lambda_m}\Phi_m^* P_K z_n\|_1 &= \|\mathbb{1}_{\Lambda_m}\Phi_m^* P_K \Phi_n^d \alpha_n\|_1 = \|\mathbb{1}_{\Lambda_m}(P_K\Phi_m)^* \Phi_n^d \alpha_n\|_1 \\ &\le \sum_{i\in\Lambda_m} \Big(\sum_j |\langle P_K\Phi_{mi}, \Phi_{nj}^d\rangle| |(\alpha_n)_j| \Big) \\ &= \sum_j \Big(\sum_{i\in\Lambda_m} |\langle P_K\Phi_{mi}, \Phi_{nj}^d\rangle| \Big) |(\alpha_n)_j| \\ &\le \mu_c(\Lambda_m, P_K\Phi_m; \Phi_n^d)\|\alpha_n\|_1 = \mu_c(\Lambda_m, P_K\Phi_m; \Phi_n^d)\|\Phi_n^* z_n\|_1.\end{aligned} \tag{5.16}$$

Similarly, we have

$$\|\mathbb{1}_{\Lambda_m}\Phi_m^* P_M z_m\|_1 \le \mu_c(\Lambda_m, P_M\Phi_m; \Phi_m^d)\|\Phi_m^* z_m\|_1. \tag{5.17}$$

Combining (5.15), (5.16) and (5.17), we obtain

$$\begin{aligned}\sum_{m=1}^N \|\mathbb{1}_{\Lambda_m}\Phi_m^* z_m\|_1 \le \sum_{m=1}^N \Big(\sum_{n\neq m} \mu_c(\Lambda_m, P_K\Phi_m; \Phi_n^d)\|\Phi_n^* z_n\|_1 + \\ \mu_c(\Lambda_m, P_M\Phi_m; \Phi_m^d)\|\Phi_m^* z_m\|_1 \Big) + \sum_{m=1}^N \|\mathbb{1}_{\Lambda_m}\Phi_m^* P_K z\|_1 \\ \le \max_n \Big(\mu_c(\Lambda_m, P_M\Phi_m; \Phi_m^d) + \sum_{m\neq n} \mu_c(\Lambda_m, P_K\Phi_m; \Phi_n^d) \Big) \mathbb{T} + \\ \sum_{m=1}^N \|\mathbb{1}_{\Lambda_m}\Phi_m^* P_K z\|_1.\end{aligned} \tag{5.18}$$

By triangle inequality, we have

$$\begin{aligned}\mathbb{T} &= \sum_{m=1}^N \|\mathbb{1}_{\Lambda_m}\Phi_m^* z_m\|_1 + \sum_{m=1}^N \|\mathbb{1}_{\Lambda_m^c}\Phi_m^*(f_m^\star - f_m)\|_1 \\ &\le \sum_{m=1}^N \|\mathbb{1}_{\Lambda_m}\Phi_m^* z_m\|_1 + \sum_{m=1}^N \|\mathbb{1}_{\Lambda_m^c}\Phi_m^* f_m^\star\|_1 + \delta \\ &= \sum_{m=1}^N \|\mathbb{1}_{\Lambda_m}\Phi_m^* z_m\|_1 + \sum_{m=1}^N \|\Phi_m^* f_m^\star\|_1 - \sum_{m=1}^N \|\mathbb{1}_{\Lambda_m}\Phi_m^* f_m^\star\|_1 + \delta \\ &\le \sum_{m=1}^N \|\mathbb{1}_{\Lambda_m}\Phi_m^* z_m\|_1 + \sum_{m=1}^N \|\Phi_m^* f_m^\star\|_1 +\end{aligned}$$

$$\sum_{m=1}^{N} \left(\|\mathbb{1}_{\Lambda_m} \Phi_m^* z_m\|_1 - \|\mathbb{1}_{\Lambda_m} \Phi_m^* f_m\|_1 \right) + \delta. \tag{5.19}$$

We note that $(f_1^\star, f_2^\star, \ldots, f_N^\star)$ is a minimizer of Algorithm 5.10. Thus

$$\sum_{m=1}^{N} \|\Phi_m^* f_m^\star\|_1 \leq \sum_{m=1}^{N} \|\Phi_m^* f_m\|_1 - \lambda \|P_K z\|_1. \tag{5.20}$$

By (5.18), (5.19), (5.20), and (5.13), we have

$$\begin{aligned}
\mathbb{T} &\leq 2 \sum_{m=1}^{N} \|\mathbb{1}_{\Lambda_m} \Phi_m^* z_m\|_1 - \lambda \|P_K z\|_1 + 2\delta \\
&\leq 2 \max_n \left(\mu_c(\Lambda_m, P_M \Phi_m; \Phi_m^d) + \sum_{m \neq n} \mu_c(\Lambda_m, P_K \Phi_m; \Phi_n^d) \right) \mathbb{T} + \\
&\quad \left(2 \sum_{m=1}^{N} \|\mathbb{1}_{\Lambda_m} \Phi_m^* P_K z\|_1 - \lambda \|P_K z\|_1 \right) + 2\delta \\
&\leq 2 \max_n \left(\mu_c(\Lambda_m, P_M \Phi_m; \Phi_m^d) + \sum_{m \neq n} \mu_c(\Lambda_m, P_K \Phi_m; \Phi_n^d) \right) \mathbb{T} + 2\delta.
\end{aligned}$$

Thus, we finally obtain

$$\mathbb{T} \leq \frac{2\delta}{1 - 2\mu_{c,N}}.$$

This concludes the claim. ∎

In our analysis, we will later provide an analysis of Algorithm 5.10 with $\mathcal{R}(x) = \|x\|_1$ for separating points from curves and texture while inpainting the missing parts of curves and texture in Section 5.4. For this, we have the following corollary.

Corollary 5.12 *Let $\Phi_1, \Phi_2, \ldots, \Phi_N$ be a set of Parseval frames. For $\delta_1, \delta_2, \ldots, \delta_N > 0$, we fix $\delta = \sum_{m=1}^{N} \delta_m$, and suppose that $f \in L^2(\mathbb{R}^2)$ can be decomposed as $x = \sum_{m=1}^{N} f_m$ so that each component $f_1, f_2, \ldots, f_N$ is $\delta_1, \delta_2, \ldots, \delta_N$−relatively sparse in $\Phi_1, \Phi_2, \ldots, \Phi_N$, respectively. Let $(f_1^\star, f_2^\star, \ldots, f_N^\star)$ solve Algorithm 5.10 with $\mathcal{R}(x) = \|x\|_1$, and we assume that $\Lambda_1, \Lambda_2, \ldots, \Lambda_N$ satisfy*

$$\sum_{1 \leq m \leq N} \|\mathbb{1}_{\Lambda_m} \Phi_m z\|_1 \leq \frac{\lambda}{2} \|z\|_1, \ \forall z \in L^2(\mathbb{R}^2). \tag{5.21}$$

If $\mu_{c,N} < \frac{1}{2}$, then we have

$$\sum_{m=1}^{N} \|f_m^\star - f_m\|_2 \leq \frac{2\delta}{1 - 2\mu_{c,N}}.$$

5.4 Inpainting and Denoising of Multiple Component Images in Applications

In image processing, the performance of existing algorithms is effective in different scenarios depending on the geometry of underlying components. Natural images may contain more than two geometric structures, for instance, astronomical images are often composed of points, curves, and texture. One interesting question in application is how to inpaint an image which is composed of multiple components the known part of the groundtruth image $f \in \mathcal{H} = L^2(\mathbb{R}^2)$. Mathematically, we assume that we have the following decomposition

$$f = \mathcal{P} + \mathcal{C} + \mathcal{T},$$

where f is the signal of our interest, $\mathcal{P}, \mathcal{C}$, and $\mathcal{T}$ are three underlying components that are unknown to us. In addition, we assume that $\mathcal{H}$ can be decomposed into the known and unknown subspace by $\mathcal{H} = \mathcal{H}_K \oplus \mathcal{H}_M$. Our goal is to recover $\mathcal{P}, \mathcal{C}$ and $\mathcal{T}$ with only the known part $P_k f$.

5.4.1 Model of Components

In this subsection, we introduce models of pointlike, curvelike, and texture structures which we aim to recover. In our analysis, the model of texture is motivated from [DLK22] with $s = 1$. We modified the model of texture for our need as follows.

Definition 5.13 Let $g \in L^2(\mathbb{R}^2)$ be a window with $\hat{g} \in C^\infty(\mathbb{R}^2)$, and frequency support $\operatorname{supp} \hat{g} \in [-1, 1]^2$ satisfying the partition of unity condition

$$\sum_{n \in \mathbb{Z}^2} |\hat{g}(\xi + n)|^2 = 1, \quad \xi \in \mathbb{R}^2.$$

Let $I_T \subseteq \mathbb{Z}^2$ be a subset of Fourier elements. A texture is defined by

$$\mathcal{T}(x) = \sum_{n \in I_T} d_n g(x) e^{2\pi i x^\top n},$$

where $(d_n)_{n \in \mathbb{Z}^2}$ denotes a bounded sequence of complex numbers.

Point-like structure $\mathcal{P}$ is modeled as

$$\mathcal{P}(x) = \sum_{1}^{K} |x - x_i|^{-3/2}.$$

Since it is certainly impossible to reconstruct point singularities in the missing part, so we assume that $x_i \in \mathcal{H}_K, \forall i = 1, 2, \ldots, K$.

Curvelike structure is modeled as a line distribution $w\mathcal{L}$ acting on *Schwartz functions* by

$$\langle w\mathcal{L}, f \rangle = \int_{-\rho}^{\rho} w(x_1) f(x_1, 0) dx_1, \ f \in \mathcal{S}(\mathbb{R}^2).$$

5.4.2 Sparse Representations

In this section, we focus on tools of harmonic analysis for sparsely approximate each component. In particular, we use the following sparsifying systems which might be best adapted to the geometry of its singularities.

- Gabor tight frames: A tight frame with time-frequency balanced elements.
- Radial wavelets: Bandlimited wavelets which form a Parseval frame of isotropic generating elements.
- Shearlets: A highly directional tight frame with increasingly anisotropic elements at fine scales.

We now fix a constant ϵ satisfying

$$0 < \epsilon < \frac{1}{4}. \tag{5.22}$$

We consider the following Gabor tight frame $\mathbf{G} = \{g_{m,n}(x)\}_{m,n\in\mathbb{Z}^2}$ defined in the frequency domain as

$$\hat{g}_{m,n}(\xi) = \hat{g}(\xi - n)e^{2\pi i\xi^\top \frac{m}{2}}.$$

This system constitutes a tight frame for $L^2(\mathbb{R}^2)$, see [DGM86] for more details. Different from [DLK22] where two conditions on the sparse set of indexes I_T were used, we assume that

$$|I_T^{\pm} \cap \mathcal{A}_j| \leq 2^{(1-\epsilon)j} \quad \text{as } j \to \infty. \tag{5.23}$$

where $I_T^{\pm} = \{n' \in \mathbb{Z}^2 \mid \exists n \in I_T : |n' - n| \leq 1\}$. Roughly speaking, we assume that at every scale j, the number of non-zero Gabor elements with the same position, generating $\mathcal{T}_j$, is not too large. We refer to Fig 5.1 for an illustration.

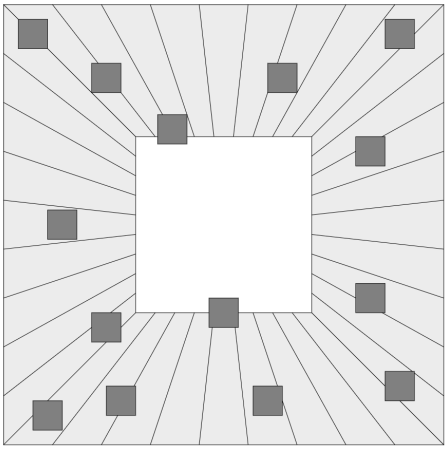

Figure 5.1: Interaction between Gabor elements (black) with wavelet and shearlet elements (gray)

For the construction of wavelets and shearlets, we choose smooth Parseval frames of shearlets [GL13] and a Parseval frame of wavelets which share the same window function.

Let Ξ be a function in $\mathcal{S}(\mathbb{R})$ satisfying $0 \leq \hat{\Xi}(u) \leq 1$ for $u \in \mathbb{R}$, $\hat{\Xi}(u) = 1$ for $u \in [-1/16, 1/16]$ and supp $\hat{\Xi} \subset [-1/8, 1/8]$. Define the *low pass function* $\Theta(\xi)$ and the *corona scaling functions* for $j \in \mathbb{N}$ and $\xi = (\xi_1, \xi_2) \in \mathbb{R}^2$,

$$\hat{\Theta}(\xi) := \hat{\Xi}(\xi_1)\hat{\Xi}(\xi_2),$$

$$W(\xi) := \sqrt{\hat{\Theta}^2(2^{-2}\xi) - \hat{\Theta}^2(\xi)}, \quad W_j(\xi) := W(2^{-2j}\xi).$$

It is easy to see that we have the partition of unity property

$$\hat{\Theta}^2(\xi) + \sum_{j \geq 0} W_j^2(\xi) = 1, \quad \xi \in \mathbb{R}^2. \tag{5.24}$$

The smooth Parseval frame of wavelets $\{\phi_{j,k}\}_{j \in \mathbb{N}_0, k \in \mathbb{Z}^2}$ is defined by

$$\hat{\phi}_{j,k} = 2^{-2j} W_j(\xi) e^{2\pi i 2^{-2j} \xi^\top k}.$$

Next, we use a bump-like function $v \in C^\infty(\mathbb{R})$ to produce the directional scaling feature of the system. Suppose $\text{supp}(v) \subset [-1, 1]$ and $|v(u-1)|^2 + |v(u)|^2 + |v(u+1)|^2 = 1$ for $u \in [-1, 1]$. Define the *horizontal frequency cone* and the *vertical frequency cone*

$$\mathcal{C}_{\text{h}} := \Big\{(\xi_1, \xi_2) \in \mathbb{R}^2 \mid \Big|\frac{\xi_2}{\xi_1}\Big| \leq 1\Big\}$$

and

$$\mathcal{C}_{\text{v}} := \Big\{(\xi_2, \xi_1) \in \mathbb{R}^2 \mid \Big|\frac{\xi_1}{\xi_2}\Big| \leq 1\Big\}.$$

Define the cone functions $V_{\text{h}}, V_{\text{v}}$ by

$$V_{\text{h}}(\xi) := v\Big(\frac{\xi_2}{\xi_1}\Big), \quad V_{\text{v}}(\xi) := v\Big(\frac{\xi_1}{\xi_2}\Big).$$

The *shearing* and *scaling matrix* are defined by

$$A_{\text{h}} := \begin{bmatrix} 2^2 & 0 \\ 0 & 2 \end{bmatrix}, \quad S_{\text{h}} := \begin{bmatrix} 1 & 1 \\ 0 & 1 \end{bmatrix},$$

$$A_{\text{v}} := \begin{bmatrix} 2 & 0 \\ 0 & 2^2 \end{bmatrix}, \quad S_{\text{v}} := \begin{bmatrix} 1 & 0 \\ 1 & 1 \end{bmatrix}.$$

Definition 5.14 The smooth Parseval of shearlets $\Psi = \{\psi'_{j,l,k}\}_{j,l,k}, j \in \mathbb{N}_0, l \in \mathbb{Z}, 0 \leq |l| \leq 2^j, k \in \mathbb{Z}^2, ' \in \{\text{v}, \text{h}\}$ is defined by

$$\hat{\psi}^{\iota}_{j,l,k}(\xi) := 2^{-3j/2} W_j(\xi) V_{\iota}\Big(\xi^T A_{\iota}^{-j} S_{\iota}^{-l}\Big) e^{-2\pi i \xi^T A_{\iota}^{-j} S_{\iota}^{-l} k}, \quad \xi \in \mathbb{R}^2.$$

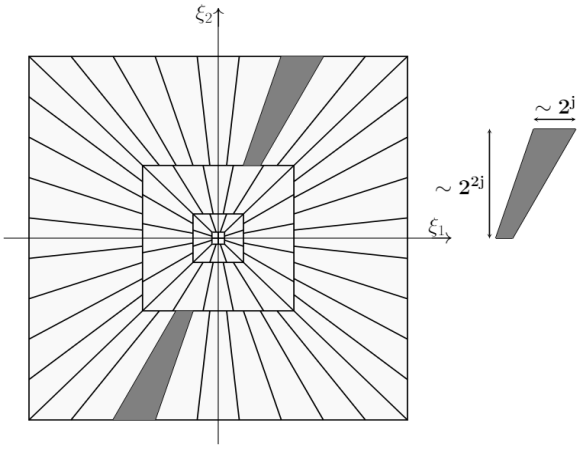

Figure 5.2: Frequency tiling of a cone-adapted shearlet.

For an illustration, the tiling of the frequency domain induced by shearlets is depicted in Fig. 5.2.

5.4.3 Multi-scale Approach

In our analysis, the simultaneous separation and inpainting problem is analyzed at each scale j. To achieve this goal we use the following class of *frequency filters* F_j

$$\hat{F}_j(\xi) := W_j(\xi) = W(\xi/2^{2j}), \quad \forall j \geq 0, \xi \in \mathbb{R}^2,$$

and in low frequency part

$$\hat{F}_{low}(\xi) := \Theta(\xi), \quad \xi \in \mathbb{R}^2.$$

By using these filters, we can decompose f into small pieces by $f_{(j)} = F_j * f,\ j \geq 0$ and $f_{low} = F_{low} * f$. Then (5.24) allows us to reconstruct f by

$$f = F_{low} * f_{low} + \sum_{j \geq 0} F_j * f_{(j)}. \tag{5.25}$$

For multi-scale separation and inpainting, we intend to apply Algorithm 5.1, Algorithm 5.10 for each sub-image $f_{(j)}$, then the whole image is reconstructed by (5.25). Here we assume that $f_{(j)} = \mathcal{P}_j + w\mathcal{L}_j + \mathcal{T}_j$. In the other words, instead of considering the whole signal we now consider the problem of simultaneous separation and inpainting at each scale. For the theoretical analysis, we assume that the model of missing subspace is chosen at each scale j to be $\mathcal{H}_M = \mathbb{1}_{\mathcal{M}_{h_j}}$ where $\mathcal{M}_{h_j} = \{x = (x_1, x_2) \mid |x_1| \leq h_j\}$ is a horizontal strip domain. This model of missing part was first introduced in [KKZ14] and then also adopted in [GK14; KDJ20]. The orthogonal projection associated with the missing trip is then defined by

$$P_{M,j} = \mathbb{1}_{\{|x_1| \leq h_j\}}.$$

For an illustration, we refer to Fig. 5.3. We now face to the task of reconstructing the sub-image $f_{(j)}$ with the knowledge of $P_{K,j} f_{(j)}$, where $P_{K,j} = 1 - P_{M,j}$.

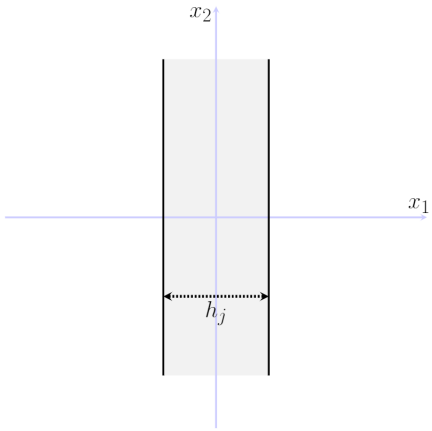

Figure 5.3: Model of the missing trip at scale j.

In addition, we assume that the energy of texture is comparable to point and curvilinear singularities, i.e., $\|\mathcal{P}_j\|_2 \approx \|w\mathcal{L}_j\|_2 \approx \|\mathcal{T}_j\|_2$. This is due to the fact that the problem becomes trivial in the case of different levels of energy. Actually, we can derive similar theoretical results by our approach if the energy of each component has a lower bound at each scale. However, for the sake of simplicity, we assume that $\|\mathcal{T}_j\|_2 \approx 2^{2j}$ since we have $\|\mathcal{P}_j\|_2 \approx \|w\mathcal{L}_j\|_2 \approx 2^{2j}$. These energy balancing conditions make the problem of geometric separation challenging at every scale.

5.4.4 Main Results

Our analysis is based on the fact that the geometric property underlying each component is often encoded in the frame coefficients. In addition, important coefficients cluster geometrically in phase space by microlocal analysis. This therefore allows us to separate components based on the machinery in Theorem 5.8 and 5.11. Thus, the correct choice of clusters plays a central role in our analysis. We aim to define the optimal set of significant coefficients to derive good cluster sparsity as well as cluster coherence. By Theorem 5.8 and 5.11, if clusters are chosen large we might have very a good approximation but the cluster coherence will be big which leads to loose control of the L_2 errors.

We now define clusters for wavelet, shearlet, and Gabor systems. First the cluster of significant wavelet coefficients is defined by

$$\Lambda_{1,j}^{\pm} := \Lambda_{1,j-1} \cup \Lambda_{1,j} \cup \Lambda_{1,j+1}, \ \forall j \geq 1,$$

where $\Lambda_{1,j} = \{p \mid p \in \mathbb{Z}^2, |p| \leq 2^{\epsilon j}\}$. For the line singularity $w\mathcal{L}_j$, we define the set of significant coefficients of shearlet system by

$$\Lambda_{2,j}^{\pm} := \Lambda_{2,j-1} \cup \Lambda_{2,j} \cup \Lambda_{2,j+1}, \quad \forall j \geq 2,$$

where $\Lambda_{2,j} := \left\{(j,l,k;\mathrm{v}) \mid |l| \leq 1, k = (k_1,k_2) \in \mathbb{Z}^2, |k_2 - lk_1| \leq 2^{\epsilon j}\right\}$. We define the cluster for texture at scale j to be

$$\Lambda_{3,j}^{\pm} := \left(\mathbb{Z}^2 \cap B(0,M_j)\right) \times \left(I_T^{\pm} \cap \mathcal{A}_j\right),$$

where $I_T^{\pm} = \{n' \in \mathbb{Z}^2 \mid \exists n \in I_T : |n' - n| \leq 1\}$, $M_j := 2^{\epsilon j/6}$ and $B(0,r)$ denotes the closed l_2 ball around the origin in $\mathbb{R}^2$. Here we remark that the index set $\Lambda_{1,j}^{\pm}, \Lambda_{2,j}^{\pm}, \Lambda_{,j}^{\pm}$ were chosen instead of $\Lambda_{1j}, \Lambda_{2,j}, \Lambda_{3,j}$ since there have overlap supports between them and their neighbors.

For later use, let us now introduce some useful notations related to shearlets

$$\begin{aligned}
\langle |x| \rangle &:= (1 + |x|^2)^{1/2} \\
\Delta &:= \left\{ (j, l, k; \acute{}) \mid j \geq 0, |l| < 2^j, k \in \mathbb{Z}^2, \acute{} \in \{\mathrm{h}, \mathrm{v}\} \right\} \\
\Delta_j &:= \{(j', k, l; \acute{}) \in \Delta \mid j' = j\}, \quad j \geq 0, \\
\Delta_j^{\pm} &:= \Delta_{j-1} \cup \Delta_j \cup \Delta_{j+1}, \text{ where } \Delta_{-1} = \emptyset.
\end{aligned}$$

By integration by parts and standard arguments, we have the decay estimates of Gabor, wavelet, and shearlet elements by the following lemma.

Lemma 5.15 *For each $N = 1, 2, \ldots$ there exists a constant C_N independent of j such that the followings hold for $j \in \mathbb{N}, m, n, l, k, p \in \mathbb{Z}, |l| \leq 2^j$.*

(i) $|g_{m,n}(x)| \leq C_N \langle |x_1 + \frac{m_1}{2}| \rangle^{-N} \langle |x_2 + \frac{m_2}{2}| \rangle^{-N}$,

(ii) $|\phi_{j,p}(x)| \leq C_N \cdot 2^{2j} \cdot \langle |2^{2j} x_1 + p_1| \rangle^{-N} \langle |2^{2j} x_2 + p_2| \rangle^{-N}$.

(iii) $|\psi_{j,l,k}^{\mathrm{v}}(x)| \leq C_N \cdot 2^{3j/2} \cdot \langle |2^j x_1 - k_1| \rangle^{-N} \langle |2^{2j} x_2 + l 2^j x_1 - k_2| \rangle^{-N}$,
$|\psi_{j,l,k}^{\mathrm{h}}(x)| \leq C_N \cdot 2^{3j/2} \cdot \langle |2^{2j} x_1 + l 2^j x_2 - k_1)| \rangle^{-N} \langle |2^j x_2 - k_2| \rangle^{-N}$,

(iv) $|\langle g_{m,n}, \phi_{j,p} \rangle| \leq C_N \cdot 2^{-2j}$,
$|\langle g_{m,n}, \psi_{j,l,k}^{\acute{}} \rangle| \leq C_N \cdot 2^{-3j/2}, \quad \forall \acute{} \in \{\mathrm{v}, \mathrm{h}\}$,
$|\langle \phi_{j,p}, \psi_{j,l,k}^{\acute{}} \rangle| \leq C_N \cdot 2^{-j/2}, \quad \forall \acute{} \in \{\mathrm{v}, \mathrm{h}\}$.

We now present the following convergence result which shows the success of Algorithm 5.1 in simultaneously inpainting and separating three components of points, curves, and texture.

Theorem 5.16 *For $0 < h_j = o(2^{-(1+\epsilon)j})$ with ϵ satisfying $0 < \epsilon < \frac{1}{3}$, the recovery error provided by Algorithm 5.1 decays rapidly and we have asymptotically perfect simultaneous separation and inpainting. Namely, for all $N \in \mathbb{N}_0$,*

$$\frac{\|\mathcal{P}_j^* - \mathcal{P}_j\|_2}{\|\mathcal{P}_j\|_2} + \frac{\|\mathcal{C}_j^* - w\mathcal{L}_j\|_2}{\|w\mathcal{L}_j\|_2} + \frac{\|\mathcal{T}_j^* - \mathcal{T}_j\|_2}{\|\mathcal{T}_j\|_2} = o(2^{-Nj}) \to 0, \quad j \to \infty,$$

where $(\mathcal{P}_j^*, \mathcal{L}_j^*, \mathcal{T}_j^*)$ is the solution of Algorithm 5.1 and $(\mathcal{P}_j, \mathcal{C}_j, \mathcal{T}_j)$ are ground truth components.

For noisy images, we have the following result.

Theorem 5.17 *For $0 < h_j = o(2^{-(1+\epsilon)j})$ with ϵ satisfying $0 < \epsilon < \frac{1}{3}$, the recovery error provided by Algorithm 5.10 decays rapidly and we have asymptotically perfect simultaneous separation and inpainting,*

$$\frac{\|\mathcal{P}_j^* - \mathcal{P}_j\|_2}{\|\mathcal{P}_j\|_2} + \frac{\|\mathcal{C}_j^* - w\mathcal{L}_j\|_2}{\|w\mathcal{L}_j\|_2} + \frac{\|\mathcal{T}_j^* - \mathcal{T}_j\|_2}{\|\mathcal{T}_j\|_2} = o(2^{-Nj}) \to 0, \quad j \to \infty,$$

where $(\mathcal{P}_j, \mathcal{C}_j, \mathcal{T}_j)$ are ground truth components and $(\mathcal{P}_j^*, \mathcal{L}_j^*, \mathcal{T}_j^*)$ is the solution of Algorithm 5.10 with $\mathcal{R}(z) = \|z\|_1, \lambda_j = 2^{(2+\epsilon)j}$.

These two theorems show that the L_2 errors of the reconstruction by Algorithm 5.1 and 5.10 can be made arbitrarily small in the limit as the scale tends to zero. We would like to remind the reader that by Remark 5.9 we need to separate each pair of components while inpaint each of them to guarantee the success of our algorithms. The proof of two main theorems relies on a number of estimates based on the general theoretical guarantee with respect to Remark 5.9.

Before giving a proof for this theorem, we consider the following materials.

5.4.5 Estimate of Approximation Errors

Lemma 5.18 *We have $\delta_{1j} = \circ(2^{-Nj}), \quad j \to \infty$.*

Proof. Without loss of generality, we can restrict the general case to $\mathcal{P}(x) = \frac{1}{|x|^{3/2}}$. By definition, we have

$$\begin{aligned}
\delta_{1,j} &= \sum_{(j',m)\notin\Lambda_{1,j}} \langle \psi_{j',m}, \mathcal{P}_j \rangle \\
&= \sum_{j'\geq 0, |m|>2^{\epsilon j}} \int_{\mathbb{R}^2} 2^{-2j} W_{j'}(\xi) e^{2\pi i \xi^T \frac{m}{2^{2j'}}} W_j(\xi) \frac{1}{|\xi|} d\xi.
\end{aligned}$$

We can assume that $j' = j$ due to the fact that $W_{j'}(\xi)W_j(\xi) = 0$ for $|j' - j| > 1$. Applying the change of variables $\eta = (\eta_1, \eta_2) = 2^{-2j}(\xi_1, \xi_2)$, we obtain

$$\delta_{1,j} \lesssim 2^j \sum_{|m|>2^{\epsilon j}} \int_{\mathbb{R}^2} \frac{1}{|\eta|} W^2(\eta) e^{2\pi i \eta^T m} d\eta.$$

We now apply integration by parts with respect to η_1, η_2, respectively, for $N = 1, 2, \ldots,$

$$\begin{aligned}
\delta_{1,j} &\lesssim 2^j \sum_{\substack{m_1,m_2\neq 0,\\ |m|>2^{\epsilon j}}} \left| \int_{\mathbb{R}^2} |m_1|^{-N} |m_2|^{-N} \frac{\partial^{2N}}{\partial \eta_1^N \partial \eta_2^N} \left[\frac{1}{|\eta|} W(\eta) \right] e^{2\pi i \xi^T m} d\eta \right| \\
&\leq C_N 2^j \sum_{|m|>2^{\epsilon j}} |m_1|^{-N} |m_2|^{-N} \\
&\leq C_N 2^j 2^{-(N-1)(\epsilon j - 1)}, \quad \forall N \in \mathbb{N}.
\end{aligned}$$

Here we note that the boundary terms vanish due to the compact support of W. This finishes the proof. ∎

Lemma 5.19 *We have* $\delta_{2j} = \circ(2^{-Nj}), \quad j \to \infty$.

Proof. This lemma is a special case of [GK14, Proposition 5.2]. It was used there universal shearlet systems with flexible scaling parameter α which coincide with our shearlets Ψ for case $\alpha = 1$. ∎

Lemma 5.20 *For every* $N \in \mathbb{N}$ *the sequence* $(\delta_{3,j})_{j\in\mathbb{N}}$ *decays rapidly, i.e.,*

$$\delta_{3,j} := \sum_{(m',n')\notin B(0,M_j)\times I_T^{\pm}} |\langle \mathcal{T}_j, g_{m',n'}\rangle| = o(2^{-Nj}).$$

Proof. The proof of this lemma follows an argument similar to that of [DLK22, Proposition 8.2]. We also include the proof here since we used a modified model of texture. By definition, we have

$$\delta_{3,j} = \sum_{(m',n')\notin B(0,M_j)\times I_T^{\pm}} |\langle \mathcal{T}_j, g_{m',n'}\rangle|$$

We now consider two cases.

Case 1: $n' \notin I_T^{\pm} \cap \mathcal{A}_j$. By Plancherel, we have

$$\begin{aligned} |\langle \mathcal{T}_j, g_{m',n'}\rangle| &= |\langle \hat{\mathcal{T}}_j, \hat{g}_{m',n'}\rangle| \\ &= \sum_{|n'-n|>1} \int \Big| \sum_{n\in I_T} d_n W_j(\xi)\hat{g}(\xi-n)\hat{g}(\xi-n')e^{2\pi i\xi^{\top}\frac{m'}{2}}\Big| \\ &= 0, \end{aligned}$$

where the last equality is due to $\operatorname{supp}\hat{g} = [-1,1]^2$, and $\operatorname{supp} W_j = \mathcal{A}_j$.

Case 2: $n' \in I_T^{\pm} \cap \mathcal{A}_j$. By Lemma 5.15 and the boundedness of $(d_n)_{n\in\mathbb{Z}^2}$, we obtain

$$\begin{aligned} \delta_{3,j} &= \sum_{\substack{m'\notin B(0,M_j)\\ n'\in I_T^{\pm}\cap\mathcal{A}_j}} |\langle \mathcal{T}_j, g_{m',n'}\rangle| = \sum_{\substack{m'\notin B(0,M_j)\\ n'\in I_T^{\pm}\cap\mathcal{A}_j}} \Big| \int_{\mathbb{R}^2} \sum_{n\in I_T} d_n g_{0,n}(x) g_{m',n'}(x)dx\Big| \\ &\le \sum_{\substack{|m'|>2^{\epsilon j/6}\\ n'\in I_T^{\pm}\cap\mathcal{A}_j}} \int_{\mathbb{R}^2} C_N\langle|x_1|\rangle^{-N}\langle|x_2|\rangle^{-N}\langle|x_1+\frac{m_1'}{2}|\rangle^{-N}\langle|x_1+\frac{m_2'}{2}|\rangle^{-N}dx \\ &\le C_N\cdot \sum_{\substack{|m'|>2^{\epsilon j/6}\\ n'\in I_T^{\pm}\cap\mathcal{A}_j}} \langle|\frac{m_1'}{2}|\rangle^{-N}\langle|\frac{m_2'}{2}|\rangle^{-N}, \end{aligned}$$

here the last equality is due to the fact that there exists a constant $C_N > 0$ satisfying

$$\int_{\mathbb{R}} \langle|t|\rangle^{-N}\langle|t+a|\rangle^{-N}dt \le C_N\langle|a|\rangle^{-N}, \quad \forall a\in\mathbb{R}.$$

Thus, by (5.23) we have

$$\begin{aligned}\delta_{3,j} &\leq C_N \cdot 2^{(1-\epsilon)j} \cdot \sum_{|m'|>2^{\epsilon j/6}} \langle|\frac{m_1'}{2}|\rangle^{-N}\langle|\frac{m_2'}{2}|\rangle^{-N} \\ &\leq C_N \cdot 2^{(1-\epsilon)j} \cdot \int_{\mathbb{R}}\int_{\frac{1}{2}2^{\epsilon j/6}}^{+\infty} \langle|\frac{t_1}{2}|\rangle^{-N}\langle|\frac{t_2}{2}|\rangle^{-N} dt_1 dt_2 \\ &\leq C_N' \cdot 2^{(1-\epsilon)j} \cdot 2^{-(N-1)\epsilon j/6}.\end{aligned}$$

This concludes the claim since we can choose an arbitrarily large $N \in \mathbb{N}$. ∎

As a direct consequence of Lemmata 5.18, 5.19, 5.20, we have the following proposition

Proposition 5.21 *For any $N \in \mathbb{N}$, we have $\delta_j := \delta_{1j} + \delta_{2j} + \delta_{3j} = \circ(2^{-Nj})$.*

5.4.6 Estimate of Cluster Coherence for Separation Task

In this section, we give an estimate for the term $\mu_{c,N}^{sep}$. The following lemma ensures the success of separating points from curves

Proposition 5.22 *We have*

(i) $\mu_c(\Lambda_{1,j}^{\pm}, \mathbf{\Psi}; \mathbf{\Phi}) \to 0,\ j \to \infty,$

(ii) $\mu_c(\Lambda_{2,j}^{\pm}, \mathbf{\Phi}; \mathbf{\Psi}) \to 0,\ j \to \infty.$

Proof. (i) By Lemma 5.15, we have

$$\begin{aligned}\mu_c(\Lambda_{1j}, \mathbf{\Psi}; \mathbf{\Phi}) &\leq \#\{(j,m) \in \Lambda_{1,j}\} \cdot C \cdot 2^{-j/2} \\ &\leq C \cdot 2^{2\epsilon j} \cdot 2^{-j/2} \\ &= C \cdot 2^{-(1-4\epsilon)j/2} \xrightarrow[j\to+\infty]{\text{By (5.22)}} 0.\end{aligned}$$

ii) Lemma 5.15 yields

$$\mu_c(\Lambda_{2j}, \mathbf{\Phi}; \mathbf{\Psi}) \leq C_N 2^{7j/2} \sum_{\substack{|l|\leq 1, |j'-j|\leq 1 \\ k\in\mathbb{Z}^2, |k_2 - lk_1|<2^{\epsilon j'}}} \int_{\mathbb{R}^2} \langle|2^{2j'}x_1 + m_1'|\rangle^{-N} \cdot$$
$$\langle|2^{2j'}x_2 + m_2'|\rangle^{-N}\langle|2^{j'}x_1 + k_1|\rangle^{-N}\langle|2^{2j'}x_2 + l2^{j'}x_1 + k_2|\rangle^{-N} dx.$$

We consider only $j' = j$ since the cases are estimated similary up to a constant.
Using the change of variable $(y_1, y_2) = (2^{2j}x_1, 2^{2j}x_2)$ yields

$$\mu_c(\Lambda_{2j}, \mathbf{\Phi}; \mathbf{\Psi}) \leq C_N 2^{-j/2} \sum_{\substack{l\in\{-1,0,1\}, k\in\mathbb{Z}^2 \\ |k_2 - lk_1|<2^{\epsilon j'}}} \int_{\mathbb{R}^2} \langle|y_1 + m_1'|\rangle^{-N}\langle|y_2 + m_2'|\rangle^{-N}$$

$$\cdot \langle |2^{-j}y_1 + k_1| \rangle^{-N} \langle |y_2 + l2^j x_1 + k_2| \rangle^{-N} dy. \tag{5.26}$$

Furthermore, we have

$$\sum_{k \in \mathbb{Z}^2} \langle |2^{-j}y_1 + k_1| \rangle^{-N} \langle |y_2 + l2^j x_1 + k_2| \rangle^{-N} \leq C'. \tag{5.27}$$

Combining (5.26) with (5.27), we obtain

$$\begin{aligned} \mu_c(\Lambda_{2j}, \mathbf{\Phi}; \mathbf{\Psi}) &\leq C'_N \cdot 2^{-j/2} \int_{\mathbb{R}^2} \langle |y_1 + m'_1| \rangle^{-N} \langle |y_2 + m'_2| \rangle^{-N} dy \\ &\leq C''_N \cdot 2^{-j/2} \xrightarrow{j \to +\infty} 0. \end{aligned}$$

We complete the proof. ∎

Proposition 5.23 *We have*

(i) $\mu_c(\Lambda_{3,j}, \mathbf{G}; \mathbf{\Psi}), \mu_c(\Lambda_{3,j}, \mathbf{G}; \mathbf{\Phi}) \to 0, \quad j \to \infty.$

(ii) $\mu_c(\Lambda_{1,j}, \mathbf{\Phi}; \mathbf{G}), \mu_c(\Lambda_{2,j}, \mathbf{\Psi}; \mathbf{G}) \to 0, \quad j \to \infty.$

Proof. i) We first consider the term $\mu_c(\Lambda_{3,j}, \mathbf{G}; \mathbf{\Psi})$. For this, we assume that the maximum is attained at $l' \in \mathbb{Z}, k' \in \mathbb{Z}^2$ and $' \in \{\mathrm{h}, \mathrm{v}\}$. We now use (5.23) and Lemma 5.15, we have

$$\begin{aligned} \mu_c(\Lambda_{3,j}, \mathbf{G}; \mathbf{\Psi}) &= \sum_{m \in B(0,M_j), n \in I_T^{\pm}} |\langle g_{m,n}, \psi^{\iota}_{j,l',k'} \rangle| \\ &\leq C_N \cdot 2^{-j} \#\{m \in B(0, M_j)\} \cdot \#\{n \in I_T^{\pm} \cap \mathcal{A}_j\} \\ &\leq C_N \cdot 2^{-j} \cdot M_j^2 \cdot 2^{(1-\epsilon)j} \\ &\overset{M_j = 2^{\epsilon j/6}}{=} C_N \cdot 2^{-2\epsilon j/3} \xrightarrow{j \to +\infty} 0. \end{aligned}$$

Similarly, we have

$$\begin{aligned} \mu_c(\Lambda_{3,j}, \mathbf{G}; \mathbf{\Phi}) &= \sum_{m \in B(0,M_j), n \in I_T^{\pm}} |\langle g_{m,n}, \phi_{j,k'} \rangle| \\ &\leq C_N \cdot 2^{-2j} \#\{m \in B(0, M_j)\} \cdot \#\{n \in I_T^{\pm} \cap \mathcal{A}_j\} \\ &\leq C_N \cdot 2^{-2j} \cdot M_j^2 \cdot 2^{(1-\epsilon)j} \\ &\overset{M_j = 2^{\epsilon j/6}}{=} C_N \cdot 2^{-j} \cdot 2^{-2\epsilon j/3} \xrightarrow{j \to +\infty} 0. \end{aligned}$$

ii) By the definition

$$\mu_c(\Lambda_{2,j}, \mathbf{\Psi}; \mathbf{G}) = \max_{(m,n)} \sum_{\eta \in \Lambda_{1,j}^{\pm}} |\langle \psi^{'}_{j,l,k}, g_{m,n} \rangle|,$$

where $\eta = (j, l, k; ')$. We assume that the maximum is achieved at $m', n' \in \mathbb{Z}^2$. By Lemma

5.15 (i),(iii), and the change of variables $(y_1, y_2) = (x_1, 2^{2j}x_2 + l2^j x_1 - lk_1)$, we have

$$\begin{aligned}
\mu_c(\Lambda_{1,j}, \mathbf{\Psi}; \mathbf{G}) &= \sum_{\eta \in \Lambda_{1,j}} |\langle \psi'_{j,l,k}, g_{m',n'} \rangle| \\
&\leq C_N 2^{\frac{3}{2}j} \sum_{\substack{|l|\leq 1, k\in\mathbb{Z}^2 \\ |k_2 - lk_1| \leq 2^{\epsilon j}}} \int_{\mathbb{R}^2} \langle |2^j x_1 - k_1| \rangle^{-N} \langle |2^{2j} x_2 + l2^j x_1 - k_2| \rangle^{-N} \\
&\qquad \cdot \langle |x_1 + \frac{m_1}{2}| \rangle^{-N} \langle |x_2 + \frac{m_2}{2}| \rangle^{-N} dx_1 dx_2. \\
&= C_N 2^{-\frac{1}{2}j} \sum_{\substack{|l|\leq 1, k\in\mathbb{Z}^2 \\ |k_2 - lk_1| \leq 2^{\epsilon j}}} \int_{\mathbb{R}^2} \langle |2^j y_1 - k_1| \rangle^{-N} \langle |y_2 + lk_1 - k_2| \rangle^{-N} \cdot \\
&\quad \langle |y_1 + \frac{m_1}{2}| \rangle^{-N} \langle |2^{-2j} y_2 - l2^{-j} y_1 + 2^{-2j} lk_1 + \frac{m_2}{2}| \rangle^{-N} dy_1 dy_2 \\
&\leq \sum_{\substack{|l|\leq 1, k\in\mathbb{Z}^2 \\ |k_2| \leq 2^{\epsilon j}}} \int_{\mathbb{R}^2} C_N \cdot 2^{-j/2} \langle |2^j y_1 - k_1| \rangle^{-N} \langle |y_2 - k_2| \rangle^{-N} \\
&\qquad \cdot \langle |y_1 + \frac{m_1}{2}| \rangle^{-N} dy_1 dy_2 \\
&= \sum_{\substack{|l|\leq 1, k_2\in\mathbb{Z} \\ |k_2| \leq 2^{\epsilon j}}} \int_{\mathbb{R}^2} C_N 2^{-j/2} \Big(\sum_{k_1 \in \mathbb{Z}} \langle |2^j y_1 - k_1| \rangle^{-N} \Big) \langle |y_2 - k_2| \rangle^{-N} \\
&\qquad \cdot \langle |y_1 + \frac{m_1}{2}| \rangle^{-N} dy_1 dy_2 \\
&\leq C_N \cdot 2^{-j/2} \cdot 2^{\epsilon j} = C_N \cdot 2^{-(1-2\epsilon)j/2} \xrightarrow{j\to+\infty} 0.
\end{aligned}$$

Similarly, we assume that the maximum of the cluster coherence $\mu_c(\Lambda_{1,j}, \mathbf{\Phi}; \mathbf{G})$ is attained for some $(m'', n'') \in \mathbb{Z}^2$. By Lemma 5.15 (iv), we have

$$\begin{aligned}
\mu_c(\Lambda_{1,j}, \mathbf{\Phi}; \mathbf{G}) &= \sum_{|p| \leq 2^{\epsilon j}} |\langle \phi_{j,p}, g_{m'',n''} \rangle| \\
&\leq C_N \cdot 2^{-2j} \cdot 2^{2\epsilon j} = C_N \cdot 2^{-(2-\epsilon)j} \xrightarrow{j\to+\infty} 0.
\end{aligned}$$

This concludes the claim. ∎

The following lemma guarantees the successful separation of curves and texture as well as points and texture.

Proposition 5.24 *We have*

(i) $\mu_c(\Lambda^{\pm}_{3,j}, P_{M,j}\mathbf{G}; \mathbf{\Psi}) \to 0, \quad j \to \infty.$

(ii) $\mu_c(\Lambda^{\pm}_{2,j}, P_{M,j}\mathbf{\Psi}; \mathbf{G}) \to 0, \quad j \to \infty.$

Proof. i) By definition, we have

$$\mu_c(\Lambda_{3,j}, P_{M,j}\mathbf{G}; \mathbf{\Psi}) = \sup_{(j,l,k)} \sum_{(m,n)\in\Lambda_{3,j}^{\pm}} |\langle P_{M,j} g_{m,n}, \psi_{j,l,k}^{'}\rangle|.$$

Without loss of generality, we may assume that the maximum is achieved at $(j, l', k'; ') \in \Delta_j$. Thus, we obtain

$$\begin{aligned}
\mu_c(\Lambda_{3,j}, P_{M,j}\mathbf{G}; \mathbf{\Psi}) &= \sum_{|m|\le 2^{\epsilon/6}, n\in I_T^{\pm}\cap\mathcal{A}_j} |\langle P_{M,j} g_{m,n}, \psi_{j,l',k'}^{'}\rangle| \\
&= \sum_{|m|\le 2^{\epsilon/6}, n\in I_T^{\pm}\cap\mathcal{A}_j} \Big| \int_{-h_j}^{h_j}\int_{\mathbb{R}} g_{m,n}(x)\overline{\psi_{j,l',k'}^{'}(x)}dx_1dx_2\Big| \\
&\le \sum_{|m|\le 2^{\epsilon/6}, n\in I_T^{\pm}\cap\mathcal{A}_j} \int_{-h_j}^{h_j}\int_{\mathbb{R}} |g_{m,n}(x)||\psi_{j,l',k'}^{'}(x)|dx_1dx_2.
\end{aligned}$$

We consider only the case $' = \mathrm{v}$, the other case can be done analogously. Indeed, we recall Lemma 5.15 (i),(iii),

$$|g_{m,n}(x)| \le C_N \cdot \langle|x_1 + \frac{m_1}{2}|\rangle^{-N}\langle|x_2 + \frac{m_2}{2}|\rangle^{-N}, \forall m, n \in \mathbb{Z}^2,$$

$$|\psi_{j,l',k'}^{\mathrm{v}}(x)| \le C_N \cdot 2^{3j/2} \cdot \langle|2^j x_1 - k_1'|\rangle^{-N}\langle|2^{2j}x_2 + l'2^j x_1 - k_2'|\rangle^{-N}.$$

We now apply the change of variable $y = S_{\mathrm{v}}^{l'} A_{\mathrm{v}}^{j} x = (2^j x_1, 2^{2j}x_2 + l'2^j x_1)$. This leads to

$$\begin{aligned}
\int_{-h_j}^{h_j}\int_{\mathbb{R}} |g_{m,n}(x)||\psi_{j,l',k'}^{\mathrm{v}}(x)|dx &\le C_N 2^{-\frac{3}{2}j}\int_{\mathbb{R}^2}\langle|2^{-j}y_1 + \frac{m_1}{2}|\rangle^{-N}\langle|y_1 - k_1'|\rangle^{-N} \\
&\quad\cdot\langle|2^{-2j}(y_2 - l'y_1) + \frac{m_2}{2}|\rangle^{-N}\langle|y_2 - k_2'|\rangle^{-N}dy \\
&\le C_N 2^{-\frac{3}{2}j}\int_{\mathbb{R}^2}\langle|2^{-j}y_1 + \frac{m_1}{2}|\rangle^{-N}\langle|y_1 - k_1'|\rangle^{-N} \\
&\quad\cdot\langle|2^{-2j}(y_2 - l'y_1) + \frac{m_2}{2}|\rangle^{-N}\langle|y_2 - k_2'|\rangle^{-N}dy.
\end{aligned} \tag{5.28}$$

In addition, we have

$$\sum_{(m_1,m_2)\in\mathbb{Z}^2}\langle|2^{-j}y_1 + \frac{m_1}{2}|\rangle^{-N}\langle|2^{-2j}(y_2 - l'y_1) + \frac{m_2}{2}|\rangle^{-N} \le C_N' \tag{5.29}$$

and

$$\int_{\mathbb{R}^2}\langle|y_1 - k_1'|\rangle^{-N}\langle|y_2 - k_2'|\rangle^{-N}dy_1dy_2 \le C_N''. \tag{5.30}$$

Combining (5.28), (5.29), (5.30) and (5.23), we finally obtain

$$\mu_c(\Lambda_{3,j}, P_{M,j}\mathbf{G}; \mathbf{\Psi}) \le \sum_{n\in I_T^{\pm}\cap\mathcal{A}_j} C_N \cdot 2^{-3j/2}\,.$$

$$\leq \quad C_N \cdot 2^{-3j/2} \cdot 2^j = C_N \cdot 2^{-j/2} \xrightarrow{j\to+\infty} 0.$$

ii) For the other term $\mu_c(\Lambda^{\pm}_{2,j}, P_{M,j}\mathbf{\Psi}; \mathbf{G})$, we assume that the maximum in the definition of the cluster is attained for some $(m', n') \in \mathbb{Z}^2 \times \mathbb{Z}^2$. Thus, we have

$$\begin{aligned}
\mu_c(\Lambda_{1,j}, P_{M,j}\mathbf{\Psi}; \mathbf{G}) &= \sum_{(j,l,k;\iota)\in\Lambda_{1,j}} |\langle P_{M,j}\psi^{'}_{j,l,k}, g_{m',n'}\rangle| \\
&= \sum_{\substack{|l|\leq 1, k\in\mathbb{Z}^2 \\ |k_2 - lk_1|\leq 2^{\epsilon j}}} \Big| \int_{-h_j}^{h_j} \int_{\mathbb{R}} \psi^{\mathrm{v}}_{j,l,k}(x)\overline{g_{m',n'}(x)}dx \Big| \\
&\leq \sum_{\substack{|l|\leq 1, k\in\mathbb{Z}^2 \\ |k_2 - lk_1|\leq 2^{\epsilon j}}} \int_{-h_j}^{h_j} \int_{\mathbb{R}} |\psi^{\mathrm{v}}_{j,l,k}(x)||g_{m',n'}(x)|dx|.
\end{aligned}$$

By Lemma 5.15 and the change of variable $y = S^l_{\mathrm{v}} A^j_{\mathrm{v}} x = (2^j x_1, 2^{2j}x_2 + l2^j x_1)$, we obtain

$$\begin{aligned}
\int_{-h_j}^{h_j} \int_{\mathbb{R}} |\psi^{\mathrm{v}}_{j,l,k}(x)||g_{m',n'}(x)|dx \leq C_N 2^{\frac{-3j}{2}} \int_{-2^j h_j}^{2^j h_j} \int_{\mathbb{R}} \langle |y_1 - k_1| \rangle^{-N} \langle |2^{-j}y_1 + \frac{m'_1}{2}| \rangle^{-N} \\
\langle |y_2 - k_2| \rangle^{-N} \langle |2^{-2j}(y_2 - ly_1) + \frac{m'_2}{2}| \rangle^{-N} dy.
\end{aligned} \tag{5.31}$$

Furthermore, we have

$$\langle |2^{-j}y_1 + \frac{m'_1}{2}| \rangle^{-N} \langle |2^{-2j}(y_2 - ly_1) + \frac{m'_2}{2}| \rangle^{-N} \leq 1 \tag{5.32}$$

and

$$\begin{aligned}
&\int_{\mathbb{R}} \Big(\sum_{\substack{|l|\leq 1, k\in\mathbb{Z}^2 \\ |k_2 - lk_1|\leq 2^{\epsilon j}}} \langle |y_1 - k_1| \rangle^{-N} \langle |y_2 - k_2| \rangle^{-N} \Big) dy_2 \\
&= \sum_{\substack{|l|\leq 1, k_1, k_3\in\mathbb{Z} \\ |k_3|\leq 2^{\epsilon j}}} \langle |y_1 - k_1| \rangle^{-N} \cdot \Big(\int_{\mathbb{R}} \langle |y_2 - k_3 - lk_1| \rangle^{-N} dy_2 \Big) \\
&\leq C_N \cdot 2^{\epsilon j} \cdot \int_{\mathbb{R}} \langle |t - y_1| \rangle^{-N} dt \leq C'_N 2^{\epsilon j}.
\end{aligned} \tag{5.33}$$

We now combine (5.31), (5.32) and (5.33) to obtain

$$\begin{aligned}
\mu_c(\Lambda_{2,j}, P_j\mathbf{\Psi}; \mathbf{G}) &\leq C''_N \cdot 2^{-3j/2} \cdot 2^j h_j \cdot 2^{\epsilon j} \\
&\leq C''_N \cdot 2^{-(1-2\epsilon)j/2} \cdot 2^j h_j \xrightarrow{j\to+\infty} 0.
\end{aligned}$$

■

Next is our final estimate.

5.4.7 Estimate of Cluster Coherence for Inpainting Task

The previous subsection ensures the success of separating three components. Now it remains to provide estimates for inpainting curves as well as texture. Indeed, by our assumption that the pointlike part has no missing content so we need only to inpaint curvilinear and texture structures. For this, we would like to recall that the inpainting task is encoded by the term $\mu_{c,N}^{inp} := \max_{1\leq m\leq N} \inf_{\Phi_m^d\in\mathbb{D}_{\Phi_m}} \mu_c(\Lambda_m, P_M\Phi_m; \Phi_m^d)$. The following lemma is what we need.

Proposition 5.25 *We have*

(i) $\mu_c(\Lambda_{2,j}^{\pm}, P_{M,j}\mathbf{\Psi}; \mathbf{\Psi}) \to 0,\ j\to\infty.$

(ii) $\mu_c(\Lambda_{3,j}, P_{M,j}\mathbf{G}; \mathbf{G}) \to 0,\ j\to\infty.$

Proof. Here we would like to remark again that universal shearlets used in [DLK22] coincide with our shearlet system Φ in case $\alpha = 1$. Now it remains to estimate the other term $\mu_c(\Lambda_{3,j}, P_{M,j}\mathbf{G}; \mathbf{G})$.

Without loss of generality, we assume that the maximum is achieved at $(m', n') \in \Lambda_{3,j}$. Thus, we obtain

$$\begin{aligned}\mu_c(\Lambda_{3,j}, P_{M,j}\mathbf{G}; \mathbf{G}) &= \sum_{(m,n)\in M_j\times(I_T^{\pm}\cap\mathcal{A}_j)} |\langle P_{M,j}g_{m,n}, g_{m',n'}\rangle| \\ &= \sum_{(m,n)\in M_j\times(I_T^{\pm}\cap\mathcal{A}_j)} \Big|\int_{-h_j}^{h_j}\int_{\mathbb{R}} g_{m,n}(x)\overline{g_{m',n'}(x)}dx\Big| \\ &\leq \sum_{(m,n)\in M_j\times(I_T^{\pm}\cap\mathcal{A}_j)} \int_{-h_j}^{h_j}\int_{\mathbb{R}} |g_{m,n}(x)||g_{m',n'}(x)|dx. \end{aligned} \tag{5.34}$$

Next, we recall Lemma 5.15 (i),

$$|g_{m,n}(x)| \leq C_N\cdot\langle|x_1+\frac{m_1}{2}|\rangle^{-N}\langle|x_2+\frac{m_2}{2}|\rangle^{-N}, \forall m,n\in\mathbb{Z}^2.$$

This leads to

$$\begin{aligned}\int_{-h_j}^{h_j}\int_{\mathbb{R}} |g_{m,n}(x)||g_{m',n'}(x)|dx \leq \int_{-h_j}^{h_j}\int_{\mathbb{R}} C_N^2\langle|x_1+\frac{m_1}{2}|\rangle^{-N}\langle|x_2+\frac{m_2}{2}|\rangle^{-N}\cdot \\ \langle|x_1+\frac{m_1'}{2}|\rangle^{-N}\cdot\langle|x_2+\frac{m_2'}{2}|\rangle^{-N}dx \\ = C_N^2\int_{-h_j}^{h_j}\int_{\mathbb{R}}\langle|y_1+\frac{m_1}{2}|\rangle^{-N}\langle|y_2+\frac{m_2}{2}|\rangle^{-N}\cdot \\ \langle|y_1+\frac{m_1'}{2}|\rangle^{-N}\langle|y_2+\frac{m_2'}{2}|\rangle^{-N}dy. \end{aligned} \tag{5.35}$$

In addition, we have

$$\sum_m\langle|y_1+\frac{m_1}{2}|\rangle^{-N}\langle|y_2+\frac{m_2}{2}|\rangle^{-N}\leq C_N',\ \int_{\mathbb{R}}\langle|y_2+\frac{m_2'}{2}|\rangle^{-N}dy_2\leq C_N''. \tag{5.36}$$

Thus, by (5.23) and (5.34) combined with (5.35) and (5.36), we obtain

$$\begin{aligned}\mu_c(\Lambda_{2,j}, P_j\mathbf{G}; \mathbf{G}) &\leq \sum_{n\in I_T^{\pm}\cap\mathcal{A}_j} C_N''' \cdot h_j \\ &\leq C_N''' \cdot 2^j h_j \xrightarrow{j\to+\infty} 0.\end{aligned}$$

This concludes the claim. ∎

Let us go back to the proof of our main theorems.

5.4.8 Proof of Theorem 5.16 and Theorem 5.17

Proof. Applying Theorem 5.8 with respect to Remark 5.9 (5), we obtain

$$\|\mathcal{P}_j^* - \mathcal{P}_j\|_2 + \|\mathcal{C}_j^* - w\mathcal{L}_j\|_2 + \|\mathcal{T}_j^* - \mathcal{T}_j\|_2 \leq \frac{\delta_{1j} + \delta_{2j} + \delta_{3j}}{1 - 2\mu_{c,3}},$$

where $\mu_{c,3}$ is bounded by (5.12). Roughly speaking, we just need to inpaint two components of curvilinear singularities and texture and simultaneously separate three geometric components including point singularities. By Proposition 5.21, we have $\delta = \delta_{1,j} + \delta_{2,j} + \delta_{3,j} = \circ(2^{-Nj}),\ \forall N \in \mathbb{N}$. In addition, Propositions 5.22, 5.23, 5.24 yield $\mu_{c,3} \to 0,\ j \to \infty$. This concludes the claim. ∎

The proof of Theorem 5.17 follows the same lines as Theorem 5.16. Here we use Theorem 5.11 instead of Theorem 5.8. Now we need to verify (5.21), i.e.,

$$\sum_{(j,p)\in\Lambda_{1,j}} |\langle \phi_{j,p}, z\rangle| + \sum_{(j,l,k)\in\Lambda_{2,j}} |\langle \psi_{j,l,k}, z\rangle| + \sum_{(j,p)\in\Lambda_{3,j}} |\langle g_{m,n}, z\rangle| \leq 2^{(2+\epsilon)j-1}\|z\|_1, \tag{5.37}$$

for all $z \in L^2(\mathbb{R}^2)$. Indeed, by Lemma 5.15 we have

$$\begin{aligned}\sum_{(j,p)\in\Lambda_{1,j}} |\langle \phi_{j,p}, z\rangle| &\leq \sum_{\substack{p\in\mathbb{Z}^2,\\ |p|\leq 2^{\epsilon j}}} C_N 2^{2j} \int_{\mathbb{R}^2} \langle |2^{2j}x_1 + p_1|\rangle^{-N} \langle |2^{2j}x_2 + p_2|\rangle^{-N} |z(x)| dx \\ &\leq C_N' 2^{2j}\|z\|_1,\end{aligned} \tag{5.38}$$

where the last inequality follows from

$$\sum_{\substack{p\in\mathbb{Z}^2,\\ |p|\leq 2^{\epsilon j}}} \langle |2^{2j}x_1 + p_1|\rangle^{-N} \langle |2^{2j}x_2 + p_2|\rangle^{-N} \leq C_N'',\ \forall x = (x_1, x_2) \in \mathbb{R}^2.$$

Similarly, we obtain

$$\begin{aligned}\sum_{(j,l,k)\in\Lambda_{2,j}} |\langle \psi_{j,l,k}^{\mathrm{v}}, z\rangle| \leq & \sum_{\substack{l\in\{-1,0,1\}\\ |k_2 - lk_1|\leq 2^{\epsilon j}}} C_N 2^{3j/2} \int_{\mathbb{R}^2} \langle |2^j x_1 - k_1|\rangle^{-N} \cdot \\ & \langle |2^{2j}x_2 + l2^j x_1 - k_2|\rangle^{-N} |z(x)| dx \\ & \leq C_N' 2^{3j/2}\|z\|_1,\end{aligned} \tag{5.39}$$

and

$$\sum_{(m,n)\in\Lambda_{3,j}} |\langle g_{m,n}, z\rangle| \leq \sum_{\substack{|m|\leq 2^{\epsilon j/6} \\ n\in I_T^{\pm}\cap\mathcal{A}_j}} C_N \int_{\mathbb{R}^2} \langle |x_1 + \frac{m_1}{2}|\rangle^{-N} \langle |x_2 + \frac{m_2}{2}|\rangle^{-N} |z(x)| dx$$

$$\overset{\text{By (5.23)}}{\leq} C'_N 2^{(1-\epsilon)j} \|z\|_1. \tag{5.40}$$

We conclude the claim (5.37) by a combination of (5.38), (5.39), and (5.40).

5.5 Summary and Conclusion

In this chapter, we provide a theoretical study of the simultaneous separation, inpainting, and denoising for multi-component signals. To achieve this, we first modify the notions of joint concentration and cluster coherence to encode the separating and inpainting tasks separately. One guarantees the success of the geometric separation and one for inpainting missing content. This is possible since the missing trip is assumed to be small which does not affect the geometry of the whole signal. Theoretical results are shown in Theorems 5.8 and 5.11 guarantee the success of our two proposed algorithms, one for constrained l_1 optimization and the other for unconstrained l_1 optimization.

Motivated by the theoretical guarantees, we aim to decompose the corrupted image into pointlike, curvelike, and texture parts as accurately as possible. In our analysis, we use a multi-scale approach that the task of simultaneous separation and inpainting is done separately at each scale j by Algorithm 5.1 and 5.10 using wavelets, shearlets, and Gabor frames. The whole image is then reconstructed from its sub-images by the reconstruction formula (5.25). The main idea for the success of the proposed algorithms is that the significant coefficients by wavelets, shearlets, and Gabor are clustered geometrically in phase space by microlocal analysis. The powerful tool based on l_1 minimization then enables us to explore the differences among these underlying components. For our main results, Theorem 5.16 and Theorem 5.17 show that at sufficiently fine scales the true components of the corrupted image are almost captured by proposed algorithms. In applications, our theory can be adapted with the change of components and sparse representation systems as long as they provide negligible cluster sparsity and cluster coherence. By choosing suitable sparsifying systems our methodology can handle the following tasks for multi-component images:

1. Simultaneous separation, inpainting, and denoising: In this case, Algorithm 5.10 is taken into account.

2. Simultaneous separation and inpainting: For this purpose, we can apply Algorithm 5.1.

3. Inpainting: Once the inpainted components are extracted, one can aggregate them again for inpainting purposes only.

4. Image separation: In this situation, we restrict our results to the case of no missing parts in the original image.

6

Numerical Implementation

6.1 Algorithms

We first consider our inpainting problem which can be solved by the following algorithm. We recall it here

$$\text{Find } f^\star = \underset{u}{\operatorname{argmin}} \|\Phi^* u\|_1, \ \text{ subject to } P_K u = P_K f,$$

as presented in Chapter 3. Note that here $P_K f$ is known to us. In term of solutions, we can recast it as a linear programming problem by adding the new variables u_1, u_2. Indeed, the nonlinearities can finally be transferred to the set of constraints as follows

$$\begin{aligned} &\text{Find } f^\star = \underset{u,z_1,z_2}{\operatorname{argmin}} \ z_1 + z_2, \\ &\text{subject to } \Phi^* u = z_1 - z_2, P_K u = P_K f, z_1, z_2 \geq 0. \end{aligned}$$

Here we applied the change of variable $z_1 = (\Phi^* u)_+$, $z_2 = (\Phi^* u)_-$, where for $x = (x_1, x_2, \ldots, x_n) \in \mathbb{R}^n$,

$$(x_+)_i = \begin{cases} x_i & \text{if } x_i \geq 0 \\ 0 & \text{else,} \end{cases} \quad \text{and} \quad (x_-)_i = \begin{cases} -x_i & \text{if } x_i \leq 0 \\ 0 & \text{else.} \end{cases}$$

This problem can be solved using any of the existing techniques, such as the primal dual interior point method.

This can be solved for instance using

$$linprog(f, A, b, Aeq, beq, lb, ub, options)$$

in Matlab.

The more general problem of simultaneous separation and inpainting, Algorithm (INP-SEP) in Chapter 4 or Algorithm 5.1 in Chapter 5, can be similarly rewritten as linear programming as follows

$$\begin{aligned} &\text{Find } f^\star = \underset{\substack{u_1,u_2,\ldots,u_N, \\ z_{11},z_{21},z_{12},z_{22},\ldots z_{1N},z_{2N}}}{\operatorname{argmin}} \ \sum_{i=1}^{N} z_{1i} + z_{2i}, \\ &\text{s.t. } \ \Phi^* u_i = z_{1i} - z_{2i}, P_K(\sum_{i=1}^{N} u_i) = P_K f, \ z_{1i}, z_{2i} \geq 0, \ \forall i = 1, \ldots, N. \end{aligned}$$

6.2 Experiments

In this section, we present some experiments for problems of inpainting an image which consists of different geometric components. By Remark 5.9, we only show the performance for inpainting each single component image.

Overall, it should be mentioned that the optimal result depends on the quality of the data.

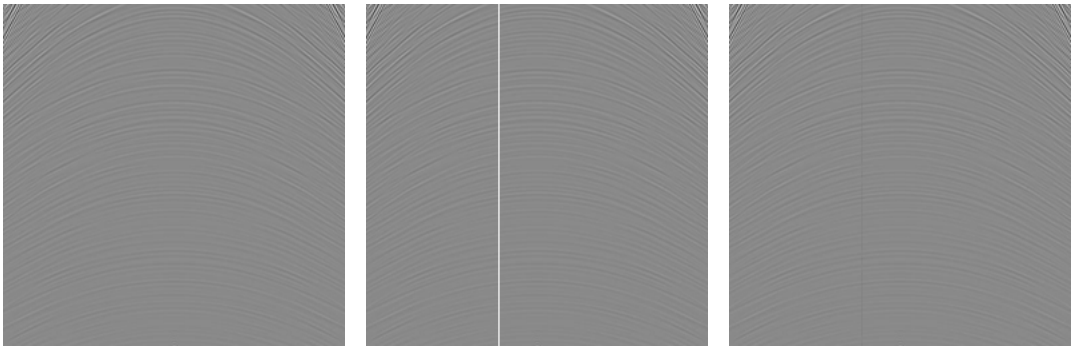

Figure 6.1: Right: Corrupted image Left: The recovered image by l_1 minimization.

Figure 6.2: Right: Corrupted image Left: The recovered image by l_1 minimization.

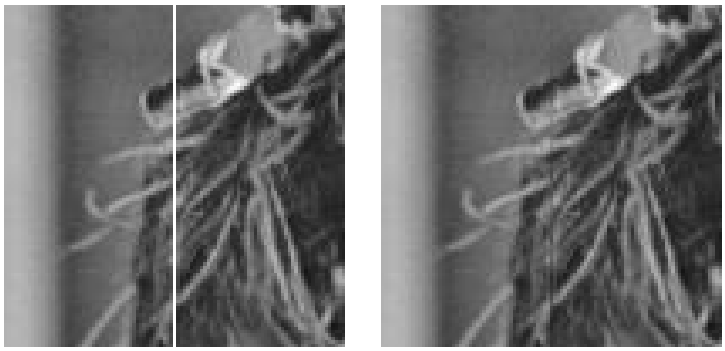

Figure 6.3: Zoom in

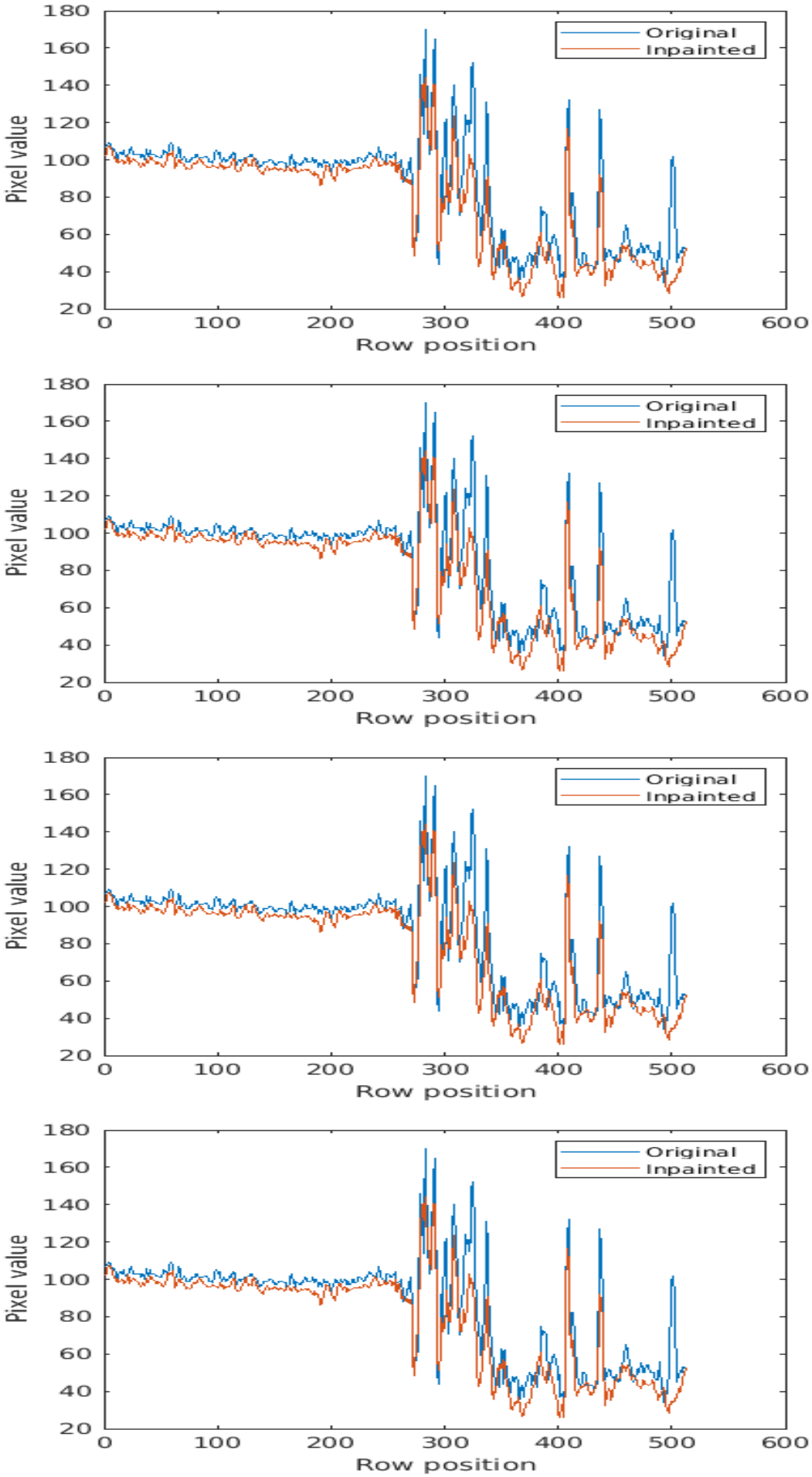

Figure 6.4: Reconstructions errors of four missing columns

For problem of separating points and curves, we refer an experiment from [KL12b]. More information can be found in shearlab.org.

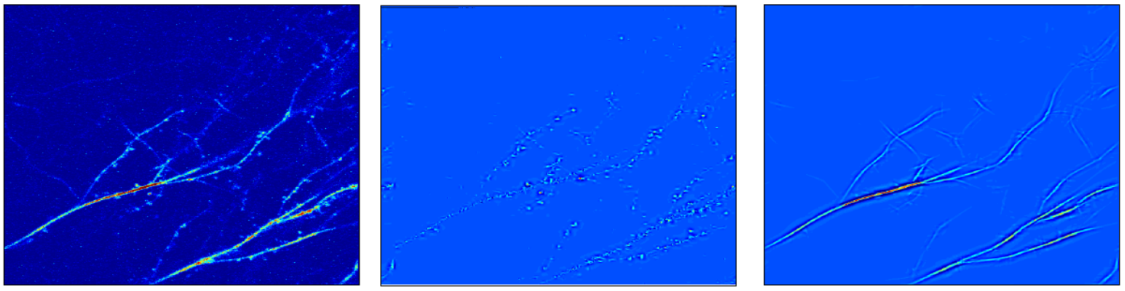

Figure 6.5: left: original image of neuron, middle: extracted spines, right: extracted dendrites. Source: [KL12b]

6.3 Discussion

In this thesis, we focus on problems of image inpainting and image separation. We provide theoretical analysis for those problems where the targets can be reconstructed by compressed sensing techniques. Some experiments in this chapter have provided a number of useful results for our theory. Our theory and experiments have shown that l_1 minimization as our reconstruction strategy is indeed a powerful tool for recovering sparse signals from underdetermined linear measurements. Although images with noise are not included in our experiments we also provide algorithms with the ability to handle additive noise as shown in our previous chapters.

Although a number of novel constructions were introduced in the past that followed the invention of directional representation systems, we throughout this thesis emphasize the role of shearlet systems with anisotropic scaling which have proved to outperform wavelets in many cases when dealing with anisotropic features such as cartoon like functions.

Bibliography

[AHP06] T. Ahonen, A. Hadid, and M. Pietikainen. *Face description with local binary patterns: application to face recognition*. IEEE Transactions on Pattern Analysis and Machine Intelligence 28(12), 2037–2041, 2006 (cit. on p. 2).

[BBCSV01] C. Ballester, M. Bertalmio, V. Caselles, G. Sapiro, and j. Verdera. *Filling-in by joint interpolation of vector fields and gray levels*. IEEE Trans. Image Process. 10(8), 1200–1211, 2001 (cit. on p. 59).

[BCL14] T. Barbu, A. Ciobanu, and M. Luca. *PDE-based image restoration using variational denoising and inpainting models*. 2014 18th International Conference on System Theory, Control and Computing (ICSTCC), pp. 688-691, doi: 10.1109/ICSTCC.2014.6982497, 2014 (cit. on p. 2).

[BZ03] O. Ben-Shahar and S. W. Zucker. *The Perceptual Organization of Texture Flow: A Contextual Inference Approach*. IEEE Trans. Pattern Anal. 25(4) , 401–417, 2003 (cit. on p. 67).

[BBS01] M. Bertalmio, A. L. Bertozzi, and G. Sapiro. *Navier-stokes, fluid dynamics, and image and video inpainting*. Computer Vision and Pattern Recognition. CVPR 2001. Proceedings of the 2001 IEEE ComputerSociety Conference on, vol. 1, IEEE, 2001, pp. I–355–I–362, 2001 (cit. on p. 59).

[BSCB00] M. Bertalmio, G. Sapiro, V. Caselles, and C. Ballester. *Image inpainting*. Proceedings of SIGGRAPH 2000, New Orleans, pp. 417–424, 2000 (cit. on pp. 1, 59).

[BVSO03] M. Bertalmio, L. Vese, G. Sapiro, and S. Osher. *Simultaneous structure and texture image inpainting*. IEEE Transactions on Image Processing, vol. 12, no. 8, pp. 882-889, Aug. 2003 (cit. on p. 3).

[BSO08] J. Bobin, J. Starck, and R. Ottensamer. *Compressed Sensing in Astronomy*. in IEEE Journal of Selected Topics in Signal Processing, vol. 2, no. 5, pp. 718-726, 2008 (cit. on p. 1).

[BGN08] L. Borup, R. Gribonval, and M. Nielsen. *Beyond Coherence : Recovering Structured Time-Frequency Representations*. Appl. Comput. Harmon. Anal.24 (1) , 120–128, 2008 (cit. on p. 59).

[CCS10] J. F. Cai, R. H. Chan, and Z. Shen. *Simultaneous cartoon and texture inpainting*. Inverse Problems & Imaging, 4 (3) : 379-395, 2010 (cit. on pp. 3, 105).

[CDOS12] J. Cai, B. Dong, S. Osher, and Z. Shen. *Image restoration: Total variation, wavelet frames, and beyond*. J. Amer. Math. Soc., 25 , pp. 1033-1089, 2012 (cit. on p. 3).

[Can98] E. Candes. *Ridgelets: theory and applications*. Ph.D. thesis, Department of Statistics, Stanford University, 1998 (cit. on p. 2).

[CD99] E. Candes and D. Donoho. *Curvelets, a surprisingly effective nonadaptive representation for objects with edges*. in: Curves and Surfaces, Vanderbilt University Press, 1999 (cit. on p. 2).

[CRT06a] E. Candès, J. Romberg, and T. Tao. *Robust uncertainty principles: Exact signal reconstruction from highly incomplete frequency information*. IEEE Transations on Information Theory, vol. 52, pp. 489–509, 2006 (cit. on p. 1).

[CRT06b] E. Candès, J. Romberg, and T. Tao. *Stable signal recovery from incomplete and inaccurate measurements*. Comm. Pure Appl. Math., vol. 59, no. 8, pp. 1207-1223, 2006 (cit. on p. 1).

[Cas00] P. Casazza. *The art of frame theory*. Taiwanese J. Math., 4, pp. 129-202, 2000 (cit. on p. 11).

[CS01] T. Chan and J. Shen. *Local in painting models and TV in painting*. SIAM Journal on Applied Mathematics, Vol. 62, pp. 1019-1043, 2001 (cit. on p. 3).

[CSZ06] T. Chan, J. Shen, and H.-M. Zhou. *Total variation wavelet inpainting*. J. Math. Imaging Vision, 25, pp. 107-125, 2006 (cit. on p. 3).

[CKS02] T. F. Chan, S. H. Kang, and J. Shen. *Euler's elastica and curvature-based inpainting*. SIAM J. Appl. Math., 63, pp. 564-592, 2002 (cit. on p. 4).

[CS02] T. F. Chan and J. Shen. *Mathematical models for local nontexture inpaintings*. SIAM J. Appl. Math., 62,pp. 1019–1043, 2001/02 (cit. on p. 59).

[CH18] Y. Chen and H. Hu. *An Improved Method for Semantic Image Inpainting with GANs: Progressive Inpainting*. Neural Processing Letters 20, 2018 (cit. on p. 3).

[Chr03] O. Christensen. "An introduction to frames and Riesz bases, Applied and Numerical Harmonic Analysis". *Birkhäuser Boston Inc., Boston, MA. MR 1946982(2003k:42001)* (2003) (cit. on pp. 4, 11, 105).

[DGM86] I. Daubechies, A. Grossman, and Y. Meyer. *Painless nonorthogonal expansions*. Journal Math. Phys.27,1271-1283, 1986 (cit. on pp. 71, 119).

[DV05] M. Do and M. Vetterli. *The contourlet transform: an efficient directional multiresolution image representation*. IEEE Transactions on Image Processing 14, 2091–2106., 2005 (cit. on p. 2).

[Do22] V. Do. *Multi-component separation, inpainting and denoising with recovery guarantees*. preprint, arXiv:2202.02806 [math.FA], 2022 (cit. on pp. 2, 5).

[DG21] V. Do and A. Goessmann. *An asymptotic analysis of separating pointlike and $C^\beta-$curvelike singularities*. preprint, arXiv:2107.01949 [math.FA], 2021 (cit. on pp. 5, 113).

[DLK22] V. Do, R. Levie, and G. Kutyniok. *Analysis of simultaneous inpainting and geometric separation based on sparse decomposition*. Analysis and Applications, Vol. 20, No. 02, pp. 303-352, 2022 (cit. on pp. 1, 4, 5, 52, 59, 111, 113, 118, 119, 125, 131).

[Don06] D. Donoho. *Compressed sensing*. IEEE Trans. Inform. Theory, vol. 52, no. 4, pp. 1289-1306, Apr, 2006 (cit. on pp. 1, 3, 4).

[Don01] D. L. Donoho. *Sparse components of images and optimal atomic decomposition*. Constr. Approx., 17:353–382, 2001 (cit. on p. 11).

[DE03] D. L. Donoho and M. Elad. *Optimally sparse representation in general (nonorthogonal) dictionaries via l_1 minimization*. Proc. Natl. Acad. Sci. USA100(5), pp. 2197–2202, 2003 (cit. on pp. 19, 59).

[DET06] D. L. Donoho, M. Elad, and V. N. Temlyakov. *Stable recovery of sparse overcomplete representationsin the presence of noise*. IEEE Trans. Inform. Theory 52(1) , 6–18, 2006 (cit. on p. 59).

[DH01] D. L. Donoho and X. Huo. *Uncertainty principles and ideal atomic decomposition*. IEEE Trans. Inform. Theory47(7) , 2845–2862, 2001 (cit. on p. 59).

[DK09] D. L. Donoho and G. Kutyniok. *Geometric Separation using a Wavelet-Shearlet Dictionary*. In L. Fesquet, B. Torrésani, editors, Proceedings of 8th International Conference on Sampling Theory, and Applications (SampTA), Marseille, 2009 (cit. on pp. 1, 2, 25, 27, 59, 107).

[DK13] D. L. Donoho and G. Kutyniok. *Microlocal analysis of the geometric separation problem*. Comm. Pure Appl. Math.66 , no. 1, 1-47. MR 2994548, 2013 (cit. on pp. 1, 2, 4, 5, 22, 24–26, 35, 50, 59, 62, 64, 74, 83, 107, 111, 113).

[DVDD98] D. L. Donoho, M. Vetterli, R. DeVore, and I. Daubechies. *Data compression and harmonic analysis*. IEEE Trans. Info. Theory 44, 2435–2476, 1998 (cit. on p. 1).

[DS52] R. J. Duffin and A. C. Schaeffer. *A class of nonharmonic Fourier series*. Transactions of the American Mathematical Society. 72 (2): 341–366. doi:10.2307/1990760. JSTOR 1990760. MR 0047179, 1952 (cit. on pp. 11, 60, 105).

[EL99] A. A. Efros and T. K. Leung. *Texture synthesis by non-parametric sampling*. IEEE International Conference on Computer Vision, Corfu, Greece, pp. 1033–1038, 1999 (cit. on pp. 2, 59).

[EB02] M. Elad and A. M. Bruckstein. *A Generalized Uncertainty Principle and Sparse Representation in Pairs of Bases*. IEEE Trans. Inform. Theory 48(9) , 2558–2567, 2002 (cit. on pp. 19, 59).

[ESQD05] M. Elad, J. L. Starck, P. Querre, and D. L. Donoho. *Simultaneous cartoon and texture image inpainting using morphological component analysis (MCA)*. Appl. Comput. Harmon. Anal.19(3), 340–358, 2005 (cit. on pp. 3, 60).

[FHMZ17] Y.-R. Fan, T.-Z. Huang, T.-H. Ma, and X.-L. Zhao. *Cartoon–texture image decomposition via non-convex low-rank texture regularization*. Journal of the Franklin Institute, Vol. 354, Issue 7, 3170-3187, 2017 (cit. on pp. 2, 48).

[FR13] S. Foucart and H. Rauhut. *A mathematical introduction to compressive sensing*. Applied and Numerical Harmonic Analysis, Birkhäuser Basel, 2013 (cit. on pp. 18, 19).

[GK14] M. Genzel and G. Kutyniok. *Asymptotic Analysis of Inpainting via Universal Shearlet Systems*. SIAM J. Imaging Sci. 7.4 , 2301-2339, 2014 (cit. on pp. 1, 2, 4, 5, 16, 26, 70–75, 87, 91, 99, 111, 113, 121, 125).

[GKHDV02] B. van Ginneken, S. Katsuragawa, B. M. ter Haar Romeny, K. Doi, and M. A. Viergever. *Automatic detection of abnormalities in chest radiographs using local texture analysis*. in IEEE Transactions on Medical Imaging, vol. 21, no. 2, pp. 139-149, doi: 10.1109/42.993132, 2002 (cit. on p. 2).

[Gra08] L. Grafakos. *Classical fourier analysis*. vol. 86, Springer, 2008 (cit. on p. 68).

[GB03] R. Gribonval and E. Bacry. *Harmonic decomposition of audio signals with matching pursuit*. IEEE Trans. SignalProc.51(1), 101–111, 2003 (cit. on p. 59).

[GN03] R. Gribonval and M. Nielsen. *Sparse representations in unions of bases*. IEEE Trans. Inform. Theory 49(12), 3320–3325, 2003 (cit. on p. 59).

[Gro13] P. Grohs. *Bandlimited shearlet frames with nice duals*. J. Comput. Appl. Math. 243, 139–151, 2013 (cit. on pp. 25, 27, 32, 34).

[GKKS16] P. Grohs, S. Keiper, G. Kutyniok, and M. Schäfer. *Cartoon approximation with α-curvelets*. J. Fourier Anal. Appl., 22(6):1235-1293, 2016 (cit. on pp. 68, 71).

[Gro04] H. Grossauer. *A Combined PDE and Texture Synthesis Approach to Inpainting*. In: Pajdla T., Matas J. (eds) Computer Vision - ECCV 2004. Lecture Notes in Computer Science, vol 3022. Springer, Berlin, Heidelberg, 2004 (cit. on p. 2).

[GKL06] K. Guo, G. Kutyniok, and D. Labate. *Sparse multidimensional representations using anisotropic dilationandshear operators*. Wavelets and Splines (Athens, GA, 2005), Nashboro Press.14, 189-201, 2006 (cit. on pp. 1, 14, 71).

[GL07] K. Guo and D. Labate. *Optimally sparse multidimensional representation using shearlets*. SIAM J. Math.Anal.39, no. 1, 298–318. MR 2318387 (2008k:42097), 2007 (cit. on p. 27).

[GL13] K. Guo and D. Labate. *The construction of smooth Parseval frames of shearlets*. Math. Model. Nat. Phenom., pp. 82–105, 2013 (cit. on pp. 1, 16, 71, 119).

[HMZZ19] B. Han, Q. Mo, Z. Zhao, and X. Zhuang. *Directional compactly supported tensor product complex tight framelets with applications to image denoising and inpainting*. SIAM J. Imaging Sci. 12, 1739-1771, 2019 (cit. on p. 60).

[HFH10] G. Hennenfent, L. Fenelon, and F. J. Herrmann. *Nonequispaced curvelet transform for seismic data reconstruction:a sparsity promoting approach*. Geophysics 75(6), WB203–WB210, 2010 (cit. on pp. 53, 70).

[HH08] F. Herrmann and G. Hennenfent. *Non-parametric seismic data recovery with curvelet frames*. Geophys. J. Int.173, 233–248, 2008 (cit. on pp. 53, 70).

[HJM10] S. Hesabi, M. Jamzad, and N. Mahdavi-Amiri. *Structure and texture image inpainting*. 2010 International Conference on Signal and Image Processing, pp. 119-124, doi: 10.1109/ICSIP.2010.5697453, 2010 (cit. on p. 2).

[Jia11] R. M. S. e. a. Jianhua Yao Andrew J. Dwyer. *Computer-aided diagnosis of pulmonary infections using texture analysis and support vector machine classification*. Academic radiology 18(3), pg. 306; doi:10.1016/j.acra.2010.11.01, 2011 (cit. on p. 2).

[KDJ20] G. Kanghui, L. Demetrio, and A. Jose. *Image inpainting using sparse multiscale representations: image recovery performance guarantees*. Appl. Comput. Harmon. Anal., 2020 (cit. on pp. 1, 3, 5, 50, 74, 111, 113, 121).

[Kei12] S. Keiper. *A flexible shearlet transform – sparse approximation and dictionary learning*. Bachelor's thesis, TU Berlin, Germany, 2012 (cit. on pp. 2, 26).

[KKZ14] E. J. King, G. Kutyniok, and X. Zhuang. *Analysis of Inpainting via clustered sparsity and microlocal analysis*. J.Math.Imaging Vis. 48 , 205-234, 2014 (cit. on pp. 1, 3–5, 26, 47, 48, 50, 62, 64, 70, 74, 109, 111, 113, 121).

[KM18] E. J. King and J. M. Murphy. *A theoretical guarantee for data completion via geometric separation*. PAMM, 2018 (cit. on p. 64).

[KKZ11] E. King, G. Kutyniok, and X. Zhuang. *Analysis of data separation and recovery problems using clustered sparsity*. Proc. SPIE, Wavelets and Sparsity XIV, vol. 8138, , pp. 813818-813818-11, 2011 (cit. on pp. 5, 25, 108).

[KKL12] P. Kittipoom, G. Kutyniok, and W.-Q. Lim. *Construction of Compactly Supported Shearlet Frames*. Constr. Approx., 35(1):21–72, 2012 (cit. on pp. 1, 16).

[Kut13] G. Kutyniok. *Clustered sparsity and separation of cartoon and texture*. SIAM J. Imaging Sci. 6 , 848-874, 2013 (cit. on pp. 2, 4, 25, 35, 48, 52, 67, 69, 83, 105, 107).

[Kut14] G. Kutyniok. *Geometric separation by single-pass alternating thresholding*. Appl. Comput. Harmon. Anal. 36, 23–50, 2014 (cit. on pp. 1, 45).

[KL09] G. Kutyniok and D. Labate. *Resolution of the wavefront set using continuous shearlets*. Trans. Amer. Math. Soc., vol. 361, pp. 2719-2754, 2009 (cit. on p. 1).

[KL12a] G. Kutyniok and D. Labate. *Introduction to Shearlets*. Applied and Numerical Harmonic Analysis. Birkhäuser Boston., 2012 (cit. on pp. 15, 16).

[KLL12a] G. Kutyniok, J. Lemvig, and W.-Q. Lim. *Optimally sparse approximations of 3D functions by compactly supported shearlet frames*. SIAM J. Math. Anal., 44 , pp. 2962–3017, 2012 (cit. on pp. 2, 15, 26, 71).

[KLL12b] G. Kutyniok, J. Lemvig, and W.-Q. Lim. *Shearlets and optimally sparse approximations*. In Shearlets, pages 145–197, Birkhäuser/Springer, New York, 2012 (cit. on p. 11).

[KLR15] G. Kutyniok, W. Q. Lim, and R. Reisenhofer. *Shearlab 3D: Faithful digital shearlet transform with compactly supported shearlets*. ACM Transactions on Mathematical Software, 42(1), 2015 (cit. on pp. 15, 70).

[KL12b] G. Kutyniok and W.-Q. Lim. *Image separation using wavelets and shearlets*. InCurves and Surfaces, Lecture Notes in Computer Science 6920, Springer, 2012 (cit. on pp. 1, 2, 4, 25, 45, 115, 138).

[KL16] G. Kutyniok and W.-Q. Lim. *Dualizable shearlet frames and sparse approximation*. Constr. Approx., 44, pp. 53–86., 2016 (cit. on p. 25).

[KL10] G. Kutyniok and W.-Q. Lim. *Compactly supported shearlets are optimally sparse*. J. Approx. Theory, 163:1564–1589., 2010 (cit. on p. 27).

[LM05] E. LePennec and S. Mallat. *Sparse geometric image representation with bandelets*. IEEE Transactions on Image Processing 14, 423–438., 2005 (cit. on p. 2).

[LW12] M. Li and Y. Wen. *A New Image Inpainting Method Based on TV Model*. Physics Procedia, Volume 33, Pages 712-717, 2012 (cit. on p. 3).

[Mal98] S. Mallat. *A Wavelet Tour of Signal Processing*. CA, San Diego:Academic, 1998 (cit. on p. 2).

[Mey01] Y. Meyer. *Oscillating Patterns in Image Processing and Nonlinear Evolution Equations*. University Lecture Series, vol. 22, Amer. Math. Soc., 2001 (cit. on p. 67).

[OSV03] S. Osher, A. Sole, and L. Vese. *Image decomposition and restoration using total variation minimization and the H^{-1} norm, Multiscale Model*. Simul. 1(3) , 349–370, 2003 (cit. on p. 67).

[PEH09] V. Patel, G. Easley, and D. M. Healy. *Shearlet-based deconvolution*. IEEE Trans. Image Process. 18(12), 2673-2685, 2009 (cit. on p. 1).

[PMSMA15] Z. Petrou, I. Manakos, T. Stathaki, C. Mücher, and M. Adamo. *Discrimination of vegetation height categories with passive satellite sensor imagery using texture analysis*. IEEE. J. Sel. Top. Appl. Earth Obs. Remote Sens. 8, 1442–1455, 2015 (cit. on p. 2).

[Rod12] D. C. P. Rodrigo Pereira Ramos Marcelo Zanchetta do Nascimento. *Texture extraction: An evaluation of ridgelet, wavelet and co-occurrence based methods applied to mammograms*. Expert Systems with Applications, Vol 39, Issue 12, 11036-11047, 2012 (cit. on p. 48).

[RMW12] M. Rostami, O. Michailovich, and Z. Wang. *Image Deblurring Using Derivative Compressed Sensing for Optical Imaging Application*. in IEEE Transactions on Image Processing, vol. 21, no. 7, pp. 3139-3149, 2012 (cit. on p. 1).

[Sch16] M. Schäfer. *The role of $\alpha-$scaling for cartoon approximation*. ArXiv:1612.01036, 2016 (cit. on pp. 68, 71).

[SHB17] Y. Shen, B. Han, and E. Braverman. *Image inpainting from partial noisy data by directional complex tight framelets*. ANZIAM J.58, 247-255, 2017 (cit. on p. 60).

[SMRR04] P. Y. Simard, H. S. Malvar, J. Rinker, and E. Renshaw. *A foreground-background separation algorithm for image compression*. Data Compression Conference, 2004. Proceedings. DCC 2004, Snowbird, UT, USA, pp. 498-507, doi: 10.1109/DCC.2004.1281495, 2004 (cit. on p. 59).

[SED05] J. .-L. Starck, M. Elad, and D. L. Donoho. *Image decomposition via the combination of sparse representations and a variational approach*. IEEE Transactions on Image Processing, vol. 14, no. 10, pp. 1570-1582, doi: 10.1109/TIP.852206, 2005 (cit. on p. 59).

[SED04] J.-L. Starck, M. Elad, and D. L. Donoho. *Redundant multiscale transforms and their application for morphological component analysis*. Adv. Imag. Electron Phys., 132, pp. 287–348, 2004 (cit. on p. 59).

[SMBED05] J.-L. Starck, Y. Moudden, J. Bobin, M. Elad, and D. L. Donoho. *Morphological Component Analysis*. Wavelets XI (San Diego, CA, 2005), SPIE Proc. 5914, SPIE, Bellingham, WA, 2005 (cit. on p. 59).

[TMY78] H. Tamura, S. Mori, and T. Yamawaki. *Textural Features Corresponding to Visual Perception*. IEEE Trans". on Systems, Man, and Cybernetics, SMC-8, pp. 460-473, 1978 (cit. on p. 67).

[TAGFG08] A. Tolouee, H. Abrishami-Moghaddam, R. Garnavi, M. Forouzanfar, and M. Giti. *Texture Analysis in Lung HRCT Images*. Digital Image Computing: Techniques and Applications, pp. 305-311, doi: 10.1109/DICTA.2008.27, 2008 (cit. on p. 2).

[Tro04a] J. A. Tropp. *Greed is good: algorithmic results for sparse approximation*. IEEE Trans. Inform. Theory50(10) , 2231–2242, 2004 (cit. on p. 59).

[Tro04b] T. A. Tropp. *Just relax: Convex programming methods for subset selection and sparse approximation*. IEEE Trans. Inform. Theory, in press, 2004 (cit. on p. 59).

[VP19] K. Vaithinathan and L. Parthiban. *A Novel Texture Extraction Technique with T1 Weighted MRI for the Classification of Alzheimer's Disease*. Journal of Neuroscience Methods, Vol. 318, pp. 84-99, 2019 (cit. on p. 48).

[VO03] L. A. Vese and S. J. Osher. *Modeling Textures with Total Variation Minimization and Oscillating Patterns in Image Processing*. J. Sci. Comput., 19(1-3) , 553–572, 2003 (cit. on p. 59).

[YSZTW10] W. Yao, J. Sun, G. Zou, S. Teng, and G. Wen. *PDE image inpainting with texture synthesis based on damaged region classification*. 2010 2nd International Conference on Advanced Computer Control, pp. 447-450, doi: 10.1109/ICACC.2010.5487104, 2010 (cit. on p. 2).

[Yeh+17] R. A. Yeh, C. Chen, T.-Y. Lim, A. G. Schwing, M. Hasegawa-Johnson, and M. N. Do. *Semantic image inpainting with deep generative models*. CVPR, 2, pp. 4, 2017 (cit. on p. 3).

[ZP01] M. Zibulevsky and B. Pearlmutter. *Blind source separation by sparse decomposition in a signal dictionary*. Neur.Comput.13, 863–882, 2001 (cit. on p. 59).